MICROBIOME ANALYSIS: TECHNICAL CONSIDERATIONS AND PRACTICAL APPLICATIONS

by

Samantha Sevilla Chill
A Dissertation
Submitted to the
Graduate Faculty
of
George Mason University
in Partial Fulfillment of
The Requirements for the Degree
of
Doctor of Philosophy
Bioinformatics and Computational Biology

Committee:

_____	Dr. Iosif Vaisman, Committee Chair
_____	Dr. Ancha Baranova, Committee Member
_____	Dr. Patrick Gillevet, Committee Member
_____	Dr. Iosif Vaisman Director, School of Systems Biology
_____	Dr. Donna M. Fox, Associate Dean, Office of Student Affairs & Special Programs, College of Science
_____	Dr. Fernando R. Miralles-Wilhelm, Dean, College of Science

Date: _____ Fall 2021
George Mason University
Fairfax, VA

Microbiome Analysis: Technical Considerations and Practical Applications

A Dissertation submitted in partial fulfillment of the requirements for the degree of Doctor of Philosophy at George Mason University

by

Samantha Sevilla Chill
Master of Forensic Science
George Washington University, 2012
Bachelor of General Science
Seattle University, 2010

Director: Dr. Iosif Vaisman, Director
School of Systems Biology

Fall 2021
George Mason University
Fairfax, VA

DEDICATION

This is dedicated to mis padres, Cruz and Dora, to whom I owe everything. I hope you know that while my name may be on the degrees and awards, they represent everything you've made me to be. Thank you for making me believe that nothing is beyond my grasp, and that where, and who, I come from is one of my greatest strengths.

Quisieron enterrarnos.

No sabían que éramos semillas.

ACKNOWLEDGEMENTS

I would like to thank committee members Dr. Baranova, Dr. Gillevet, and Dr. Vaisman, for their support, wisdom, and encouragement. They each helped guide me at various points of this program, and their work is endlessly appreciated. I would also like to Dr. Emily Vogtmann, who was major support during the early stages of my program, particularly when I wavered during the pandemic. She is a brilliant example of what a positive, female, mentor should be.

I would like to thank my husband, Stephen, for whom without, this would never have been possible. Between providing meals, taking on extra childcare time, and being the #1 sample donor, he provided me support and encouragement through each step of this degree. I would also like to thank my dear friend, Maria, who helped keep me motivated and self-assured during the beginning of my program. They both heard about this work and my anxieties through each academic milestone, more than anyone else. Despite this, they somehow never wavered in their positivity and celebration of each of my successes, and in at least feigning to be as excited about each new finding as I was. Finally, I would like to thank my dear friends Sara, Veronica, and Zuzana who have become supports through the writing and defense stages, encouraging me to triumph. I am so lucky to know you all.

I would like to thank my extended Guerrero family, who taught me how to argue hard and loud, and who always welcomed me home with open arms. I especially want to thank my tíos and tías, who have shown me that a fulfilled, successful, life is about much more than the degrees you earn. I would like to thank my siblings, Cruzer and Nessie, who are finding their ways to success with such incredible dedication, I'm in awe. They have made being a big sister one of the best parts of my life.

Finally, I would also like to acknowledge my two sons, whose lives have been marked by the various phases of this dissertation. Lorenzo George, who was growing internally when I defended my dissertation proposal, and who has since grown into a rambunctious one-year-old as I completed the final stages. Stephen Isaac, who kicked and squirmed through months of writing and who served as motivation to complete my final requirements, before he made his arrival. I hope that one day, when you find yourselves on a similar journey, marked by excitement, frustration, unbelievable growth, and the most unforeseen circumstances (like a global pandemic), that you'll too persevere.

TABLE OF CONTENTS

LIST OF TABLES

LIST OF FIGURES

LIST OF EQUATIONS

LIST OF ABBREVIATIONS

16S ribosomal RNA subunit	16S rRNA
American Type Culture Collection	ATCC
Amplicon sequence variant	ASV
Base pair (s)	bp
Basic Local Alignment Search Tool	BLAST
Co-Occurrence of Domains Analysis	CoDA
Divisive Amplicon Denoising Algorithm, version 2	DADA2
Earth Microbiome Project	EMP
Human Microbiome Project	HMP
Internal transcribed spacer	ITS
Next-Generation Sequencing	NGS
Operational taxonomic unit	OTU
Polystyrene	PS
Principal Coordinates Analysis	PCoA
Ribosomal ribonucleic acid	RNA
Quantitative Insights into Microbial Ecology	QIIME
Taxonomic accuracy rate	TAR
Taxonomic detection rate	TDR

ABSTRACT

MICROBIOME ANALYSIS: TECHNICAL CONSIDERATIONS AND PRACTICAL APPLICATIONS

Samantha Sevilla Chill, Ph.D.

George Mason University, 2021

Dissertation Director: Dr. Iosif Vaisman

Continued advances in high-throughput sequencing have created new opportunities to discern microbiome composition from a variety of samples and to develop applications in ecological recycling efforts and health and disease exploration. In this work, the Tenebrio molitor Linnaeus microbiome elucidated how these mealworms adapt to consuming biodegradable-resistant materials, including polystyrene (PS), on a varied diet. With 14 million US tons generated yearly, PS is a considerable environmental contaminant. Determining the mechanism behind the digestion of PS into biodegradable components would have significant ecological implications. Additionally, this work seeks to add to the understanding of the gut-brain axis through microbiome profile examination, recently implicated in mental health disorders. The dysbiosis observed between healthy patients and those afflicted with mental health disorders highlights the potential of differential microbial composition and functional predictive modeling. However, for either of these applications to be most meaningful, the implicit technical bias in microbiome research must be understood. Previous studies have attempted to assess these variations with simplistic and unreliable models, failing to

reflect a complexity seen in either human or environmental samples. Along with the practical ecological and health-related findings, this study highlights that the careful designing of microbiome-related comparisons, and matching data processing pipelines, are necessary to ensure the reproducibility and reliability of results.

1. INTRODUCTION

When the first microbes were observed between 1665 and 1678 by Robert Hooke and Antoni van Leeuwenhoek, it is unlikely that these esteemed scientists could have readily imagined how integral these tiny organisms would be to all aspects of life (Gest, 2004). These microbes were found to have an unusually high level of diversity, not only in shape and structure but also in function (Willey et al., 2014). The human body is colonized by the diverse collection of archaea, bacteria, and fungi from birth, a complex collection that continues to evolve throughout one's life (Aagaard et al., 2014; Wampach et al., 2017). This community is now referred to as the microbiome, a combination of unique microorganisms and the environment that they occupy that creates a unique relationship by simultaneously performing essential functions for the hosts and being implicated in both overt infections and slowly developing chronic diseases (Jandhyala et al., 2015; Libertucci & Young, 2019; Prescott, 2017). The study of metagenomics, the genomic material which reflects this community, is the primary type of microbiome research utilized today (Aguiar-Pulido et al., 2016). Understanding the relationships within the microbiome, both symbiotic and parasitic, is a primary focus in current microbiome studies, requiring the identification of the individual microbes within the communities and the function of genes and systems defining the balance of unique species within the microbe consortium and looking at just two of many striking examples, *Ophiocordyceps unilateralis s.l.* Affects the host ant *Camponotus Leonardi*, and causing its death just as the ant reaches an optimal location for parasitic development, and

Lactobacillus Plantarum, who influences the mating preferences of *Drosophila melanogaster*, by changing the cuticular hydrocarbon sex pheromones, it has become apparent that microorganisms are potent in steering their hosts (Hughes et al., 2011; Sharon et al., 2010). It is not surprising then that understanding the microbiome in its entire complexity is essential to not only human and animal health but also to environmental conservation efforts (Ley et al., 2006).

While early cell-culturing techniques provided small glimpses into the microbial communities within sampled hosts, it was the significant technological advancements of sequencing methods that led to the most considerable breakthrough of the field. The sequencing evolution began with Sanger sequencing in 1977, achieving it with chain-terminating reactions, through further development of the techniques through an invention of pyrosequencing and eventually, next-generation sequencing (NGS) (Sanger et al., 1977). With these advancements also came new analytical tools, as the data generated were able to answer further questions, stretching much beyond simple maps of phylogenetic relationships. This intersection of novel technologies, both in the laboratory and in the data analysis field, continues to revolutionize the face of microbiology.

1.1 Human and animal microbiome

The human microbiome consists of an estimated 10-fold value over human nucleated cells and a 1.3 value overall human cells, whereas the animal microbiome numbers vary greatly depending on species and circumstances (Qin et al., 2010; Sender et al., 2016). The typical microbiome consists of an extensive range of species and cell

types, of which the microbial genomes account for more genes than are the human genome (Gilbert et al., 2018). Even the early, most conservative estimations of nearly 500-1,000 species found in our mucosal, skin, reproductive, and digestive tracts illustrate not only the complexity of this community but also the difficulties of presenting an accurate census (Turnbaugh et al., 2007). Early studies of bacterial species relied on cell-culture techniques, which severely limited the ability to comprehend the complexity of a community as our ability to identify the species was directly related to the ability of a species to be cultured *in vitro* (Pace et al., 1986). Later, sequencing-based techniques began targeting the small ribosomal RNA subunit gene (16S rRNA) to establish relationships between the species, their local distributions, and the evolution of these communities (Amann et al., 1995; Woese, 1987). It is this ribosomal gene that served as the foundation to the numerous microbiome-related studies and as the target for most attempts of community-based microbial identification.

Within the total human microbiome, the two most profiled communities are the microbiome of the gastrointestinal tract (commonly referred to as the "gut microbiome") and the microbiome of the oral cavity. Isolating and studying these two microbiomes has become essential for researchers for several reasons. First, it's a matter of expediency and accessibility. Both the gut microbiome and the oral microbiome lend themselves to collections directly at the source – for the gut microbiome, fecal samples may be obtained, and for the oral microbiome, oral rinses or swabs may be obtained, both of which are representative of their respective sources. Second, each of these locations represents a different part of the digestion process and where mutualistic relationships

develop and thrive. These relationships, when well-balanced, are believed to be crucial for human health. However, as research has shown, dysbiosis is always looming, and behind it, the possibility of the disease is lurking.

In animals, the relationship between bacteria and their host is a bit more complex. There are animals in which there is a strong symbiotic relationship, such as in cows, those with a weak connection, such as those in red pandas, and those with no apparent symbiosis, as seen with the *Crematogaster* ant (Hammer et al., 2019). It is even more critical then, in the study of various animal species, to determine where on the spectra the relationships fall, that is, on top of understanding its composition. For example, when researchers of the *Homarus americanus*, the American lobster, examined the microbiome of lobsters with epizootic shell disease, they found the bacterium *Aquimarian homaria i*n high abundances. Because of the identification of the dysbiosis of this bacterium, as compared to healthy lobsters, researchers may have identified a possible contributor to (decipher) ESD and can better design solutions to overcome this ailment. We see this also true in human-related research, as the identification of microbial species as drivers of disease, such as *Helicobacter pylori's* association with gastric cancer and gastric mucosa-associated lymphoid tissue (MALT) lymphoma, may be identified in a relatively straightforward fashion, with limited bias (Atherton, 2006). Generating accurate descriptions of healthy microbiomes is necessary to differentiate between the presence/ absence of invading species and to accurately estimate relative abundances in control and disease groups has implications both to environmental conservation efforts and to human health and disease.

1.2 Sequencing 16S rRNA Genes

The 16S rRNA gene is highly conserved between species of bacteria and archaea, approximately 1500 bp in length. It is often referred to as a 'molecular clock,' as it is functionally constant, shows mosaic heterogeneity across the entire gene, and occurs in all organisms (Tsukuda et al., 2017). Additionally, it is an ideal candidate for phylogenetic relationships as horizontal gene transfer rarely affects this gene as it's considered to be part of the core of informational genes (Acinas et al., 2004). The 16S rRNA gene has nine unique variable regions (V1-V9), each with varying lengths (Table 1) and levels of intragenomic heterogeneity (Coenye & Vandamme, 2003; B. Yang et al., 2016). Because of this, variable regions may be sequenced in groups or individually, with sequencing platform selection depending on the length of the selected region (Table 2) (Omega BioTek, n.d.). The combination of stretches of highly conserved sequences and variable regions enables the design of PCR primers, which can be exploited as a measure of diversity, now used in the field of microbiology.

Table 1. Nine variable regions of the 16S rRNA gene in Escherichia coli, with a start and end base pair positions listed.

Variable Region	Start position (bp)	End position (bp)
V1	8	96
V2	97	306
V3	307	487
V4	488	746
V5	747	885
V6	886	1029
V7	1030	1180
V8	1181	1372
V9	1373	1468

Table 2. 16s rRNA gene variable regions commonly sequenced, by length and common platform used.

Region (s)	Approximate length (bp)	Common Platform (s) Used
V1-V3	510	Roche 454
V3-V4	428	Illumina MiSeq
V3-V5	548	Roche 454
V4	252	Illumina HiSeq, Illumina MiSeq
V4-V5	411	Roche 454, Illumina MiSeq
V6-V9	562	Roche 454
V1-V9	1500	Pacific Biosciences

It became clear early in the that the 16S rRNA gene was helpful for establishing relationships between species. Using RNase T1 oligonucleotides, researchers were able to move away from FISH staining and begin to create catalogs of phylogeny-based relationships (Fox et al., 1980). Using reverse transcriptase and synthesis oligodeoxynucleotide primers at three sites, researchers created autoradiograms to view nucleotide data, specifically identifying differences between phylogeny (Lane et al., 1985). Pyrosequencing, a method of sequencing by synthesis, was the following breakthrough method developed in the 1990s, proving 'target amplicon-based sequencing' technology was sufficient for accurate microbial community analysis (Liu et al., 2007; Novais & Thorstenson, 2011). This sequencing method also was found to be highly correlative to DNA microarrays, a key feature for study continuity, while offering broader taxa identification and increased sensitivity (Ahn et al., 2011). Amplicon sequencing allowed for the comparison of sequencing results to detailed, and curated taxonomic databases, of which phylogenetic information regarding community profiles could be obtained. The "454" method, performed using a Roche 454 instrument that was first described in 2007,

used designed primers that flanked the variable regions, thereby classifying each read into a taxonomic unit. This method also led to sample barcoding, allowing for multiple samples to be sequenced in one run (Christensen et al., 2018). The most impactful advancement, not just to microbiology but in all scientific fields, came in the form of next-generation sequencing. This technique not only continued short-read sequencing methods but made both the human genome and the microbiome alike less elusive and more available to the scientific community at large.

Illumina sequencers are one of the most common sequencing platforms utilized to perform this sequencing, with single or paired-end reads of varying lengths. Two primers developed by the Earth Microbiome Project are typically used for the most common V4 region are the 515F (forward) and 806R (reverse), which were initially described in 2011 (Werner et al., 2011). These primers include a 10-nucleotide primer pad that helps prevent hairpin formation, a 2-nucleotide primer that shares no similarity to the 16S rRNA sequence, and a locus-specific sequence that binds to evolutionarily conserved regions (Earth Microbiome Project, 2011). Additionally, these primers also contain an Illumina sequence adaptor that attaches to a corresponding Illumina flow cell, which is then typically sequenced on an Illumina MiSeq or an Illumina HiSeq instrument (Caporaso et al., 2012). These primers have been updated since their first release, including having degeneracy added to both primers, eliminating unwanted bias toward specific taxa (Parada et al., 2016). The second change altered the forward primer (515F), adding barcodes, enabling the usage of reverse primer constructs, allowing for longer amplicons to be obtained. A sample-specific barcode that allows for multiplexing of samples to reduce

overall costs (Apprill et al., 2015). Despite amplicon-based sequencing being the most cost-effective approach to the characterization of the microbiome to date, other methods may provide more robust information on the functional and compositional microbiome profiles generated.

These metagenomic sequencing approaches include whole-genome shotgun sequencing, in which the genome of all microorganisms in a sample is sequenced. Metatranscriptomics, or the sequencing of the complete transcriptome, informs which genes are expressed within the population and has advantages over sequencing only the single 16S rRNA gene by increasing the detection of diversity and adding functional prediction (Ranjan et al., 2016). The cost and time constraints of this sequencing type, however, are not always feasible, despite the fine granularity made possible by this method (Jovel et al., 2016). Commercial manufacturers have attempted to address the cost and multiplexing concerns of whole-genome sequencing by creating custom 16S rRNA gene "panels" that include combinations of, or all, the variable regions (Qiagen, 2019f; SwiftBiosciences, n.d.). Such panels can sequence the specified variable regions in a single sequencing run, as well as primers for the internal transcribed spacer (ITS) gene region, a marker gene for fungal identification. Both shotgun sequencing and 16S rRNA gene panels offer a better resolution to the taxonomic profiles of the sample and provide a way to obtain functional level information of the various encoded microbial genes. It is pertinent then to the researcher to determine which method, if any, will be able to answer the biological questions being asked.

These biological questions have expanded in breadth and scope because of the advancements made in the field of microbiology. Being able to determine the microbiota of various environments requires that researchers not only determine which sequencing methodology to adapt but, due to the complex nature of these communities, have several other laboratory considerations to determine. To maintain the most accurate compositional profile of the microbiome, intentional decisions are required throughout the laboratory process, beginning with collection through the bioinformatic assignment of taxonomic units. These parameters, if not chosen correctly, will introduce significant bias to the analysis and may lead to spurious results and incorrect conclusions despite a solid study design in all other aspects.

1.3 Pre-Processing

Sequencing data directly from a sequencer must undergo pre-processing before any statistical analysis, often beginning with demultiplexing. During the library preparation, unique barcodes are added to each sample via an adaptor that identifies a sample as unique. Samples are then pooled together into one larger sample, added to flowcells, and sequenced. Splitting pools into their samples via barcode is the first step of most workflows and must be done before reads can be assessed for sample-level information. After demultiplexing, the depth of sequencing can be reviewed to determine the overall coverage of each project, as well as by sample.

Significant variations in sample depths may lead to an inflation of sample diversity (beta diversity) as relative abundances of species counts would be unevenly distributed (Weiss et al., 2017). Each biological sample may vary in the depth of sequencing that was

achieved, representing either a sequencing processing variation or a biological variation. Sequencing processing variation can be mitigated through sequencing controls, used to monitor the depth of reads per flow cell. To mitigate natural variation, a process of data normalization, or transformation, to make accurate comparisons between samples can be performed. Normalization in the microbiome field takes the form of rarefying data, correcting sequencing depth differences between samples. The process of rarefaction includes reviewing the entire project's species counts and then selecting a number representing a sub-selection of species. This number is then chosen randomly without replacement, discarding reads beyond this number. This threshold will also eliminate samples that do not have this minimum number of reads, eliminating low-read and possibly low-quality samples.

1.4 Operational Taxonomic Units and Amplicon Sequence Variants

Once sequences have been normalized and filtered, Operational Taxonomic Units (OTUs) are generated. Rather than using each sequence, a more computational beneficial approach is to cluster similar reads into similar 'bins,' based on an assigned level of similarity. This level of similarity can vary, depending on the stringency of the reads within bins or on the similarity to a reference database. Closed-reference clustering clusters OTU's against a selected reference database at a similarity threshold, discarding reads that do not match the database (Edgar, 2017). The fastest of all these approaches is closed-referenced and has been shown to improve accuracy over other OTU-clustering approaches, as it is classified against a known and curated reference database (Allali et al., 2017).

An alternative to the faster OTU-clustering method is amplicon sequence variants (ASV). Recent efforts have been made to urge the use of ASV's over OTU's, as they allow for a finer resolution of sequence differences and are correlated with their biological meaning, independently from any reference database (Callahan et al., 2017). ASV processing involves the removal of spurious sequences and chimeras, followed by the dereplication of sequences. These exact nucleotide sequences are then binned, creating more consistent analysis, as ASV's are not based on a reference database or various percent similarities. There are several methods capable of creating ASV's; however, DADA2 has been shown to not only improve accuracy over OTU's but better resolution over other similar methods (Callahan et al., 2016).

1.5 Assigning Taxonomy

Once OTU's or ASV's have been generated, a taxonomic assignment must be performed. There are three major taxonomic assignment parameters used in metagenomics to be tested for their accuracy and precision: BLAST+, VSEARCH, and scikit-learn multinomial naïve Bayes classifier. BLAST+ performs a local alignment between the query sequence and reference reads, then assigns consensus taxonomy to each query sequence from among top hits, of which share a minimum consensus taxonomic assignment (Camacho et al., 2009). With this method, the first N hits greater than the set percent identity similarity are included, not the top N matches. VSEARCH is a multithreaded tool that performs a global alignment between query and reference reads, then assigns consensus taxonomy to each query sequence from among top hits, of which share a minimum consensus taxonomic assignment (Rognes et al., 2016). Unlike the BLAST+

method, this method searches the entire reference database before choosing the top N hits in rank order; it does not simply select the first of the top N hits. Finally, a naïve Bayes classifier that integrates several machine-learning algorithms with training possible on a reference database chosen was implemented (Pedregosa et al., 2011). Each method presents unique approaches to the taxonomic classifier and will be benchmarked against both the complex human samples and artificially created communities.

Two publicly available 16s rRNA gene databases are commonly used in the field, each of which has differences in curation, taxonomic level, and creation, leading to differences in taxonomic calls, alpha and beta diversity abundances, and comparative statistics gleaned from a dataset. The Silva rRNA database project includes a comprehensive library of ribosomal RNA sequence data, including both small (16S and 18S) subunits, as well as large (23S and 28S) subunits (Quast et al., 2013). This database includes the domains Bacteria, Archaea and Eukarya; however, it is not regularly curated and has not been updated since 2017 (The SILVA ribosomal RNA database project, 2017). It takes taxonomic rank information from several sources, including Bergey's Taxonomic Outlines, List of Prokaryotic Names with Standing in Nomenclature (LPSN), and the International Society of Protistologists, to generate the taxonomic relationships and classifications. Additionally, all taxonomic rank assignments in this database are manually curated, based on literature and communications, by the Silva database team.

The second database often utilized is the GreenGenes database, the oldest (2013) but still widely used curated database (DeSantis et al., 2006; GreenGenes, 2019). This database only contains 16s rRNA genes, and its classification is based on automatic de

novo tree construction and mapping from mainly NCBI taxonomic sources. The phylogenetic tree is generated after a quality filtering step and is based on publicly available databases. This tree is constructed using FastTree, where inner nodes are assigned from NCBI and previous databases.

1.6 Diversity and Statistical Analyses

Alpha diversity summarizes a community's richness, or the number of features, evenness, or the distribution of these groups, or both. These diversity metrics include observed species, Abundance-based Coverage Estimator (ACE), Shannon, and Simpson. Observed species metrics represent the number of observed species for each class, whereas the ACE metric is an estimate of the richness of the samples, using a correction factor (Chao & Lee, 1992). Shannon and Simpson's indexes are diversity indices, where Shannon's Index is more sensitive to species richness while Simpson's Index is more sensitive to species evenness (Shannon & Weaver, 1949; Simpson, 1949). Shannon's Index calculates the predictability of species in a sample, with less diverse species having a higher predictability score. Simpson's Diversity Index represents the probability that two randomly chosen individuals belong to different species. In both indices, as species richness and evenness increase, so diversity increases, as well as their values.

The counterpart to alpha diversity is beta diversity, which compares how the microbiomes of one community compare to another. Two methods are commonly included (Bray-Curtis dissimilarity and Jaccard distance), both of which present the differences in taxonomic abundance profiles or taxonomic presence/absence profiles between different environments. The Bray-Curtis dissimilarity matrix determines the differences between

two samples, on a scale between 0 and 1, with 0 being the same species, at the same abundances between samples and one being they have completely different species or abundances. The Jaccard distance differs in that it includes a comparison of the presence or absence of species and does not include abundances, although it does use the same scale of 0 to 1.

Two additional methods can be employed to help reduce the dimensionality of the data using ordination techniques. These include the Principal Component Analysis (PCA), which finds a set of orthogonal linear combinations that explain all the variation in the data, using an input of presence/absence. Principal Coordinate Analysis (PCoA) is another ordination method, which utilizes distance matrices (of similarities or dissimilarities) and generates plots that can be used to visualize the distance matrix of beta diversity. The distance matrix is transformed to an orthogonal axis, reducing the dimensionality of the data. This takes a complex distance matrix down to a 2-D or 3-D scatterplot, visualizing microbial community compositional differences between samples.

Clustering algorithms are utilized to organize groups of samples by these distance matrices and metadata provided. Hierarchical clustering is used to organize items into dendrograms, where more similar objects are closer to one another on the tree. Two items start as the roots, which are most closely related, and each object next most closely related is added, based on the distance matrix. Two types of discrete clustering algorithms can be employed as well, k-means clustering and partitioning around medoids (PAM) clustering. K-means clustering is an unsupervised machine learning approach, where K random points are selected as a cluster center, and points are assigned to the cluster center, minimizing

the distance between clusters. PAM clustering selects K points to be the center of the clusters, and points are assigned to the cluster center, again minimizing the distance between the clusters. Both approaches are useful to determine if there are clustering patterns between metadata groups and to visualize the difference or calculate the significance between the centers of each cluster.

Statistical tests can be employed to determine the significance between the quantitative measures (relative abundance and the presence/absence of species) and metadata, to determine if there is statistical significance between groups (for example, healthy and unhealthy) or methods (for example, extraction methodology). These methods will include the Mann-Whitney-Wilcoxon test (Mann-Whitney *U* test), a one-way analysis of variance (ANOVA) test, and the PERMANOVA (Adonis) test. The Mann-Whitney *U* test is a non-parametric statistical method in which data is not required to fit a normal distribution and assumes unequal variances between species (Kallner, 2018). This test determines if there is significance between the means of two groups and was performed with the Bonferroni correction. This correction is applied to account for the multiple-comparison assessment, as there are multiple statistical tests performed simultaneously. Alternatively, an ANOVA test may be employed to analyze the diversity between beta diversity levels, as well as relative abundance values, assuming normal distributions (Xia & Sun, 2017). Finally, Adonis analysis is a multivariate analysis that draws upon the variance between distances matrices of an object. It can be used to interpret differences between grouping factors of samples and may be integrated with PCoA to visualize significant community-level differences.

It is important that the type of variation addressed using these statistical methods also be explored. It is known that repeated measurements of most scientific processes may not lead to the same measurement, a value represented in standard deviation (Bland & Altman, 1996). However, due to the multiple replicates within the project, variation can be determined on several levels. First, variations between biological replicates processed using the same extraction methods and bioinformatic methods would be expected to be small, indicating reproducibility of the workflow. Variations within the same sample types processed using the same extraction and bioinformatic methods can help to elucidate the reliability of artificial controls and the robustness of the workflow to handle human variation. Between methods, variations can help to understand better the bias of extraction methods, extraction method manufacturers, and bioinformatic variables. These are all important to better understanding, designing, and optimizing a workflow for any microbiome study.

Software packages are widely available to employ these statistical methods. The use of R, a programming language and environment, is common to utilize these types of statistical analysis and graphical representations (R Core Team, 2014). Python is a second programming language that is employed to perform complex statistical analysis and data management (van Rossum, G.; Drake, 2009). Both R and python incorporate 'packages' that are publicly created and maintained, which expand basic utilizations provided. Specific to microbiome analysis, the Statistical Analysis of TaxonoMic and functional Profiles (STAMP) can be employed to perform statistical hypothesis testing (ANOVA), determine effect size and confidence intervals, and provide filtering features based on p-value or other

set values (Parks et al., 2014). Although STAMP is used through a GUI, both R and Python programs can be implemented in a reproducible and robust workflow, which is highly valuable when processing a significant number of samples.

1.7 Functional Approaches

While current trends in microbiome research have seen an expansion of sequencing methodology beyond the 16S rRNA gene, this approach is still highly used in research. Being able to take this type of data, and glean functional annotation, only increases the power and value of these types of studies. Publicly available predictive tools have been created to fill this need, including PICRUSt 2.0 (https://github.com/picrust/picrust2) and Tax4Fun. These predictive methods provide functional annotations based on 16S OTU clustering techniques, employing different statistical models and references (Langille, 2018). These prediction tools utilize Kyoto Encyclopedia of Genes and Genomes (KEGG) pathways, which are manually curated pathway maps that integrate molecular interactions, reaction, and relational networks (Kanehisa Laboratories, n.d.).

PICRUSt 2.0 performs prediction by examining the gene family contribution to a metagenome based on the 16srRNA sequencing results (The PICRust Project, 2013). It uses a Hidden State Prediction (HSP) method to estimate the gene content through the sequences of related species as a reference. It relies on the plasticity theory of the microbial genome and that more recently diverged species will be more similar than more distant relatives. Gene families can then be predicted based on the microbial OTU's present. This prediction tool utilizes either GreenGenes or SILVA references, although the previous version (1.0) relied on GreenGenes alone. One primary concern with this prediction tool is

that all OTU's are linked within the phylogenetic tree, even if distances between relationships are large. Alternatively, Tax4Fun utilizes the nearest neighbor statistical approach, based on 16s rRNA sequence similarity (Aßhauer et al., 2015). The SILVA database is used as a reference, and the profile generated is transformed by a precomputed association matrix, and KEGG abundances are normalized through NCBI annotations. These abundances are then used to combine functional profiles of the KEGG organisms for the final prediction, functional profile of the community.

1.8 Technical Considerations

Technical considerations have been an unsettled topic in the microbiome community, as multiple factors in the microbiome study workflow can alter the accuracy and reliability of the full microbial community representation. While a single, standardized method, appropriate for all sample types and projects, does not seem feasible given the emergence of new technologies and the specific considerations of microbiome sample types, understanding the effects of each variable is critical to assessing the accuracy of the community-generated and potentially limiting the conclusions drawn (Editorial, 2017; Sinha et al., 2017). Studies have been completed and consortiums created to begin to understand such technical and analytical concerns, illuminating confounding sources of error and bias from sample collection, sample storage, DNA extraction, library preparation, sequencing, and informatics. One example, the Microbiome Quality Control (MBQC) consortium, attempted to create reproducible parameters for microbiome studies, including extraction, 16S amplification, and sequencing. Initial assessments from this consortium, and other published research, have further illustrated the need for a clear understanding of

each step in the workflow from extraction to bioinformatic analysis to understand better bias and project to project technical variations at each level of processing (Sinha et al., 2017).

From the moment of collection, each choice within a workflow must be carefully considered. Collection material, sample storage conditions, and storage medium have all been shown to have an impact on detected microbial communities (Choo et al., 2015; Song et al., 2016). The very nature of microbe analysis presents complications as extracting bacterial, virus, or fungal DNA in any combination requires careful consideration. Extraction methodology has shown to have a significant effect on sample diversity, with the rise and variance of the commercial protocol only exacerbating this effect (Gerasimidis et al., 2016; Salonen et al., 2010). Methods, even from the same manufacturer, may differ in several variables, including mechanical and chemical lysis of samples, the removal of inhibitors, host depletion, the addition of heat, and the strength and type of clean-up methods (Claassen et al., 2013). Mechanical disruption, often by bead beating or acoustics, has been reported as being the most efficient way to achieve cell wall lysis; however, it may also cause DNA shearing, thus limiting further molecular analyses and so must be carefully implemented. Complicated by the release of new or updated extraction methods by commercial manufacturers, or the addition of automated instruments for liquid handling or clean-up, it is how the bias of commonly used extractions protocols relate. Providing a more robust analysis of the impact of each variable on the overall profile, comparing complex and known samples, will help drive extraction decisions and may elucidate explainable differences between studies that obtain varying phenotypic results.

Sequencing methodology also plays a role, as library preparation and the primers or platform was chosen can preferentially bias samples (Gohl et al., 2016; Jones et al., 2015; Thomas et al., 2015). Determining the bias between individual sequencing runs, if any, is important to understand the internal variations caused by the technician or robotics. The depth of coverage and PCR cycle number are two other parameters that must be examined, playing a role in both cost and potential artifacts, such as chimera formation. Determining which variable region or regions are used is essential for study design. Many microbiome studies rely solely on the V4 region for taxonomic analysis due to cost and sequencing constraints (Chakravorty et al., 2007). While all regions should result in the same community profile, it has been shown that the entire gene is the best at estimating the richness of the microbiota, as variable region selection can alter taxonomic assignment (Kim et al., 2011). For example, sequencing regions V2-V3 or V3-V4 often map to higher levels of taxa than other varying combinations, although this can vary depending on whether Archaea or bacteria are targeted (Bukin et al., 2019; Davidson & Epperson, 2018). Additionally, regions V3-V4 and V4-V5 have been shown to produce more reliable results over V1-V3 (Teng et al., 2018). These combinations, as well as the method of sequencing chosen, must then be carefully considered to reduce the bias and inaccurate profile generation. Once the laboratory effects have been fully understood, the analysis parameters also must be considered, as there is also no true consensus on how data should be appropriately handled.

Finally, a bioinformatic analysis pipeline must be examined at each significant step: filtering, taxonomic assignment, and comparative analysis. Filtering settings are essential

for all genomic data, and denoising parameters have all been shown to impact the resulting microbiome profile to varying degrees (Bokulich et al., 2018). Filtering can include removal of low abundance taxonomic species, rarifying datasets to even sample read counts, and identifying and removing chimeras. Determining whether to bin reads by OTU or utilize ASV's is an important consideration as well. In addition, the reference database used to perform the taxonomic assignment is another consideration, as different databases have been created with other methods, have been updated on different schedules, and have different standards for distinguishing between species. Finally, determining the function of these microbes is often necessary, and a variety of functional tools have been created to explore these connections and answer more extensive, more impactful biological relationships.

One way to explore the various parameters discussed is by using artificially created or mock communities. An artificial community can vary significantly in the field of microbiome, representing a single species or a complex community. They can be designed to verify sequencing parameters, by being already extracted, or as an extraction control, as unlysed cells. They may be formed as an even community, with similar estimated concentrations of each community, or as a logarithmic community, where the most common species are much more prevalent. They may also represent a variety of species, both expected and unexpected, in the source or organism being investigated. Finally, they may be composed of not only bacteria but yeast and fungi, which may prove beneficial to the study design. The best use of artificial communities to assess the differences in microbiome study should represent the diversity and complexity a human sample provides,

as opposed to a single strain community, which many studies have used in the past. In addition to these communities, other types of controls, such as extraction blanks, PCR blanks, and non-template controls, must be included at each level of analysis to allow researchers to parse the impact and necessity of technical, biological, and spatial replicates within a study design.

While there have been attempts to identify how these variables impact the microbiome analyzed, there has not been one study to compare the impact of all variables using a single dataset. By examining controls at each level of analysis, within each of the variables can help to provide a much-needed robust analysis of the specific impacts of DNA extraction, sequencing, and bioinformatic approaches. It is the intersection of carefully considered technical parameters with the functional annotations, where relationships may emerge between the microbiome and disease.

1.9 Microbiome Applications

Global pollution has increased at alarming rates, with potential consequences for both human health and the environment. The production of plastic has grown over the last several decades, reaching nearly 350 million tons per year, earning our current period the title as the "Plastics Age" (Bokulich et al., 2018; Heidbreder et al., 2019). This waste is of particular concern, with the discovery of microplastics and nano-plastics detected in air, rain, tap water, beverages, and food, and with over 6300 million metric tons of plastic generated to date (Bojic et al., 2020; Geyer et al., 2017). The largest source of this waste is polystyrene (PS), a durable and often considered biodegradation-resistant material commonly known as Styrofoam, with nearly 14 US metric tons generated annually (Earth

Day Network, 2019). This polymer ([-CH (C_6H_5) CH_2-]$_n$) had a global market value of $32 billion in 2014, which has since risen to a projected $42 billion this year (Borrelle et al., 2020; Market Research Store, 2015). Numerous efforts are underway to both curtail plastic generation and to aid in its environmentally conscious disposal; however, current approaches are not sufficient to meet up with the demand and usage worldwide (Borrelle et al., 2020; Sina, 2003).

Due to the large portion of waste that PS accounts for, efforts have attempted to find ways to help with the degradation or disposal of this material with little success due to the cost to recycle and the cost of raw material. Then, in 2003, scientists discovered the larvae of *Tenebrio molitor* (mealworms) were able to digest Styrofoam food containers into biodegradable components successfully (Gilbert et al., 2014; Sina, 2003). By collecting samples from the guts of the *T. molitor* after consumption, as well as their feces, the 16s rRNA gene was analyzed for community profiling. Studies have since shown variation in diets contributing to PS consumption rate, including soy protein and bran diets, as well as the generational affinity for PS consumption being passed to new generations. This focus of research has several practical implications not only for the recycling of PS but for other plastics that resemble PS in structure. Limited, however, is information on the functional pathways that may be contributing to this digestion, as well as information on how other diets may affect the PS consumption. Both approaches may help to elucidate additional details on the mechanism of consumption and help better enable environmental applications.

Functional analysis is an essential part of understanding the true impact of microbiome community differences. Due to the limitation of 16S rRNA sequencing, practical applications must be predicted utilizing commercially available software. These include packages such as Tax4Fun, which indicates functional capabilities of microbial communities based on 16S rRNA data using the SILVA database as a reference. This package links gene sequences with the nearest neighbor approach, based on a minimum of 16s rRNA gene similarity (Aßhauer et al., 2015). After identifying the top differentiated OTU's for each metadata feature, a functional prediction may provide essential insights into understanding the mechanisms behind the digestion of polystyrene in the *T. molitor*.

Other applications where technical pipelines are necessary for largely expanding areas include human health and disease. Beginning from birth through life changes such as pregnancy, the microbiome has been shown to fluctuate over time. Source locations are also important for evaluation, like the gut, mouth, skin, and reproductive organs such as the vagina, all have unique microbiomes in both quantity and composition.

Due to the variations are seen within individuals, populations, and ecosystems, study designs for microbiome research often include a population of healthy groups and those who are afflicted with the disease/disorder/issues of interest. These types of consortiums have been developed with a focus on environmental or human aims, with intersections between the fields of ecological research and human health. One example, the Earth Microbiome Project (EMP), was started in 2010 to characterize microbial ecosystems, gathering over 30,000 samples. Then, in 2012 a collaboration between the EMP and the Human Food Project (HMP) formed the American Gut (AGP), which focused

on enhancing our understanding of microbiomes found throughout the world[92–94]. As of May 2017, the AGP had sequenced over 15,000 samples, representing over 11,000 sequences using the 16S rRNA V4 gene. All information is publicly available, as is a dense database of metadata associated with the individual donors. This dataset will be used further to examine differences in mental health diagnosis and the microbiome, utilizing both alpha and beta diversity differences, species identification, and functional approaches. Being able to elucidate potential modifiers related to the diagnosis of mental health disorders has considerable implications for both diagnosis and treatment.

In a clinical context, these large consortiums are highly valuable. The microbiome has gained significant focus recently, as studies have shown the influence that specific community changes, or even individual species presence, have on a wide range of illnesses. Diseases such as fatty liver disease, cirrhosis, cancer, inflammatory bowel disease, bipolar disorder, and autism have had associations with the microbiome, with dysbiosis correlating with disease (Bajaj, Fagan, Sikaroodi, et al., 2019; Caussy et al., 2019; Evans et al., 2017; Greenblum et al., 2012; Gudra et al., 2018; Hsiao et al., 2013). Not only are there developed links between the microbiota of an individual and these diseases, but their treatments may also be affected, as seen with some antipsychotic treatment outcomes and differences in the patient's gut microbiota (Flowers et al., 2017).

In addition, humans may be even more complex than some environmental work, as body sites often act as separate ecosystems with significant microbiome variations seen within an individual (Methé et al., 2012). These variations appear to be primarily influenced by social (environmental, dietary, etc.) rather than genetic relationships, with

studies showing spouses having more closely related microbiomes than siblings (Dill-Mcfarland et al., n.d.; Rothschild et al., 2018). It is no wonder, then, those microbiome-related studies have been on the rise since the early 2000's (NIH Human Microbiome Portfolio Analysis, 2019). To achieve the significant aim of predicting human health based on the personal microbiome, in conjunction with genetic information, further research must be conducted (Andersen et al., 2019).

2. AIMS.

There are three AIMs for this current study:

AIM 1: To determine the impact of technical (laboratory, sequencing and bioinformatic) variation on 16S rRNA gene microbiome analysis, using artificial communities and fresh-frozen human fecal samples.

AIM 2: To examine 16S rRNA gene differences between *Tenebrio molitor* communities primed on differing diets, to determine likely candidates responsible for the digestion of polystyrene.

AIM 3: To examine 16S rRNA gene differences between humans diagnosed mental health disorders and their healthy counterparts, to utilize microbiome-related functional prediction tools that may help to elucidate the biological pathways responsible for these dysfunctions.

3. TECHNICAL VARIATIONS

3.1 Background

The advancements made in genomics, with the introduction of amplicon-based next-generation sequencing, have made significant impacts in microbiology. These studies have far reached applications – from understanding the psychological effects of post-traumatic stress disorder to the intestines of mealworms that can digest polystyrene – and require special considerations. However, unlike most human genomic studies, there is no global standard for all microbiome data due to the complexity of source material and despite the attempts of consortiums, like the Microbiome Quality Control Project (MBQC). In addition, variations in sample types, the complexity of data generated, and the bias inherent to laboratory techniques require researchers to be even more intentional when designing methodologies. This will ensure that the study results have limited bias and enable researchers to understand when, if ever, two studies may be compared.

Unlike other common genomic source material, such as whole blood, microbiome studies often have individual biases that must be addressed in study design. Ensuring a sterile environment where samples aren't contaminated with the technician's microbiome profile is a critical and unique concern compared to other more robust genomic sample types. As the urine microbiome is a new field being explored, it is also essential to ensure that fecal microbiomes are not confounded by species originating from the kidney, for example (Frimodt-Møller, 2019). Extraction has been shown to significantly vary the alpha and beta diversity of studies due to the varying lysis solutions, the addition of inhibition

reagents, homogenization methods, and mechanical instrumentations used (Ferrand et al., 2014; Z. Wang et al., 2018; Yuan et al., 2012). These confounding variables are found throughout the extraction process and are only made more challenging to identify the proprietary nature of publicly available extraction kits. Each stage of the extraction process, from lysis to clean-up to elution, must be considered and measured to determine the final impact on the generated community profile.

Unlike whole human blood, one must consider the target microbial cells, which vary in their composition and the thickness of the bacterial cell walls. Balancing the community composition of complex to lyse Gram-positive cells and easier to lyse Gram-negative cells with thin cell walls is crucial to obtain a complete profile (Smith et al., 2011). Previous work has shown that bead-beating and freeze-thaw cycles significantly impact the amount of DNA obtained from these two cell types (Bahl et al., 2012; Wesolowska-Andersen et al., 2014). The introduction of heat during lysis may be an additional consideration, as this may influence more difficult to lyse cells. Because of this balance, microbiome sample lysis often requires a combination of chemical and mechanical techniques, with automation considerations regularly integrated with standard protocols for the mechanical bead-beating. Mechanical lysis is most performed using robotic instrumentation, whether in simple foam vortex adaptors or more robust instruments such as the SPEX instrument or Qiagen TissueLyzer (Qiagen, 2019i; SPEX Sample Prep, 2010). These methods introduce variation to the sample, as each has different intensity, speed, and pattern of bead-beating. In addition, the container used for homogenization and material used for the mechanical lysis must be considered. As the surface area difference of a well

in a 96-well SBS-formatted plate and an individual tube varies, so too will the ability for a single source particle to interact with the container wall. The contents of each of these source materials also vary. The beads used in processing bead-beating protocols can vary in material (most commonly glass, zirconia, or silica beads, and in size (ranging from .5 to over 1 mm). Research has shown that size variations alter the alpha diversity of samples, however, is limited information on the overall effect of these homogenization variations on sample diversity (Costea et al., 2017).

Once samples have been lysed, considerations must be made to remove contaminants present in the sample. Most commonly, clean-up can be performed with either magnetic bead-based chemistry or column-based chemistry. However, there may again be inherent bias with the bead selection (both material type and bead size) and the matrix of the column selected. Extraction methods may induce a microbiome-specific removal reagent designed to combat the difficulties of source samples that not only contain bacterial and host cells, but substances derived from food or proteins. While these removal reagents are essential to ensure that PCR or sequencing-related artifacts are removed, they may also add bias to the sample by eliminating species unequally within the sample. Human host-cell reagents may be required for specific sample types, as the host composition may constitute a significant portion of the genomic content (Heravi et al., 2020). Like other inhibitor removal reagents, this may also lead to an unbalanced microbiome profile and must be carefully considered when included as a part of the extraction workflow.

In addition to the protocol chemistry variations, many genomic centers have moved to include automation, thereby limiting the cumbersome and time-consuming extraction components. Whether implementing a liquid-handling robotic system or a magnetic clean-up robotic system implementing automated robotic approaches can yield reductions in time, improve batch-to-batch variation, and reduce contamination. Two robotic platforms are commonly used within the microbiome field, compatible with magnetic bead-based methods, produced by Qiagen and ThermoFisher Scientific. These include the Qiagen QIAsymphony instrument, which processes samples in a closed-system unit, and the ThermoFisher Scientific KingFisher Flex, which processes samples in an open-source platform (Qiagen, 2019h; ThermoFisher Scientific, n.d.-b). The QIAsymphony instruments have liquid handling capabilities on deck and can therefore complete the clean-up and elution of samples with minimal human interaction. The KingFisher Flex has no liquid handling capabilities and therefore requires user interaction to prepare the necessary reagent plates. While all instruments improve the speed of the reaction, it is another consideration to extraction study design.

After considering each of these extraction parameters, sequencing must then be assessed. Targeted amplicon sequencing is the most prevalent sequencing method used today in the microbiome community. This method targets a conserved DNA region, the 16s rRNA gene subunit, present in all bacteria and amplifies the region through polymerase chain reaction (PCR). This allows each sequence to be read, annotated, and counted with relatively low cost and low overall sequencing depth. Researchers can also keep expenses for sequencing low by multiplexing or using targeted barcoding to increase the total sample

number on each plate. While this eliminates flow cell bias in small projects, most large studies require more than one sequencing run to complete and run-to-run consistency is paramount. Understanding these variations on the microbiome profile will offer researchers another layer of clarity and confidence in their results.

The final component of the microbiome workflow that must be considered is the bioinformatic impact. This analysis begins as sequence data leave the sequencing instrument, starting with demultiplexing. Multiple samples are often pooled with labeled barcodes before sequencing to help reduce sequencing costs, sorting reads back to their source is required. After demultiplexing, the depth of sequencing should be reviewed to determine the overall coverage of each project, as well as by sample. Significant variations in depth that are not addressed may lead to an inflation of sample diversity (beta diversity) as relative abundances of species counts would be unevenly distributed (Weiss et al., 2017). In addition, each biological sample may vary in the achieved depth of sequencing, representing either a sequencing processing variation or a natural variation. To rule out sequencing variation, controls can monitor the depth of reads per flow cell. One way to mitigate these challenges, data is normalized or transformed to make accurate comparisons between samples. Normalization in the microbiome field can take the form of rarefying or drawing randomly without replacement so that all samples have the same total read counts. This threshold will also eliminate samples that do not have this minimum number of reads, eliminating low-read and possibly low-quality samples.

Reads are then grouped into similar sequences through two main approaches: clustering or denoising. Clustering methods involve grouping individual reads into similar

'bins' based on an assigned level of similarity. In closed-reference clustering, OTU's are clustered against a selected reference database at a similarity threshold, discarding reads that do not match the database will be used to create OTU's at a 97% similarity score (Edgar, 2017). These reads will be mapped using two different reference databases: the GreenGenes and the Silva databases. Alternative to the OTU-clustering method, denoising techniques are often performed, involving the removal of spurious sequences and chimera, followed by the dereplication of sequences, with amplicon sequence variants (ASV) as the output data (Callahan et al., 2016). Features can then be mapped to these sequences for taxonomic classification. Recent efforts have been made to urge the use of ASV's over OTU's, as they allow for a more acceptable resolution of sequence differences and are correlated with their biological meaning, independently from any reference database (Prodan et al., 2020). Both ASV's and OTU's will be explored to determine if sequencing controls can assess which method better determines the taxonomic classification of sequences.

Once OTU's or ASV's have been generated, taxonomic assignments must be performed. There are three major taxonomic assignment parameters used in metagenomics to be tested for their accuracy and precision: BLAST+, VSEARCH, and scikit-learn multinomial naïve Bayes classifier. BLAST+ performs a local alignment between the query sequence and reference reads, then assigns consensus taxonomy to each query sequence from among top hits, which share a minimum consensus taxonomic assignment (Camacho et al., 2009). With this method, the first N hits greater than the set percent identity similarity to the query are included, not the top N matches. VSEARCH is a multithreaded tool that

performs a global alignment between query and reference reads, then assigns consensus taxonomy to each query sequence from among top hits, sharing a minimum consensus taxonomic assignment (Rognes et al., 2016). Unlike the BLAST+ method, this method searches the entire reference database before choosing the top N hits in rank order; it does not simply select the first of the top N hits. Finally, the naïve Bayes classifier uses a Python module (scikit-learn) that integrates several machine-learning algorithms with training possible on a selected reference database (Pedregosa et al., 2011). Each method presents unique approaches to the taxonomic classifier and will be benchmarked against the complex human samples and artificially created communities.

The last area of comparison is the reference databases used. Two publicly available 16s rRNA gene databases are commonly used in the field, of which have differences in curation, taxonomic level, and creation, leading to differences in taxonomic calls, alpha, and beta diversity abundances comparative statistics gleaned from a dataset. Silva's rRNA database project includes a comprehensive library of ribosomal RNA sequence data, including both small (16S and 18S) subunits, as well as large (23S and 28S) subunits (Quast et al., 2013). These include Bacteria, Archaea and Eukarya; however, it is not regularly curated and has not been updated since 2017. It takes taxonomic rank information from several sources, including Bergey's Taxonomic Outlines, List of Prokaryotic Names with Standing in Nomenclature (LPSN), and the International Society of Protistologists. Additionally, all taxonomic rank assignments in this database are manually curated. Two versions of the database, one released in 2014 and the second released in 2017, were chosen for comparative analysis. Finally, the GreenGenes database is the oldest but widely used

curated database (2013) but only contains 16S rRNA genes (DeSantis et al., 2006; GreenGenes, 2019). Its classification is based on automatic de novo tree construction and rank mapping from mainly NCBI taxonomic sources. This tree is constructed using FastTree, where inner nodes are assigned from NCBI and previous databases (Price et al., 2009).

While some of this assessment will require the direct implementation of a tool, most of the bioinformatic evaluation was performed utilizing the second version of Quantitative Insights into Microbial Ecology (QIIME) pipeline, updated, and renamed in 2019 (QIIME2) (Bolyen et al., 2019; Caporaso et al., 2010). This is an open-source bioinformatics resource for 16s rRNA gene analysis that packages many analysis features into a multi-stepped workflow for microbial data. This pipeline, however, cannot run multiple steps simultaneously, take in a configuration file for systematic tracking, or provide speed-related parameters inherently. To improve this, Snakemake, a workflow management system that can be used to create reproducible and scalable analyses, was utilized to allow for the maintenance of unique parameters, downstream tracking, and parallelization of data processing (Chill et al., 2020). In addition, R, an open-source statistical computing and graphics software program, was utilized with publicly available packages to visualize and run additional statistical measurements (R Core Team, 2014).

3.2 Study Design

3.2.1 Overview

The study design includes two analyses: extraction method and bioinformatic processing. Fourteen types of specimens, totaling 996 samples, were included: fresh-frozen human stool (n = 1), human "robogut" samples (N=1), MBQC produced artificial chemostat stool-derived samples (n=2), commercially produced unextracted artificial samples (n=1), commercially produced extracted artificial samples (n=7) and negative reagent controls (n=3) (Table 3). All samples were pooled and randomly aliquoted prior to extraction or sequencing. Extraction was performed using seven extraction methods, organized into two groups, depending on sample types tested (Figure 1). Although both groups included all sample types in extraction, group 1 failed to produce any reads for fresh-frozen human samples or negative control samples. For this reason, group 1 analysis included extraction methods with data on artificial, robogut-derived, and chemostat-derived sample types, whereas group 2 included these types plus fresh-frozen human samples and negative controls. Twelve different bioinformatic processing methods were also included, varying ASV or OTU assignment, reference database, and taxonomic classification method (Figure 2). Controls varied in terms of number of species, as well as composition of community (Table 4).

Table 3. Overview of variables tested within extraction, sequencing, and bioinformatic evaluation. Identifiers will be used as a shorthand throughout analysis. Extraction Group ID includes extraction methods grouped by sample types evaluated.

Variable Category	Category defined	Sample Description	Identifier	Group ID
Artificial community, unextracted	Extraction	D6300	Z00	1,2
Chemostat stool derived community	Extraction	DZ35316	M16	1,2
	Extraction	DZ35322	M22	1,2
Robogut stool derived community	Extraction	DZ35298	M98	1,2
Artificial community, extracted	Sequencing	D6305	Z05	
	Sequencing	D6306	Z06	
	Sequencing	D6311	Z11	
	Sequencing	MSA1000	A00	
	Sequencing	MSA1001	A01	
	Sequencing	MSA1002	A02	
	Sequencing	MSA1003	A03	
Negative reagent controls	Extraction	Water	BW	2
	Sequencing	NTC_Blank	BN	
	Sequencing	PCR_Blank	BP	
Fresh-frozen human	Extraction	human_1	H01	2
Extraction Methods	Extraction	Qiagen DSP Virus Kit	EX-1	1
	Extraction	Qiagen MagAttract PowerMicrobiome Kit	EX-2	2
	Extraction	Qiagen DNeasy PowerSoil Pro kit	EX-3	1
	Extraction	Qiagen MagAttract PowerSoil DNA Kit	EX-4	2
	Extraction	Qiagen QIAamp with Modifications	EX-5	2
	Extraction	ThermoFisher MagMax Microbiome Ultra Kit	EX-6	1
	Extraction	ZymoBiomics 96 MagBead DNA Extraction Kit	EX-7	2

Bioinformatic Methods	Bioinformatics	blast_gg_dada.qza	BINF-01	1
	Bioinformatics	blast_silva_dada.qza	BINF-02	2
	Bioinformatics	scikit_gg_dada.qza	BINF-03	1
	Bioinformatics	scikit_silva_dada.qza	BINF-04	2
	Bioinformatics	vsearch_gg_dada.qza	BINF-05	1
	Bioinformatics	vsearch_silva_dada.qza	BINF-06	2
	Bioinformatics	blast_gg_closed_gg.qza	BINF-07	3
	Bioinformatics	blast_silva_closed_silva.qza	BINF-08	4
	Bioinformatics	scikit_gg_closed_gg.qza	BINF-09	3
	Bioinformatics	scikit_silva_closed_silva.qza	BINF-10	4
	Bioinformatics	vsearch_gg_closed_gg.qza	BINF-11	3
	Bioinformatics	vsearch_silva_closed_silva.qza	BINF-12	4

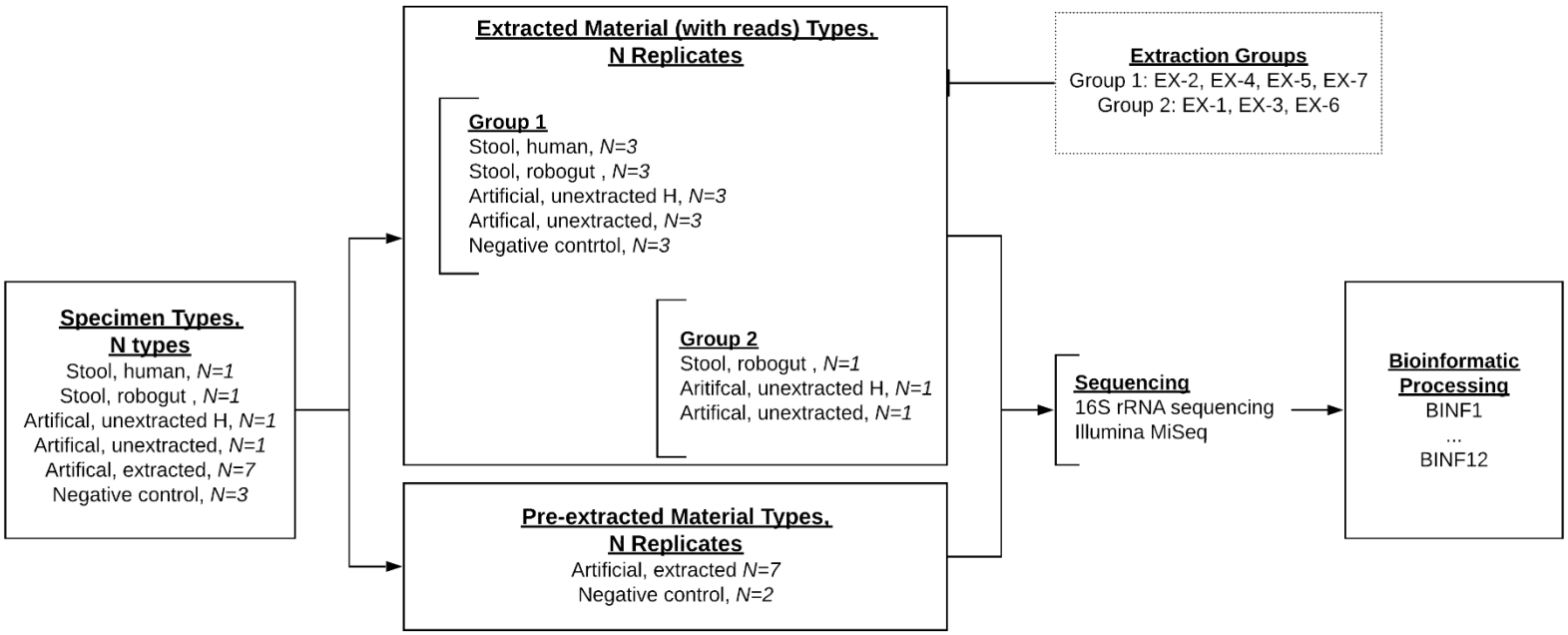

Figure 1. Overview of extraction, sequencing, and bioinformatics processes. Extraction methods were grouped based on sample type extracted. All extracted and pre-extracted materials were processed with the same sequencing methods and analyzed using various bioinformatic parameters (BINF1…BINF12).

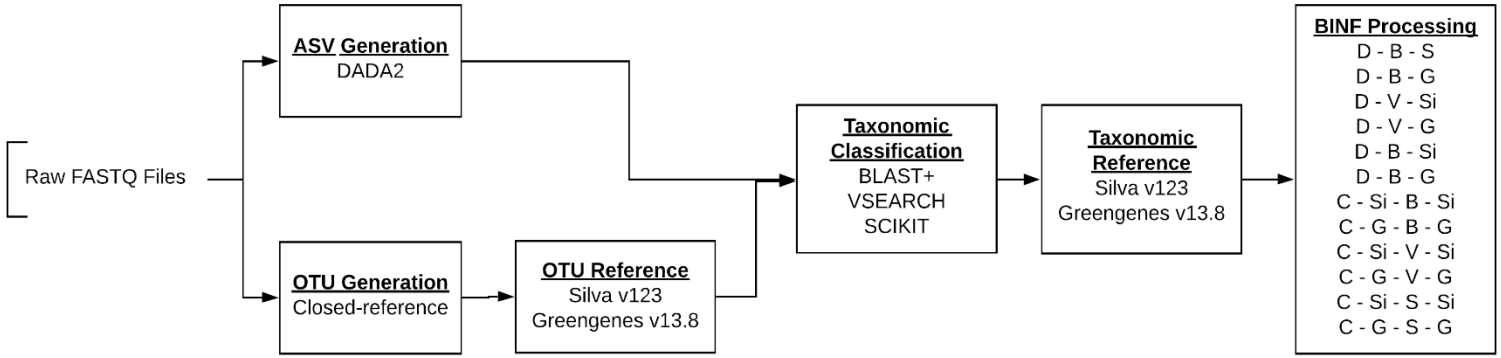

Figure 2. Workflow of bioinformatic variables tested. ASV/OTU generation type (D = Dada2, C.= Closed-reference cluster) followed by OTU reference, if applicable (Si = Silva v123, G = GreenGenes v13.8); taxonomic classification type (B = BLAST+, V = VSEARCH, S = SciKit) followed by Taxonomic reference (Si = Silva v123, G = GreenGenes v13.8).

Table 4. Artificial community composition. Controls are listed by abbreviation and sample number included in project. They also include taxonomic assignment (Species and Family), positive (P) and negative (N) gram staining, and expected relative abundance percentage, based on manufacturer provided information.

	Species	**Family**	**Gram Staining**	**Expected Relative Abundance (%)**
M22 (N=20)	*Alistipes shahii*	*Rikenellaceae*	N	3.7E+00
	Anaerostipes hadrus	*Lachnospiraceae*	P	6.3E+00
	Bacteroides caccae	*Bacteroidaceae*	N	6.3E+00
	Bifidobacterium angulatum	*Bifidobacteriaceae*	P	6.3E+00
	Bilophila wadsworthia	*Desulfovibrionaceae*	N	2.4E+00
	Clostridium bolteae	*Lachnospiraceae*	P	6.3E+00
	Collinsella aerofaciens	*Coriobacteriaceae*	P	6.3E+00
	Coprobacillus cateniformis	*Erysipelotrichaceae*	P	3.7E+00
	Enterococcus gallinarum	*Enterococcaceae*	P	6.3E+00
	Escherichia coli	*Enterobacteriaceae*	N	6.3E+00
	Fusobacterium gonidiaforman	*Fusobacteriaceae*	N	6.3E+00
	Fusobacterium varium	*Fusobacteriaceae*	N	6.3E+00
	Lactobacillus iners	*Lactobacillaceae*	P	3.7E+00
	Paenibacillus barengoltzii	*Paenibacillaceae*	P	3.7E+00
	Parabacteroides merdae	*Porphyromonadaceae*	N	6.3E+00
	Pediococcus acidilactici	*Lactobacillaceae*	P	4.2E+00
	Propionibacterium acnes	*Propionibacteriaceae*	P	6.3E+00
	Pyramidobacter piscolens	*Synergistaceae*	N	2.1E+00
	Ralstonia pickettii	*Burkholderiaceae*	N	6.3E+00
	Subdoligranulum variabile	*Ruminococcaceae*	N	1.6E+00
M16 (N=22)	*Bacillus licheniformis*	*Bacillaceae*	P	4.2E+00
	Barnesiella viscericola	*Porphyromonadaceae*	N	6.3E+00
	Bifidobacterium longum	*Bifidobacteriaceae*	P	6.3E+00
	Campylobacter concisus	*Campylobacteraceae*	N	3.1E+00
	Capnocytophaga sputigena	*Flavobacteriaceae*	N	5.2E-01
	Dialister pneumosintes	*Veillonellaceae*	N	1.0E-01
	Eggerthella lenta	*Coriobacteriaceae*	P	3.7E+00
	Eikenella corrodens	*Neisseriaceae*	N	4.2E+00
	Fusobacterium periodonticum	*Fusobacteriaceae*	N	6.3E+00
	Gemella morbillorum	*Tenericutes IncertaeSedis X*	P	5.2E+00
	Granulicatella adiacens	*Streptococcaceae*	P	6.3E+00

	Klebsiella pneumoniae	*Enterobacteriaceae*	N	6.3E+00
	Leptotrichia goodfellowii	*Leptotrichiaceae*	N	5.2E+00
	Mogibacterium timidum	*Eubacteriaceae*	P	1.0E-01
	Neisseria sicca	*Neisseriaceae*	N	6.3E+00
	Parvimonas micra	*Peptoniphilus*	P	3.1E+00
	Prevotella oralis	*Prevotellaceae*	N	6.3E+00
	Slackia exigua	*Coriobacteriaceae*	P	3.7E+00
	Stomatococcusmucilaginosu	*Brevibacteriaceae*	P	6.3E+00
	Streptococcus gordonii	*Streptococcaceae*	P	6.3E+00
	Veillonella parvula	*Veillonellaceae*	N	5.2E+00
	Weissella cibaria	*Leuconostocaceae*	P	5.2E+00
A00 (N=10)	*Bacillus cereus*	*Bacillaceae*	P	1.0E+01
	Bifidobacterium adolescentis	*Bifidobacteriaceae*	P	1.0E+01
	Clostridium beijerinckii	*Clostridiaceae*	P	1.0E+01
	Deinococcus radiodurans	*Deinococcaceae*	P	1.0E+01
	Enterococcus faecalis	*Enterococcaceae*	P	1.0E+01
	Escherichia coli	*Enterobacteriaceae*	N	1.0E+01
	Lactobacillus gasseri	*Lactobacillaceae*	P	1.0E+01
	Rhodobacter sphaeroides	*Rhodobacteraceae*	N	1.0E+01
	Staphylococcus epidermidis	*Staphylococcaceae*	P	1.0E+01
	Streptococcus mutans	*Streptococcaceae*	P	1.0E+01
A01 (N=10)	*Bacillus cereus*	*Bacillaceae*	P	4.5E+00
	Bifidobacterium adolescentis	*Bifidobacteriaceae*	P	4.0E-02
	Clostridium beijerinckii	*Clostridiaceae*	P	4.5E-01
	Deinococcus radiodurans	*Deinococcaceae*	P	4.0E-02
	Enterococcus faecalis	*Enterococcaceae*	P	4.0E-02
	Escherichia coli	*Enterobacteriaceae*	N	4.5E+00
	Lactobacillus gasseri	*Lactobacillaceae*	P	4.5E-01
	Rhodobacter sphaeroides	*Rhodobacteraceae*	N	4.5E+01
	Staphylococcus epidermidis	*Staphylococcaceae*	P	4.5E+01
	Streptococcus mutans	*Streptococcaceae*	P	4.5E-01
A02 (N=20)	*Acinetobacter baumannii*	*Moraxellaceae*	N	5.0E+00
	Bacillus cereus	*Bacillaceae*	P	5.0E+00
	Bacteroides vulgatus	*Bacteroidaceae*	N	5.0E+00
	Bifidobacterium adolescentis	*Bifidobacteriaceae*	P	5.0E+00

	Clostridium beijerinckii	*Clostridiaceae*	P	5.0E+00
	Cutibacterium acnes	*Propionibacteriaceae*	P	5.0E+00
	Deinococcus radiodurans	*Deinococcaceae*	P	5.0E+00
	Enterococcus faecalis	*Enterococcaceae*	P	5.0E+00
	Escherichia coli	*Enterobacteriaceae*	N	5.0E+00
	Helicobacter pylori	*Helicobacteraceae*	N	5.0E+00
	Lactobacillus gasseri	*Lactobacillaceae*	P	5.0E+00
	Neisseria meningitidis	*Neisseriaceae*	N	5.0E+00
	Porphyromonas gingivalis	*Porphyromonadaceae*	N	5.0E+00
	Pseudomonas aeruginosa	*Pseudomonadaceae*	N	5.0E+00
	Rhodobacter sphaeroides	*Rhodobacteraceae*	N	5.0E+00
	Schaalia odontolytica	*Actinomycetaceae*	P	5.0E+00
	Staphylococcus aureus	*Staphylococcaceae*	P	5.0E+00
	Staphylococcus epidermidis	*Staphylococcaceae*	P	5.0E+00
	Streptococcus agalactiae	*Streptococcaceae*	P	5.0E+00
	Streptococcus mutans	*Streptococcaceae*	P	5.0E+00
A03 (N=20)	*Acinetobacter baumannii*	*Moraxellaceae*	N	1.8E-01
	Bacillus cereus	*Bacillaceae*	P	1.8E+00
	Bacteroides vulgatus	*Bacteroidaceae*	N	2.0E-02
	Bifidobacterium adolescentis	*Bifidobacteriaceae*	P	2.0E-02
	Clostridium beijerinckii	*Clostridiaceae*	P	1.8E+00
	Cutibacterium acnes	*Propionibacteriaceae*	P	1.8E-01
	Deinococcus radiodurans	*Deinococcaceae*	P	2.0E-03
	Enterococcus faecalis	*Enterococcaceae*	P	2.0E-03
	Escherichia coli	*Enterobacteriaceae*	N	1.8E+01
	Helicobacter pylori	*Helicobacteraceae*	N	1.8E-01
	Lactobacillus gasseri	*Lactobacillaceae*	P	1.8E-01
	Neisseria meningitidis	*Neisseriaceae*	N	1.8E-01
	Porphyromonas gingivalis	*Porphyromonadaceae*	N	1.8E+01
	Pseudomonas aeruginosa	*Pseudomonadaceae*	N	1.8E+00
	Rhodobacter sphaeroides	*Rhodobacteraceae*	N	1.8E+01
	Schaalia odontolytica	*Actinomycetaceae*	P	2.0E-03
	Staphylococcus aureus	*Staphylococcaceae*	P	1.8E+00
	Staphylococcus epidermidis	*Staphylococcaceae*	P	1.8E+01
	Streptococcus agalactiae	*Streptococcaceae*	P	1.8E+00
	Streptococcus mutans	*Streptococcaceae*	P	1.8E+01
Z00,-05,-06 (N=8)	*Bacillus subtilis*	*Bacillaceae*	P	1.7E+01

	Enterococcus faecalis	*Enterococcaceae*	P	9.9E+00
	Escherichia coli	*Enterobacteriaceae*	N	1.0E+01
	Lactobacillus fermentum	*Lactobacillaceae*	P	1.8E+01
	Listeria monocytogenes	*Listeriaceae*	P	1.4E+01
	Pseudomonas aeruginosa	*Pseudomonadaceae*	N	4.2E+00
	Salmonella enterica	*Enterobacteriaceae*	N	1.0E+01
	Staphylococcus aureus	Staphylococcaceae	P	1.6E+01
Z11 (N=9)	Bacillus subtilis	Bacillaceae	P	1.2E+00
	Enterococcus faecalis	Enterococcaceae	P	6.7E-04
	Enterococcus gallinarum	Enterococcaceae	P	6.7E-04
	Escherichia coli	Enterobacteriaceae	N	6.9E-02
	Lactobacillus fermentum	Lactobacillaceae	P	1.2E-02
	Listeria monocytogenes	Listeriaceae	P	9.6E+01
	Pseudomonas aeruginosa	Pseudomonadaceae	N	2.8E+00
	Salmonella enterica	Enterobacteriaceae	N	7.0E-02
	Staphylococcus aureus	Staphylococcaceae	P	1.0E-04

3.2.2 Commonalities

Specimens were processed using one of the selected extraction methods provided by publicly available manufacturing companies, using manufacturer recommended parameters, including homogenization and clean-up parameters (Table 5, Table 6). The 16S rRNA gene amplicons were generated using an Illumina MiSeq instrument, targeting the v4 region. FASTQ files were demultiplexed and analyzed using varied bioinformatic variables for ASV or OTU generation (DADA or closed reference), reference database (Silva v123 or GreenGenes), and taxonomic classification method (BLAST+, VSEARCH, SciKit). Filtered counts and taxonomically classified output were generated for review.

Table 5. Extraction and bioinformatic variations summary. Includes methodologies, variables tested within each method, and the number of instances that the variable is tested. For example, the extraction manufacturer Qiagen is tested in multiple extraction kits (N=5), of which one is the Qiagen DSP Virus kit, which has multiple samples tested (N=3).

	Methodology	*Variable*	*N Methods*
Extraction Methods	Extraction Kit Manufacturer	Qiagen	5
		Thermofisher	1
		ZymoResearch	1
	Extraction Kit	Qiagen DSP Virus	3
		Qiagen MagAttract PowerMicrobiome	12
		Qiagen Dneasy PowerSoil Pro	12
		Qiagen MagAttract PowerSoil	12
		Qiagen QIAamp (Modified)	3
		ThermoFisher MagMax Microbiome Ultra	3
		ZymoFisher 96 MagBead DNA Extraction	12
	Homogenization Method	Plate vortex adaptor	1
		TissueLyzer	3
		Vertical vortex adaptor	3
	Homogenization Format	Plate	4
		Tubes	3
	Cleanup Method	Column	2
		Magnetic	5
	Inhibitor Removal Method	None	2
		Solution	4
		Tablet	1
Bioinformatic Methods	ASV or OTU generation method	Dada2 (ASV)	1
		Closed-Reference (OTU)	2
	Taxonomic Classifications	BLAST+	2
		VSEARCH	2
		SCIKIT	2

Table 6. Extraction variable summary, including information on each methods manufacturer, homogenization variables, clean-up variables, and inhibitor removal variables.

Extraction Method	*Extraction Manufacturer*	*Homogenization Method*	*Homogenization Format*	*Clean-up method*	*Inhibitor Removal Method*
Qiagen DSP Virus	Qiagen	Vertical vortex adaptor	Tubes	Magnetic	Tablet
Qiagen MagAttract PowerMicrobiome	Qiagen	TissueLyzer	Plate	Magnetic	Solution
Qiagen Dneasy PowerSoil Pro	Qiagen	TissueLyzer	Plate	Magnetic	Solution
Qiagen MagAttract PowerSoil	Qiagen	TissueLyzer	Plate	Magnetic	Solution
Qiagen QIAamp (Modified)	Qiagen	Vertical vortex adaptor	Tubes	Column	Solution
ThermoFisher MagMax Microbiome Ultra	ThermoFisher	Plate vortex adaptor	Plate	Magnetic	None
ZymoFisher 96 MagBead DNA Extraction	ZymoBiomics	Plate vortex adaptor	Tubes	Column	None

Fresh-frozen specimen. Fresh stool samples were collected in a plastic commode and transferred to a clinical urine collection container from a single volunteer (H01). They were stored at 4*C for one night prior to freezing at -80*C. Samples were thawed on ice and aliquoted into 200 mg samples, for extraction, using a plastic spatula. Aliquots were stored at -20*C until extraction.

Robogut specimens. Specimens were obtained that had been generated under the MBQC study and described previously (Sinha et al., 2017). Briefly, one healthy donor (male, 25 years old) provided fresh fecal samples on two separate occasions, 3 months apart that were used to inoculate two separate chemostat runs (M98).

Chemostat specimens. Specimens were obtained from three sources for use. First, artificial communities (M16, M22) were obtained from previously described MBQC research, which were isolated from human subjects (Sinha et al., 2017). Briefly, each strain was separately cultured on Fastidious Anaerobe Agar (FAA) (Acumedia, Lansing, MI) and supplemented with 5% defibrinated sheep's blood (Hemostat, Dixon, CA) for 72 h at 37 °C under anaerobic conditions in a Concept 300 anaerobe chamber, with the exceptions of 1_1_55 (*K. pneumoniae*), 30_1 (*Ent. saccharolyticus*), 1_1_43 (*Esch. coli*), 5_7_47FAA (*R. pickettii*), GT4ACT1 (*N. mucosae*) and CC94D (*G. adiacens*).

Artificial communities. Artificial communities were purchased from ZymoBIOMICs Research in two formats: unextracted, mixtures of ten inactivated microorganisms (Z00) and extracted, genomic DNA mixtures of ten microbial strains (Z05, Z06, Z11) (ZymoResearch, 2019). Although the composition of both Z05 and Z06 were identical, recommended input amounts varied due to the composition of the cell pellets.

Finally, artificial communities were purchased from the American Type Culture Collection (ATCC) (A00, A01, A02, A03) (extracted genomic DNA mixtures) of varying numbers of microbial strains (ATCC, n.d.).

Negative control blanks. Blank samples were included at various stages of processing: diH20 was used during extractions and as a non-template control and diH20 and PCR reagents were used during amplification.

3.2.3 Extraction

Overview. All samples were thawed on ice, from -80*C storage, prior to extraction. Seven extraction protocols were used, with chemistries representing three major manufacturers (Qiagen, ThermoFisher Scientific, and ZymoBIOMICs Research), performed on three automated platforms (QIAsymphony, KingFisher, and QIACube). These protocols included: Qiagen's DSP Virus Kit, Qiagen's QIAamp kit (with modifications based a comparative extraction project), Qiagen's (formerly MoBIO) MagAttract PowerSoil DNA kit, Qiagen's (formerly MoBIO) MagAttract PowerMicrobiome DNA Kit, Zymo Research 96 MagBead DNA/RNA Kit, Qiagen's DNeasy PowerSoil Pro kit and ThermoFisher' s MagMAX Microbiome Ultra Nucleic Acid Isolation Kit (Qiagen, 2019g, 2019e, 2019b, 2019c, 2019a; ThermoFisher Scientific, n.d.-c).

Groups. Extraction methods were placed into two groups, determined by the number fand types of samples included. Both groups included methods tested with extraction artificial communities (Z00), robogut-derived communities (M16, M22), and chemostat-derived communities (M98). The first group (EX-G1) also included a negative

extraction control (BW) and fresh-frozen human sample (H01). All sample types for this first group were done in triplicate and included extractions methods 2, 4, 5, and 7 (Table 7). Extraction group 2 (EX-G2) only included one replicate for each type, and methods in this group included extraction methods 1, 3, and 6 (Table 7).

Table 7. Extraction group and id by method name and manufacturer.

Extraction Group	*Extraction ID*	*Extraction Method*	*Extraction Manufacturer*
EX-G1	EX-1	Qiagen DSP Virus	Qiagen
EX-G2	EX-2	Qiagen MagAttract PowerMicrobiome	Qiagen
EX-G1	EX-3	Qiagen Dneasy PowerSoil Pro	Qiagen
EX-G2	EX-4	Qiagen MagAttract PowerSoil	Qiagen
EX-G2	EX-5	Qiagen QIAamp (Modified)	Qiagen
EX-G1	EX-6	ThermoFisher MagMax Microbiome Ultra	ThermoFisher
EX-G2	EX-7	ZymoFisher 96 MagBead DNA Extraction	ZymoBiomics

Qiagen DSP Virus Kit (EX-G2, EX-1). Non-homogenous samples were transferred into a Qiagen Pathogen Lysis Tube L, containing proprietary beads (unknown material or size) (Qiagen, 2019d). A chemical lysis buffer was added to the sample, and homogenization was performed by vortexing on a vertical vortex-adaptor. The supernatant was transferred to a new tube containing an InhibitEx tablet (a PCR inhibitor absorption matrix), vortexed, incubated, and centrifuged. After lysis was complete, the lysate was transferred to the QIAsymphony for the remaining clean-up, and elution, following manufacturer protocols.

Qiagen MagAttract PowerMicrobiome DNA kit (EX-G1, EX-2). Non-homogenous samples were transferred into a lysis plate, pre-filled with glass beads. A chemical lysis buffer was added to the sample, and homogenization was performed using

a TissueLyzer II. After lysis was complete, the lysate was transferred to the KingFisher Flex instrument for the remaining clean-up, and elution, following manufacturer protocols.

Qiagen DNeasy PowerSoil Pro Kit (EX-G2, EX-3). Non-homogenous samples were transferred to a Qiagen PowerBead Pro Tube, containing proprietary beads (unknown size or material). A chemical lysis buffer was added to the sample, loaded to the TissueLyzer II for homogenization. After lysis was complete, the lysate was transferred, and a manual column-based approach was performed.

Qiagen MagAttract PowerSoil DNA kit (EX-G1, EX-4). Non-homogenous samples were transferred into a lysis plate, pre-filled with garnet beads. A chemical lysis buffer was added to the sample, and homogenization was performed using a TissueLyzer II. After lysis was complete, the lysate was transferred to the KingFisher Flex instrument for the remaining clean-up, and elution, following manufacturer protocols.

Qiagen QIAamp Kit with modifications (EX-G1, EX-5). This method has been compared to other extraction methods in oral samples with more robust results (M. Chen et al., 2016). An optimized protocol was published with variations from manufacturer recommendations which was followed (Costea et al., 2017). Non-homogenous samples were transferred into a Qiagen Pathogen Lysis Tube L, containing proprietary beads (unknown material or size) (Qiagen, 2019d). A chemical lysis buffer was added to the sample after the samples were cooled on ice, and homogenization was performed by vortexing on a vertical vortex-adaptor. Ammonium acetate was added to the solution to precipitate proteins, the solution pelleted, and then added to the QIAamp spin column for clean-up. Samples are washed and eluted, via manually processing.

ThermoFisher MagMAX Microbiome Ultra Nucleic Acid Isolation Kit (EX-G2, EX-6). Non-homogenous samples were added to a lysis plate, pre-filled with glass beads. A chemical lysis buffer was added to the sample, and homogenization was performed using a TissueLyzer II. After lysis was complete, the lysate was transferred to the KingFisher Flex instrument for the remaining clean-up, and elution, following manufacturer protocols.

Zymo Research 96 MagBead kit (EX-G1, EX-7). Non-homogenous samples were added to a lysis plate, pre-filled with proprietary ultra-high-density beads A chemical lysis buffer was added to the sample, and homogenization was performed using a TissueLyzer II. After lysis was complete, the lysate was transferred to the KingFisher Flex instrument for the remaining clean-up, and elution, following manufacturer protocols.

3.2.4 Sequencing

16S rRNA gene amplification primers. Extraction samples were randomized and multiplexed using unique identifying barcodes. V4 forward 515 primer (GTGYCAGCMGCCGCGGTAA) and 806R (GGACTACNVGGGTWTCTAAT) primer were used, as described by the Earth Microbiome project (Gilbert et al., 2014). After extraction samples were stored at -20*C before amplification. 5 PRIME Hot Master Mix was utilized for PCR (Quantabio).

Post-PCR Processing. Following PCR amplification, samples were stored at 4*C prior to sequencing. An Illumina MiSeq instrument was used, generating paired end reads, at a length of 150 base pairs (Illumina, 2019). The V2 Illumina chemistry was used with a

PhiX spike-in of 20pM (Caporaso et al., 2012). Four sequencing runs were performed, with controls on each run, to examine bias between individual runs.

Quantification. All samples were quantified using the Quant-iT PicoGreen dsDNA reagent and fluorescence measured with a SpectraMax Gemini (Molecular Devices) spectrophotometer. DNA yield ranged from 0 ng to > 75 ng/uL (Molecular Devices, n.d.).

Sequencing Library. Enzymatic fragmentation was performed, to create Illumina paired-end library fragments of ~300–400 base pairs. Following fragmentation, end-repair, A-tailing, and the ligation of Illumina multiplexing PE adaptors was performed. Products were then amplified through Ligation Mediated-PCR (LM-PCR) on a ThermoFisher 9700-thermal cycler (ThermoFisher Scientific, n.d.-a). Samples were amplified at a total of 20 cycles, and purification performed with Beckman Coulter Agencourt AMPure XP beads after enzymatic reactions (Beckman Coulter, n.d.). Following the final XP bead purification, quantification and size distribution of the LM-PCR product was determined using an Agilent Bioanalyzer 7500. Samples were pooled to a final concentration of 5 pM, and templates prepared and loaded.

3.2.5 Bioinformatics

Clustering and grouping. Raw reads were demultiplex using Illumina software post-sequencing, following default parameters. Grouping of sequences was performed next with two approaches, clustering OTU's and denoising's ASV. Clustering sequences into OTU's was performed using a closed-reference technique which clustered OTU's against a selected reference database at a similarity threshold, discarding reads that do not match. Denoising ASV's, which removes and corrects reads before deduplicating similar

sequences, was performed using the second version of the Divisive Amplicon Denoising Algorithm (DADA2) (Callahan et al., 2016).

Reference database. Silva (release SILVA 132) database, and GreenGenes (release 13_8) database, were both utilized as a reference for taxonomic identification of OTUs and ASV's (DeSantis et al., 2006; Quast et al., 2013).

Taxonomic classification. Three taxonomic methods were used: BLAST+, VSEARCH, and sci-kit learn. BLAST+ took sequences and performed an alignment against a given reference sequence (GreenGenes or Silva), assigning taxonomy at a maximum hit (Camacho et al., 2009; Rognes et al., 2016). The default settings (10 maximum hits, with 80 percent identity) were used. VSEARCH consensus was achieved by assigning taxonomy to sequences by performing a global alignment, with the default maximum number of hits (10) and percent identity (80%) used. Finally, scikit-learn was performed by training reference sequences at 99% similarity, using two different publicly available reference databases (Pedregosa et al., 2011).

3.2.6 Data Integration

Overview. ASV and OTU tables generated were merged for comparative analysis at the Genus level. The databases used (either GreenGenes or Silva) are identified in each comparison, as other bioinformatic or extraction variables.

Diversity measurements. Several metrics were used to determine the influence of extraction and bioinformatic variables on microbiome analysis. Alpha diversity was examined using the inverse Simpson metrics, and beta diversity was measured using Bray-Curtis dissimilarity. First, bioinformatic diversity was explored within a bioinformatic

method, within (Bray-Curtis and Inv. Simpson) and between (Bray-Curtis) sample types. This allows for the exploration of alpha and beta-diversity within and between sample types in each bioinformatic method. Beta-diversity was explored across all variables, using extraction groups 2 and 4, and a subset (N=3) of human, blanks, and chemostat replicates:

1. technical replicates come from identical specimens and have the same bioinformatic, and extraction method;
2. bioinformatic replicates come from identical specimens and have the same extraction method;
3. sequencing replicates come from identical specimens and have the same bioinformatic and extraction methods;
4. extraction replicates come from identical specimens and have the same bioinformatic and extraction methods;

Accuracy Assessment. To determine the accuracy of our extraction and bioinformatic methods, four measures were used to determine: Taxon Accuracy Rate (TAR), Taxon Detection Rate (TDR), F-measure (F1), and Bray-Curtis dissimilarity. Each of these measures can be used to assess the presence/absence of the expected artificial communities tested, and aid in the objective determination of the best-performing protocol.

The first three measures rely on a classification of results as one of the following:

- Taxon is observed, and was expected (true positive, TP)
- Taxon is observed, but was not expected (false positive, FP)
- Taxon is not observed, but was expected (false negative, FN)

From these classifications, assessments can be made regarding the precision of the workflow (TAR) or the recall of the workflow (TDR). The TAR was calculated by determining the fraction of observed taxa that were expected (TP) to all taxa that were observed (TP + FP) (Equation 1). While the TDR was calculated by determining the fraction of observed taxa that were expected (TP) to all taxa that were expected in the sample (TP + FN) (Equation 2). Finally, to compare both values, the f-measure (F1), a weighted average, was calculated for each control (Equation 3).

Equation 1. **Taxonomic Accuracy Rate, a measure of precision, measured as a fraction of observed taxa that were expected.**

$$Taxonomic\ Accuracy\ Rate\ (TAR) = \frac{TP}{TP + FP}$$

Equation 2. Taxonomic Detection Rate, a measure of recall, measured as a fraction of expected taxa that were observed.

$$Taxonomic\ Detection\ Rate\ (TDR) = \frac{TP}{TP + FN}$$

Equation 3.F Measure (F1), a weighted average of TAR (precision) and TDR (recall).

$$F - measure\ (F1) = 2\ X\ \frac{TAR\ x\ TDR}{TAR + TDR}$$

3.3 Results

3.3.1 General Extraction

Samples were thawed on ice prior to extraction using one of the seven extraction protocols. Manufacturer recommendations were followed for all methods, except for EX-5, which was performed following a published, optimized method[12]. All protocols, briefly, following a mechanical and chemical homogenization, a clean-up method was performed.

Purification and collection of DNA varied by method. Following extraction, samples were quantified using a SpectraMax Gemini (Molecular Devices) and stored at 4*C for sequencing. Extraction concentration varied by extraction method, with standard deviation ranges variable (Table 8).

Table 8. Concentration values by extraction kit, with listed standard deviation, standard error of the mean and confidence intervals.

Extraction Kit	*N samples*	*QDNA (ng/uL)*	*standard deviation*	*standard error of the mean*	*confidence interval*
EX-1	3	2.67	4.19	2.42	10.42
EX-2	15	6.24	13.42	3.47	7.43
EX-3	3	10.13	16.17	9.33	40.16
EX-4	15	6.27	11.80	3.05	6.53
EX-5	15	5.86	14.43	3.73	7.99
EX-6	3	3.67	1.90	1.10	4.72
EX-7	15	11.81	18.26	4.71	10.11

3.3.2 General Sequencing

Sequencing was performed using an Illumina MiSeq sequencer, following the recommendations of the Earth Microbiome Project. This included the updated 515F/806R forward and reverse primers specifically adapted for the 16s rRNA gene V4 region. Samples were normalized, pooled, and sequenced using custom sequencing primers that overlap the amplification primer. A primary amplification was performed with a single pair of PCR primers, with adaptor tails to amplify samples. A secondary amplification was performed to add flow cell adaptors and indices.

A total of 303 samples were sequenced, of which 10 were negative sequencing controls, 40 were negative extraction controls and 253 were fresh-frozen, robogut-derived, chemo-stat derived, and artificial communities. Of these, 10/10 negative sequencing

controls, 11/40 negative extraction controls, 1/32 sequencing artificial communities, 2/41 extraction artificial communities, 2/77 robogut-derived, chemo-stat derived, and 37/103 fresh-frozen samples failed to produce reads above threshold. To ensure balance between each dataset, extracted samples were randomly subsampled down according to their assigned extraction group (Group 1 N=1, Group 2 N=3), for a total of 83 (unextracted samples N=69, extracted samples N=14) samples. Samples were subset by extraction groups (Group 1 through Group 4) and replicates (N=3) when indicated. A single, healthy, female donor, with normal BMI, was used for the fresh-frozen human replicate (H01). The average number of reads per sample type varied depending on the complexity of the sample, as expected, with a range of ~48,055 (extraction blank) to ~104,209 (robogut-derived) reads (Table 9, Figure 3).

Table 9. Number of reads by sample type, including standard deviation, standard error, and confidence intervals.

Sample Type	***N of Samples***	***N of reads***	***Standard Deviation***	***Standard Error***	***Confidence Intervals***
Artificial-E	31	78,161	39,851	7,157	14,617
Artificial-U	46	86,522	35,100	5,175	10,423
Blank	29	48,056	37,265	6,920	14,175
Chemostat	29	90,631	38,179	7,090	14,523
Human	66	103,482	27,150	3,342	6,674
Robogut	46	104,210	28,776	4,243	8,546

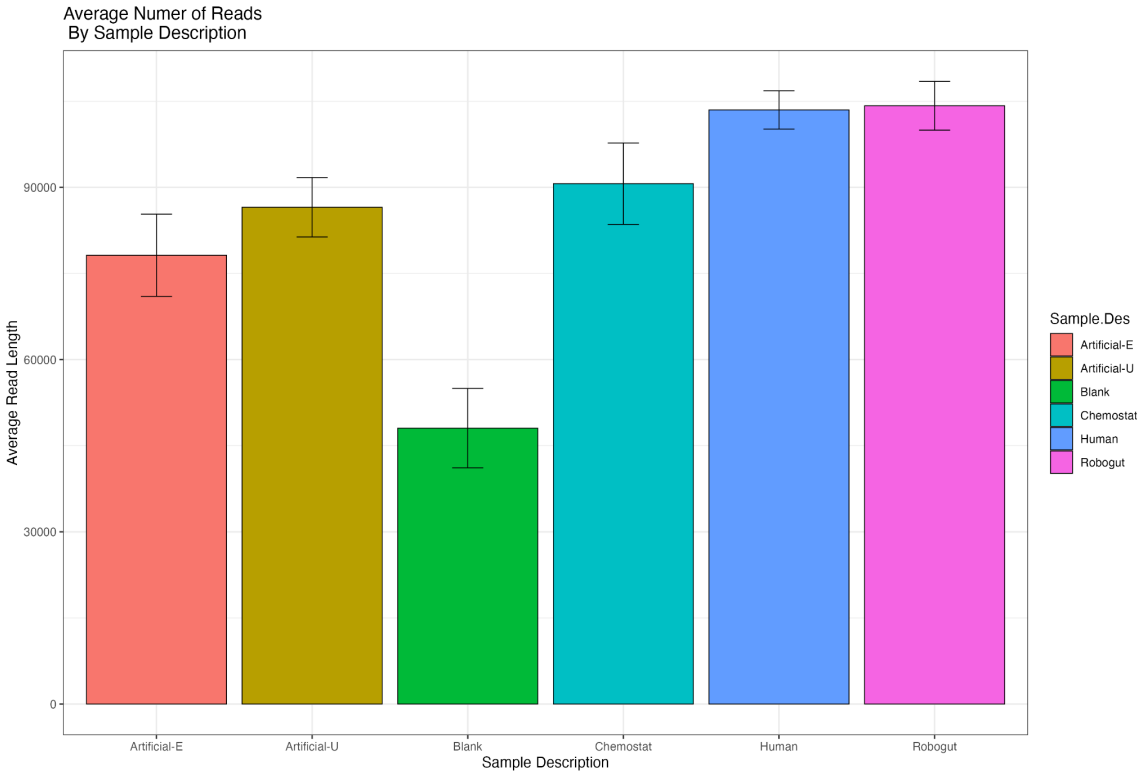

Figure 3. Raw FASTQ read length by sample type

Due to the sequencing depth graphs showing multiple peaks, read counts across all four flow cells were then reviewed to ensure that sequencing bias had not been introduced. A processing deviation was of note and would likely explain at least one of these peaks – variation in depth of coverage. To expand the number of samples processed, flowcells 1-3 had 96 barcoded samples included, and flow cell 4 had 182 samples included. We expect no significant differences in per-sample read counts between these first three flow cells, and no significant differences in total read counts between all flowcells.

To test this, blanks were first removed, as their total counts were not consistent throughout all flow cells due to the variance in number of samples. Mann-Whitney-

Wilcoxon test was performed with Bonferroni correction, to determine significance between the mean read counts of samples and controls, and as expected, flowcells 1-3 were found to be significantly different ($p<=1.00 \times 10^{-4}$) than flow cell 4 (Figure 4). Significance (p <=1.00 X 10-2) was also noted between flow cell 1 and 2, with flow cell 2 showing a larger range in sequencing variation. In reviewing the sample types by flow cell, significance was also noted. However, when viewing samples by the sample type, no significance was found. This was also true when viewing the fraction of samples filtered for controls, indicating consistency between the filtering parameters (Figure 5). This provides further justification for subsampling, as an uneven distribution of reads, would lead to an unweighted community, and could lead to spurious correlations.

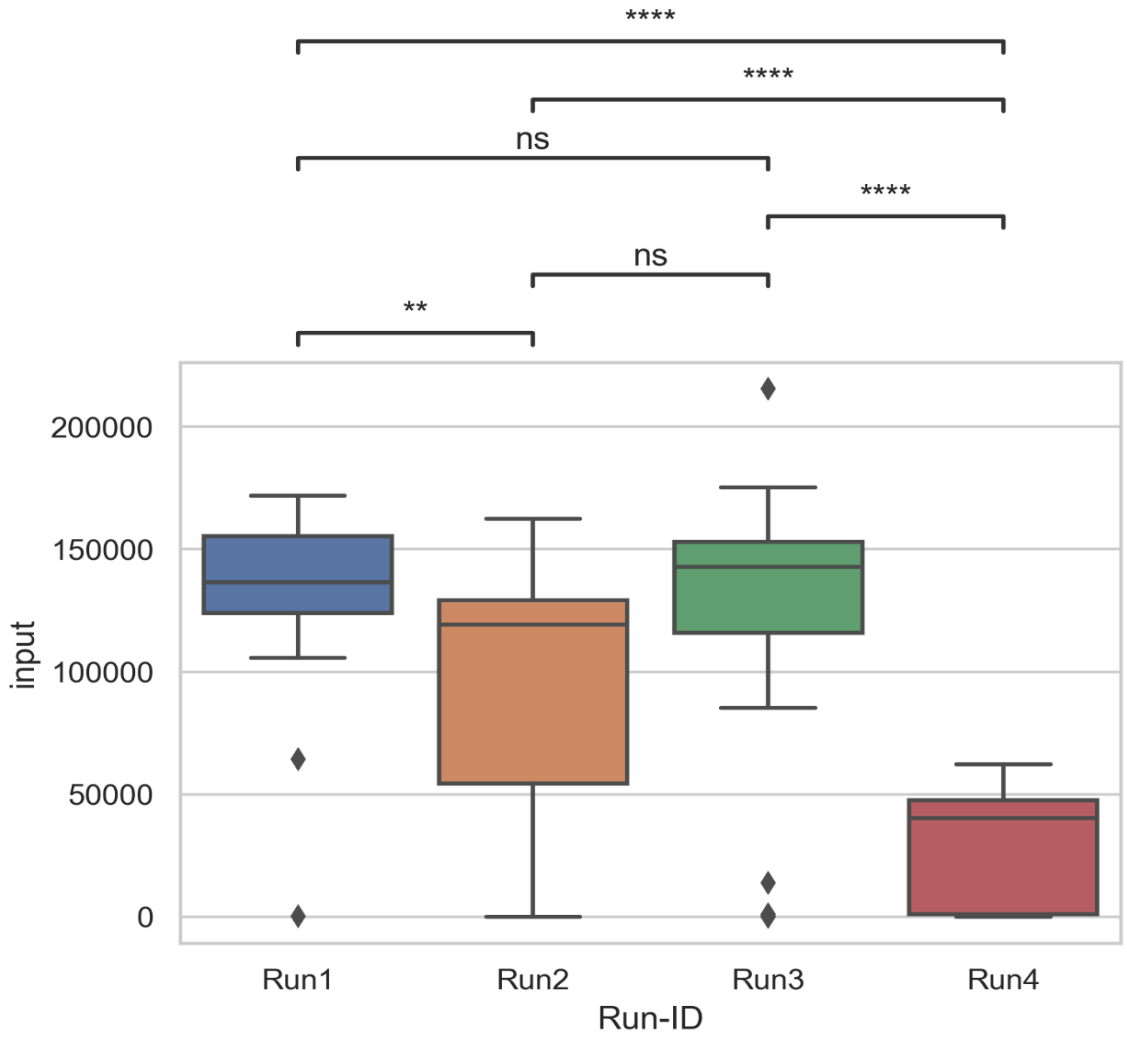

Figure 4. Sequencing read count by flow cell with mean and quartiles identified. Mann-Whitney-Wilcoxon test performed with Bonferroni correction, indicating non-significance (ns) and significant values (** p<=1.00 X 10-4) against flowcell 4.**

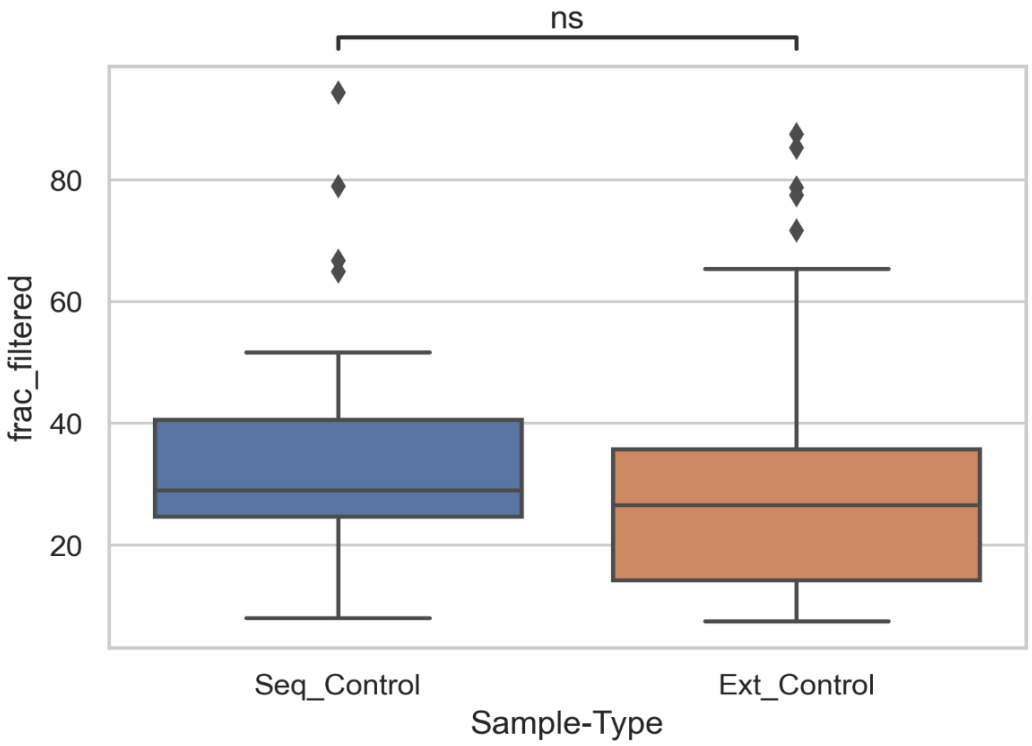

Figure 5. Fraction of reads filtered for sequencing and extraction controls. Mann-Whitney-Wilcoxon test performed with Bonferroni correction indicates no significant difference between datasets.

3.3.3 General Bioinformatics

Raw reads were demultiplex using Illumina software post-sequencing, following default parameters. Grouping of sequences was performed next with two approaches, clustering OTU's and denoising's ASV. Clustering sequences into OTU's was performed using a closed-reference approach, and denoising ASV's was performed with the Divisive Amplicon Denoising Algorithm (DADA2). The impact of taxonomic classifiers was evaluated using three methods: BLAST+, VSEARCH, and sci-kit learn. Both Silva (release SILVA 132) database, and GreenGenes (release 13_8) database, were implemented into

these methods as references, to determine their impact on the expected assignment of genera to controls.

3.4.4 Taxonomic Analysis

Each of the 12 bioinformatic protocols had a dataset of 86 samples, totaling 996 samples across all variables. This equated to 504 human, robogut-derived, chemostat-derived fecal replicates, 324 extraction artificial community and negative control replicates, and 168 sequencing artificial community replicates. Mean OTU count, median OTU count, and standard deviations were noted for each bioinformatic protocol (Table 10). Reviewing these figures highlighted the impact of the OTU/ASV generation method and associated reference database, over taxonomic classification method. Bioinformatic groups were assigned due to the non-variance, collapsing the 12 methods to four, identified by clustering method and taxonomic reference database.

Table 10. Summary of OTU/ASV counts by bioinformatic method. Methods have been grouped by taxonomic reference method, as there were no differences at this level of analysis.

BINF ID	*Clustering Method*	*Taxonomic Classification Method*	*mean otu/asv*	*median otu/asv*	*Standard Deviation*
BINF-01,03,05 BINF-G1	DADA2	Blast, SciKit, VSEARCH with GreenGenes reference	63,313.41	48,368.00	36,273.10
BINF-02,04,06 BINF-G2	DADA2	Blast, SciKit, VSEARCH with Silva reference	63,313.41	48,368.00	36,273.10
BINF-07,09,11 BINF-G3	Closed reference with GreenGenes reference	Blast, SciKit, VSEARCH with GreenGenes reference	70,816.95	48,635.00	42,279.36
BINF-08,10,12 BINF-G4	Closed reference with SILVA reference	Blast, SciKit, VSEARCH with SILVA reference	71,085.53	48,730.00	42,420.81

Prior to filtering, alpha diversity metrics were calculated for each of the 12 bioinformatic protocols after removing species missing from any sample. Richness measures (Inverse Simpson, Chao1, Observed Species) highlighted similarities between Group 1 and Group 2 (BINF-G1, BINF-G2), as all their metrics were identical (Table 11). Groups 3 and 4 (BINF-G3, BINF-G4) were more similar in values than Groups 1 and 2, however there were differences noted.

Table 11. Alpha diversity measurements per bioinformatics group, stratified by sample type. Mean values were calculated for each measurement with standard deviation indicated in parenthesis. Sequencing artificial communities (Artificial-E) and extraction artificial communities (Artificial-U) are separated into two categories for review.

Specimen Type	*Bioinformatics Group*	*Inverse Simpson*	*Chao1*	*Observed Species*
Artificial-E	BINF-G1	5.81 (3.05)	13.57 (5.95)	13.57 (5.95)
Artificial-E	BINF-G2	5.81 (3.05)	13.57 (5.95)	13.57 (5.95)
Artificial-E	BINF-G3	7.64 (3.87)	763.66 (257.32)	583.43 (213.25)
Artificial-E	BINF-G4	8.85 (4.55)	1469.75 (478.22)	1053.07 (361.91)
Artificial-U	BINF-G1	6.67 (1.37)	33.4 (18.62)	33.4 (18.62)
Artificial-U	BINF-G2	6.67 (1.37)	33.4 (18.62)	33.4 (18.62)
Artificial-U	BINF-G3	9 (2)	1060.27 (265.05)	834.33 (226.71)
Artificial-U	BINF-G4	11.19 (2.51)	2038.93 (470.55)	1578.2 (461.64)
Blank	BINF-G1	19.11 (11.25)	143.25 (75.39)	143.25 (75.39)
Blank	BINF-G2	19.11 (11.25)	143.25 (75.39)	143.25 (75.39)
Blank	BINF-G3	26.26 (15.69)	2482.5 (1252.97)	1632.83 (1019.02)
Blank	BINF-G4	28.5 (16.93)	3203.71 (1544.87)	2065.67 (1240.67)
Chemostat	BINF-G1	13.67 (3.42)	77 (38.51)	77 (38.51)
Chemostat	BINF-G2	13.67 (3.42)	77 (38.51)	77 (38.51)
Chemostat	BINF-G3	15.76 (3.79)	1484.28 (695.14)	1056.6 (563.96)
Chemostat	BINF-G4	16.9 (4.21)	2192.8 (966.67)	1512.8 (777.27)
Human	BINF-G1	20.12 (4.71)	163.5 (24.45)	163.5 (24.45)
Human	BINF-G2	20.12 (4.71)	163.5 (24.45)	163.5 (24.45)
Human	BINF-G3	29.62 (7.66)	3594.34 (506.38)	2624.58 (604.57)
Human	BINF-G4	32.53 (8.46)	4554.06 (653.48)	3278.17 (787.9)
Robogut	BINF-G1	8.12 (1.84)	114.33 (17.15)	114.33 (17.15)
Robogut	BINF-G2	8.12 (1.84)	114.33 (17.15)	114.33 (17.15)
Robogut	BINF-G3	9.04 (2.16)	1447.53 (266.08)	1050.4 (227.8)
Robogut	BINF-G4	9.91 (2.39)	1886.97 (352.16)	1354 (309.15)

A comparison of the impact of diversity between wet and dry procedures (extraction method, bioinformatic group) was highlighted in both alpha and beta diversity analysis. Alpha diversity varied by extraction method, however, bioinformatic grouping had a more distinguishable impact (Figure 6). This was highlighted most significantly in the Observed Species metric between bioinformatic protocol Groups 1/2 and Groups 3/4, which is not seen to the same degree in the extraction protocols. Beta diversity analysis of extraction methods and bioinformatic protocols revealed similar trends - bioinformatic Groups 1 and 2 (BINF-G1, BINF-G2) were almost indistinguishable from one another, whereas groups 3 and 4 showed slight differences (Figure 7). Extraction methodologies did not show significant clustering differences at this level, although clustering groups are noted throughout, likely due to a different variable.

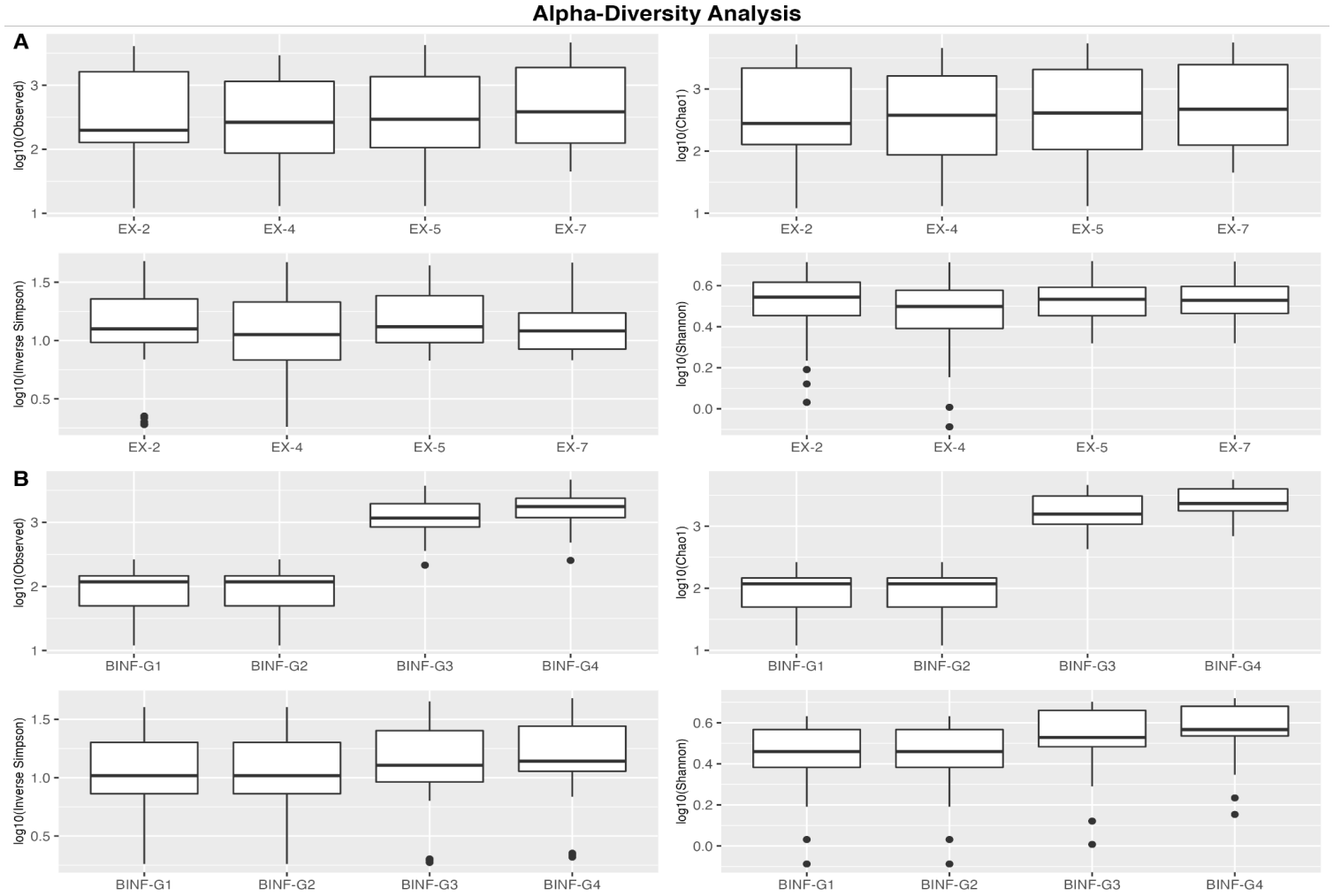

Figure 6. Alpha diversity measurements (Observed, Chao1, Inverse Simpson, Shannon) stratified by A) extraction method and B) bioinformatic group. Only extraction group two data is used in this comparison.

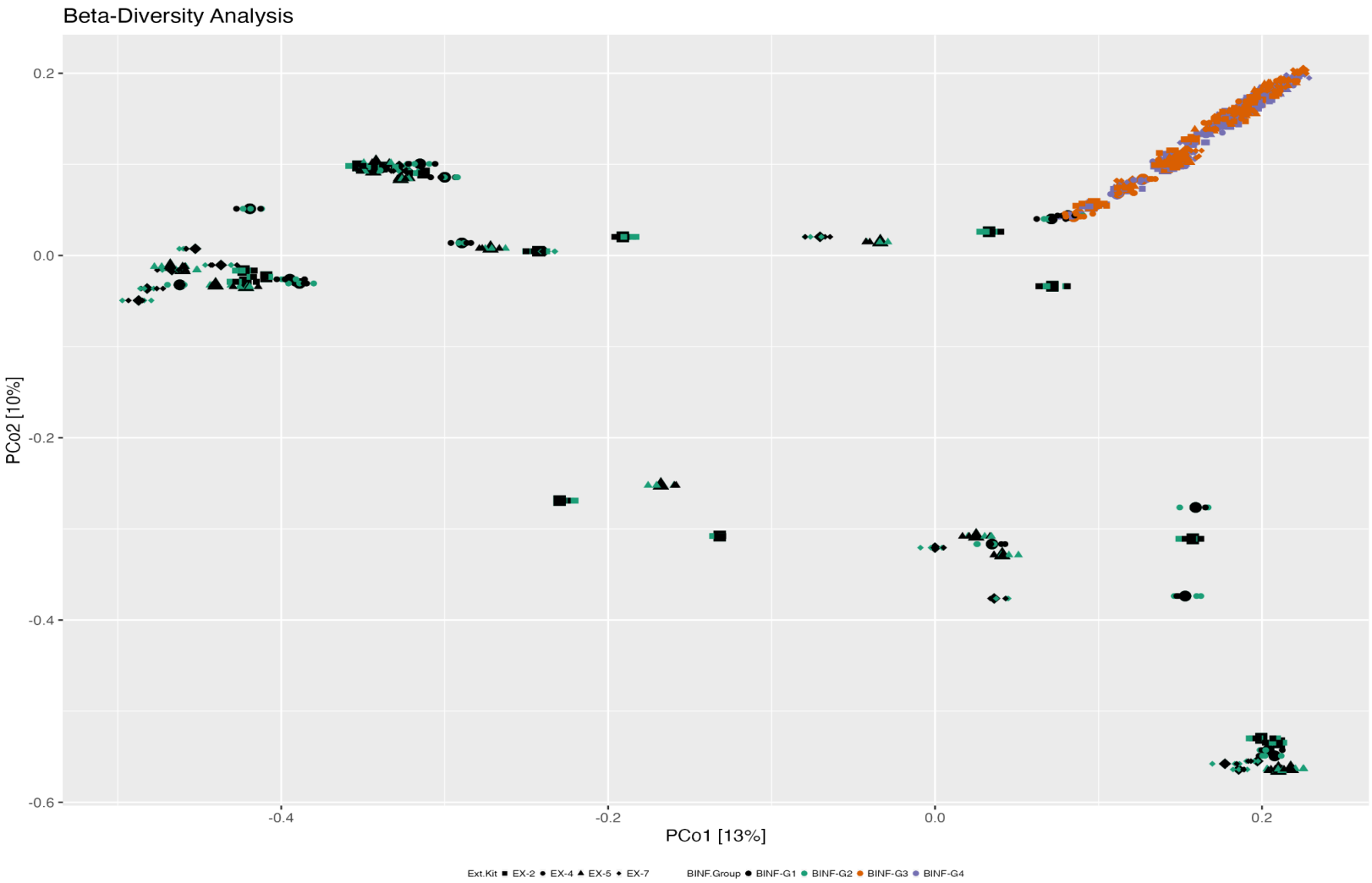

Figure 7. Beta-diversity ordination of 720 samples, corresponding to 60 replicated sequencing results of 6 different physical specimens (human-derived, chemostat, and oral and gut artificial communities, negative controls), using Bray-Curtis dissimilarities. Figure is stratified by the bioinformatic protocol used (color) as well as extraction protocol (shape). Only extraction group two data is used in this comparison.

After this initial review, filtering was performed to remove low abundance OTU's from all samples. The total number of OTU's (N=38,360) were filtered for rare OTU's by ensuring that an OTU was present at least once in at least 10% of all samples (N=623). Fresh-frozen human fecal samples (H01) averaged 111 +/- 6 ASV's with BINF-G1/BINF-G2 parameters, whereas they averaged 177 +/- 24 OTU's with BINF-G3 parameters and 185 +/- 29 OTU's with BINF-G4 parameters (Table 12). Negative extraction control samples (BW) had surprising values, with OTU's averaging 134 +/- 45 to 139 +/-48, whereas AVS were 86 +/- 40, nearly as high as the fresh-frozen human sample. Positive controls varied, with sequencing positive controls having lower ASV/OTU counts (7 +/- 2 to 113 +/-7) than extraction positive controls (28 +/14 to 156 +/- 36). Sequencing artificial communities (Artificial-E) were stratified by manufacturer and showed fewer observed OTU's/ASV's between those communities developed by ATCC (A00-A03) than those developed by ZymoBiomics (Z00), despite having a higher average number of genera (ATCC N=15 to ZymoBiomics N=9.5).

Table 12. Mean ASV (BINF-G1, BINF-G2) and OTU (BINF-G3, BINF-4) values with standard deviation in parentheses, stratified by sample type. Sequencing artificial communities (Artificial-E) are stratified by manufacturer (ATCC: A00-A03 and ZymoBiomics: Z00) to help assess potential differences.

	BINF-G1	***BINF-G2***	***BINF-G3***	***BINF-G4***
Artificial-E (A00-A03)	5.5 (1.77)	5.5 (1.77)	98.75 (6.56)	113.88 (6.96)
Artificial-E (Z00)	28.33 (14.68)	28.33 (14.68)	141.73 (34.01)	156.73 (36.19)
Artificial-U (Z05,Z06,Z11)	7.67 (1.94)	7.67 (1.94)	71.67 (39.19)	81.83 (46.21)
Chemostat (M16,M22)	80.47 (9.35)	80.47 (9.35)	124.27 (14.82)	127.53 (14.5)
Extraction Negative Control (BW)	85.58 (40.71)	85.58 (40.71)	134.17 (44.44)	139.17 (47.69)

Human (H01)	111.42 (5.93)	111.42 (5.93)	177.75 (23.91)	185.5 (28.89)
Robogut (M98)	52 (33.83)	52 (33.83)	139.73 (64.14)	149.8 (73.83)

Continuing the comparison between the effects of extraction and bioinformatic protocol differences post filtering, within and between sample diversity was evaluated stratifying both variables (Figure 8). Alpha diversity showed clear differences between bioinformatic groups 1/2 (BINF-01 to BINF-06) and groups 3/4 (BINF-07 to BINF-12). Diversity differences were not as significant between bioinformatic processing methods, although differences were noted between extraction protocols. Significance testing highlighted beta-diversity differences between extraction protocol (both method and group), bioinformatic protocol (both method and group) and sample type (Table 13). Reviewing individual comparisons with spearman correlation matrices of log10 Inverse Shannon values for both bioinformatic and extraction protocols, illustrate the tightness of fit between the bioinformatics protocol (values range from 0.73 to 0.75), whereas low index values indicate a low level of correlation (or inconsistent bias) between extraction methods (values range from 0.3 to 0.47) (Figure 9).

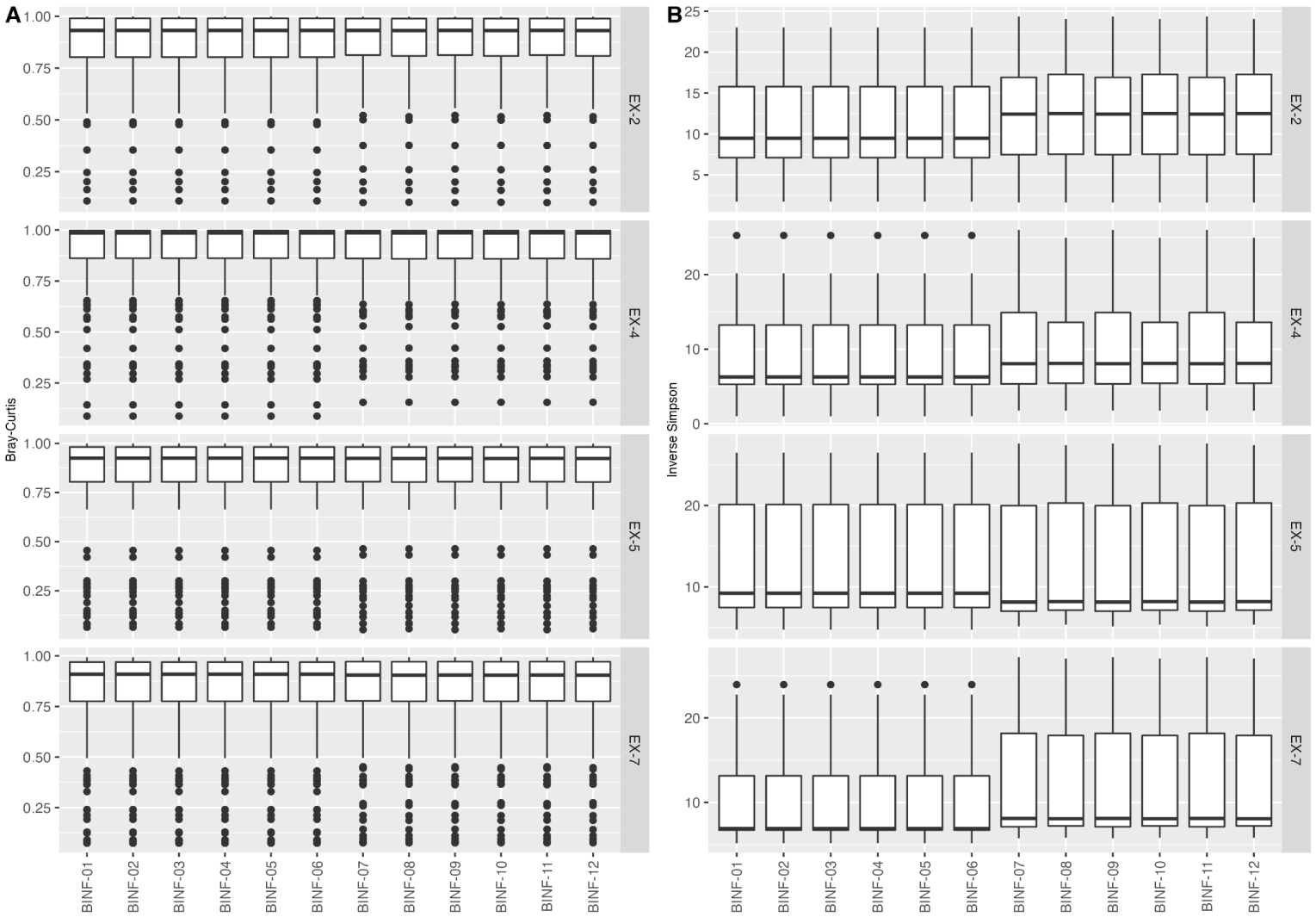

Figure 8. Bray-Curtis dissimilarity values and inverse Simpson values stratified by bioinformatic methods and extraction methods

Table 13. PERMANOVA analysis performed at each stratification level, holding all other variables constant, with 1000 iterations.

Stratification	p-value
Sample Type	0.000999
Extraction Method	0.000999
Extraction Group	0.000999
Bioinformatic Method	0.000999
Bioinformatic Group	0.000999

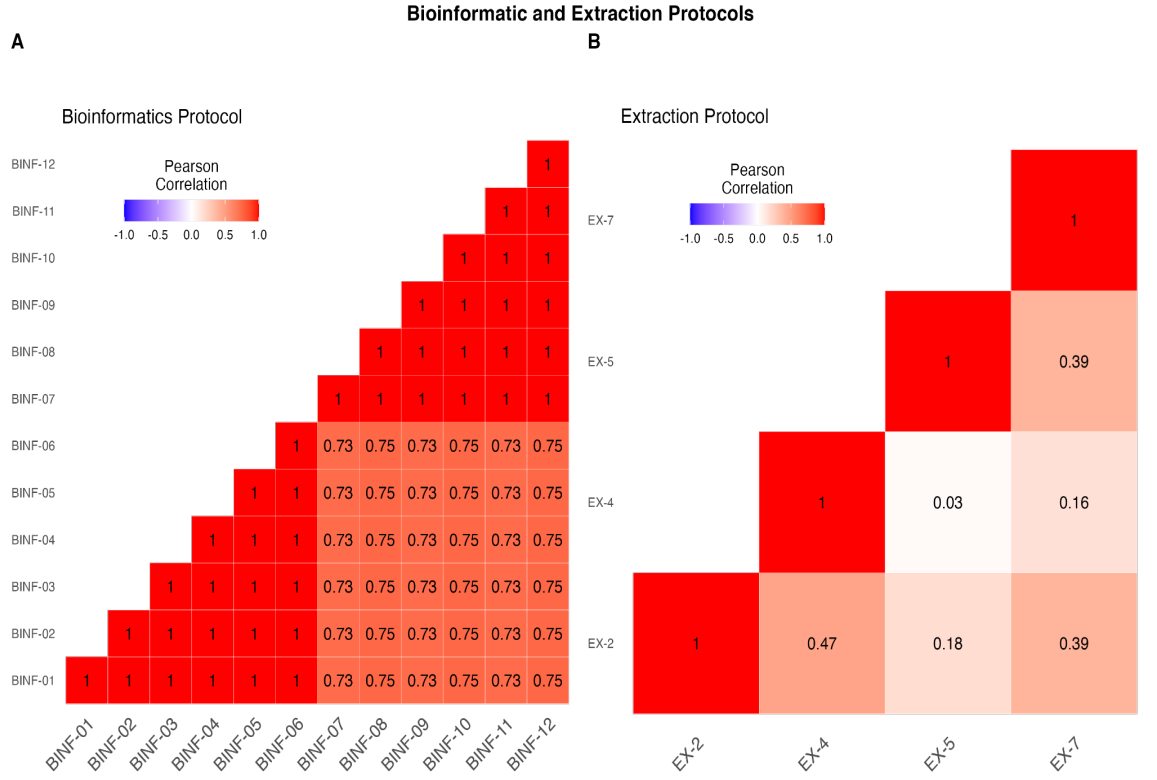

Figure 9. Correlations of alpha diversities for samples, stratified by A) bioinformatics protocol and B) extraction method. Each tile represents a Spearman rank coefficient between the pairwise comparison of log10 transformed Inverse Simpson index estimates at that grouping.

After reviewing the absolute levels of diversity, quantitative diversity was assessed (Figure 10). For each, Bray-Curtis within dissimilarities for bioinformatic methods were computed between technical replicates (same source material) extracted with the same

extracted protocol, whereas for extraction protocols were computed between technical replicates processed with the same bioinformatic method. Bray-Curtis between dissimilarities were calculated between non-technical replicates and non-identical extraction or bioinformatic methods. These two comparisons offer insight then, into the reliability and reproducibility of replicates within any bioinformatic or extraction protocol, and the dissimilarity between protocols. Reviewing within, and between beta diversity levels at each bioinformatic processing level stratified by sample type illustrated the differences between sample type over bioinformatic processing method. In the same figure, reviewing the alpha diversity, with the Inverse Simpson metric highlighted differences in ASV generation (BINF-01 to BINF 06) representing BINF-G1 and BINF-G2, as compared to OTU generation (BINF-07 to BINF-12) representing BINF-G3 and BINF-G4. Extraction methods did not follow the same trend, with variation noted between technical replicates extracted with different methods, and between sample types within the same method.

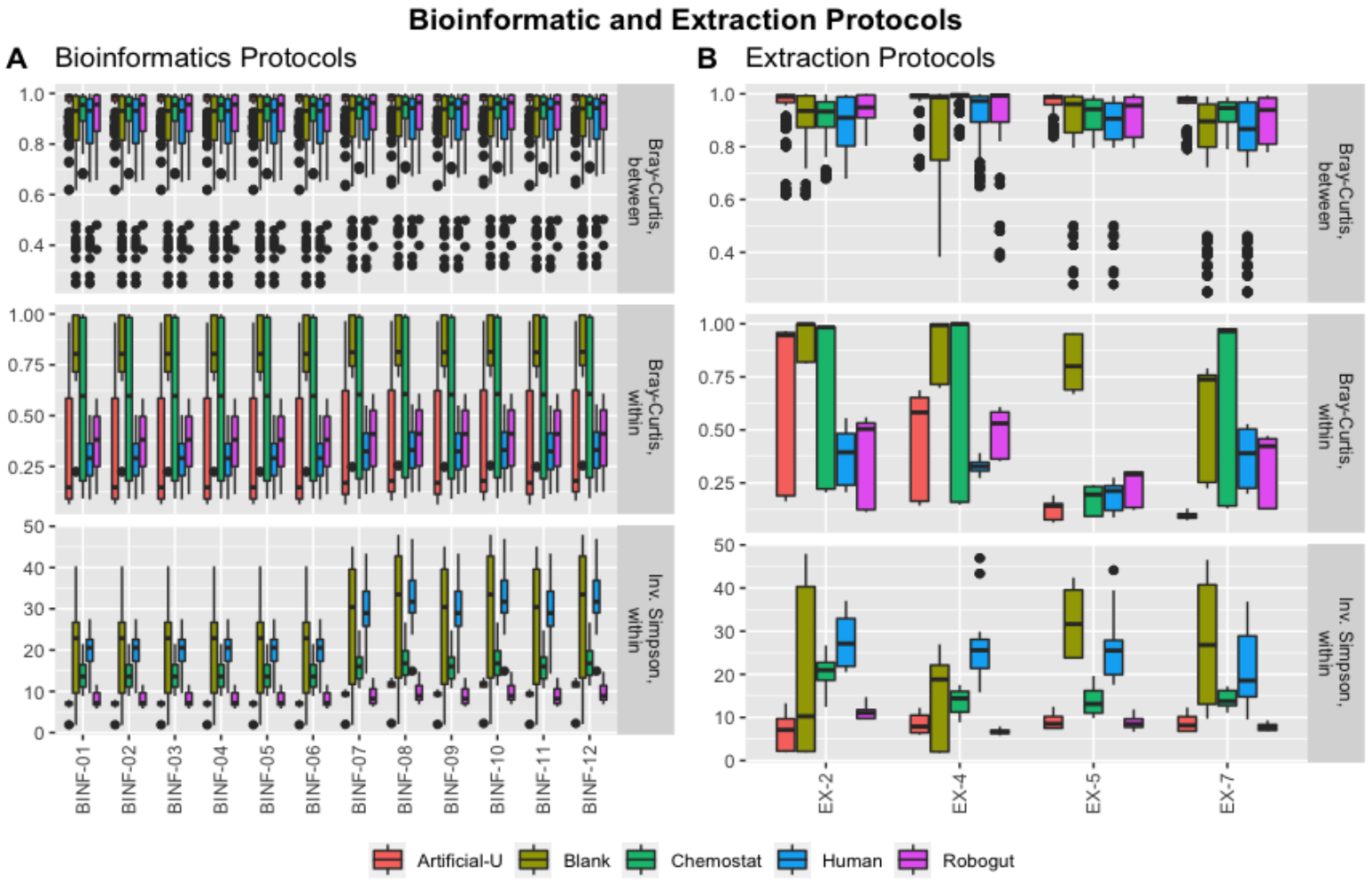

Figure 10. Effects of bioinformatics and extraction protocols on alpha and beta diversity levels. Distributions are stratified by extracted sample material, including extraction group 2 only. Sample types included extraction artificial communities (artificial-u N=1), extraction negative controls (blank N=1), chemostat-derived samples (chemostat N=1), human-derived samples (human N=1), and robogut-derived samples (robogut N=1).

To further explore these differences, Bray-Curtis dissimilarity matrices were created to isolate the variability introduced by bioinformatic protocol, extraction protocol, subject and sample type (Figure 11). For each of these variables, all other variables were held constant; for example, in bioinformatic variability the subject, extraction protocol and sample type were held constant, and compared to all other bioinformatic protocols. This allowed for the assessment of each individual variable against all others. The effect size of this distribution highlighted the variability of every aspect of analysis, particularly on low-complexity sample types (extraction artificial communities, extraction negative controls) over higher-complexity sample types (human-derived, robogut-derived). It also highlighted the impact of bioinformatic processing (likely related to OTU and ASV generation) over extraction processing.

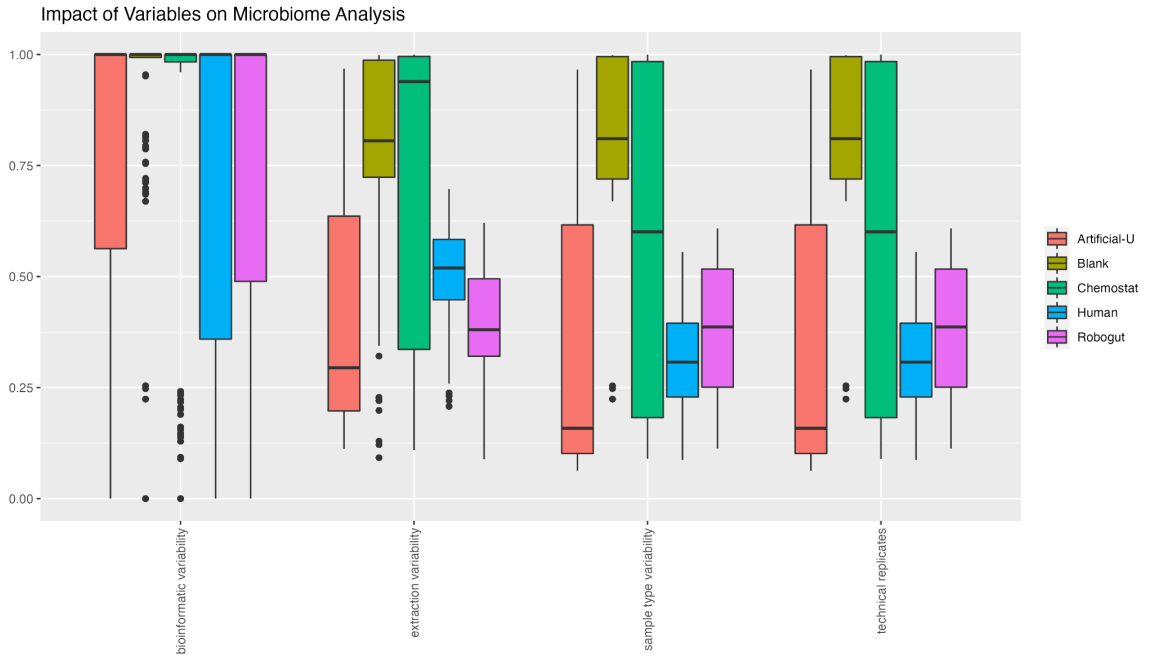

Figure 11. Bray-Curtis dissimilarity comparisons between variations, comparing all bioinformatic methods, all extracted material, and only extraction group 2. Bioinformatic variability compares the same subject's, extracted with the same extraction protocol, but analyzed with different bioinformatic protocols. Extraction variability compares the same subjects analyzed with the same bioinformatic protocol but extracted with different extraction methods. Sample type variability compares different subject's, extracted with the same extraction protocol, and analyzed with the same bioinformatic protocol. Technical replicates compare the same subject, extracted with the same extraction protocol, and analyzed with the same bioinformatic method.

Stratifying the data between biological, laboratory and bioinformatic variables all appear to contribute to between-sample variations (Figure 12). Human-derived samples (H01) clustered the most tightly together, with the negative controls (BW), likely indicating the source contamination of these samples. Robogut-derived samples (M98) clustered near these samples as well, with sequencing controls from ZymoBiomics (Z05, Z06, Z11) and ATCC (A00-A03) clustering a distance away. The tightness of clustering of the human-derived and robogut-derived samples does point to the importance of these samples, and possible use as positive controls in future experiments. Computational protocols (BINF-A through BINF-D) were the most distinct of all clustering methods, specifically with the

clustering method of ASV's (BINF-A, BINF-B) or OTU's (BINF-C, BINF-D) illustrating profound differences.

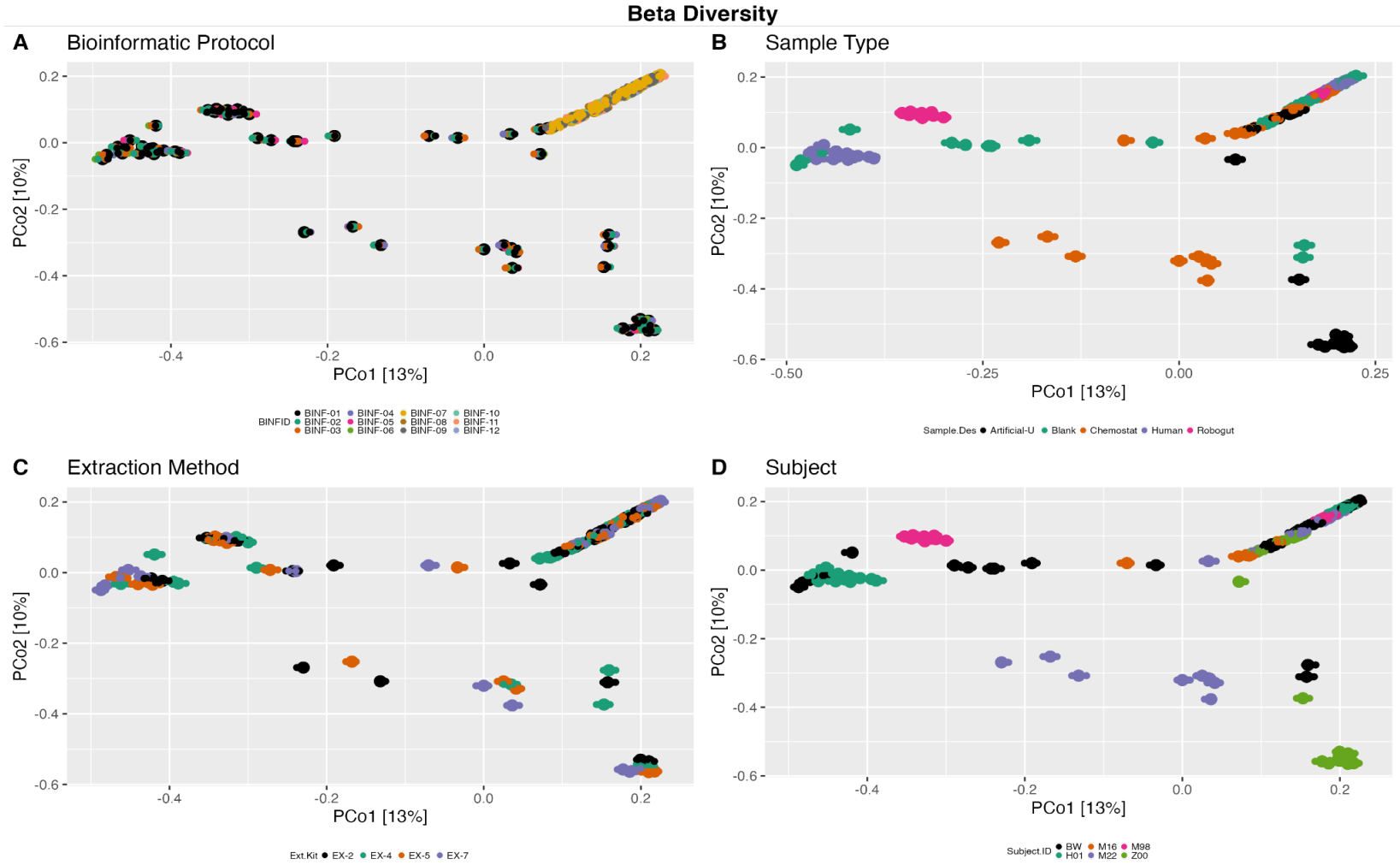

Figure 12. Beta-diversity ordination of 5,258 samples, corresponding to 232 replicated sequencing results of 14 different physical specimens (human-derived, chemostat, and oral and gut artificial communities, negative controls), using Bray-Curtis dissimilarities. Figures are stratified by bioinformatic protocols (a), sample description (b) sample type (c), and extraction method (d).

Sample type was differentially affected by extraction method, with extraction artificial communities (Z00) minimally affected and extraction negative controls (BW) showing large distributions within methods (Figure 13). One way analysis of variance (ANOVA) testing was performed on each type, with significance between samples noted with sample type M98 (Table 14). A Tukey's Honest Significant Difference (HSD) test was performed to determine the pairwise comparisons of each type's mean to determine which means are different or grouped. Within M98, three groups were identified: extraction group 1 and 5, group 2 and 3, and group 4, 6, and 7. Sample specific diversity was also noted within bioinformatic methods on sample types of robogut-derived (M98) and chemostat-derived communities (M22) (Figure 14).

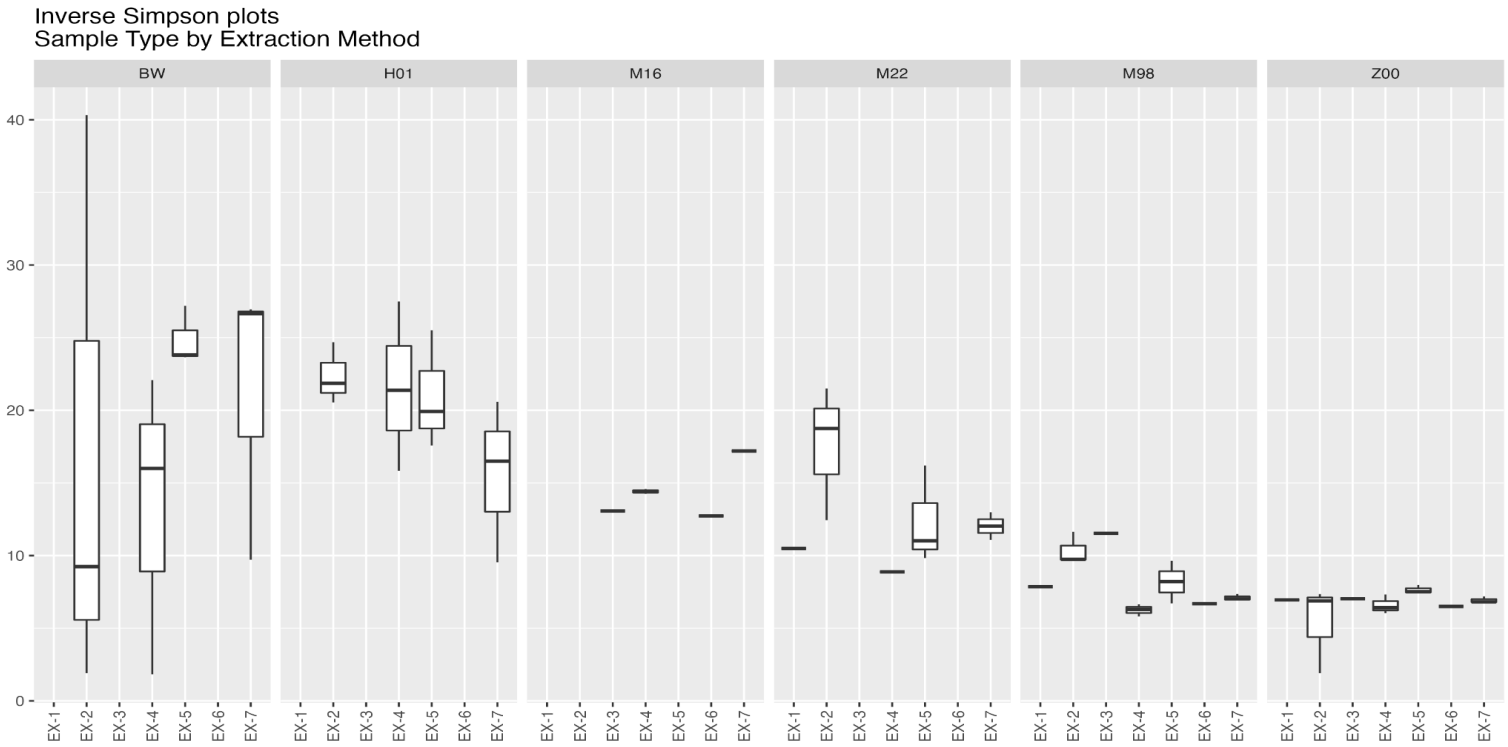

Figure 13. Inverse Simpson diversity estimates for sample type, stratified by extraction method, analyzed under one bioinformatic protocol (BINF-01).

Table 14. One way ANOVA tests performed to determine whether the difference of diversity means is significantly different (*), by sample type within an extraction method.

Sample Type	ANOVA p-value
BW	0.71
M98	0.01*
M16	0.08
H01	0.33
M22	0.30
Z00	0.74

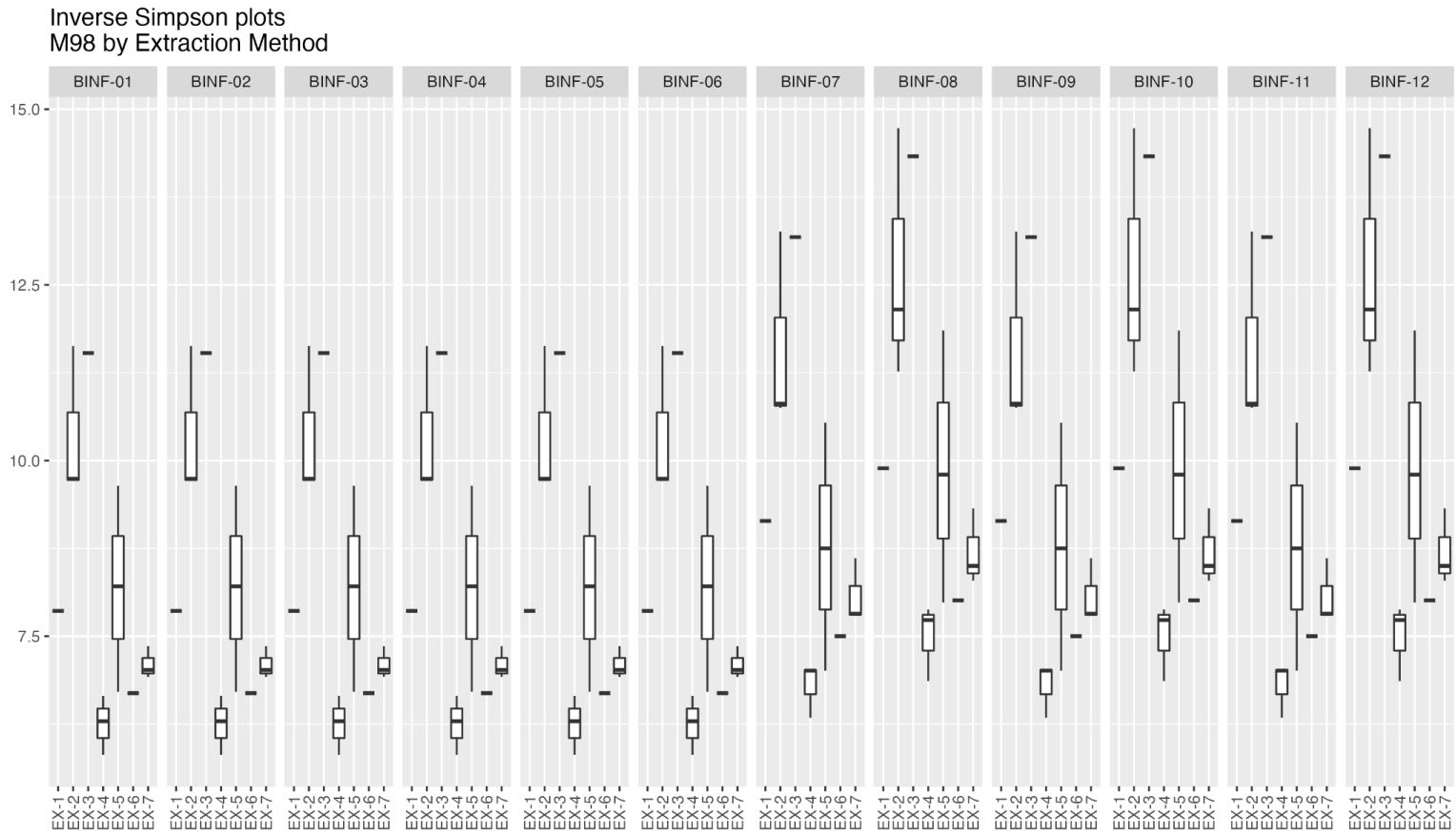

Figure 14. Inverse Simpson diversity estimates for robogut-derived (M98) sample, stratified by bioinformatic method and extraction method.

Significant p-values were identified for these derived communities (M22, M98), although not all complex communities (H01) were identified as significant (Table 15). This highlights the complicated relationship between the handling of bioinformatic and extraction methods, compounded by the complexity of community sample type. Reviewing the p-values associated with the ANOVA tests, plotted at sample type for each bioinformatic method, the distribution can be reviewed (Figure 15). The significant effect of handling lab on Inverse Simpson diversity is varied by sample type, as the lowest complexity sample (Z00) had the least significance. Underlying the variation of alpha and beta diversity seen within extraction methods, is variation in relative abundance. One-way ANOVA tests were performed to determine significance differences between Phyla within an extraction method or extraction manufacturer, stratified by bioinformatic methods (Figure 16). Different Phyla did show varying significance between both stratification methods, which was consistent between extraction methods and companies, such as with Firmicutes.

Table 15. One way ANOVA tests performed to determine whether the difference of diversity means is significantly different (*), by sample type within a bioinformatic method.

BINF Group	M22 p-value	M98 p-value
1	0.30	0.01*
2	0.30	0.01*
3	0.30	0.01*
4	0.30	0.01*
5	0.30	0.01*
6	0.30	0.01*
7	0.07*	0.01*
8	0.04*	0.01*
9	0.07*	0.01*
10	0.04*	0.01*
11	0.07*	0.01*
12	0.04*	0.01*

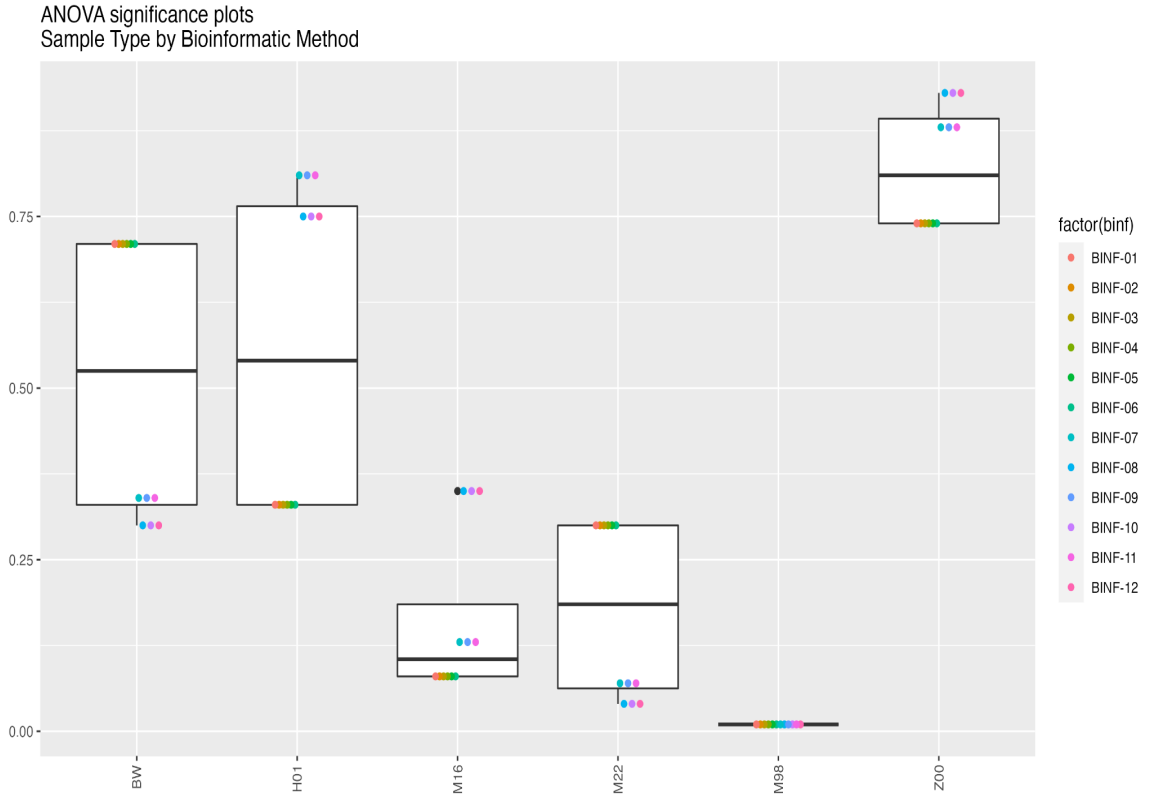

Figure 15. Distribution of p-values by bioinformatic method (color), testing for the significance of extraction method on inverse Simpson diversity, stratified by sample type.

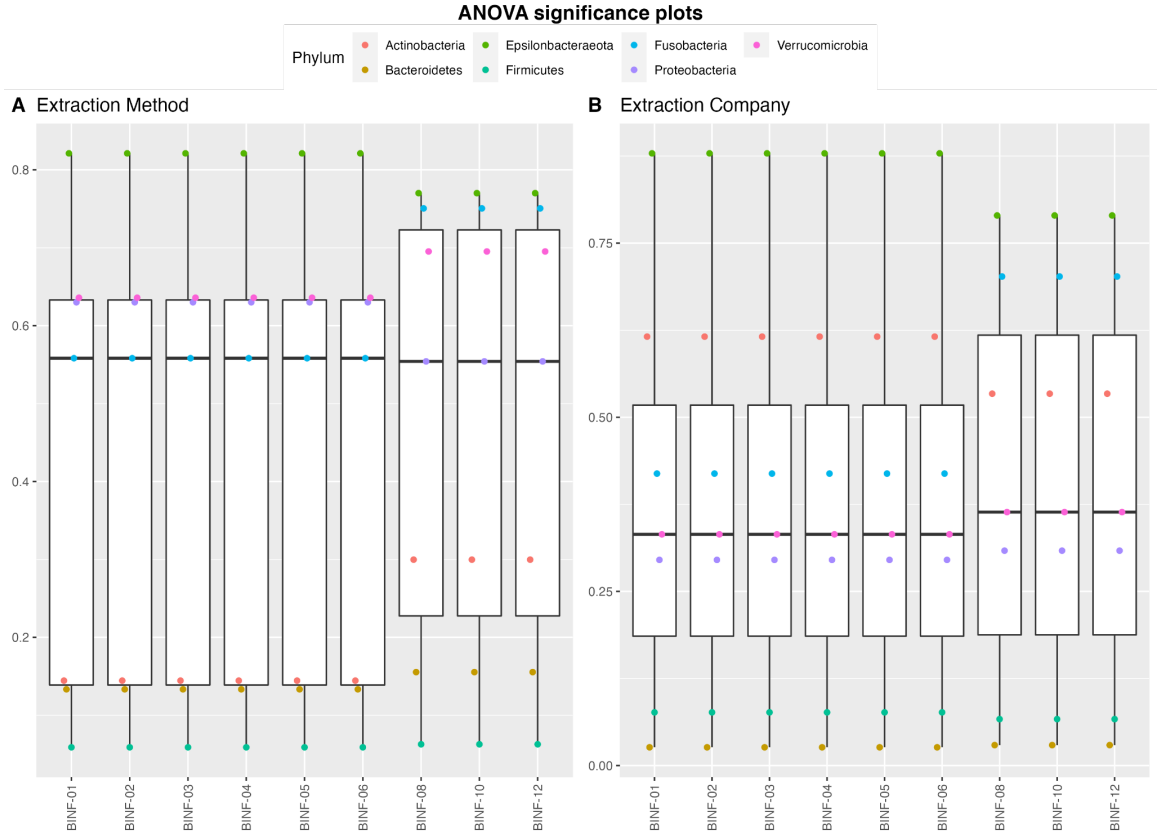

Figure 16. ANOVA significance plots, comparing the relative abundance of Phyla between extraction methods (A) or extraction companies (B), within a bioinformatic method.

Controls were assessed, including positive sequencing controls, positive extraction controls, and negative extraction controls. Each bioinformatic method included 5 positive artificial sequencing communities, 1 negative extraction control, and 1 positive artificial extraction community. Extraction method contributed significantly to the negative extraction controls, with variation between abundance levels observed within the method, and between methods. Common Phyla were observed, such as *Firmicutes*, although percent composition did vary (Figure 17A). The positive extraction and sequencing communities contained anywhere between 10 and 20 species (table old), whereas the negative controls

were not expected to have any communities produce sequencing results. Bioinformatic methods contributed to positive control abundance most significantly in two groups: ASV methods (BINF-01 through BINF-06) and OTU's annotated with Silva reference database as compared to OTU's annotated with GreenGenes reference database (Figure 17B).

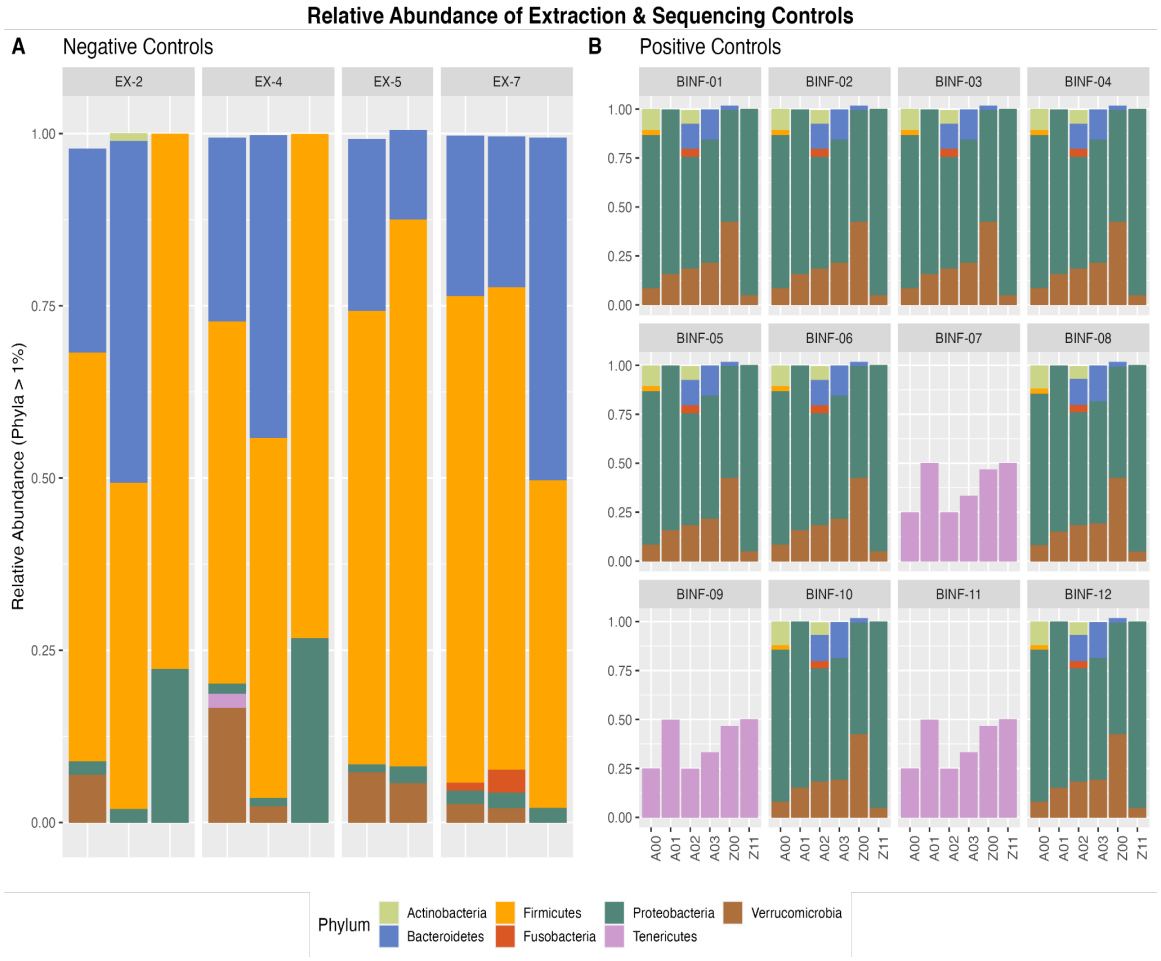

Figure 17. Relative abundance of negative extraction controls (A) and positive extraction and sequencing controls (B) at the Phylum level.

Bray-Curtis dissimilarity plots expanded these differences, with the variation between extraction methods, stratified by sample type and bioinformatic method had some

differences between bioinformatic methods BINF-01 to BINF-06 and BINF-07 to BINF-12 (Figure 18). Evaluation of the reproducibility of these results was performed by reviewing the Bray-Curtis dissimilarity differences between positive extraction control (Z00) replicates, stratified by extraction method and bioinformatics method (Figure 19). Some extraction methods (EX-2) showed little variation between bioinformatic methods, whereas other extraction methods (EX-7) showed significant differences between ASV and OTU generation. This was also reflected in the variation in rarefaction curves, with low depth observed in all extraction methods stratified by sample type, and in all sample, types stratified by bioinformatic methods BINF-04 to BINF-09 (Figure 20).

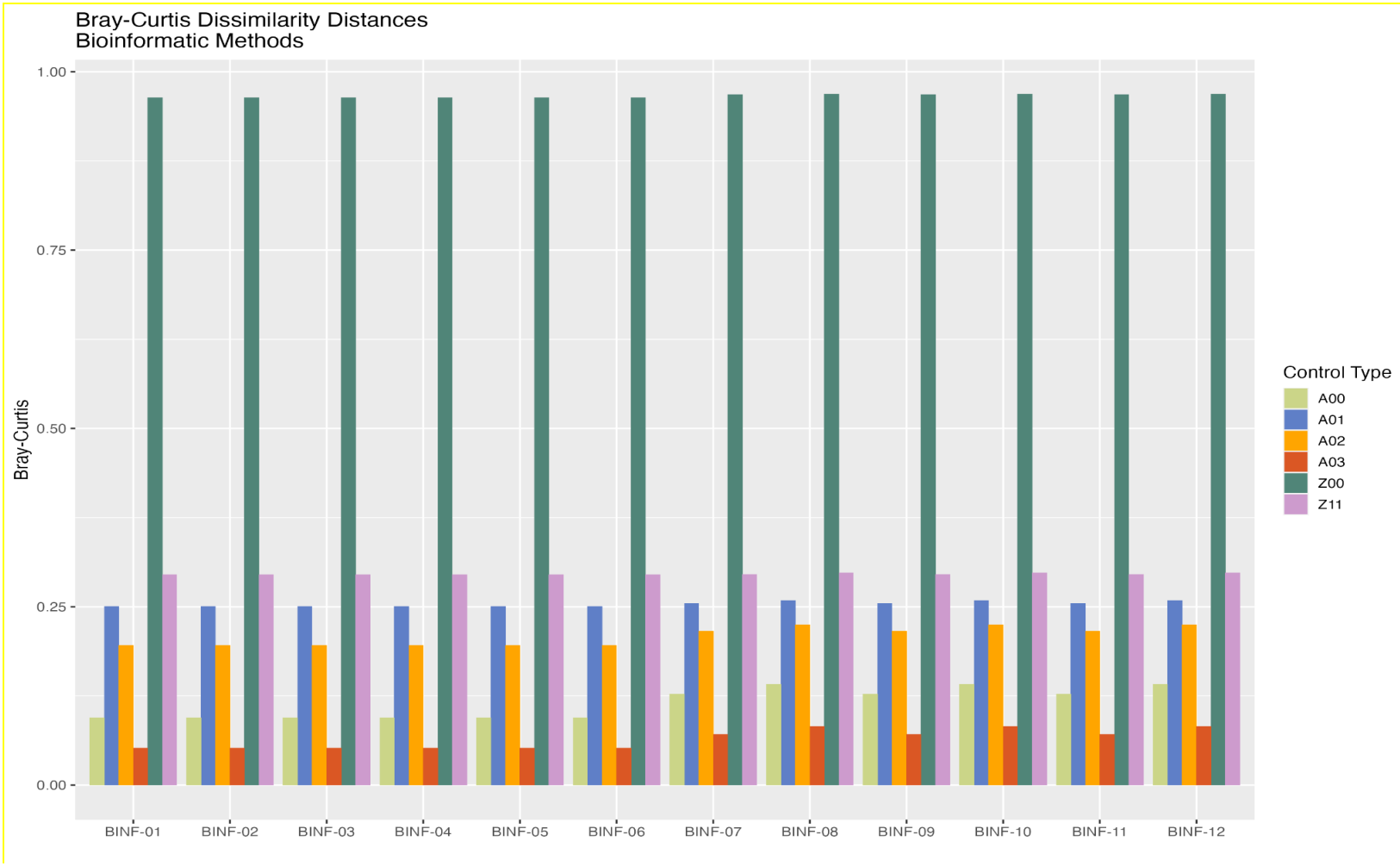

Figure 18. Bray-Curtis dissimilarity matrix by bioinformatic method, stratified by control type.

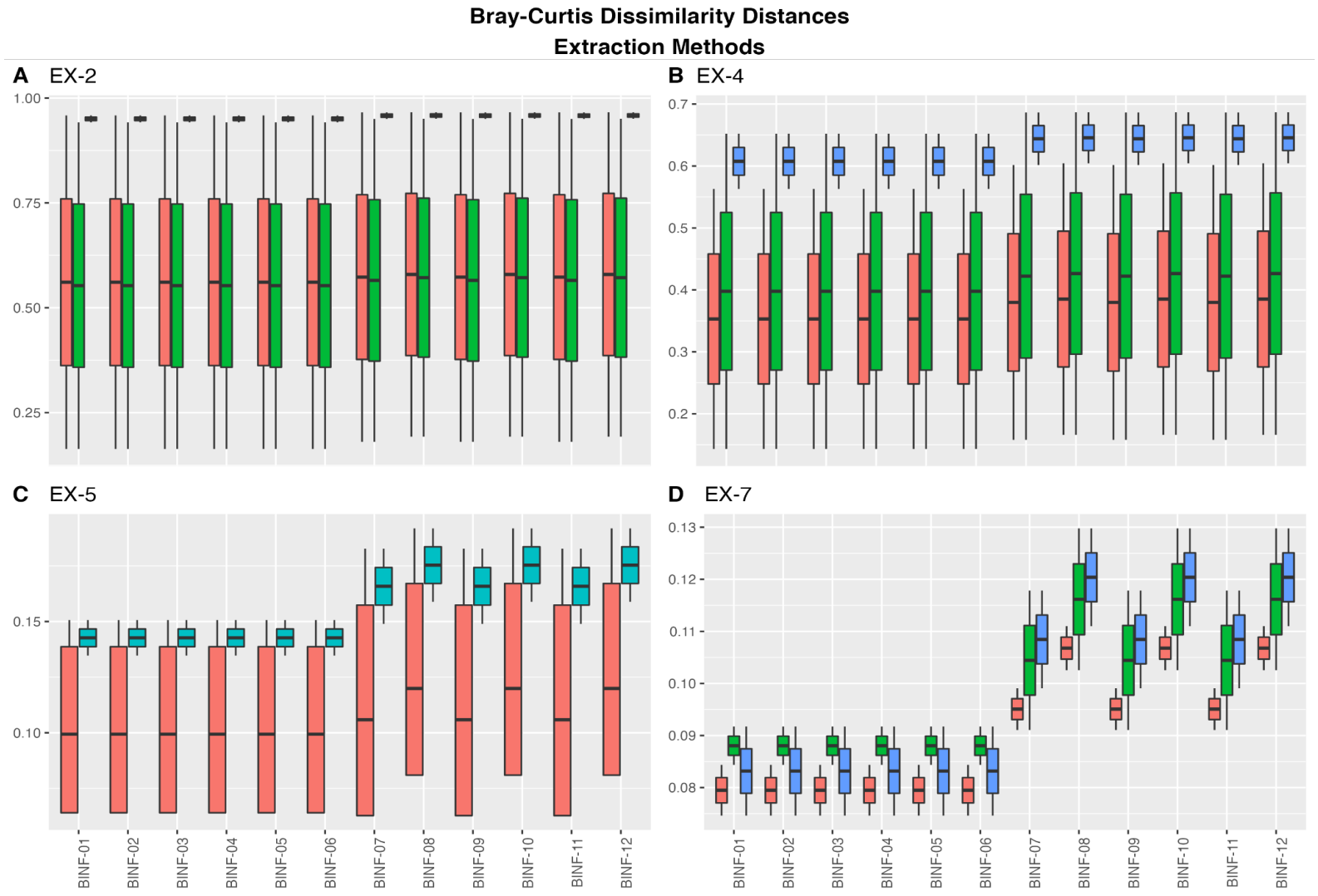

Figure 19. Bray-Curtis dissimilarity matrix of replicate extraction positive control (Z00) stratified by extraction method and bioinformatic method.

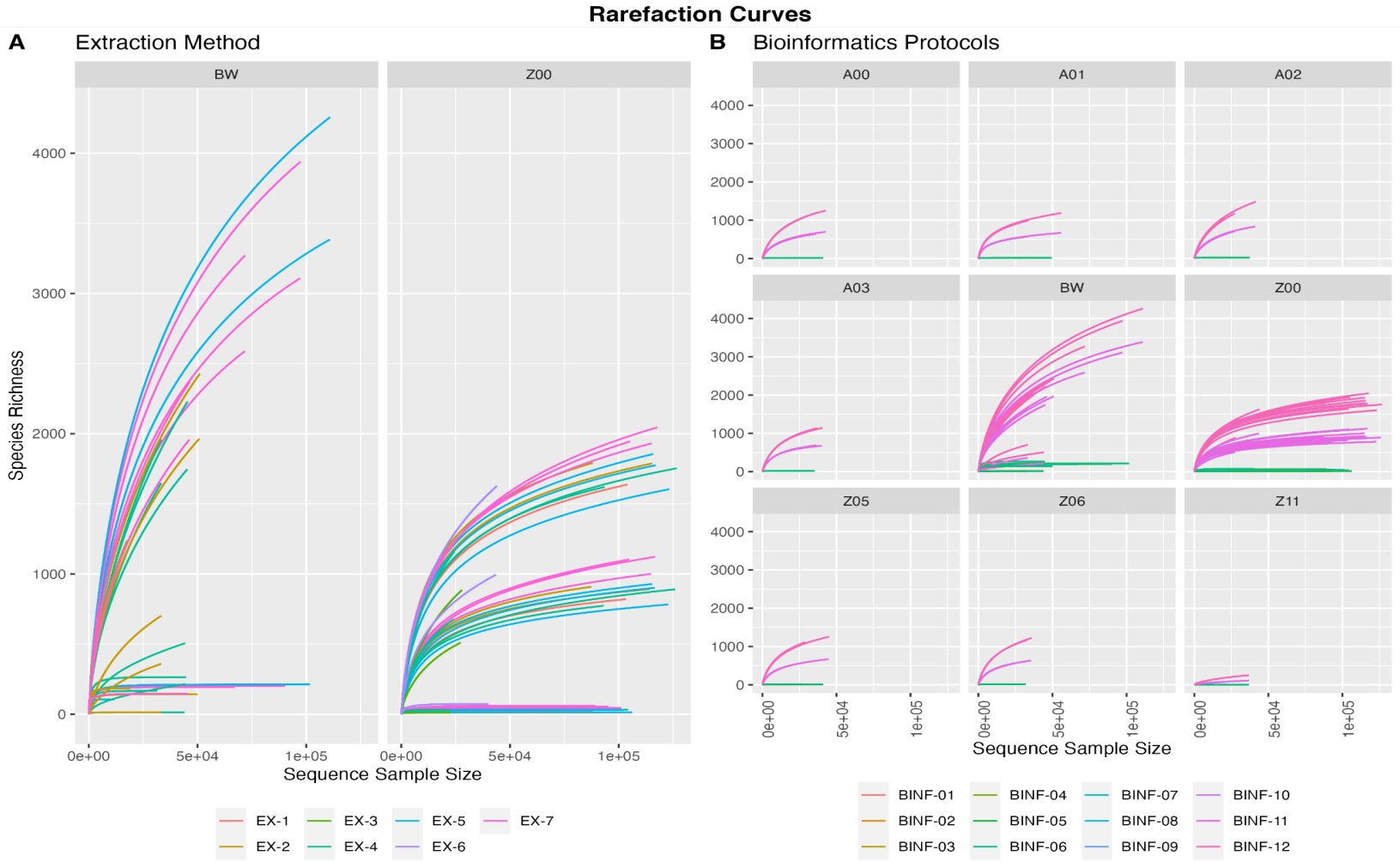

Figure 20. Rarefaction curves for the mean OTU's by rarefaction depth, stratified by extraction method and bioinformatic method. Both methods include both negative and positive controls, however, extractions methods only include extraction controls, whereas bioinformatic methods include both extraction and sequencing controls.

Accuracy of each control was considered next. Each control was assessed to the expected genera first, using a present/absence scoring to determine the following values: true positives, false positives, false negatives, TAR scores, TDR scores, and F1 scores. Differences were noted in each of these values, with A03 having the highest true positive and false negative count, however, this must be weighed by the fact that this control also had the highest (18) number of expected genera (Figure 21). TAR scores did not show significant variation in the mean of values but did show variation in the individual sample values. The weighted average of TAR and TDR scores, the F1 score, also showed variations, with Z05 (8 expected genera) having the highest mean F1-score regardless of the bioinformatic method used measure (Figure 22). Some variation is noted within extraction method as well when reviewing the extraction positive control (Z00), with EX-2 and EX-4 showing lower values than other methods, again illustrating the impact of extraction method on extracted material over bioinformatic method.

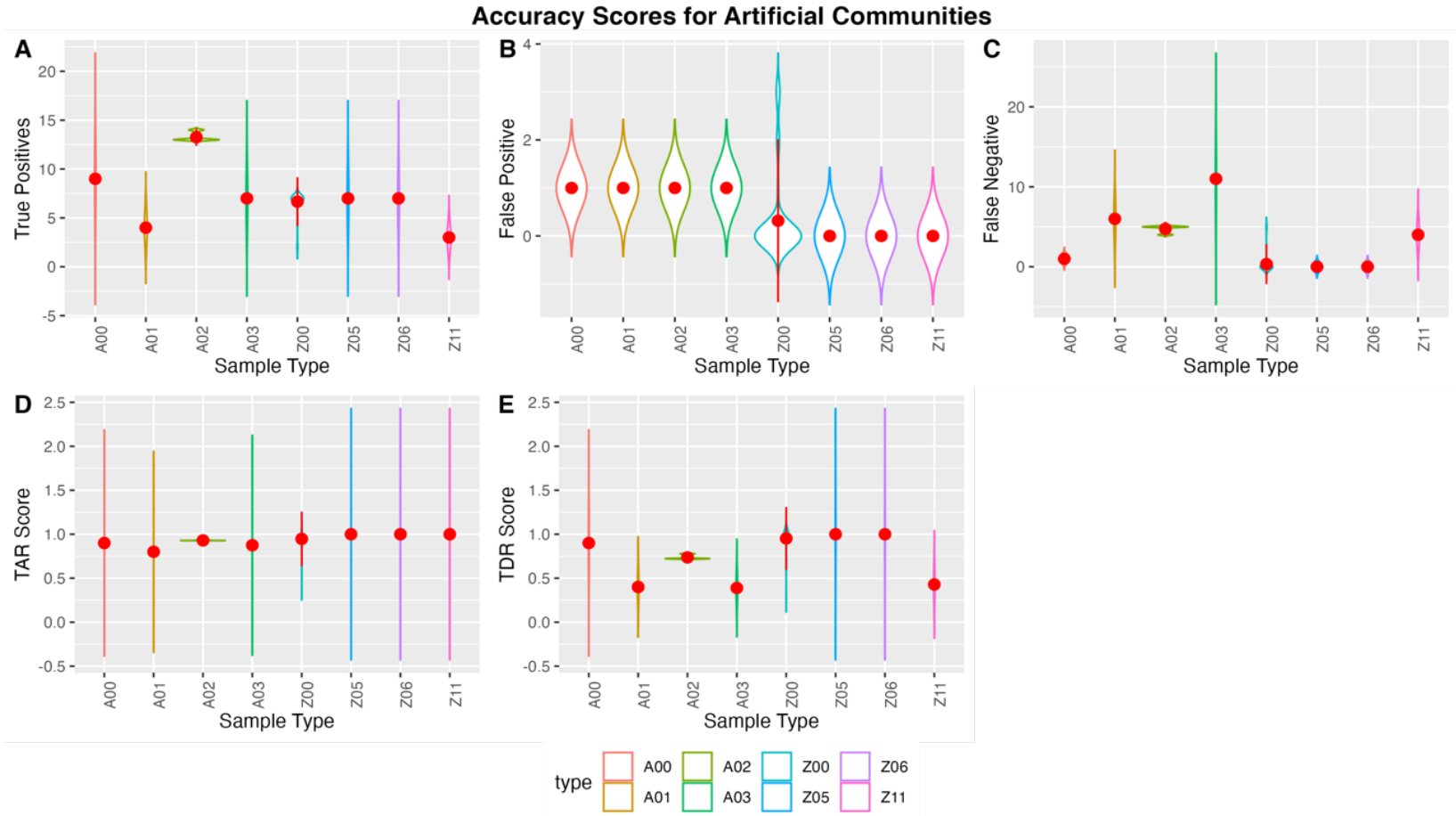

Figure 21. Individual counts of false negative, false positive, and true positive values of genera, as compared to the expected positive controls. Violin plots show distribution of controls averaged by all methods, with mean values indicated with a red dot.

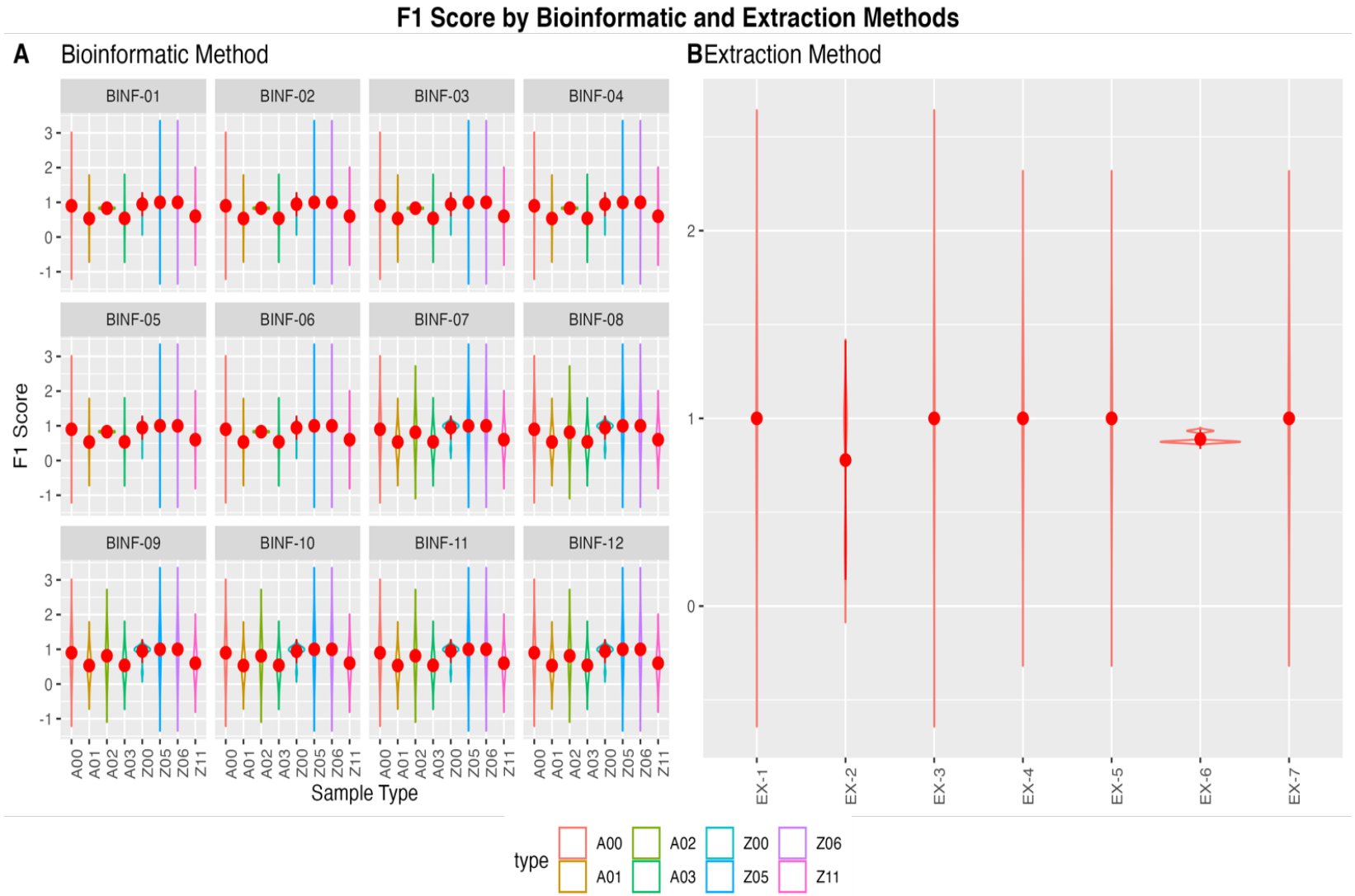

Figure 22. F-Measure (F1) stratified by bioinformatic method (A) for sequencing artificial communities and by extraction method (B) for extraction artificial communities. Violin plots show distribution of controls averaged by method, with mean values indicated with a red dot.

Bray-Curtis dissimilarity distances were calculated to determine the effects of bioinformatic and extraction method on sample type. Differences were noted by sample type, with some sequencing artificial communities (A00-A03, Z05) performing worse than others (Z06, Z11) (Figure 23). When stratifying by both extraction and bioinformatic method for the artificial extraction control, no difference is noted between the bioinformatic method, however, differences are noted within the extraction methods (Figure 24). This illustrates the importance of extraction method on extracted samples, compounded by bioinformatic method on sequenced-only samples.

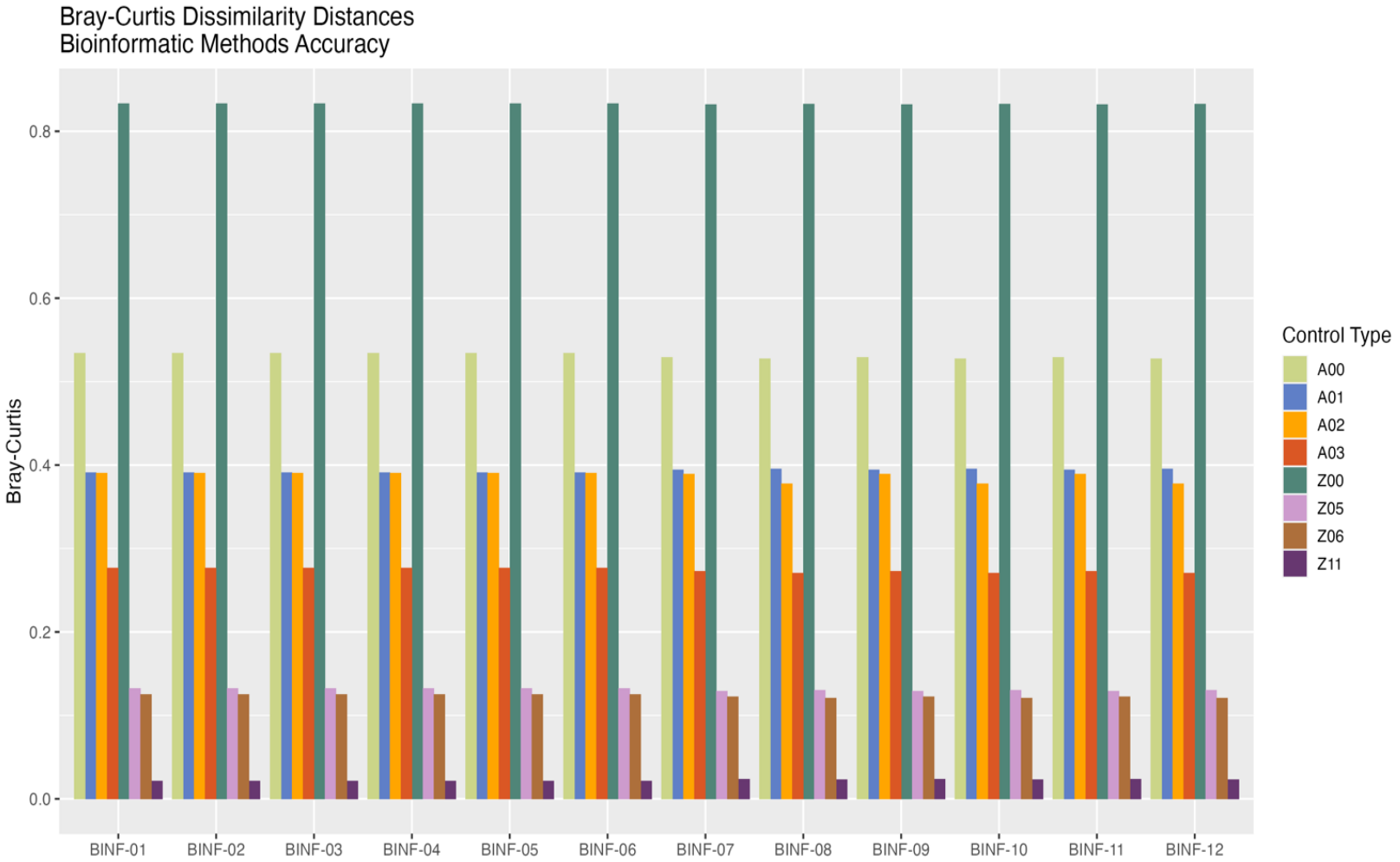

Figure 23. Bray-Curtis dissimilarity distances averaged by extraction method, stratified by bioinformatic method and sample type, for positive controls.

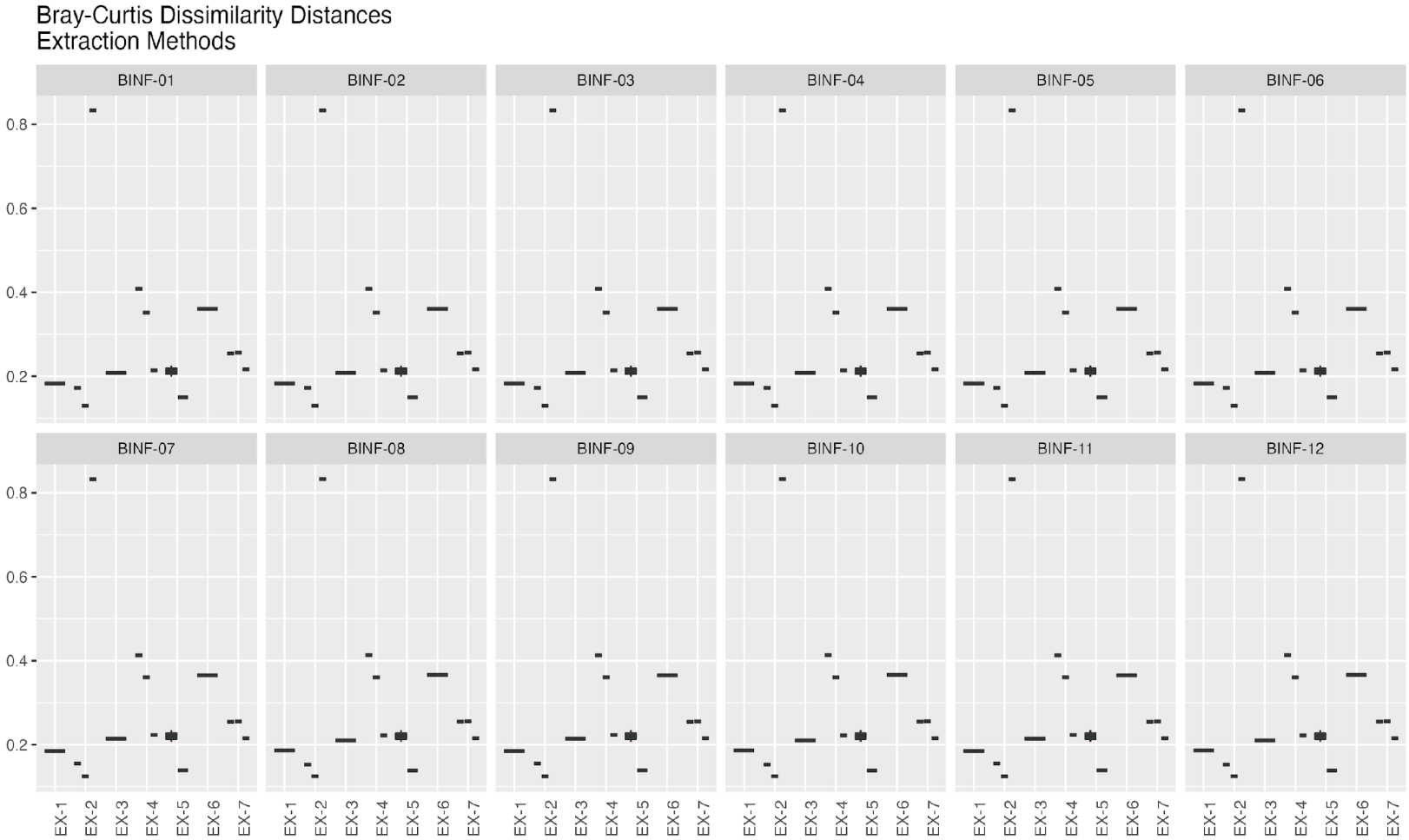

Figure 24. Bray-Curtis dissimilarity distance of extraction artificial community (Z00) stratified by bioinformatic and extraction method.

To assess the performance of relative abundance levels for each control, scatter plots were generated for each control, and R^2 values assessed (Figure 25). A00 was not included in these plots, as this community was evenly distributed, and therefore did not have a linear correlation. Z11 had the highest performance, however, this was reliant on the uneven, logarithmic distribution of abundances. For example, the expected value of *listeria* was 96%, whereas the expected value was 94.3%. While the remaining seven genera were inaccurate, because of this uneven distribution, the control still had a high R value. Of the remaining five controls, four (A01, A03, Z05, and Z06) had significant (<0.05) R values, indicating a high degree of correlation to the expected relative abundance values. While A02 outperformed the other controls in terms of presence and absence, it did not perform best in terms of the expected observed relative abundance levels. The ZymoBiomics controls were also not in agreement with the previous metrics, as the Z06 control performed better in terms of the correlation to the relative abundance, than did the Z05 controls.

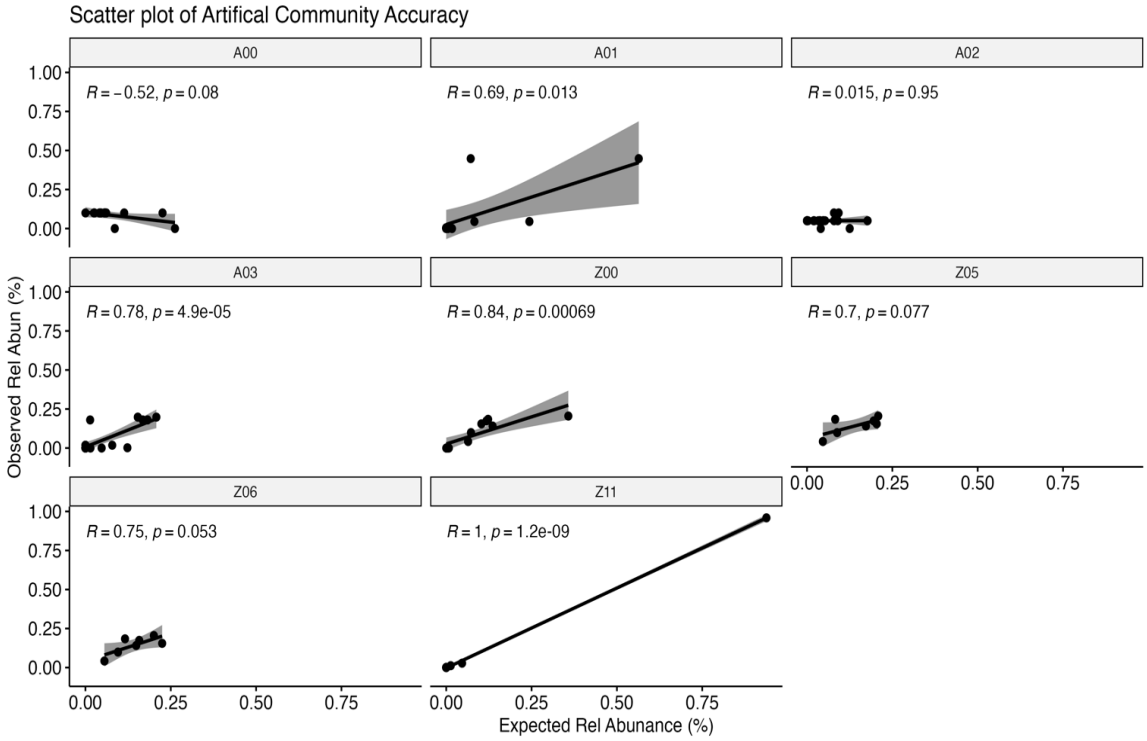

Figure 25. Scatter plots of the artificial communities, averaged across all bioinformatic and extraction methods.

3.4 Discussion

There are a considerable number of variables within any microbiome workflow, beginning with the extraction methods and ending with the bioinformatic parameters set, that must be carefully chosen to provide the most accurate profile. These parameters are also important when choosing which controls to include at the extraction and sequencing levels, as they have been shown to vary in performance. If controls will be used to assess the performance of human samples, for example, complex communities must be included. While this study attempted to address most of these questions, there were limitations to the study design and a need for future work in both development and as clinical projects are being implemented.

The quality assessment performed illustrated that reducing the depth of coverage of samples, while significantly reducing the number of sequencing reads, did not cause significant differences between sample types. This is important information as researchers look to increase sample size, while working with strict budgetary constraints. It was also evident that even with this reduction, rarefaction levels could be set to a high value of 20,000 reads, while still being inclusive of most samples. As has been previously reported, rarefaction levels should be reviewed for each project to determine this exact threshold, however, these results are encouraging to maintain a significant number of samples and sequence information, even if samples have varying input concentrations.

It was determined that there was significant influence by both bioinformatic and extraction methodology. First reviewing alpha diversity metrics, differences were noted between each extraction method. Bioinformatic methods however, appeared to group by cluster/OTU method, and by reference database. When exploring beta-diversity between these two sets of variables this was only further highlighted, with bioinformatic clustering methods being identical, and grouping methods by taxonomic reference being identical. When comparing the Pearson correlation values of bioinformatic and extraction methods, it was seen that extraction method more significantly impacted the overall profile generated. This is an important finding, as it points to the importance of study design, and in the cross-comparison compatibility of study's not extracted utilizing the same extraction methodology.

The bioinformatic assessment highlighted not only the number choices one can make when assessing microbiome data, but how these choices impact the resulting profile.

Significant differences were not noted between the clustering/grouping methods, specifically with clustering methods remaining relatively stable regardless of taxonomic method and grouping methods differentiating by the reference database used. The SILVA database was shown to outperform the GreenGenes database, in all metrics, as several reads were unable to be identified at the phylum level within controls. Due to the biological representation of ASV's, DADA2 was used as the clustering method, and due to the improved reproducibility of sci-kit, the highest performing bioinformatic variables were the SILVA reference database, with DADA2 as the clustering method, and sci-kit as the taxonomic assignment method.

The sequencing assessment performed had several insights, consistent with the bioinformatic assessment. First, utilizing multiple metrics beyond the accuracy and precision of controls is critical to drive project control inclusion became clear. Moreover, it is also evident that not all commercially available sequencing controls perform equally, whether due to their manufacturing, community composition, or the availability of their referenced sequences in the databases examined. This assessment highlighted the strength of the ZymoBiomics generated controls, although they were low in complexity. It highlighted the need to balance complex controls such s though from the ATCC with precision and accuracy, particularly those that were evenly distributed. Researchers should utilize these controls in groups, when designing pipelines, to have the largest number of species, in attempts to replicate the diversity of the target human sample. Once the pipeline has been optimized, a smaller subset of these controls should be included on each sequencing run, thereby enabling quality control to be monitored throughout a project. This

approach balances both the complexity necessary for pipeline verification, and cost of including multiple controls in a sequencing run.

The extraction assessment presented several insights, many in agreement with current research. The first, was the variation in extraction performance, as measured by the number of samples passing QC thresholds, and the number of extraction blanks failing to pass QC thresholds. Both values indicate the intrinsic impact that processing methodology has on sample performance, and how some methods are more prone to contamination due to the number of transfers, homogenization format, and reagent addition. The community profiles generated most resembled an average of the most complex human samples, rather than any one individual sample. This likely indicates that the cross-contamination is occurring during either extraction or sequencing processing, where high-yield samples are mixed with negative samples and then amplified. When researchers are looking to implement a method into their pipelines, these are important considerations, particularly when considering time-constraints, limited sample material, and low-biomass samples.

Congruent with sequencing results, the extraction assessment also illustrated varying performance of extraction controls, on average, as well as by method. A trade-off was also noted in assessing the accuracy and precision of these controls – lower complexity was found to have better accuracy and precision. Despite having lower results, the more complex samples there were not significant differences noted in Bray-Curtis distances, when compared to the expected abundance values. This again illustrates that while the controls may not be used as an absolute control, they can be implemented into workflows to ensure the reproducibility of pipelines and to identify problems at the extraction level. It

was also shown that the commercially prepared communities performed better than the alternatively prepared communities, likely due to the precision that is implemented during commercial manufacturing.

In addition to the controls, human samples illustrated significant differences between methodologies. Alpha diversity metrics (richness, Simpson, and Shannon), for example, showed significant differences between the average values of methods as well as the distribution of values by method. Similarly, clustering patterns of controls and fresh-frozen human samples differed by method, when reviewing beta-diversity PCoA plots. The human samples also showed less intra-sample-type variation in the more complex human and robogut samples than the artificial colonies, indicating that variation is method is more susceptible to perturbations when relatively few, or low-level communities are present.

These lead to the overall conclusions of this study, and recommendations to be used in the second and third aim. Clustering sequencing reads to ASV's using DADA2 will be implemented with the taxonomic method scikit-learn. Reference database Silva will be used as the reference database, to ensure a greater assignment of taxonomy at lower levels of phylogeny. Extraction methods will not be able to be selected, as samples had been pre-extracted prior to analysis, however, within aim 3, only samples extracted within the same methodology will be compared. The use of statistical methods and predictive modeling tools will be added to the analytical workflow to explore functional implications within the data, not explored in this technical exploration.

A significant limitation found in this assessment was the complexity of the controls, despite their advantages. Although six sequencing artificial community controls from two

manufacturers representing 20 different species, and one extraction artificial community controls from one manufacturer representing 8 species, were used, this still is not representative of the complexity found in human samples. Currently, this is a tradeoff, for the ability to assess the accuracy of a sample with known expected values is an important metric for quality control. Improving this limitation would include additional sequencing controls that could increase the total number of species and varying the type of species to ensure a more representative profile of typical human genera. Commercially available controls that are more representative of human samples would strongly increase the efficacy of their use, and likely lead to improved bioinformatic pipelines.

Additional limitations include the use of only one human donor sample. Future studies should include multiple donors to determine the impact that extraction might have on unique individuals, particularly those with outlying microbiomes. Varying the age, sex, and health status of these donors will increase the ability to assess the robustness of any method. While not limited to this project, the constant evolution of publicly available extraction methodologies is also problematic to microbiome research. As this study illustrated, it is imperative that extraction methods be standardized and consistently utilized within a single methodology. If these methods are being replaced by newer methods, even if improved, previously resulted data may not be comparable. Finally, using 16s rRNA sequencing alone, rather than incorporating shotgun sequencing approaches limits the type of studies that can be assessed with these methods. A more complete study, with both amplicon-based and shotgun sequencing data would provide a more complete picture of microbiome processing, consistent with current trends and study designs.

4. ENVIRONMENTAL APPLICATIONS

4.1 Background

One of the foremost global environmental concerns of our generation is the usage of plastics in everyday life. Having tripled over the last 25 years to nearly 350 million tons a year, plastic production is exponentially growing at alarming rates[82]. Problems with waste management, including limited space in landfills, and low recycling rates, have only exacerbated these issues (Jeftic et al., 2009). In addition, with the discovery of microplastics and nano-plastics detected in air, rain, tap water, beverages, and food, plastics are a complex and imminent threat to our planet that must be addressed with innovative solutions84.

The impact of this usage is widespread, as based on published literature, plastics are among the most readily found debris in oceanic environments (Eriksen et al., 2014; Thompson, 2006). The global sea surface is estimated to be covered by approximately .25 trillion plastic particles, weighing over 250,000 tons. It has been estimated that nearly 10% of plastic debris finds its way to oceanic waters and has drawn international attention as early as 2006 in scientific conferences abroad (Bourne et al., 2016; Bräger, 2006). As coral microbiome research has expanded to better understand the interactions of microhabitats and the overall coral health, these microplastics may be significantly contributing to (Gall & Thompson, 2015).

Whether entering through intentional placement or through sewerage systems, the properties that make plastic desirable to human use, namely the durability and buoyancy,

are causing significant negative impacts (Kiessling et al., 2015). While the durability of plastics is one of their strengths in commercial use, it is also a detrimental feature that makes them long-lasting and resistant to degradation (Bräger, 2006; Kiessling et al., 2015). The lightweight nature of most plastics is another positive feature of usage; however, the characteristic leads to plastics being buoyant. When plastic material enters a water system, for example then, it can travel beyond its initial entry point. This movement is dangerous for the animals who may interact with the plastics and who may be subject to entanglement, suffocation, and debilitation and because it can serve as a transport for invasive species that would not otherwise be possible (Brennecke et al., 2016). It is not only dangerous transportation, but the absorption of heavy metals was shown possible in plastics, presenting an additional concern in consumption (de Stephanis et al., 2013).

Consumption of plastics by marine life has also been shown to be devastating. A large-scale review of the impact on marine life illustrated the urgency to address this threat – nearly 690 species encountered marine debris, with 92% explicitly being plastic, and 10% of these species have ingested some form of microplastics. These effects are seen widely between animals, with one study of 24 Caretta post-hatchling loggerhead turtles dying after eating anthropogenic debris, 9% of which were plastic. Another study reviewing the death of sperm whales indicated the cause of death to be gastric rupture following impaction with debris (Murphy et al., 2016; Ryan et al., 2016; Turner, 2016). Ingestion of these microplastics also impacts the physical damage they may cause due to their chemical absorption. Studies have found that plastics may serve as a transfer vector within the host, carrying toxic pollutants from either the manufacturing process or the

environment it interacted with (Murphy et al., 2016). The impact that these toxins may have on the marine animals that then consume them could be significant for their health and the humans that subsequently consume them.

While wastewater treatment plants attempt to reduce the concentration of microplastics, an estimated 65 million microplastics are still found in daily water sources (Rochman et al., 2015). This is not only impactful on humans who use this source for consumption but also for aquatic habitats where this water is dumped, with estimates of approximately 8 trillion microbeads entering these habitats daily. Just as with marine life, the negative consequences of the ingestion of microplastics by humans must be addressed. Microplastics have been reported in several types of seafood, including mussel and seabass, with levels of polyethylene reported up to 48 hours after ingestion (Browne et al., 2008; Mazurais et al., 2015). These findings are not limited to sea animals - honey, German beer, and even bottled water have been cited with some levels of microplastic (Liebezeit & Liebezeit, 2013, 2014; Mason et al., 2018). It is hypothesized that high levels of exposure could lead to embolization of small vessels, tissue damage, and fibrosis (Lundqvist et al., 2008). Nanoparticles maybe even more dangerous, with toxicity potentially affecting the central nervous system at high levels (Waring et al., 2018).

Response to this growing problem has been seen locally and internationally, with varying success. National movements to address plastic bags and reduce microbeads in cosmetics led to several pieces of legislation within the United States and Canada, including the Microbead-Free Waters Act of 2015 (Pallone, 2015; The Nicholas Institute for Environmental Policy Solutions, n.d.). The United Nations Environment Assembly

(UNEA) has several resolutions published addressing these plastics and marine impacts, but with limited oversight, significant impacts have not been achieved (Solutions, n.d.). The Group of Seven Summit (including Canada, France, Germany, Italy, Japan, the United Kingdom, and the United States) also outlined specific reduction measures and presented solutions to improve the current ecological imbalance entitled the G7 Ocean Plastics Charter with five members (excluding the United States and Japan) signing (Canada, n.d.; Niaounakis, 2017). These measures included making all plastics recyclable by 2030, reducing single-use plastics, promoting the use of recycled plastics, and innovating sustainable, long-lasting technologies (Niaounakis, 2017). Other focuses vary from cleanup programs for the current plastic waste to treatment and recycling programs to reduce plastic usage (Krueger et al., 2015). The complexity of this problem makes a single solution improbable. Instead, it means that multiple solutions will be required to address different facets of the problem if we are to see long-term and sustainable improvements.

The reduction of Polystyrene has received particular interest due to its increasing usage and resistance to biodegradation. The potential for bacteria or fungi to aid in this degradation has elicited several studies, some of which indicated that while bacterial isolates are capable of degradation, they only do so with low efficacy (Y. Yang et al., 2020). The Pseudomonas strain, for example, was shown to involve the degradation of low-molecular-weight PE through its alkane hydroxylase gene alkB. Despite this promising finding, the consumption rate varied considerably (4.9-28.6% of the carbon) after 80 days and was only applied to low-molecular-weight polyethylene. Research searching for ways to address this plastic-type has been an essential focus of environmental cleanup efforts.

Scientists were rightfully hopeful when research showed that the larvae of Tenebrio molitor were not only able to digest Polystyrene to CO2 and other compounds of low molecular weight but readily did so (Alves et al., 2016; Brandon et al., 2018; Y. Yang et al., 2015a, 2015b). Mealworms are omnivorous species, and much has been known regarding their standard diet (bran) and related microbiome, with the anterior gut dominated by the *Bacillaceae* family and the poster gut representing a diverse species. Reports of this PE degradation ability have been noted in other insect larvae, including the Indian meal moths and wax moths, which may indicate broader implications of the insect gut microbiome. Follow-up studies illustrated that their ability to digest this material was likely to be related to the microbiome found in the digestive tracts of the mealworms, both the cleavage of long-chain PS molecules and formation of low molecular weight metabolites were formed in the gut of the mealworms (Y. Yang et al., 2015a). In addition, when mealworms were given gentamicin, an effective inhibitor of the gut microbiome, the mealworms were unable to depolymerize PS (Y. Yang et al., 2015b). While mealworms with gut microbiomes intact were able to consume PS with a rate of approximately half their gut in 12-15 hours, significantly faster than the bacterial isolates could do alone, research into the impact of dietary changes has promising results (Ercolini & Fogliano, 2018; Y. Wang & Zhang, 2015; Y. Yang et al., 2015a).

Studies have shown that mealworms fed various diets that ranged in carbohydrate to sugar content showed significant variations in lipid, protein, fiber, and starch concentration after 30 days. The correlation of dietary changes with microbiome gut changes in humans has led to the plausible conclusion that a shift in the diet of mealworms

may influence the gut microbiota, and significantly influence the consumption and digestion of PE (Y. Wang & Zhang, 2015). When co-fed on a PS and bran diet, research showed that the rate of PS degradation almost doubled, with the anterior gut being dominated by anaerobes Lactococcus and Pantoea. While different regions of the gut exhibited differences, none were explicitly identified as responsible for the overall consumption of PS. This leaves several questions to be explored, with significant implications for PS and environmental sustainability.

4.2 Materials & Methods

Tenebrio molitor Linnaeus mealworms were purchased through a pet supply company (Exotic Nutrition, n.d.; Fisher Scientific, n.d.). Mealworms were subjected to an initial feeding stage before introduction to Polystyrene (Figure 26). Mealworms (N=14) were housed in two cages and were fed a rice bran diet for five days. Mealworms were then divided into two groups, where group 1 was continued on rice bran (N=9), and group 2 was changed to apple slices (N=5) for ten additional days. After this initial period, polystyrene (Styrofoam) cups were introduced to each population (referred to as time point baseline). Collections were then taken from the mealworm gut (rice bran N=6, apple slices N=4) at four subsequent time points (Day 5, Day 8, Day 12), indicating the length of time Styrofoam diet. Additional collections were obtained from feces (rice bran N=3, apple slices N=1) at two-time points (baseline and Day 12) for comparison. All collections were taken in triplicate, ensuring the reliability of the results.

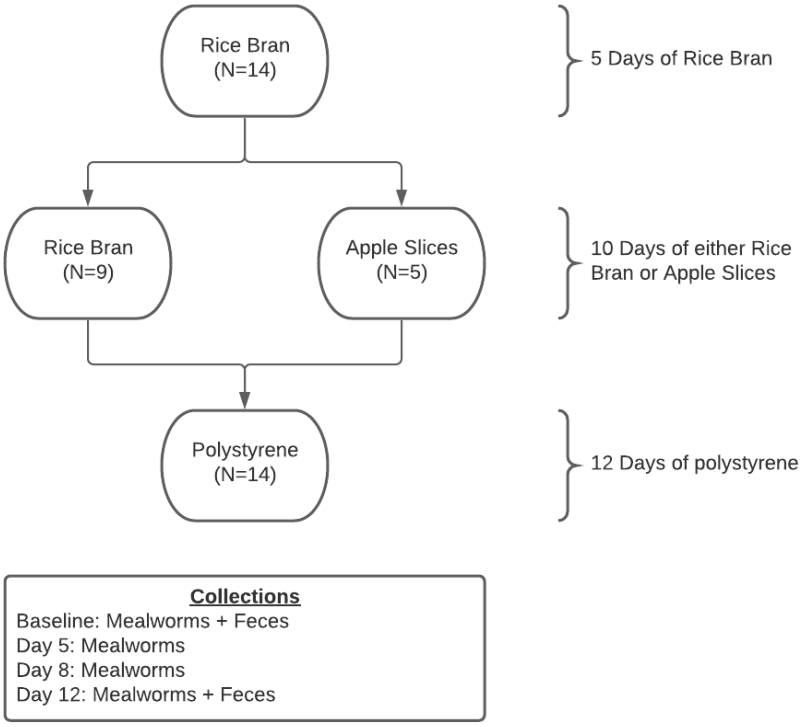

Figure 26. Mealworms were first subjected to an introductory rice bran diet (5 days) before being split into continued rice bran, or apple slices, groups (10 days). After this period, all mealworms were given Polystyrene, and samples were collected from either the mealworm gut or a fecal sample at four-time points (Baseline, Day 5, Day 8, Day 12).

Mealworm samples and fecal material were collected and frozen at -80*C until all collections had been performed. The material was extracted using the FastDNA Spin kit from MP Biomedical Inc, per manufacturer instructions. Next-generation sequencing was performed, isolating the 16S rRNA gene subunit in the V4 hypervariable region. Samples were prepared in duplicate using Multi-tag Sequencing, barcoded with varied forward and reverse sequences utilizing universal 16s rRNA gene primers. Barcoding strategies followed previously published work to ensure that distortion of community abundance was not a factor (Gotelli & Colwell, 2001). Pooling was performed (up to 48 samples), and 16S

sequencing was conducted in two trials using an Ion Torrent PGM. Samples were sequenced in duplicate or triplicate across the two sequencing runs.

Raw reads were demultiplexed using QIIME2 (v2019.1) software post-sequencing, following default parameters (Bolyen et al., 2019; Chill et al., 2020). A denoising technique, which removes and corrects reads before deduplicating similar sequences, was utilized next. For this, the second version of the Divisive Amplicon Denoising Algorithm (DADA2) was used to generate ASV's. Next, samples were automatically filtered due to the quality (Q) score, merging errors, and identification of chimeric reads. The Phred quality score measures the quality of identifying nucleotides, which relates logarithmically to the base-calling error probabilities (Illumina, 2011). Sequences that cannot be merged either because the sequences are too short and do not overlap or because the sequence ends do not align were also filtered, as were chimeric sequences identified. Finally, taxonomic classification was performed next, with the scikit-learn method (Pedregosa et al., 2011). This was achieved by training reference sequences at 99% similarity, using Silva's reference databases (release SILVA 132) (Quast et al., 2013).

Alpha metrics were reviewed to determine the overall distribution of diversity. The Simpson indexes are a diversity index, more sensitive to species evenness than other methods available (Willis, 2019). Simpson's Diversity Index represents the probability that two randomly chosen individuals belong to different species. Because it is the inverse measurement, the Simpson value indicates that the diversity index value increases as species richness and evenness increase. Beta diversity metrics include the use of Principal Coordinates Analysis (PCoA) which includes an eigenanalysis performed on the

abundance matrix derived from a given dataset. This matrix can be calculated through different measures; either quantitative (weighted UniFrac and Bray-Curtis) or qualitative (unweighted UniFrac and Binomial). Bray-Curtis dissimilarity was chosen because a matrix can be created to compare the degree of dissimilarity between the abundance of each species in a tested variable versus the expected abundance of that species. It can assess the distance, then, between these expected abundances and those observed through the processing, and all distances are compared to determine whether the distances are significant. Values are bound between 0 and 1, where 0 indicates that the two samples share the same species, whereas one suggests that they do not share any species. Bray-Curtis may also be illustrated with the largest Eigenvalue that accounts for the most significant variance lying on one axis. In contrast, the second greatest variance (or other chosen value) is placed on the second axis.

Multiple tests were considered to determine the correlation of each of these expected control values to their observed values. First, a permutational multivariate analysis of variance (PERMANOVA) test quantifies multivariate community-level differences between groups (Anderson, 2005). This PERMOVA test was performed, analyzing the variance using distance matrices of relative abundance tables. To determine if the distances between groups had any statistical significance after creating the Bray-Curtis distance matrices, p-values were evaluated. The Bonferroni correction was applied, as this was a multiple-comparison assessment.

Rarefaction usage in microbiome data has been controversial and was used for all but the differential analysis to help normalize the presence of rare OTU's or ASV's. Curves

are created that graphically represent the number of samples by the number of species or the sequencing depth by the number of samples, showing an exponential curve, with an asymptote. This asymptote represents the point of saturation, where no further taxa will be added, regardless of the increases in the number of reads included. These curves were created and assessed to determine the target sequencing depth to normalize the data, recognizing that samples with low-read counts would be removed. While this subsetting is often performed on alpha and beta diversity analysis, a comparative study illustrated the negative impact that rarefying samples had on differential analysis (McMurdie & Holmes, 2014). As such, all raw OTU counts were in differential analysis.

Taxonomic, functional prediction analysis is implemented to provide insights into the possible functional mechanisms utilized by the microbiome community identified. The Kyoto Encyclopedia of Genes and Genomes (KEGG) is a database of functions that can be mapped to genes, or in the case of microbiome research, taxonomic information generated from OTU's (Kanehisa Laboratories, n.d.). Tax4Fun, an open-source R package that predicts the functional capabilities of microbial communities using 16S rRNA datasets, was used to create KEGG pathways related to specified OTU's (Aßhauer et al., 2015). To visualize and run additional statistical measurements, R, an open-source statistical computing and graphics software program, was utilized with publicly available packages (R Core Team, 2014).

4.3 Results

Samples had an average number of 9,088 reads (min. 1,345, max. 41,515), with 1240 unique OTU's identified. Raw OTU counts were used, without rarefaction, due to

previous studies' bias when subsetting datasets before this type of analysis. The number of reads was stratified by sample type and showed some variation, with the mealworm samples had 1,000 more reads than the fecal samples (Table 16, Figure 27). An average number of reads stratified by timepoint showed more significant variation, with baseline samples having the lowest (~6215) and Day 8 samples having the highest (12,152) average number of reads (Table 16, Figure 27).

Table 16. An average number of reads by sample type.

Sample Type	N	reads	Standard deviation	Standard Error	Confidence interval
Feces	12	8,369	9624.216	2778.272	6114.935
Mealworm	29	9,386	8546.928	1587.125	3251.077

Table 17. The average number of reads by timepoint.

Timepoint	N	reads	Standard deviation	Standard Error	Confidence interval
Baseline	15	6,215	3119.371	805.4182	1727.45
Day05	6	7,592	4844.256	1977.6594	5083.735
Day08	5	13,152	15874.062	7099.0963	19710.251
Day12	15	11,205	10435.252	2694.3705	5778.85

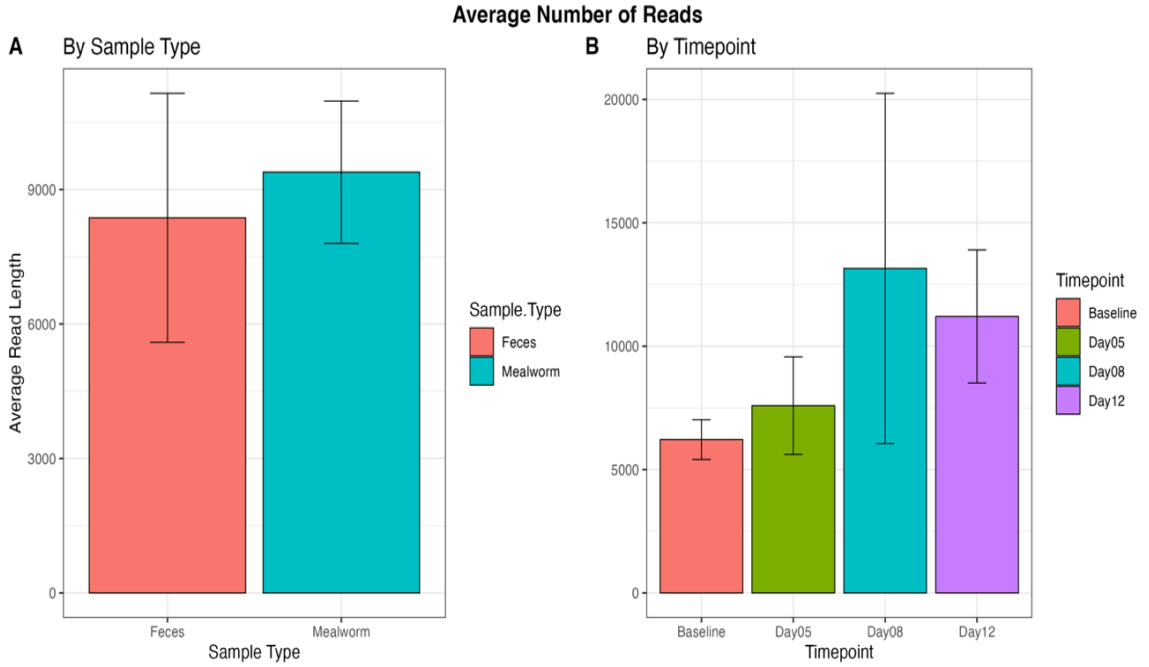

Figure 27. The average number of reads is stratified by sample type and timepoint.

All reads were identified as belonging to the bacterial kingdom, and the most abundant microorganisms were the Phylum *Proteobacteria* and *Firmicutes*, consistent with the previous studies (Urbanek et al., 2020). Also consistent with previous findings were the top bacterial OTUs identified at the class level: *Gammaproteobacteria, Bacilli,* and *Alphaproteobacteria*. Relative abundance differences by Phylum show apparent differences between diet types, consistent with previous studies (Figure 28). However, utilizing the Dirichlet-multinomial distribution for the relative abundance of Phylum stratified by diet (control group = rice bran), a non-significant p-value was obtained (p-value = 1) for the null hypothesis there were no differences between groups (la Rosa et al., 2012). This was not the case for the Genus level, indicating significant p-values (0.013) between the two diets. Absolute abundances were also compared, stratified by diet and

timepoint, and differences were noted between the two groups (Figure 29**).** In addition, heatmaps of abundance levels stratified by diet and timepoint also highlighted these differences (Figure 30).

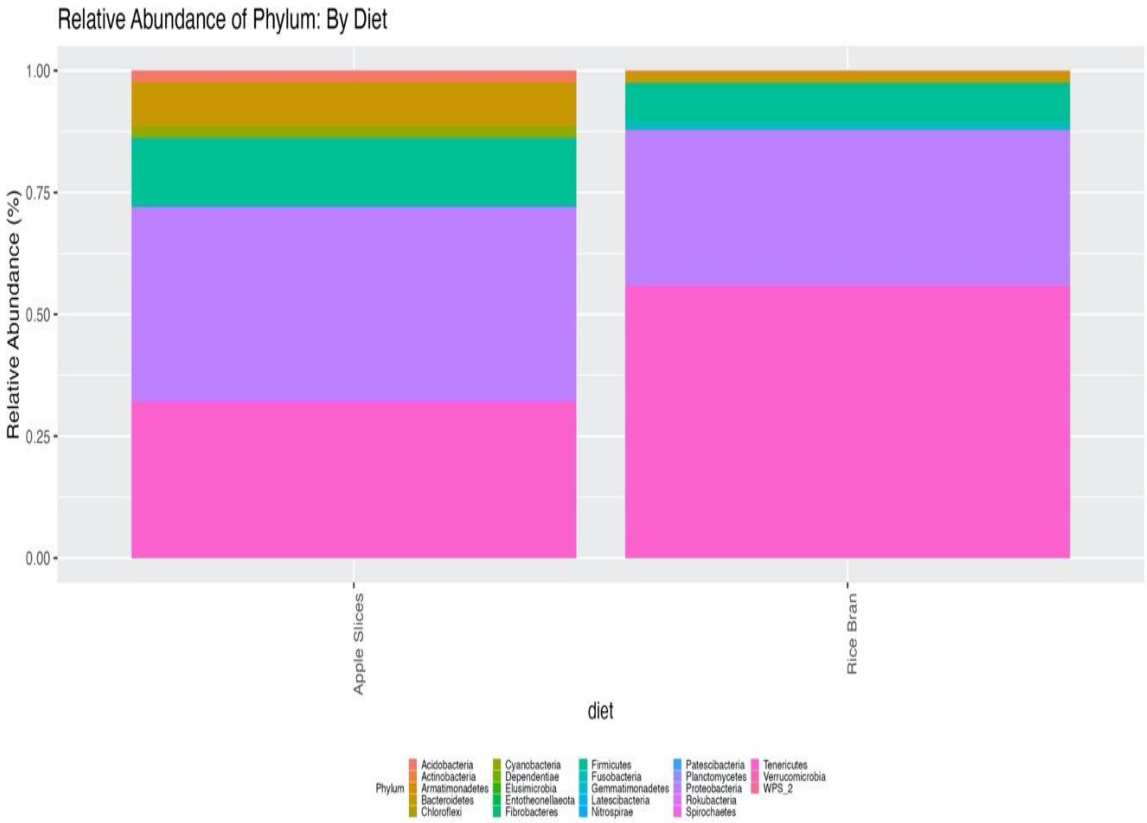

Figure 28. Relative abundances averaged stratified by diet.

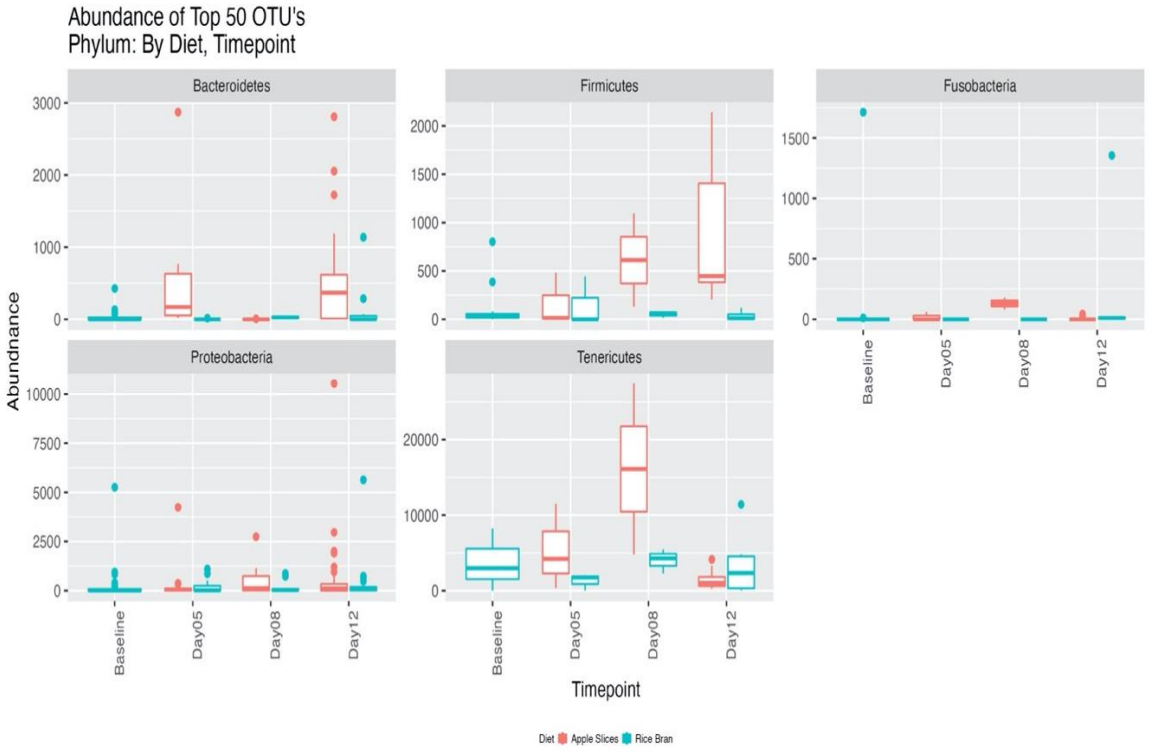

Figure 29. Absolute abundances of Phyla stratified by diet and timepoint, sub-sampled for the top 50 most abundant OTU's.

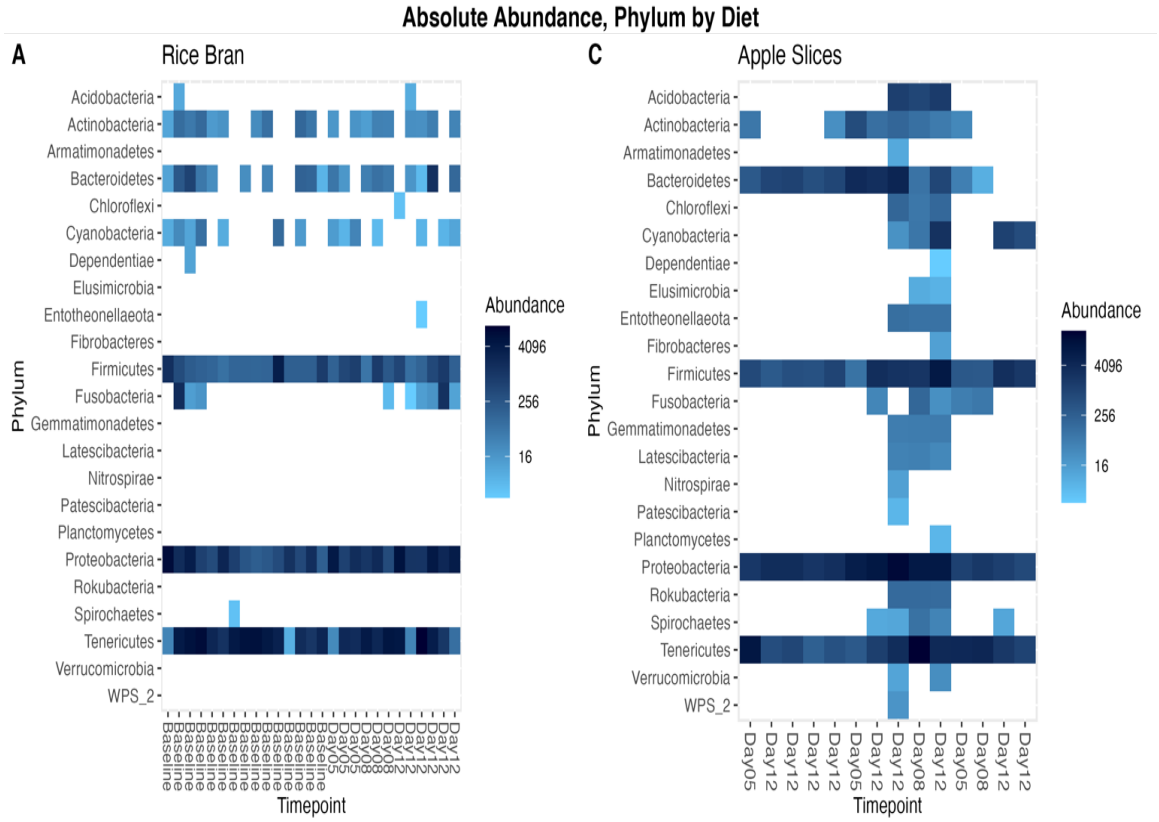

Figure 30. Heatmap of sample absolute abundance, stratified by diet and timepoint.

Alpha diversity was measured using the following metrics: Inverse Simpson, Chao1, and Observed species. Diversity increased throughout the time series, with a baseline for both sample types (Table 18). Each of these metrics had significant differences between the diet and timepoint when performing a Wilcox test. Because of the multiple tests being performed, an ANOVA analysis was performed, with a Tukey multiple test correction. Reviewing Inverse Simpson results after this correction illustrated significance between groups of timepoints (baseline/Day05/Day08 vs. Day12) and diet (apple slices vs. rice bran) (Figure 31). This was not true of the sample type, which did not have significant

Wilcox p-values (p-value = 0.934). To determine if timepoint or sample type influenced the samples were stratified further (Figure 32). There was no consistency between the cause of increases across each of these variables and their associated values.

Table 18. Alpha diversity measurements are stratified by sample type and timepoint.

Sample Type	***Timepoint***	***Inverse Simpson***	***Chao1***	***Observed Species***
Feces	Baseline	3.85 (1.51)	32.67 (24.33)	32.67 (24.33)
Feces	Day5	NA	NA	NA
Feces	Day8	NA	NA	NA
Feces	Day12	15.86 (5.87)	79 (88.78)	79 (88.78)
Mealworm	Baseline	6.26 (3.93)	33.56 (25.23)	33.56 (25.23)
Mealworm	Day5	6.34 (3.19)	43.83 (22.01)	43.83 (22.01)
Mealworm	Day8	4.17 (1.46)	73.4 (101.61)	73.4 (101.61)
Mealworm	Day12	19.88 (15.36)	82.11 (118.13)	82.11 (118.13)

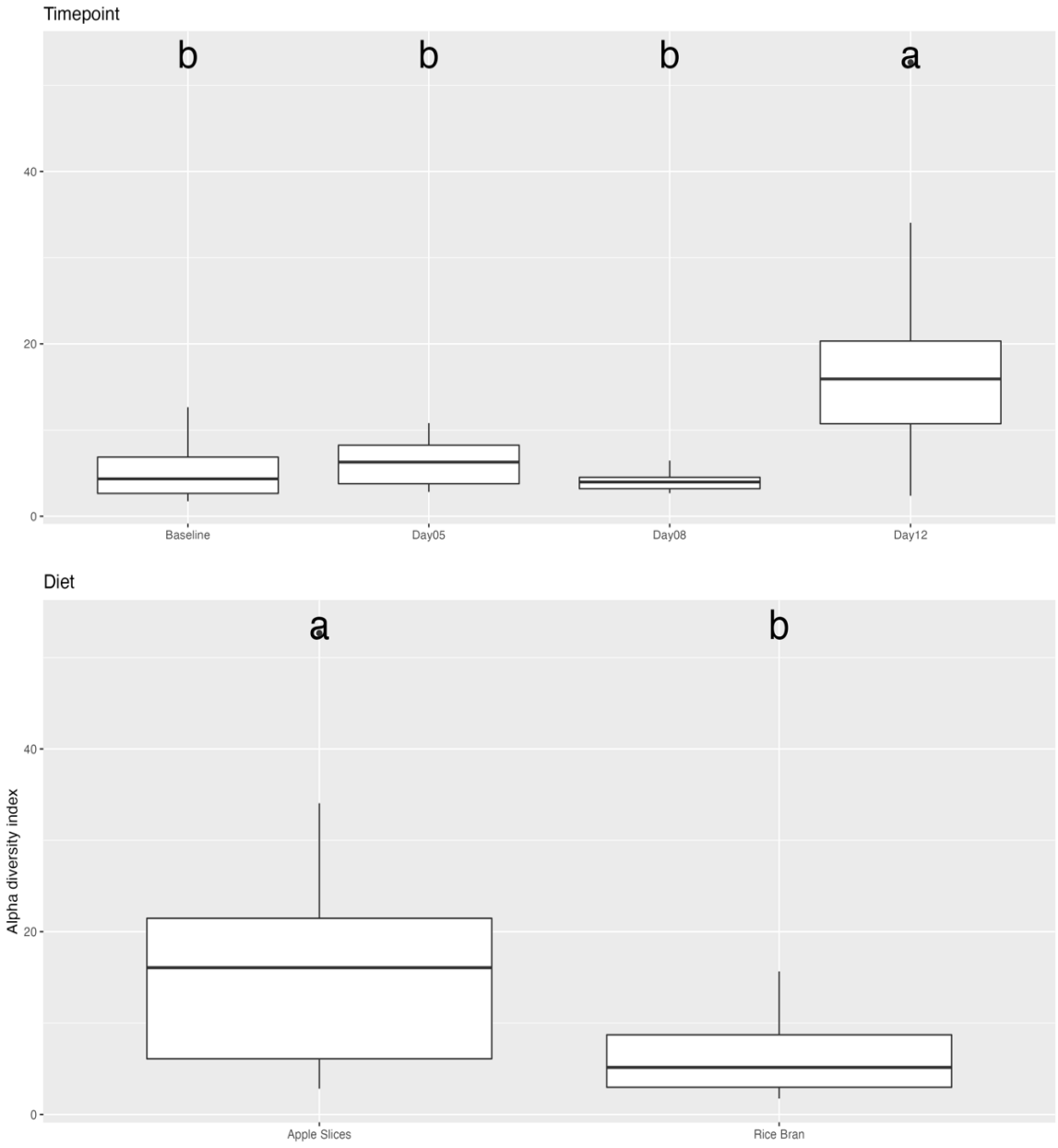

Figure 31. Inverse Simpson alpha diversity, by timepoint (TOP) and diet (BOTTOM) showing groupings after multiple test corrections (ANOVA, Tukey's multiple test correction).

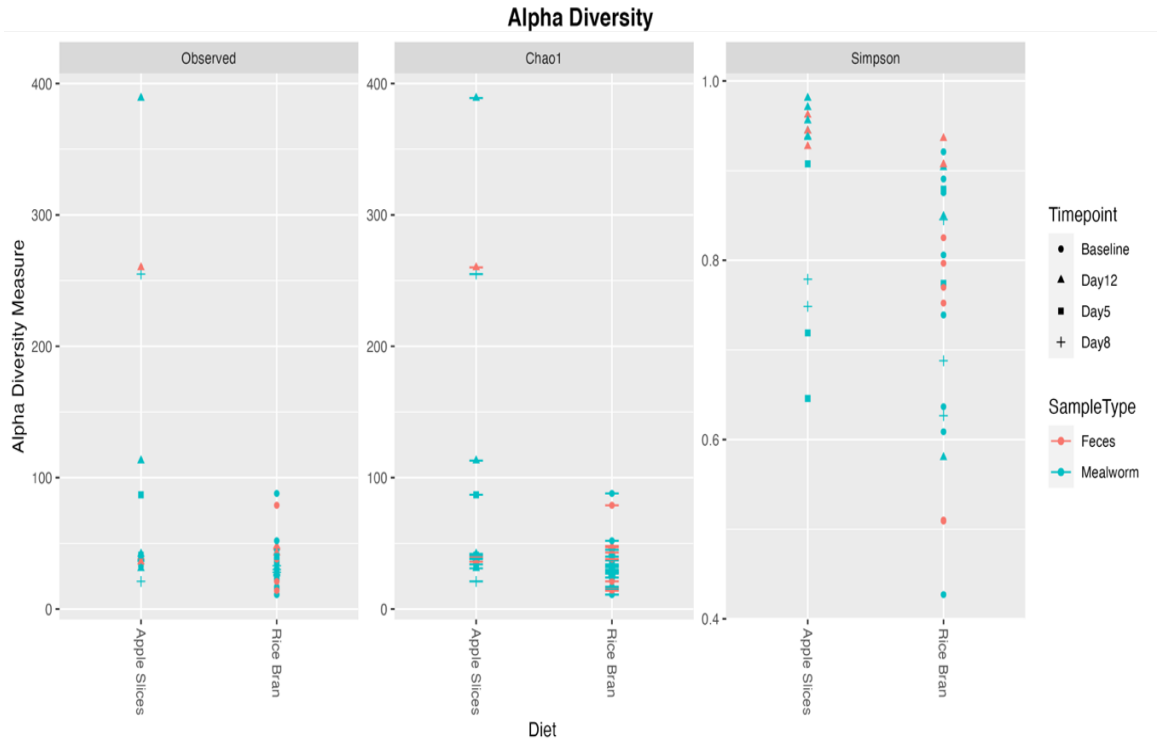

Figure 32. Alpha diversity metrics are stratified by metric and diet, colored by sample type, and shaped by timepoint.

Beta diversity analysis was performed using principal coordinate analysis (PCoA) and NMDS using the Bray-Curtis dissimilarity index. Stratifying by sample type, diet, and timepoint and highlighting clustering within the samples. This analysis presents points in which the distance along the x and y-axis represents the similarity of communities. Clusters revealed similarities between diet and time within the apple slices diet, not seen with the rice bran diet group (Figure 33). An ordination plot using the Aitchison Distance was generated, and overlapping values were observed between the health statuses, with the noted distribution of samples distance from the centroid (Figure 34). A permutational multivariate analysis (PERMANOVA) was performed and found to be significant by diet ($p = 0.07$) when comparing between baseline (rice bran) and timepoint Day 12 (apple

slices). At the same time, the variance of homogeneity was non-significant (p = 0.952). This indicates we would reject the null hypothesis of no difference in the centroid location according to diet at these two-time points.

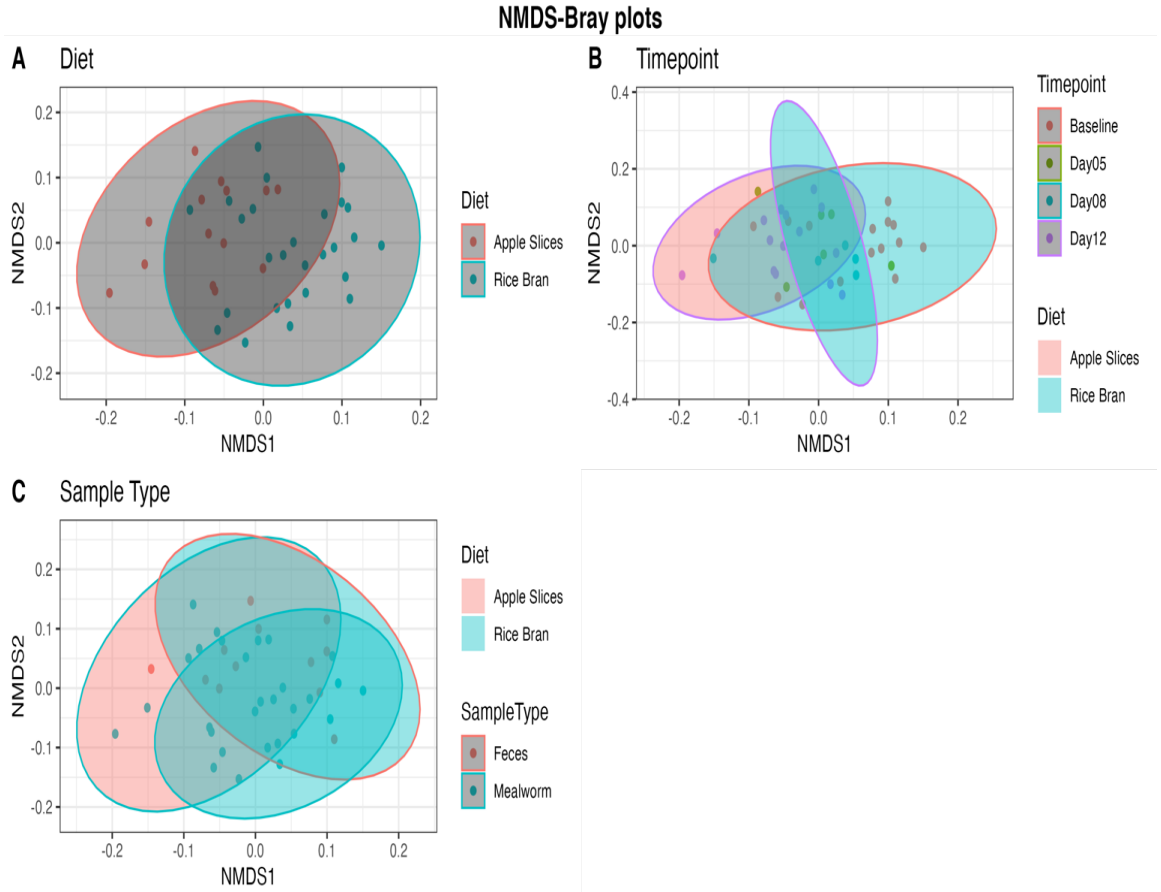

Figure 33. NMDS-Bray plots stratified by Diet (A), time point (B), and sample type (C).

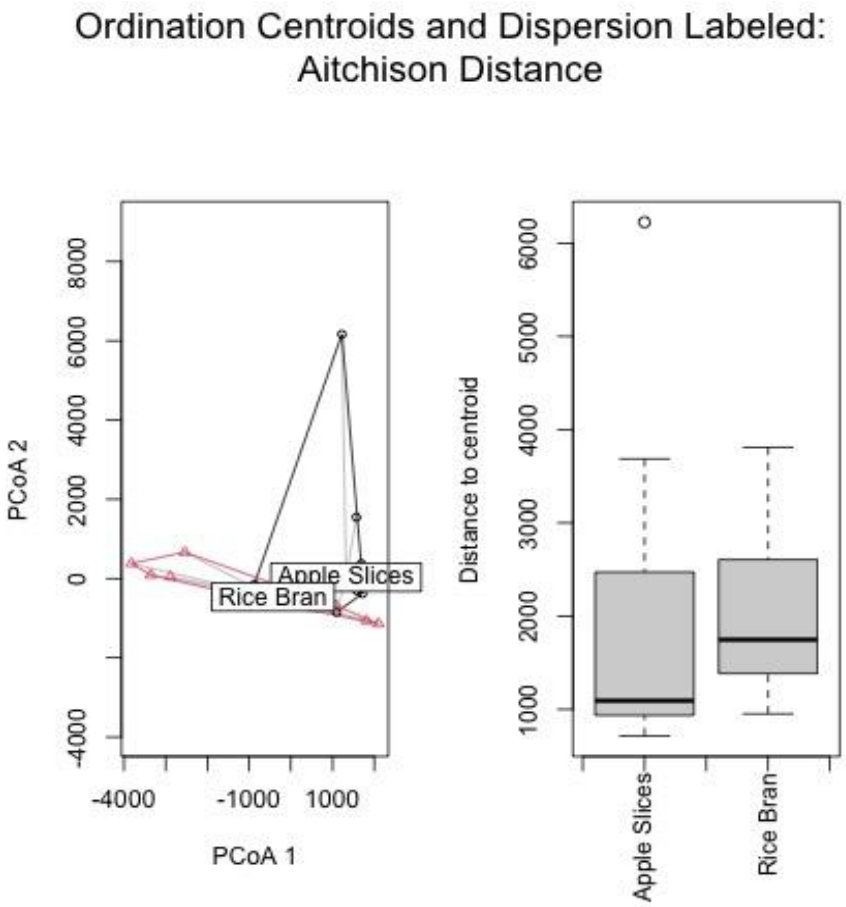

Figure 34. Ordination using Aitchison Distance (left) and stratified by diet at timepoint baseline (rice bran) and day 12 (apple slices).

Differential analysis was performed to determine significant differences in the Genera present between two groups within variables. Three approaches were employed: the non-parametric Wilcoxon test, the second is ANOVA-like differential expression (ALDEx2), and finally, a differential algorithm based on the negative binomial distribution (DESeq 2). In addition, because of the multiple comparisons being performed, the Benjamini and Hochberg (BH) correction was applied to the p-values, as appropriate. Each

test has features that are particularly useful when performing differential analysis and were used to determine the continuity of results.

The Wilcoxon method indicated significantly differentiated taxa by diet, regardless of timepoint (p-value 0.01), with seven Phylum specifically contributing to significance even after BH FDR corrections (Table 19). When comparing the baseline value (rice bran diet) to the day 12 value for apple slices, although all phyla did not produce significant differences (p-value= 0.8), comparisons between Phylum did produce meaningful results (Table 20). ALDEx2 is a Co-Occurrence of Domains Analysis (CoDA) method, developed for next-generation sequencing analysis, which employs Monte-Carlo sampling from a Dirichlet distribution with a small non-zero-sum. The ALDEx2 is a much more conservative approach and did not identify any significant OTU's falling within the first and third quartiles after the CLR transformation (Figure 35).

Table 19. Significant Phylum between diet, calculated with a Wilcoxon rank-sum test, with continuity correction (p-value) and BH FDR correction (BH_FDR).

Phyla	**p-value**	**BH_FDR**
Firmicutes	0.003	0.003
Bacteroidetes	0.004	0.004
Spirochaetes	0.005	0.005
Proteobacteria	0.005	0.005
Gemmatimonadetes	0.015	0.015
Rokubacteria	0.015	0.015
Candidatus Latescibacteria	0.015	0.015

Table 20. Significant Phylum between baseline samples (rice bran diet) and timepoint Day 12 samples (apple slices diet), calculated with a Wilcoxon rank-sum test, with continuity correction (p-value) and BH FDR correction (BH_FDR).

Phlya	**p-value**	**BH_FDR**
Firmicutes	0.002	0.00234719
Proteobacteria	0.004	0.00435027
Bacteroidetes	0.013	0.01332045
Spirochaetes	0.023	0.02333027

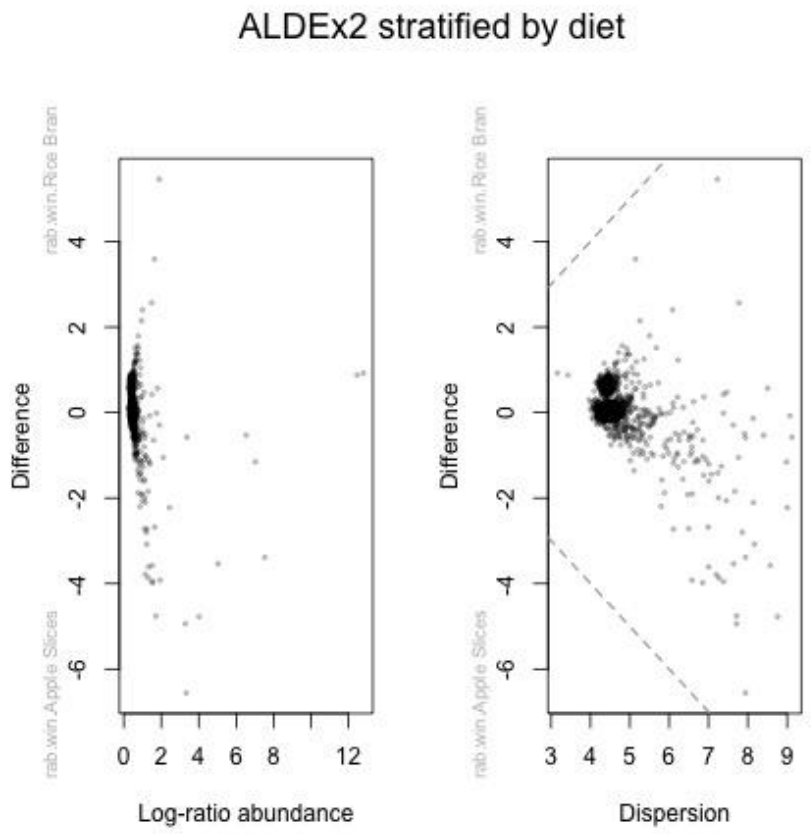

Figure 35. ALDEx2 log-ratio abundance (left) and dispersion (right) plots for OTU's stratified by diet, indicating no significant results.

Genera were found to be significantly different between diets using the DESeq2 method (N=3), two associating to the apple slice (positive), and one to rice bran (negative) diets, in line with previous results (Figure 36). Stratifying by timepoint and performing a crosswise comparison between each of the times highlighted several significant genera. Of note, since OTU identified were mapped to their genus as listed in the Silva (version 132) database, some OTU's have "Higher Taxonomic Level" listed, as these OTUs were only mapped to a higher taxonomic value. Each time point had significant genera differentiated,

with the highest being the differences in Day 05 to Day 08 (N=39) (Table 21). In this comparison, more genera were significantly differentiated in Day 08 over Day 05, indicating the peak of the microbiome transition between the rice bran diet-fed on the baseline and the apple slice diet (Figure 37).

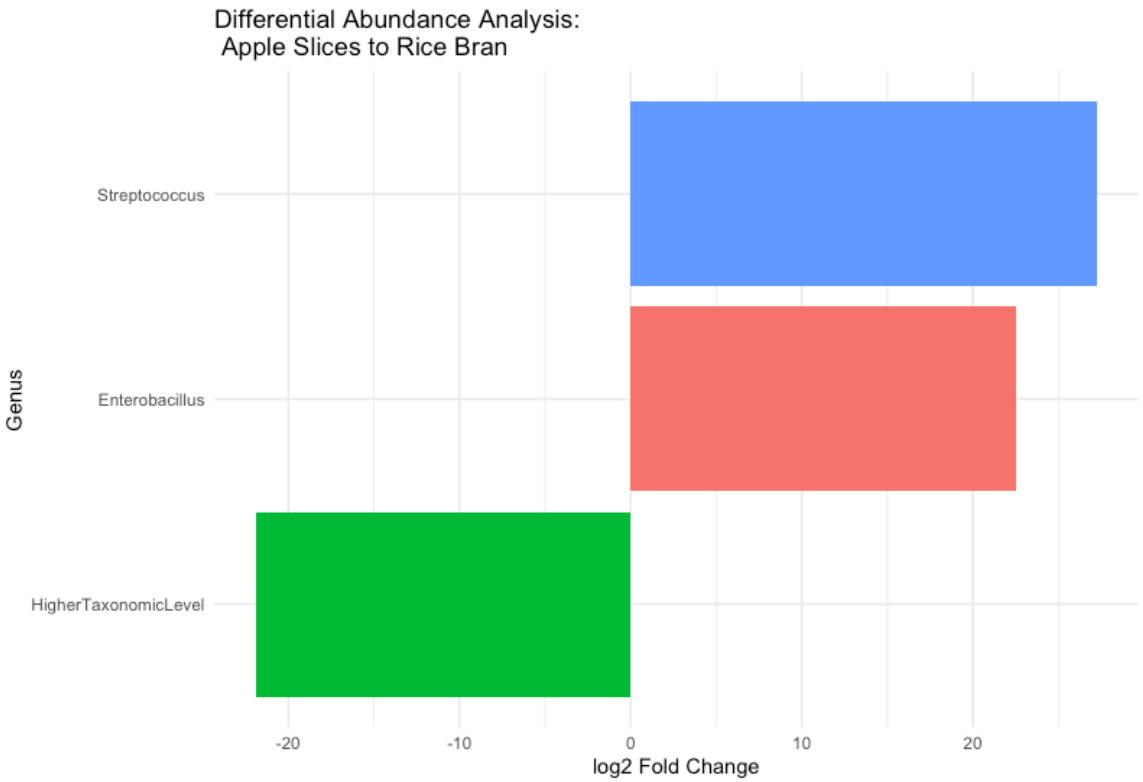

Figure 36. Differential abundance analysis, between varying diets (apple slices and rice bran). P-values were adjusted using the BH correction and filtered (p-value <0.05). The fold change direction (log2) relates to the stronger association with apple slices (positive) or rice bran (negative

Table 21. Top significant genera differentially expressed by a variable with BH corrected p-value shown.

Genera	Diet	Bto5	Bto8	Bto12	5to8	8to12
Chryseobacterium	0	2.61E-10	0	0	1.32E-11	0
Delftia	0	0	0	0	8.78E-12	0
Enterobacillus	1.89E-10	0	7.12E-09	0	1.84E-10	1.39E-10
Enterococcus	0	0	8.37E-09	0	8.78E-12	1.36E-10
Enterococcus.1	0	0	6.38E-09	0	2.59E-11	1.36E-10
Enterococcus.2	0	0	3.05E-09	0	1.39E-10	1.36E-10
Enterococcus.3	0	0	3.05E-09	0	6.04E-11	1.39E-10
Enterococcus.4	0	0	3.05E-09	0	3.93E-11	0
Higher Taxonomic Level	4.29E-10	2.11E-11	3.05E-09	4.33E-10	1.10E-11	1.39E-10
Higher Taxonomic Level.2	0	2.58E-09	9.83E-09	9.44E-12	2.37E-10	2.92E-10
Higher Taxonomic Level.3	0	2.61E-10	9.83E-09	0	4.03E-10	3.59E-10
Sphingobacterium	0	0	0	9.73E-11	3.60E-11	5.86E-06
Streptococcus	3.68E-22	0	3.05E-09	0.04478376	0	0
Weissella	0	0	0	1.20E-10	0	1.89E-07

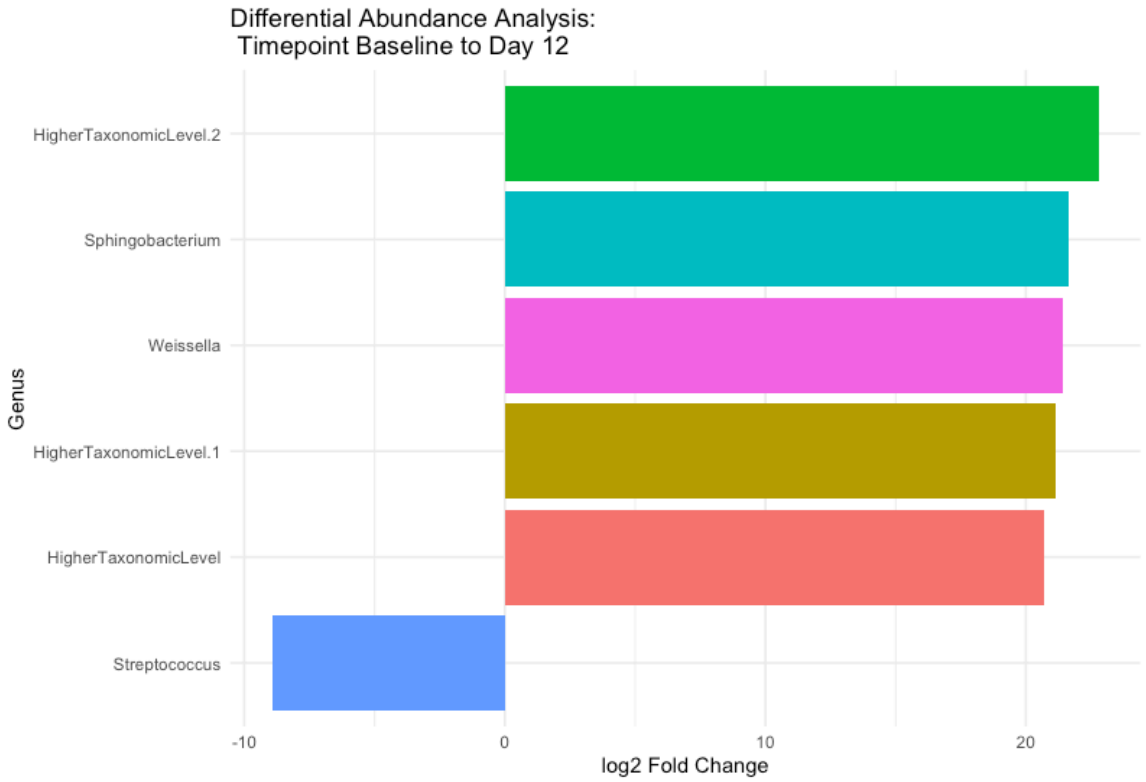

Figure 37. Differential abundance analysis, between varying time points (before PS consumption, Day 12 after PS consumption). P-values were adjusted using the BH correction and filtered (p-value <0.05). The fold change direction (log2) relates to the stronger association to the baseline before PS consumption (positive) or Day 12, after PS consumption (negative).

Prediction modeling was performed in R using two methods – the first is a CODA method using an R software package called rms, and the second is a R software package Selabl179,180. To begin, the full model was fit, and a grid search was performed to determine the optimal value for a penalty (simple penalty = 1, non-linear penalty = 200). Plotting the resulting log odds ratio showed the associations were linear; however, a cubic spline was used in the full model (Figure 38). PC1 – PC3 were reviewed to determine the prediction strength, with PC1 having the highest strength, representing 75% of the

diversity. A full bootstrap resampling was then performed to determine the model performance, with poor results for the model prediction (Figure 39)

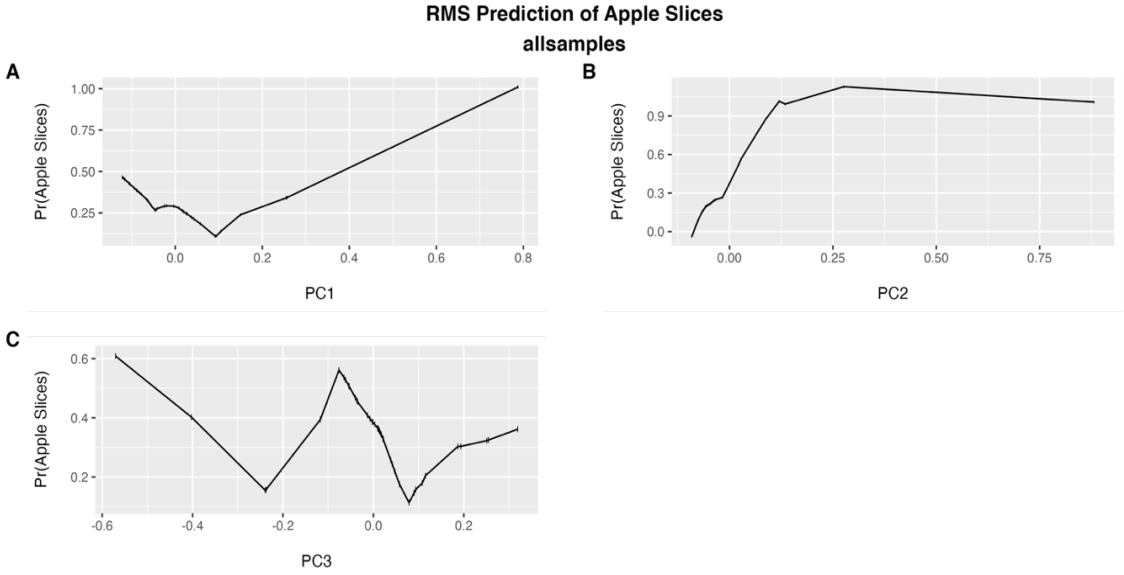

Figure 38. RMS prediction values of all samples for apple slices, stratified by PC1, PC2, and PC3.

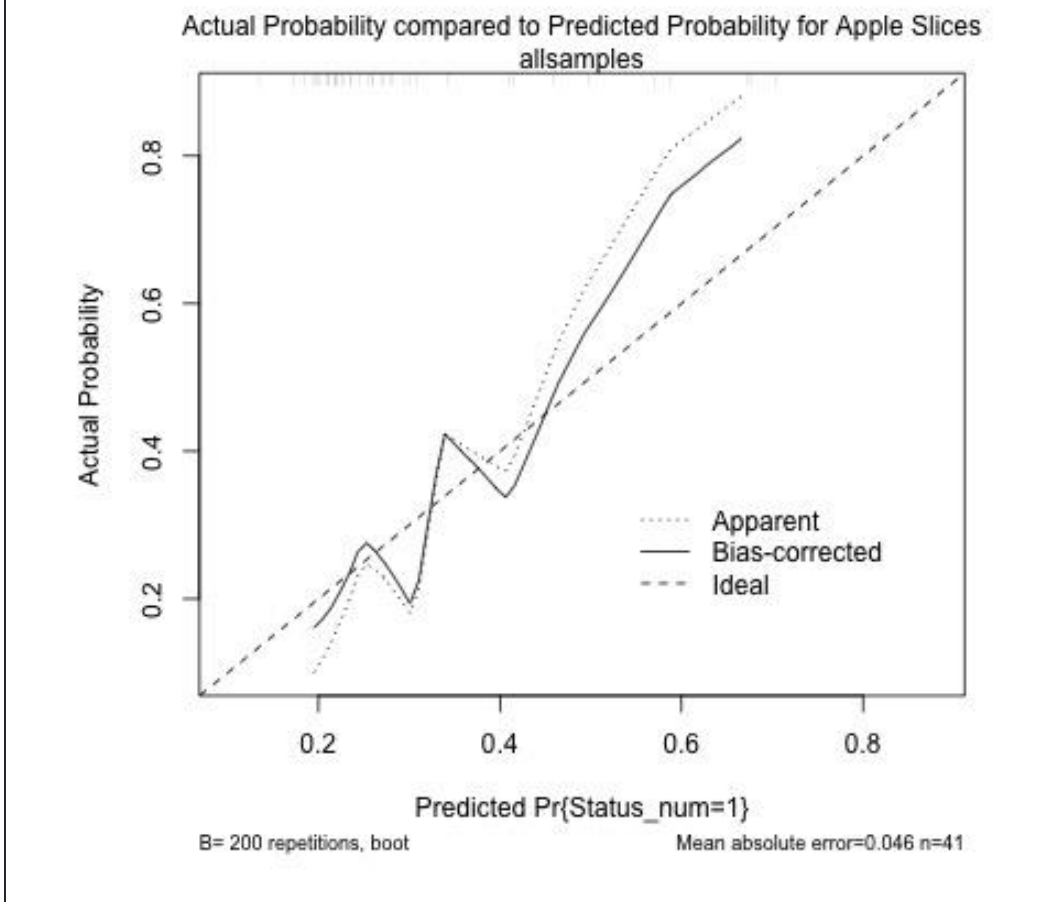

Figure 39. RMS prediction performance probability for all samples to determine diet.

Selbal uses a forward-selection method to identify taxa groups whose relative abundance is associated with a particular response variable (UVic-omics, n.d.). This microbial signature can then be used as a predictor for group identification by performing multiple regressions, adding a new taxon with each iteration. Rare taxa were removed (N<200) to balance bias. The two Phyla that were the strongest predictors were

Bacteroidetes for apple slices and Actinobacteria for rice bran (Figure 40). The discrimination value of the area under the curve (AUC) is established when no additional variable (taxa) improves the current optimization parameter (Figure 41). In addition, a cross-validation procedure is performed to explore the robustness of the balance between taxa. The AUC-CV for this prediction is 0.775, with each Phylum being found in 80% of the cross-validations performed.

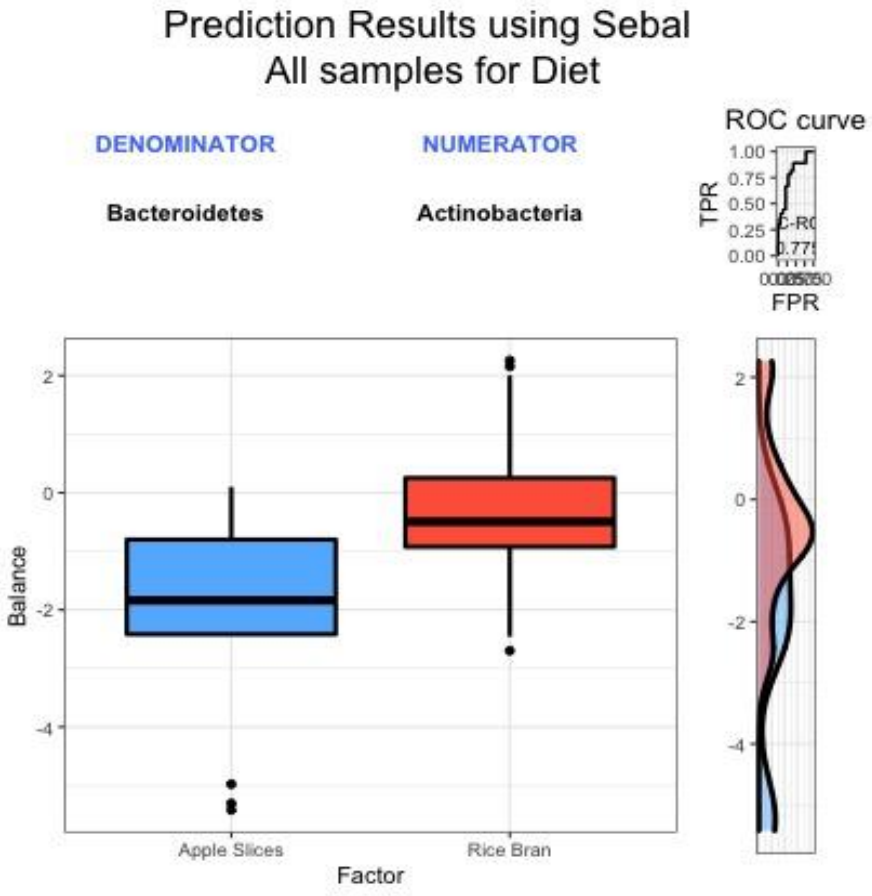

Figure 40. Selbal prediction analysis for diet, with all samples, included.

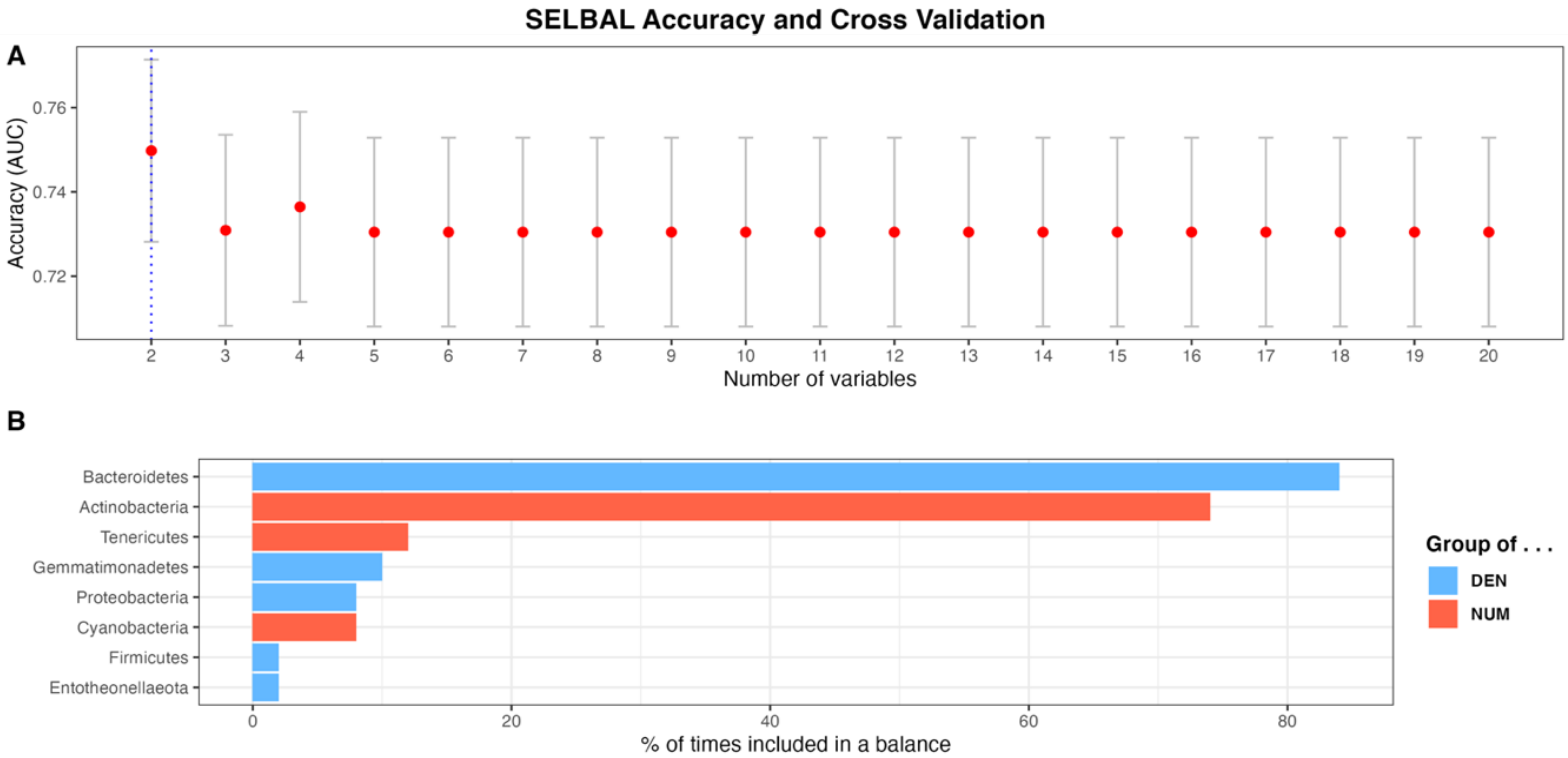

Figure 41. AUC (A) for variables and bar plot (B) representing the frequency of variables selected in the CV process, defined by the numerator (rice bran) and denominator (apple slices).

The functional prediction was performed using an R software package Tax4Fun and a QIIME2 plugin for PICRUST2 (Caporaso et al., 2010; Chill et al., 2020; The PICRust Project, 2013). An exploration of significant OTU's (p-value <0.01) using Tax4Fun analysis revealed several predicted pathways related to metabolism, with the top 10 KO pathways and the top 10 Molecular descriptions reviewed (Table 22, Table 23). Utilizing a structural topic model (STM), which uses a machine learning approach to estimate relationships between text inputs, in this case, KEGG pathways, top pathways can be grouped, identified, and visualized (Roberts et al., n.d.). Associations are assigned as 'topics' and plotted as an estimation towards healthy status (red) or unhealthy status (blue) (Figure 42, TOP). Then, these topics can be examined in the heatmap, showing the function-topic interaction. Yellow and dark blue is representative of relative abundances (high and low, respectively) and were used to explore relevant pathways (Figure 42, BOTTOM).

Table 22. Top 10 KEGG KO pathways determined by Tax4Fun.

Pathway Descriptions
alcoholism
carbon metabolism
oxidative phosphorylation
longevity regulating pathway – multiple species
nucleotide excision repair
porphyrin and chlorophyll metabolism
RNA degradation
purine metabolism
starch and sucrose metabolism
purine metabolism

Table 23. Top 10 KEGG KO descriptors determined by Tax4Fun.

Molecular Descriptions
adenylate cyclase [EC:4.6.1.1]
ATP-dependent Clp protease ATP-binding subunit ClpB
calcium/calmodulin-dependent protein kinase 1 [EC:2.7.11.17]
DNA helicase II / ATP-dependent DNA helicase PcrA [EC:3.6.4.12]
DNA-directed RNA polymerase subunit beta' [EC:2.7.7.6]
glycogen phosphorylase [EC:2.4.1.1]
magnesium chelatase subunit H [EC:6.6.1.1]
molecular chaperone DnaK
NAD (P)H-quinone oxidoreductase subunit 4 [EC:1.6.5.3]
pyruvate, water dikinase [EC:2.7.9.2]

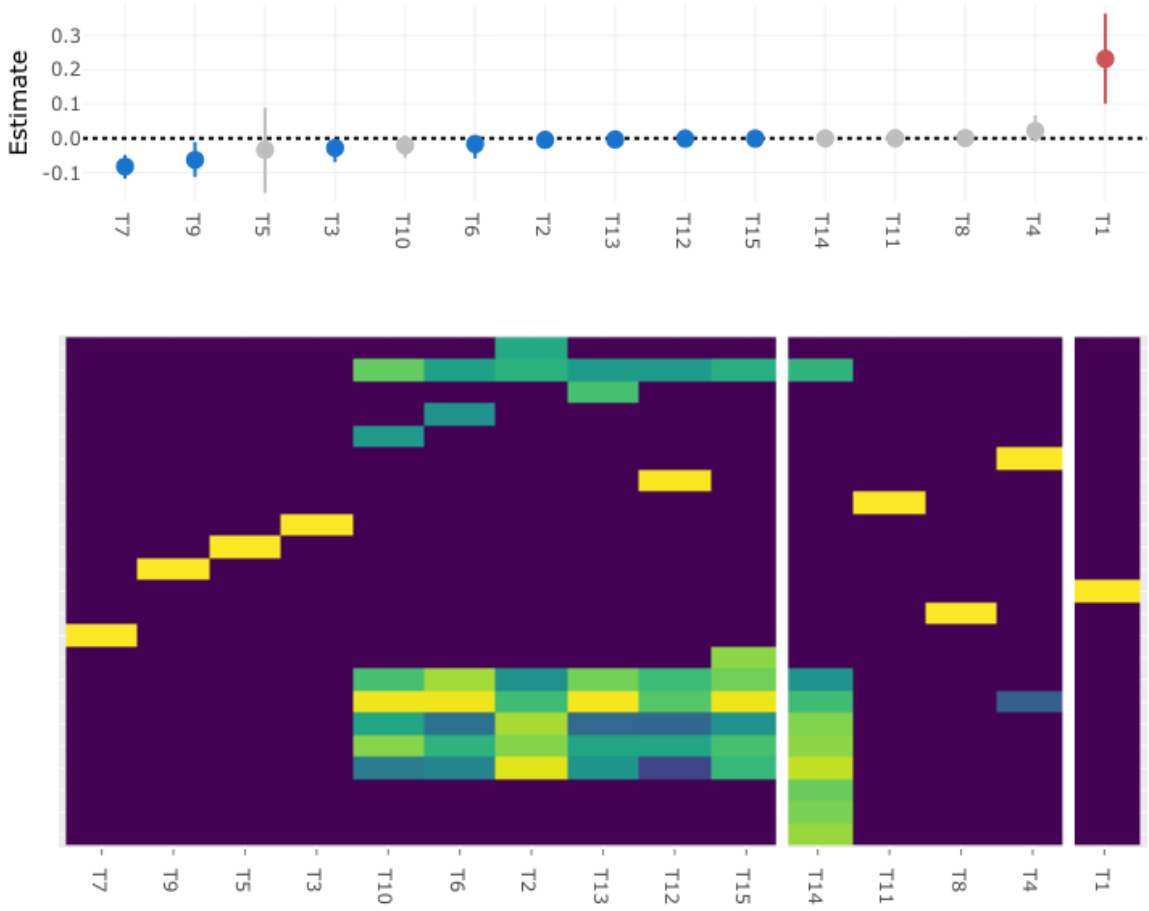

Figure 42. Functional prediction by topic with estimate cause of variance (TOP) and heat map (BOTTOM).

PICRUST2 and STAMP were employed next to determine additional functional significance and differentiation between healthy and afflicted individuals (Figure 43, Figure 44). Results from this prediction tool highlighted 51 significant pathways (corrected p-value <0.01), of which the top 5 significant pathways are shown (Table 34). Pathway PWY-6263 is related to methyl-accepting chemotaxis, a transmembrane receptor that mediates chemotactic responses in certain bacteria, specifically in response to toxin

chemicals[180]. The top path highlighted in the heatmap, and differentially regulated in several samples, is the PWY-7219, representing the adenosine ribonucleotides de novo biosynthesis (Figure 45). In addition, P122-PWY (corrected p-value 7.47E-06) is found to be related to heterolactic fermentation, recently shown to be important in improving both the digestibility of fiber, but also increasing water-soluble carbohydrates available (Figure 46) (H. Zahiroddini et al., 2006).

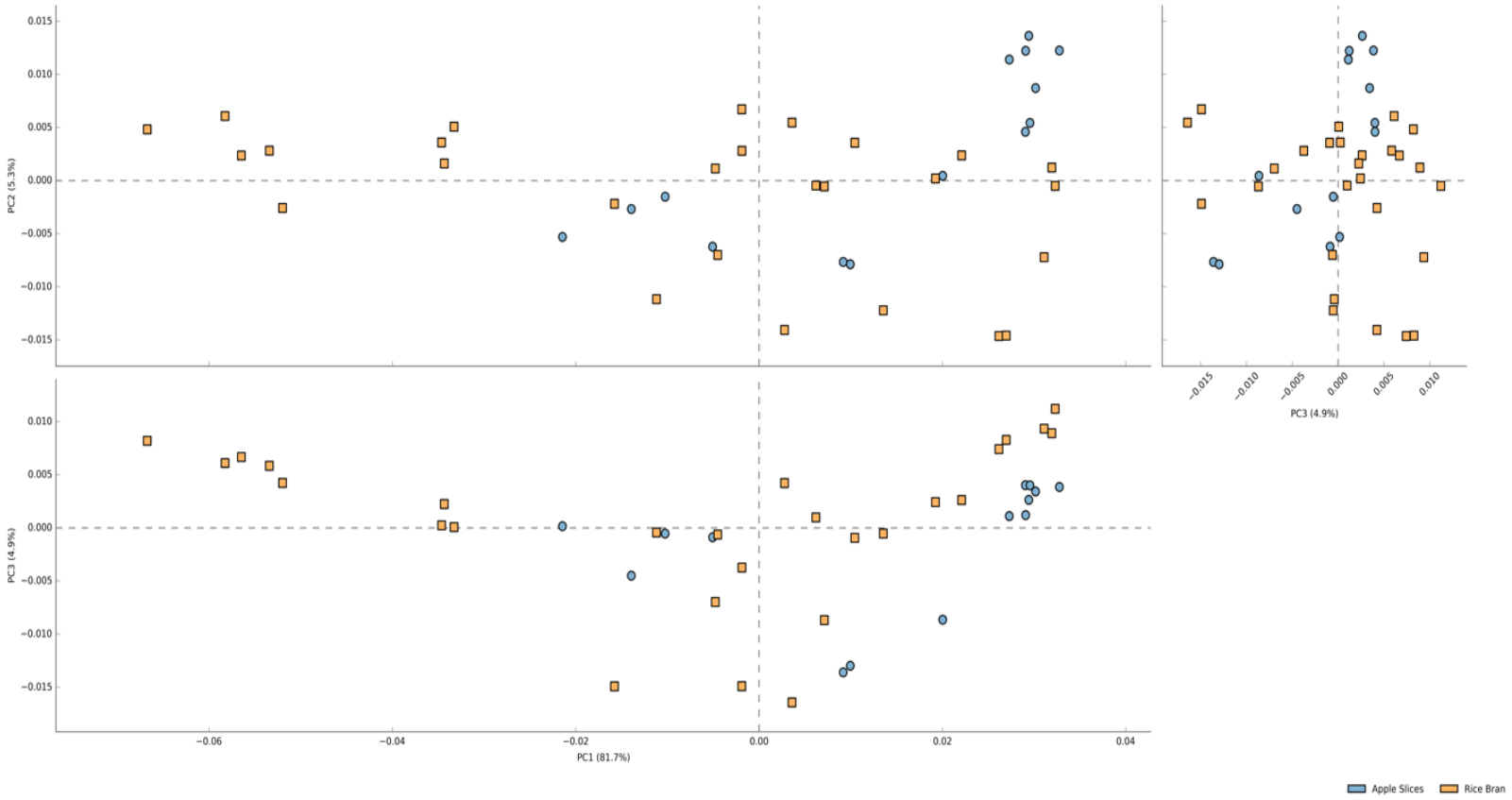

Figure 43. Crosswise comparison of PCoA 1 through PCoA3, for diet (color), from PICRUST2 and STAMP analysis.

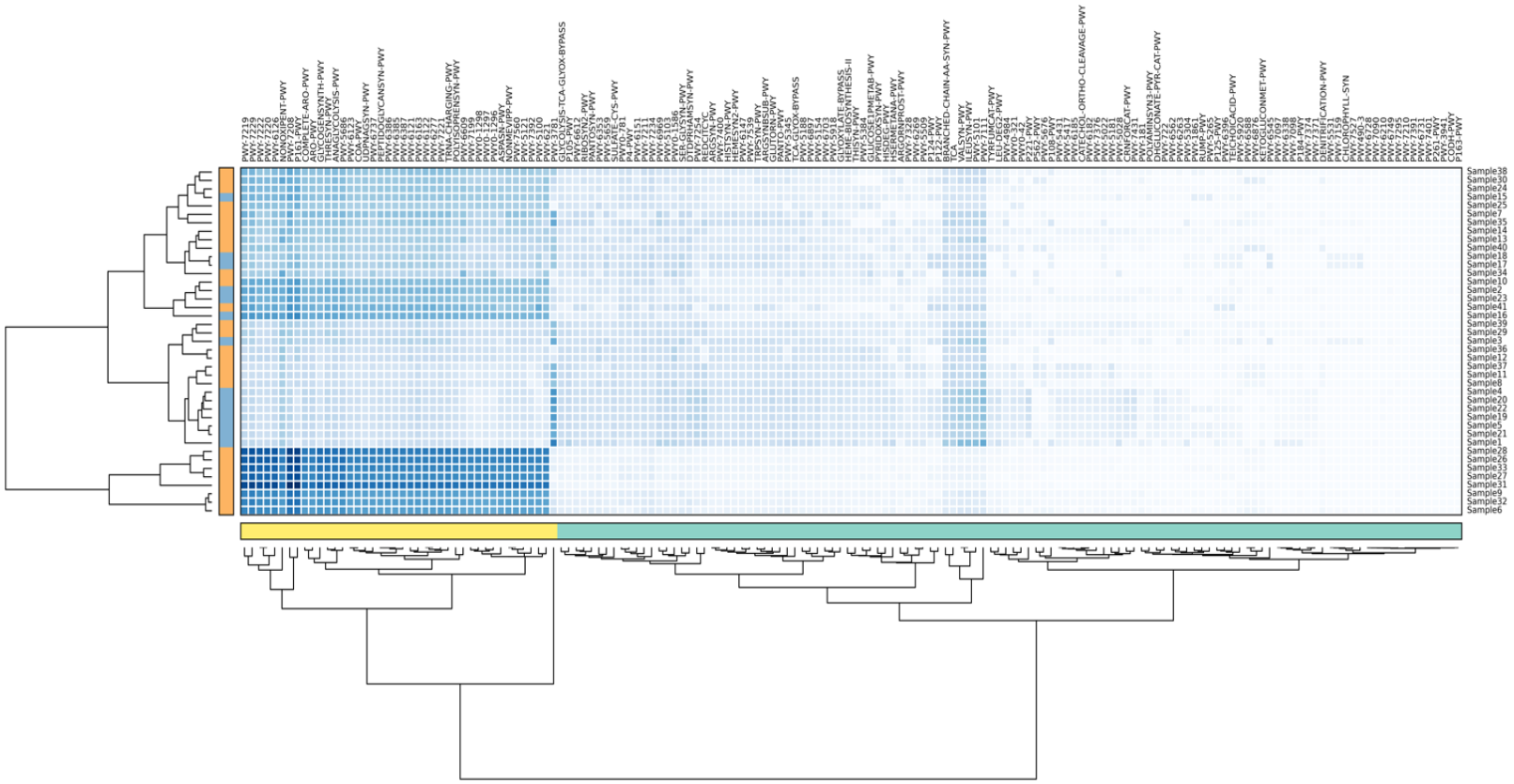

Figure 44. Heatmap for diet (apple slices – orange, rice bran - blue) by columns and significant pathways (rows), from PICRUST2 and STAMP analysis.

Table 24. Top 5 significant differentiated pathways generated from PICRUST2.

OTU ID	p-values (corrected)	Effect size	Apple Slices: mean rel. freq. (%)	Apple Slices: std. dev. (%)	Rice Bran: mean rel. freq. (%)	Rice Bran: std. dev. (%)
PWY-7371	2.87E-06	0.433566944	0.035755434	0.025757285	0.0053044	0.008345809
PWY-6263	3.98E-06	0.424316062	0.080637618	0.055936549	0.01396224	0.020908052
PWY-7374	6.04E-06	0.412265156	0.032980372	0.024238317	0.005252398	0.008345216
P122-PWY	7.47E-06	0.406052592	0.298310813	0.098370328	0.115999467	0.107626932
P124-PWY	1.32E-05	0.388967425	0.314207797	0.101512731	0.127507422	0.115561001

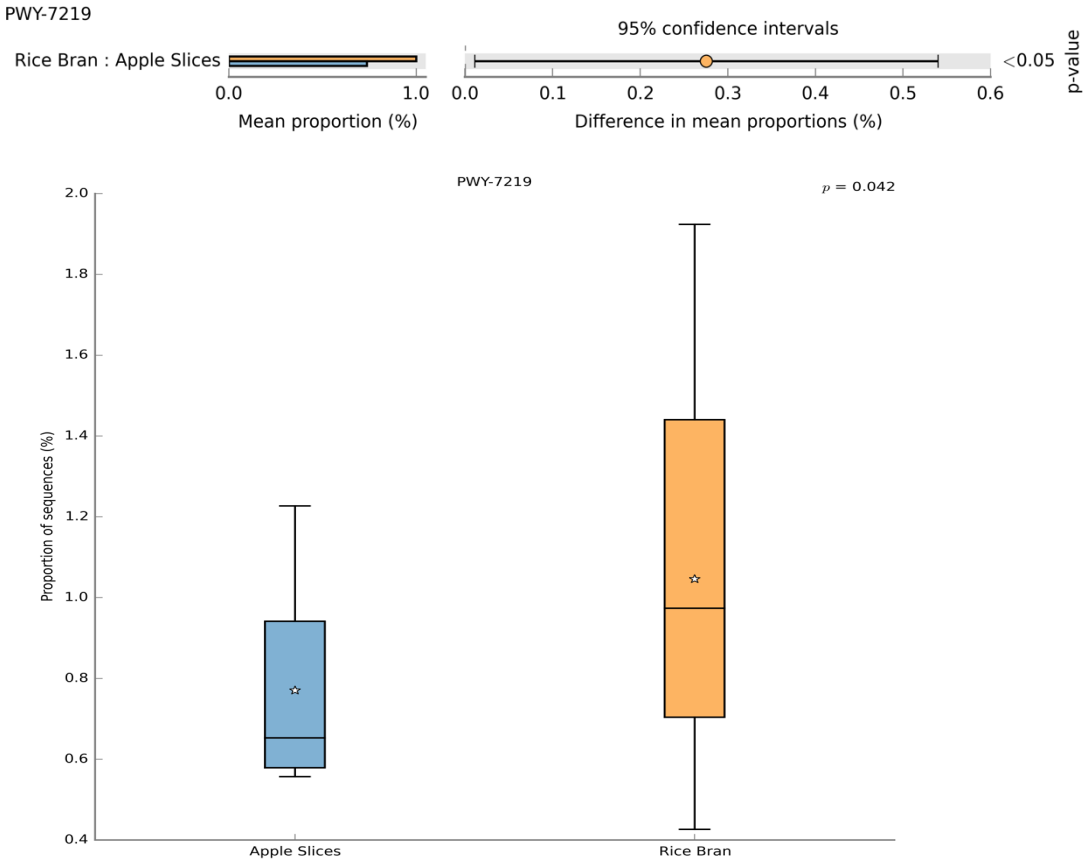

Figure 45. Significantly differentially regulated pathway (PWY-7219) between diet groups, using PICRUST2 and STAMP for visualizations.

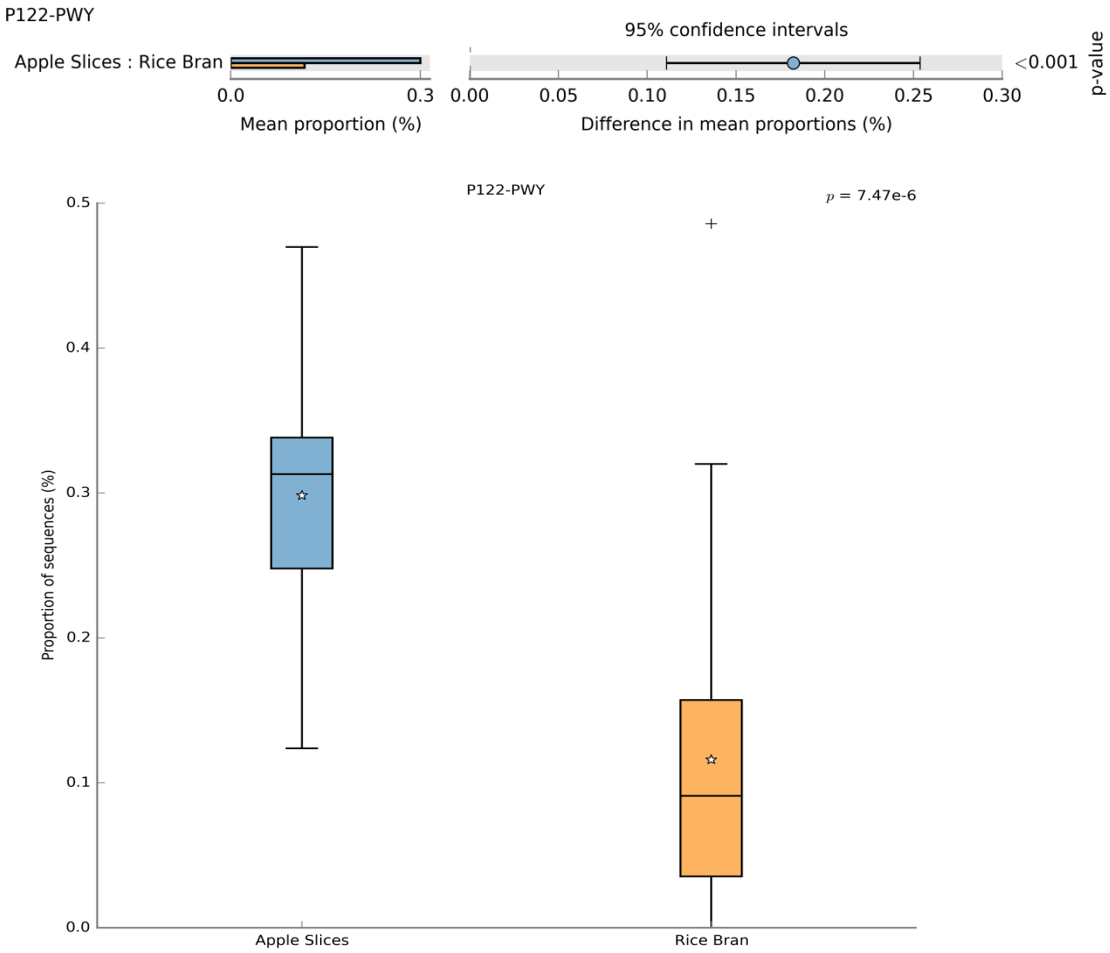

Figure 46. Example of a significant functional pathway, significantly differentiated between the two diet groups (P122-PWY), using PICRUST2 and STAMP for visualizations.

4.4 Discussion

Relative abundance differences were noted between diets, with higher abundance levels at later time points in apple slices. This was also the case with variance, both higher in apple slice samples and at later time points. Consistent findings with previous work for T. molitor who consume Polystyrene indicates some community divergences within the larger homeostasis of the gut from baseline. The top phylum in both apple slice and rice

bran diets groups were *Bacteroidetes*, consistent with the previous characterization of the *T. molitor* gut microbiome (Brandon et al., 2018). Differences are noted between the diets at the second and third highest OTU's; however: *Pseudomonas* and *Enterobacillus*, in the apple slices diet, *Enterobacillus* and *Escherichia-Shigella* in the rice bran diet. This may indicate specific differences related to the diets of the T. molitor, as opposed to bacteria that are inherent to the mealworms. Follow-up sequencing for differentially abundant species is essential to identify the key players within these communities that may be responsible for consumption response.

Rice brain is created from the milling process of rice and stabilized through a heating process (Kahlon, 2009). It consists of a higher amount of fiber and is commonly used as an animal feed or dietary supplement in some low and middle-income countries (Zambrana et al., 2019). This can be compared to that type of whole-grain diet, which typically consists of wheat and brown rice. A change to a more sugar-based diet in the *T. molitor*, such as with the apple slices, showed an increase in alpha diversity over the rice bran. This is consistent with human studies that showed between whole grain and fruits diet; the fruit diet had a significantly higher alpha diversity (Zambrana et al., 2019). In addition, as these alpha diversity differences were noted with greater diversity levels noted at later time point, this may be an indication that there is not an immediate conversion of microbiome. This appears to be confirmed by the alpha diversity groupings of early time points (Baseline, Day 05, Day 08) to later time points (Day12) showing significant divergence, thereby highlighting a possible transition period of the gut microbiome. These

differences lead to implications regarding the complexity of priming diet and community and the amount of Polystyrene consumed and are findings to explore in future studies.

Differences in alpha diversity were supported by the distance measurements performed using both PC plots and Aitchison Distance plots. PC1 was found to describe 15% of the diversity and was responsible for the clustering that was achieved by diet. PC2 represented 8.9% of the sample diversity and subsequently did not have as much of an effect on the clusters formed by diet. By performing a log transformation of the matrix counts, the positive skew towards zero, which confounds PCA, can be overcome[186]. This provided a similar representation of clustering as the PC plots, with similarly significant results. Differences in NMDS clustering highlight timepoint differences within diets, as well as sample types within diets, with the apple slices and rice brans creating two clusters with an overlapping center. This center, however, was defined by the timepoint of Day 12, further implicating a potential priming event, as described earlier.

In studying the degradation of PS material, it has been shown that there are two distinct phases: the first is the adsorption of enzymes on the polymer surface, and the second is the hydroperoxidation and or hydrolysis of C-O bonds (Mohanan et al., 2020). These two phases were considered through each step of the differential expression and prediction analysis. Starting with the differential analysis of diet, the Wilcoxon rank-sum test produced seven differentially expressed phyla, including Firmicutes and Proteobacteria, both of which were previously highlighted as likely responsible for the second phase of degradation, through depolymerization of PS and degradation of intermediates (S. S. Yang et al., 2018). The stricter ALDEx2 method did not produce any

significant OTU's. However, this is not unexpected given the distribution matrix used and as mentioned, the more stringent methodology. Finally, DeSeq2 presented results at the genus level. Both *Streptococcus* and *Enterobacillus* were positively associated with apple slices, whereas OTUs identified at a higher taxonomic level than genus was associated with rice bran. Furthermore, the association of *Enterobacillus* to apple slices strengthens this argument as previous work has also hypothesized that the depolymerization and eventual degradation of PS are likely due to this gram-negative bacterium.

The prediction balance approach of Selbal found that the combination of *Bacteroidetes* and *Actinobacteria* were the strongest predictor for diet source and may provide insight into diet-based changes that link consumption-based differences. Functional prediction allowed for the analysis of differentially expressed OTU's and mapping to their functional counterparts. Tax4Fun analysis utilized KEGG pathways for associations and found starch and sucrose metabolism to be significantly differentiated between all samples. Of particular interest is starch and sucrose metabolism, which is associated with anti-oxidative enzymatic properties (J et al., 2019). Previous research into the hypothetical degradation pathway indicates that PS-degrading bacteria are likely responsible for secreting oxidative enzymes that can break down PS polymer chains, thereby generating C-O bonded intermediates (S. S. Yang et al., 2018). In that case, this may be a pathway that can elucidate these differences – the mealworms that were able to digest the most Polystyrene likely had a decrease in starch and sucrose metabolism, thereby increasing oxidative enzymes and an increase in PS polymer change intermediates.

Utilizing PICRUST2 with STAMP, additional pathways were highlighted, found methyl-accepting chemotaxis protein-associated (PWY-7219), the most common receptor in bacteria and archaea, which may play a role in biodegradation (Salah Ud-Din & Roujeinikova, 2017). Other vital pathways related to menaquinone and naphthoate, both of which are components of the cytoplasmic membrane (Biocyc, n.d.). Finally, P122-PWY was highlighted found to be related to heterolactic fermentation. This was found to be important in improving the digestibility of fiber and increasing water-soluble carbohydrates available (H. Zahiroddini et al., 2006). This finding is in line with previous research, which showed that the degraded PS had higher water-soluble daughter products detected, indicating the possible importance of these carbohydrates to the degradation process (Y. Yang et al., 2015b).

Significant limitations were also found within this study design. The low number of samples is the first limitation, and future studies would aim to expand the sample count for each of the study aims. Additional sampling should also be performed for both fecal and mealworm guts, to be better able to ascertain the differences between the two source materials. It is also imperative that the timeline of the study be expanded to included additional timepoints. Findings in this study implicated a priming event is occurring following the introduction of polystyrene into the diet. Additional time points will help to determine if there are additional changes that occur within the microbiome following subsequent days of consumption.

Beyond the limitations of the study, future work should include follow-up studies on the most significant, and theoretically functionally pathways. Determining the impact

of specific species on the rate of consumption is important to accurately identify the species that are responsible for consumption rate. Utilizing the functional prediction results as a baseline to design in-vitro studies would be beneficial to elucidate some of these questions, and to best develop more flexible results, that would have long-lasting impacts in environmental clean-up efforts of polystyrene.

5. HUMAN APPLICATIONS

5.1 Background

Innovation in DNA sequencing technology began with Sanger sequencing in 1977 with chain-terminating sequencing, becoming more complex and available to researchers and physicians alike, with techniques like pyrosequencing and eventually, next generation sequencing (NGS) (Klindworth et al., 2013). Over the span of 4 years, research awards at the NIH went from 60 awards in 2012 to 140 awards in 2016, representing nearly 728 million dollars (NIH Human Microbiome Portfolio Analysis, 2019). Most research during this period focused on colonization of the host including microbial community impacts on physiology, metabolism, and the immune system. Community interactions was the largest aim of projects examined (approximately $551 million dollars of budget) over the presence of a specific microbe ($112 million dollars of budget). This is an important statistic when reviewing research related to the microbiome and human health, as single microbe targets for all health-related diseases may not be observable due to the focus of research. When reviewing the time of 1977 to 2017, nearly 80% of all publications related to microbiome-research were published in a four-year period of 2013-2017, thus highlighting the recent explosion of both research in this field, and promising future for human health, and disease (Cani, 2018).

5.1.1 Microbiome Consortiums

Although still in its infancy when compared to other human disease associated fields, the intersection between decrease in cost of sequencing and increase in interest in

the microbes that live within us, reached new heights in 2007 when the Human Microbiome Project (HMP) was created by the National Institutes of Health (NIH) (National Institutes of Health, n.d.-b). This 10-year, $215 million dollar initiative was launched to examine diversity and the composition of the human microbiome, in hopes to evaluate diversity patterns associated with health, and whether features of the microbiome correlated with diseases. Several important insights have been made over the decade that followed, including adjusting the view that microbes are "bad", and instead understanding the of the mutualism between the human microbiome of the gut, for example, and the host (Bäckhed et al., 2005). This understanding has setoff other large consortium-based projects, in addition to individual research experiments. The American Gut Project was launched in 2012, to explore microbes and microbiomes of a "self-selected citizen-scientist cohort" and has since sequenced over 15000 samples from over 11,000 human participants (McDonald et al., 2018). Individuals volunteer for this project through an online forum, collection kits are sent to individuals' homes, and results are compiled by organizers. These types of open-source projects offer a unique insight into a wide array of health-related questions, and in conjunction with more traditional research, contribute to our understanding of the human microbiome.

5.1.2 Microbiome Variation

Studies have shown that starting from birth, differences in the delivery method (cesarean section vs vaginal delivery) and whether a child was breastfed, key factors in microbiome composition (Gomez-Gallego et al., 2016; Moossavi et al., 2019). These breastfeeding studies have expanded the impact by having shown the impact that

breastmilk, as opposed to formula, has on microbiome formation, and immune health demonstrating one example of the interdependence between the microbiome, and its host (Morgan & Huttenhower, 2012; Walker & Shuba Iyengar, 2014). Even before the child is 3 years of age, there are three distinguished microbiome profiles, which include a development, transitional and stable phase (Stewart et al., 2018). This early development of a mature gut microbiome has even been shown to reduce the risk of disease, such as asthma, in early life, although not necessarily being a permanent part of the individual (Stokholm et al., 2018). Stability is also achieved in healthy individuals during adulthood, with limited variation not contributed to significant dietary changes or disease (Yatsunenko et al., 2012). Studies have also found that the elderly (>60) show significant microbiome shifts, over their younger counterparts (Martin et al., 2016). This does vary by source site, however, and notably must be a considering factor when analyzing data (Chaudhari et al., 2020). Understanding the pivotal milestones that causes these shifts is the focus of studies today and begets the need for age-related cohorts in disease studies as well, to not only understand causality, but also what these shifts might mean to our long-term health.

Gender-related alpha diversity differences have been noted. For example, differences in the colonization of specific species, such as the *L. ruminis* subgroup are often found over-represented in women (C. Chen et al., 2017). While it is believed that hormonal changes during puberty may be the reason for these differences, animal models have not been replicated in humans to date. Pregnancy is a significant event that may also play into these changes, as well as whether a mother decides to breastfeed. It has been shown that various parts of the female reproductive system, such as the cervical canal and uterus, have

distinct microbiomes, that may be affected during childbirth (C. Chen et al., 2017). Exacerbating these differences is the consideration of the body mass index (BMI) of an individual. Strong relationships between the gut microbiota and obesity have been observed, despite limited understanding of the mechanism behind this link (Maruvada et al., 2017). Even more specifically, significantly BMI-related differences have been noted within the female subgroups, exacerbating these relationships (Gao et al., 2018). These relationships may have foundations in gene expression, as shown in one large population-based twin study in which the human microbiome explained over 67% of the variance of the NAT2 gene, a gene responsible for visceral-fat mass (Zierer et al., 2018). This only confounds microbiome data, as the interaction of other systems may be impacting the role of the community, or this community may be having additional effects on outside systems.

Each of these factors must be balanced in a study design to ensure the confounding variables do not impact the diversity observed. To design the least biased dataset factors such as the gender, age, and BMI of study participants must be balanced to limit the demographic role that each may play in the microbiome diversity that is observed between groups. The demographic location of study participants is also important, as geographical location is likely to play a role as well, particularly if the submitting areas are different in terms of food and water supplies.

5.1.3 Microbiome and human health

Our knowledge and understanding of the human microbiota have evolved significantly over the past 20 years. Current research has shown that in healthy donors, two phyla dominate the gut microbiome (*Bacteroidetes* and *Firmicutes*), however, these

percentages can vary between 10% to 90% (Allaband et al., 2019). Significant differences in microbial diversity between healthy donors and donors diagnosed with rectal and sigmoid cancers, for example, have highlighted the potential for microbiome sampling for both diagnosis and prognosis (Xi et al., 2019). Similar potential for prognosis has been illustrated in lung cancer models, with the enrichment of oral microbes being associated with decreased survival (Segal et al., 2016).

Treatment of disease is a particularly interesting topic of research and of societal concern. Academic studies have highlighted how the gut microbiome may play a role in treatment outcomes, such as with melanoma patients who responded to immunotherapy, showing a significantly higher alpha diversity ($P < 0.01$) than those who did not respond (Gopalakrishnan et al., 2018). Clinical questions also have begun to form around microbiome-specific interventions, with the introduction of new medical treatments like the fecal transplants, where a donor fecal microbiome is "implanted" in an individual with dysbiosis; of which long term side-effects are not completely known (Bajaj, Fagan, Gavis, et al., 2019). The increase in antimicrobial resistance genes also raises new clinical questions and has led to warnings by US government and health organizations world-wide and a call for the need of better annotation, classification, and functional effects as well (Ventola, 2015).

5.1.4 Mental illness

Despite the large number of studies that have been conducted to date, there are still gaps in the research, where fields have not yet been fully explored to determine the true impact that the microbiome may have on disease physiology. One area where the

microbiome may prove to have a significant impact, is on mental health-related disease. Mental illness in the United States alone affects nearly 1 in 5 individuals, or approximately 51.5 million adults aged 18 or older (National Institutes of Health, n.d.-c). This is a complicated category of illness, with varying conditions, symptoms, onset, and treatment. Some of the most prevalent of these conditions include bipolar disorder, depression, post-traumatic stress disorder, and schizophrenia. Any understanding of their development, selection of treatment, or prevention strategies would bring significant improvements to the lives of millions of individuals worldwide.

Depression is the most common mental disorder in the United States, affecting 7.1% of adults and 13.3% of adolescents between 12-17 (National Institutes of Health, n.d.-a). This disease describes a period of at least two weeks, where an individual loses interest in daily activities, and is often accompanied by issues with sleeping, eating, and concentration. Bipolar disorder is a mental disorder, which can be categorized into three types, all which change the mood, energy, or activity levels of the individual (National Institutes of Health, 2017b). It can vary between and within an individual, with periods of elation, known as manic episodes, to periods of indifference or hopelessness, known as depressive episodes. Approximately 2.8% of U.S. adults have this disorder at any given point, and approximately 4.4% of U.S. adults are estimated to experience bipolar disorder at some point in their life. These numbers are similar in adolescents, with 2.9% of US adolescents diagnosed. Research into these diseases, not only seek to understand the mechanism between their onset, but to develop new therapeutic techniques to manage the symptoms.

Other mental disorders are not as transient and have differing mechanisms of onset and treatment options. Exposure to a potentially traumatic event may develop into post-traumatic stress disorder (PTSD), affecting approximately 3.6% of adolescents and 5% of U.S. adults (National Institutes of Health, 2017a). Symptoms of this disorder can be debilitating, ranging from frightening thoughts, to sleep problems, to being easily startled. Schizophrenia is another disorder, with an onset in the late teens to early thirties and affecting only 0.25 – 0.64% of U.S. adults today (National Institutes of Health, n.d.-d). This disorder consists of psychotic symptoms and can vary in both the frequency of episodes (although commonly persistent) and severity. These symptoms can include hallucination, unusual ways of thinking, and a reduction in the motivation to accomplish goals. Like PTSD, however, there may be events in the individual's life that reflect a significant change in brain development.

5.1.5 Mental Illness and the microbiome

Unlike many other areas of microbiome-related research, few intersections with bacteria and the brain were noted in history (Bastiaanssen et al., 2018). In the 1920's psychiatric patients had colectomies and their teeth removed under a procedure termed 'surgical bacteriology', under a physician who believed bacteria was poisoning these individuals (Wessely, 2009). While these procedures would never be performed today, this premise, that bacteria could affect the mental health of an individual, has become more supported by today's research. Through the development of sequencing and bioinformatics, several studies have been able to investigate the relationship between

microbes of the gut, and the brain focusing on the formation of the gut-brain axis (GBA) and its variation over time.

The central nervous system components of the GBA communicate through a variety of pathways, and it is understood that stress may mediate parts of this axis (Cryan et al., 2017). Research has shown a link between microbial tryptophan metabolism, influencing the GBA by producing important neurotransmitters like serotonin in tryptophan-rich media (Knecht et al., 2016). Colonization of microbiome in early life may influence the development of the serotonergic system, as well as in late life, influencing age-related health problems. Variations in the tryptophan metabolism may also be linked to cognitive deficit disorders, through a kynurenine pathway, which has been linked to cognitive changes that closely resemble Huntington's disease (Kaur et al., 2019). In addition, the vagus nerve represents the main afferent pathway between the abdominal cavity and the solitary tract in the brain. It is believed that the gut microbiota may be capable of effecting behavioral and physiological effects, which has been shown in *lactobacilli* (Bravo et al., 2011; Vécsei et al., 2013). Exploring these pathways, with a stable and well-balanced cohort, may yield important discoveries for not only the overall understanding of these diseases, but also for diagnosis and intervention.

Current research has highlighted the importance of inflammation as well, in depressive disorders. It is believed that the gastrointestinal (GI) tract's microbiome may trigger the onset of neuroinflammation, thereby triggering microglial action, and the depression pathway (Limbana et al., 2020; Sherwin et al., 2016). Microbial dysbiosis has been noted in patients with mental disorders, including depression, with variance in

Firmicutes, Bacteroides and Actinobacteria (Hemmings et al., 2017; Huang et al., 2018). The connection between inflammation and high levels of neurotransmitters has been shown, indicating the importance in regulating inflammation to curb depression-related symptoms (Jiang et al., 2015; Serafini et al., 2011). While the impact potential on diagnosis, prognosis, and treatment has clear impacts for human health, understanding microbiome differences between study attributes is key in study design.

5.2 Materials & Methods

Participants to the AGP were volunteers, who contributed a monetary donation and a biological sample. Oral samples were collected using BBL culture swabs and sent using domestic shipping to domestic posts located in Australia, the United Kingdom, and the United States. Participants also provided metadata through a web portal, which was later de-identified and published. Metadata was downloaded through NCI's portal and FASTQ files were downloaded through the European Nucleotide Archive (ENA) (European Nucleotide Archive (ENA), n.d.).

Sample groups were created based on the subject's responses to the provided AGP questionnaire. Subjects who did not answer the selected criterion questions were eliminated. Subjects who answered "yes" to the question regarding whether they had a mental illness were placed into the "afflicted" group and those that answered "no" were placed into the "healthy" group. The group was not heterogeneous for race for subsequent factors, and only individuals who identified as Caucasian were included. Groups were then stratified by additional features, including age, BMI, and sex. Age groups were identified

by decade, and subjects below the age of 20 years and over the age of 70 removed, due to low participation counts. Similarly, individuals with a BMI <18.5 were also removed from the dataset. Remaining subjects were then categorized into two BMI categories: normal (BMI between 18.5 – 30) and overweight/obese (BMI > 30). A total of 386 individuals remained. To balance the dataset between the health statuses and each sub-category, 116 individuals were used, of which 114 had sequencing data sufficient for analysis.

Raw reads were demultiplexed using QIIME2 (v2019.1) software post-sequencing, following default parameters. A denoising technique, which removes and corrects reads, before deduplicating similar sequences was utilized next. For this, the second version of the Divisive Amplicon Denoising Algorithm (DADA2) was used to generate ASV's (Callahan et al., 2016). Samples were automatically filtered due to the quality (Q) score, merging errors, and identification of chimeric reads. The Phred quality score is a measure of the quality of the identification of nucleotides, which relates logarithmically to the base-calling error probabilities (Illumina, 2011). Sequences that cannot be merged either because the sequences are too short and do not overlap, or because the sequence ends do not align, were also filtered, as were chimeric sequences identified. Finally, taxonomic classification was performed next, with the scikit-learn method (Pedregosa et al., 2011). This was performed by training reference sequences at 99% similarity, using the reference databases Silva (release SILVA 132) (Quast et al., 2013).

Alpha metrics were reviewed to determine the overall distribution of diversity. The Simpson indexes are a diversity index, more sensitive to species evenness than other methods available. Simpson's Diversity Index represents the probability that two randomly

chosen individuals belong to different species. Because it is the inverse measurement, the Simpson value indicates that as species richness and evenness increase, so does the diversity index value. Beta diversity metrics include the use of Principal Coordinates Analysis (PCoA), an eigenanalysis performed on the abundance matrix derived from a given dataset. This matrix can be calculated through different measures; either quantitative (weighted UniFrac and Bray-Curtis) or qualitative (unweighted UniFrac and Binomial). Bray-Curtis dissimilarity was chosen because a matrix can be created to compare the degree of dissimilarity between the abundance of each species in a tested variable, versus the expected abundance of that species. It can assess the distance then, between these expected abundances and those observed through the processing, and all distances are compared to determine whether there is significance to the distances. Values are bound between 0 and 1, where 0 indicates that the two samples share the same species, whereas 1 indicates that they do not share any species. Bray-Curtis may also be illustrated with the largest Eigenvalue that accounts for the greatest variance lying on one axis while the second greatest variance (or other chosen value) is placed on the second axis.

To determine the correlation of each of these expected control values, to their observed values, multiple tests were considered. A permutational multivariate analysis of variance (PERMANOVA) test, quantifies multivariate community-level differences between groups (Anderson, 2005). This PERMOVA test was performed, analyzing the variance using distance matrices of relative abundance tables. To determine if the distances between groups had any statistical significance, after creation of the Bray-Curtis distance

matrices, p-values were evaluated. The Bonferroni correction was applied, as this was a multiple-comparison assessment.

Rarefaction usage in microbiome data has been controversial and was used for all but the differential analysis, to help normalize the presence of rare OTU's or ASV's. Curves are created that graphically represent the number of samples by the number of species, or the sequencing depth by number of samples, showing an exponential curve, with an asymptote. This asymptote represents the point of saturation, where no further taxa will be added, regardless of the increases in number of reads included. These curves were created, and assessed, to determine the target sequencing depth to normalize the data, recognizing that samples with low-read counts would be removed. While this subsetting is often performed on alpha and beta diversity analysis, a comparative study illustrated the negative impact that rarefying samples had on the results of differential analysis. As such, all raw OTU counts were in differential analysis.

Taxonomic, functional prediction analysis is implemented to provide insights into the possible functional mechanisms utilized by the microbiome community identified. The Kyoto Encyclopedia of Genes and Genomes (KEGG) is a database of functions that can be mapped to genes, or in the case of microbiome research, taxonomic information generated from OTU's (Kanehisa Laboratories, n.d.). Tax4Fun, an open-source R package that predicts the functional capabilities of microbial communities using 16S rRNA datasets, was used to create KEGG pathways related to specified OTU's (Aßhauer et al., 2015). To visualize and run additional statistical measurements, R, an open-source statistical

computing and graphics software program, was utilized with publicly available packages (R Core Team, 2014).

5.3 Results

Of the 386 individuals that met the criteria, 116 samples were analyzed, subset to ensure a balanced cohort. Two samples (ERR4020670 and ERR4019056) failed to produce any sequencing reads and were dropped from subsequent analysis. The remaining cohort included the "afflicted" mental disease group (N=57) and the "healthy" mental disease group (N=55). Categorization by BMI, age and sex are described, separated by mental health status (Table 20). A binomial test was performed for percent female to ensure even distribution between the two groups (Table 25). A Welch two-sample t-test was performed for age and BMI category to ensure an even distribution between age, health status and sex and BMI, health status, and sex (Table 26). Additional stratifying by mental health sub-type was performed, with many of the subjects identifying with more than one mental illness (Table 27). For this reason, most analysis will consist of a comparison between mental health status (afflicted versus healthy) and indicate when sub-types are used for informational purposes.

Table 25. Demographic information of study samples by mental health status (healthy, afflicted), sex (male, female), BMI category (18.5-30 and >30) and age category (30,40,50,60).

		Healthy		Afflicted	
		male	female	male	Female
BMI 18.5 - 30	30	4	4	4	4
	40	4	4	4	4
	50	4	4	4	4
	60	2	4	2	4
BMI 30<	30	3	3	3	3
	40	4	1	4	1
	50	4	4	4	3
	60	4	4	3	4

Table 26. Demographic information of study samples, including a binomial test (% female) and t-test test for age and BMI by sex and health status.

	Healthy	Afflicted	p-value
Total number	57	55	
Number female (%)	27 (47.3%)	28 (50.9%)	0.55
Mean age category (female)	46.42	46.43	1
Mean age category (male)	44.14	43.33	0.7881
Mean BMI category (female)	26.5	24.68	0.42
Mean BMI category (male)	25.62	26.81	0.607

Table 27. Demographic information of mental health sub-type counts, by gender, post-sequencing filtering.

Mental Health Sub-type	**male**	**female**
healthy	29	28
bipolar, depression, PTSD	0	2
depression	25	19
depression, PTSD	0	5
depression, schizophrenia	1	1
depression, substance abuse	2	0
PTSD	1	0
PTSD, schizophrenia, substance abuse	0	1

Samples had an average number of 23,478 reads (min. 4,772, max. 45,514), with 2716 unique OTU's identified. Raw OTU counts were used, without rarefaction, due to the bias previous studies showed when subsetting datasets before this type of analysis [190]. The number of reads was stratified by mental health status showed little variation, with the healthy status (mental illness = "N") samples having ~21,131 reads and affected status (mental illness = "Y") having ~25,826 reads (Table 28, Table 29). Average number of reads stratified by IBD health status showed greater variation (healthy ~23,3212 to afflicted ~30,810), however, with large variation in data set size (afflicted N=4, health N=110) further stratification by IBD will not be used (Table 29, Figure 47).

Table 28. Average number of reads by mental health status.

Mental Health Status	N	reads	Standard deviation	se	Confidence interval
afflicted	57.00	25,826.91	9,694.19	1,284.03	2,572.22
healthy	57.00	21,131.04	3,440.06	455.65	912.77

Table 29. Average number of reads by IBD health status.

IBD Health Status	N	reads	Standard deviation	se	Confidence interval
afflicted	4.00	30,810.25	13,647.22	6,823.61	21,715.78
healthy	110.00	23,212.38	7,277.18	693.85	1,375.19

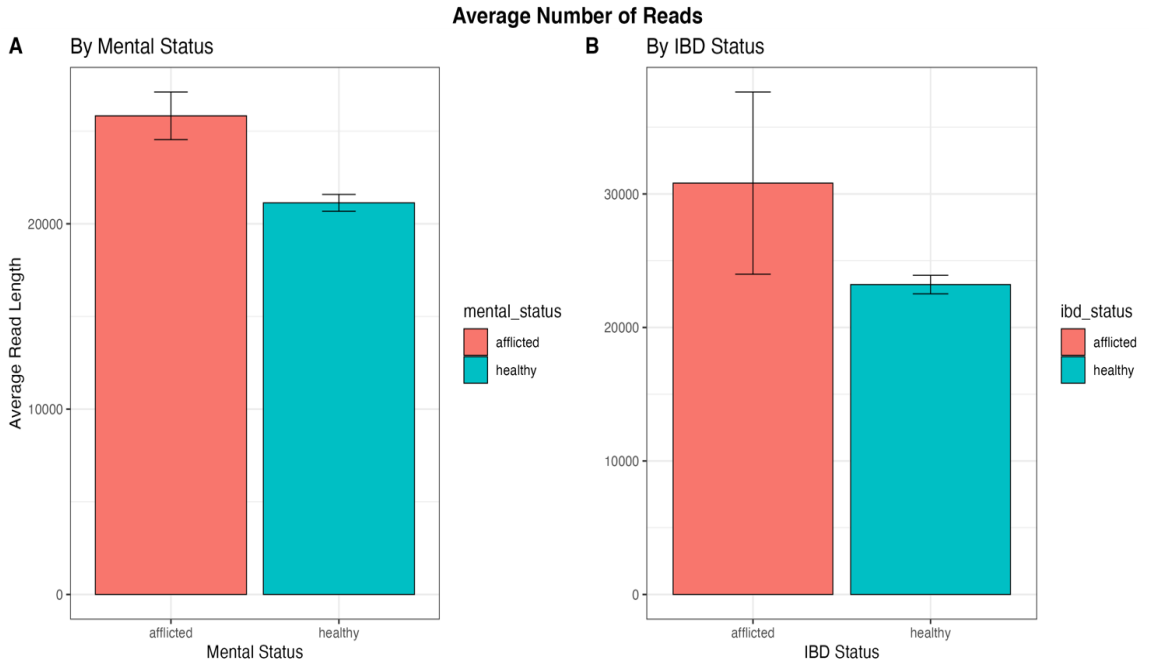

Figure 47. Average number of reads stratified by sample type and timepoint.

Most reads were identified as belonging to the bacterial kingdom (99.7%*)*, and the most abundant microorganisms were the phylum *Bacteroidetes* and *Firmicutes*, consistent with previous studies (Huang et al., 2018). Relative abundances were calculated between healthy and unhealthy groups, and differences were noted between the health statuses (Figure 48). Utilizing the Dirichlet-multinomial distribution for the relative abundance of Phylum stratified by mental health status, a significant p-value was obtained (p-value = 1.11 e-05) for the null hypothesis that there were no differences between groups. Absolute abundances were also compared, stratified by health status and mental illness sub-type, and differences noted between the two groups and within groups (Figure 49). In addition, heatmaps of abundance levels stratified by these groups also highlighted these differences (Figure 50).

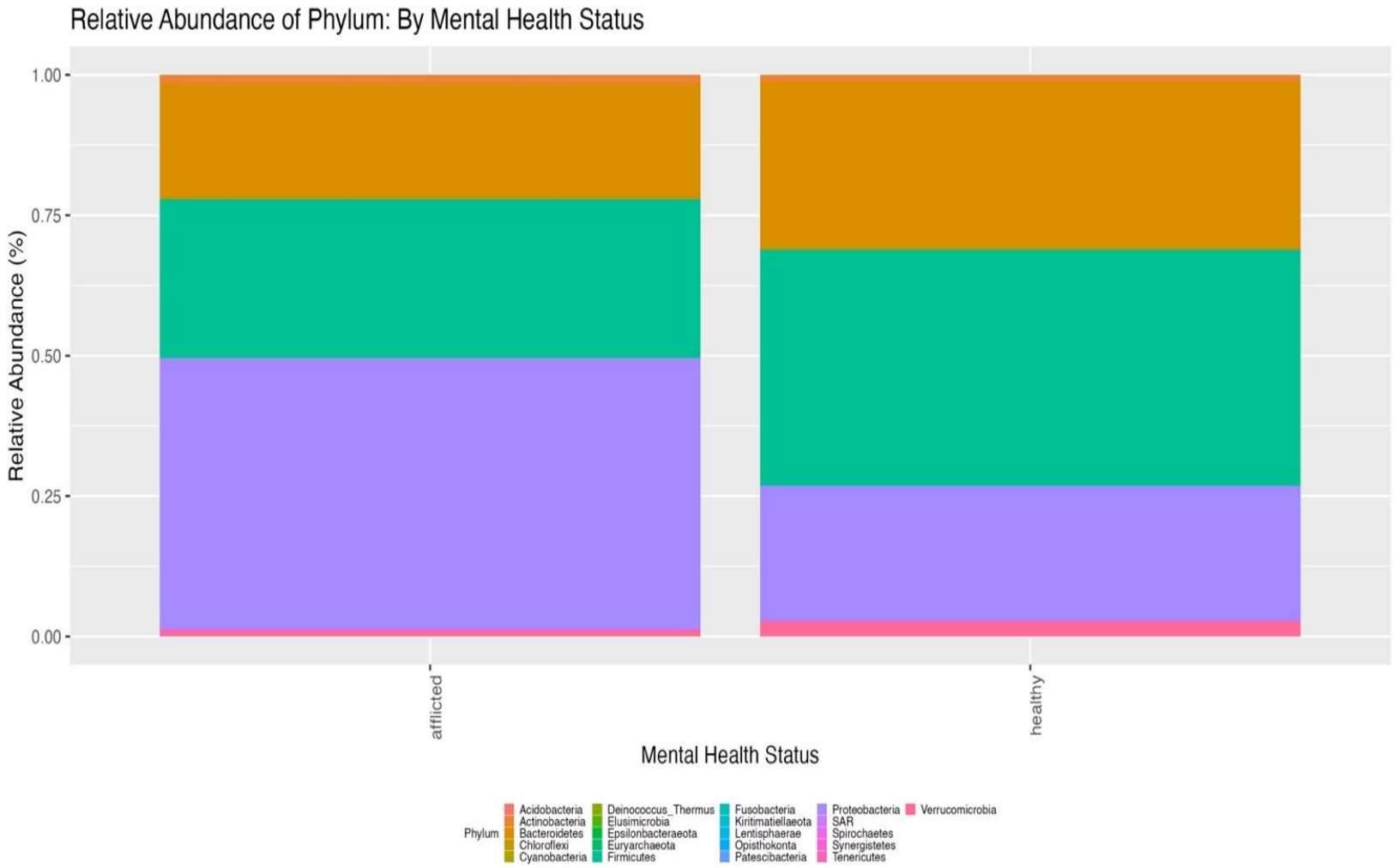

Figure 48. Relative abundances averaged stratified by diet.

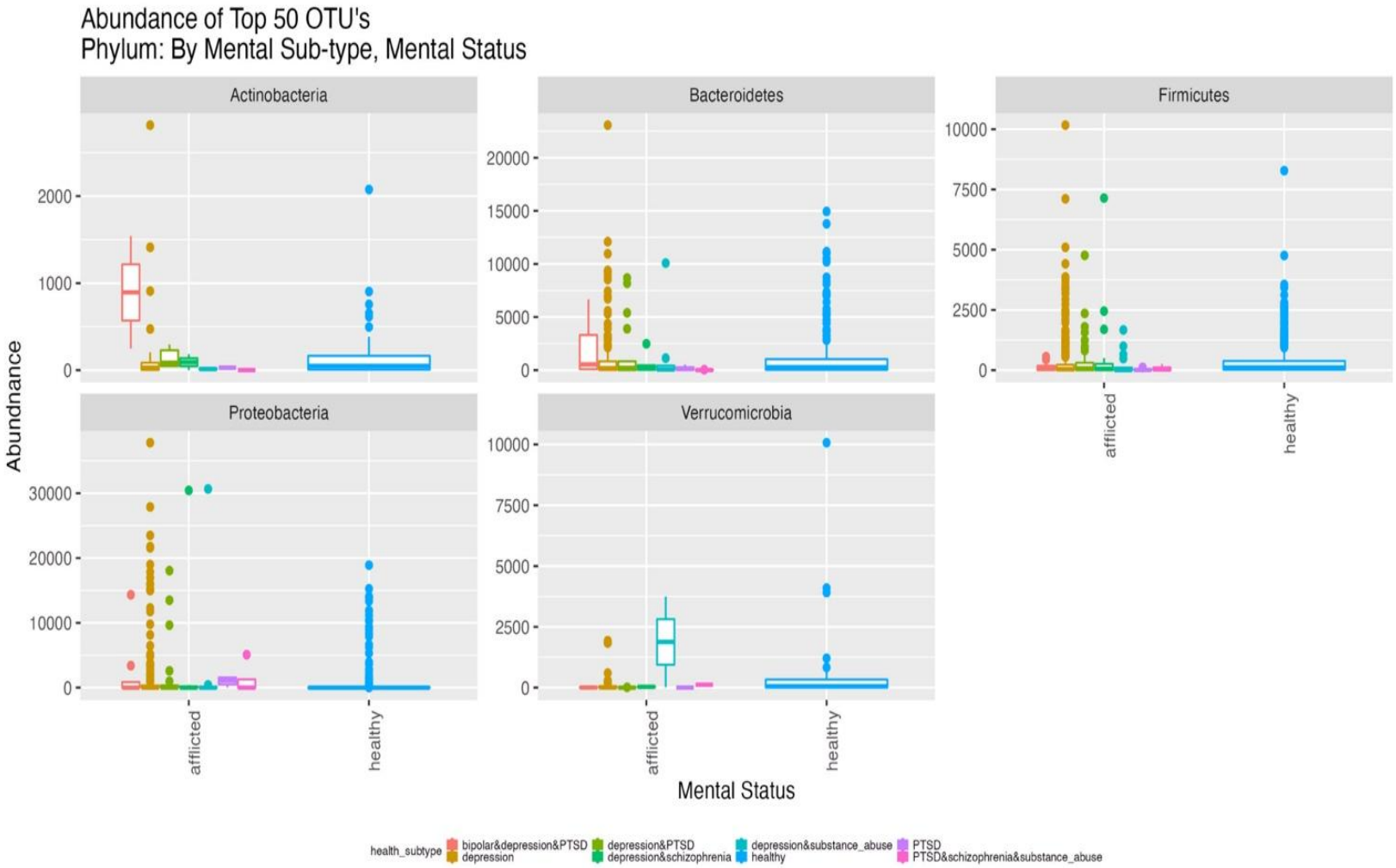

Figure 49. Absolute abundances of Phyla stratified by diet and timepoint, sub-sampled for the top 50 most abundant OTU's.

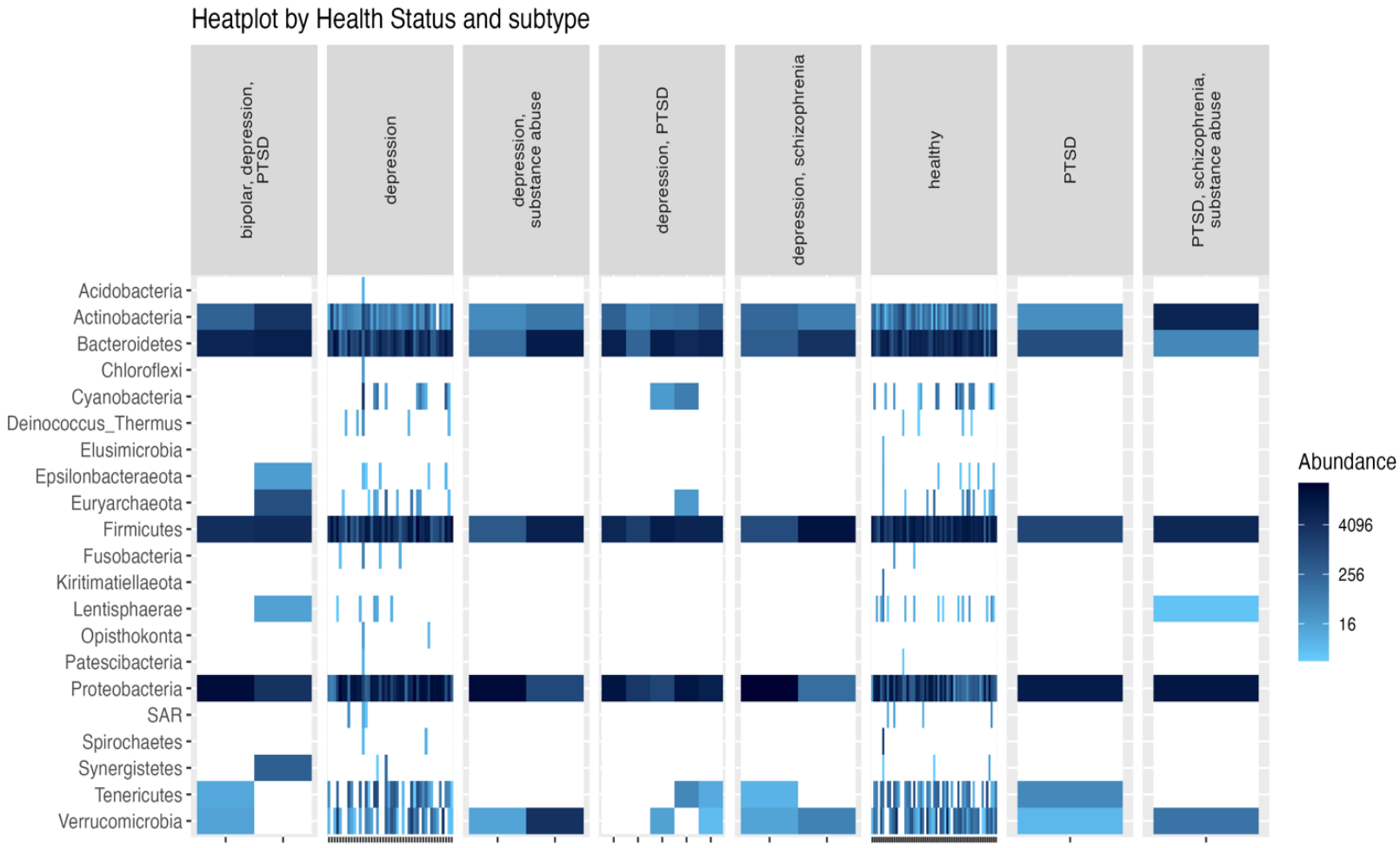

Figure 50. Heatmap of sample absolute abundance, stratified by mental health subtype.

Alpha diversity was measured using the following metrics: Inverse Simpson, Chao1 and Observed species. Diversity decreased with afflicted mental health sub-types as compared to the healthy across all three metrics (Table 30). This decrease in alpha diversity is consistent with previous studies who observed similar decreases when examining individuals with major depressive disorder[223]. Each of these metrics had significant differences between the diet and timepoint when performing a Wilcox test. Because of the multiple tests being performed, an ANOVA analysis was performed, with a Tukey multiple test correction. Reviewing Inverse Simpson results after this correction illustrated significance between mental health status (p-value 0.00102), but not between sub-type (p-value 0.128) or IBD health status (p-value 0.756) (Figure 51). As suggested by the non-significant p-value, there is no obvious trend when reviewing these metrics by health-subtype (Figure 52).

Table 30. Alpha diversity measurements stratified by mental health sub-type.

Sample Type	Mental Health Subtype	Inverse Simpson	Chao1	Observed Species
healthy		17.17 (13.7)	151.16 (58.13)	151.16 (58.13)
afflicted		9.84 (9.02)	124.16 (63.75)	124.16 (63.75)
afflicted	bipolar, depression, PTSD	12.54 (10.89)	126.5 (37.48)	126.5 (37.48)
	depression	10.35 (9.67)	129.93 (67.61)	129.93 (67.61)
	depression, substance abuse	6.28 (7)	79 (65.05)	79 (65.05)
	depression, PTSD	7.81 (7.06)	124.4 (47.32)	124.4 (47.32)
	depression, schizophrenia	8.1 (8.38)	87.5 (55.86)	87.5 (55.86)
	PTSD	7.41 (NA)	61 (NA)	61 (NA)
	PTSD, schizophrenia, substance abuse	5.49 (NA)	91 (NA)	91 (NA)

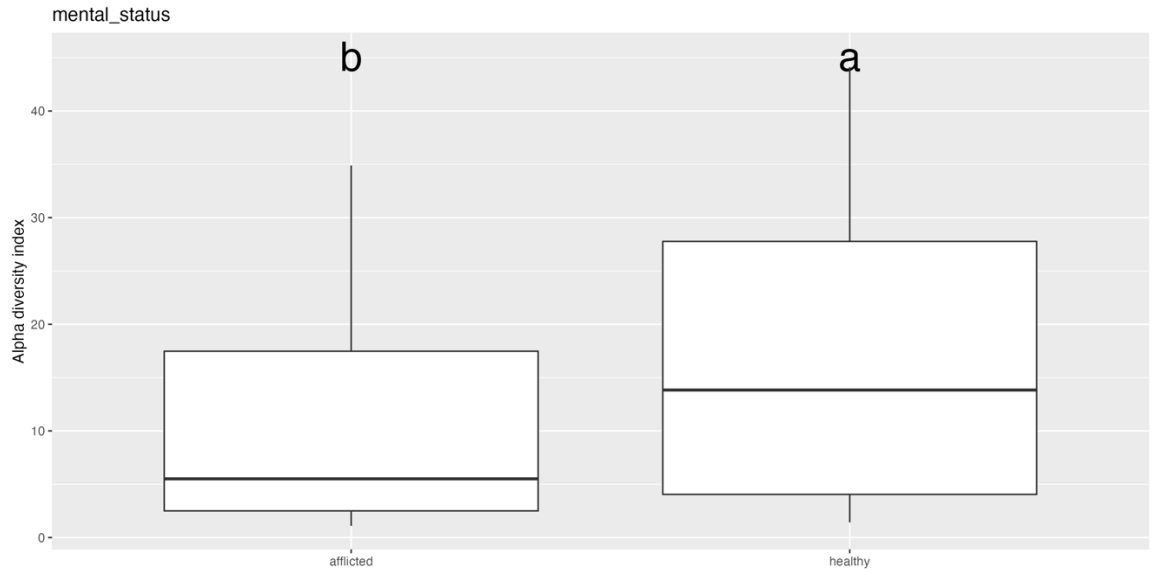

Figure 51. Inverse Simpson alpha diversity, by mental health status showing significant groupings after multiple test corrections (ANOVA, Tukey's multiple test correction).

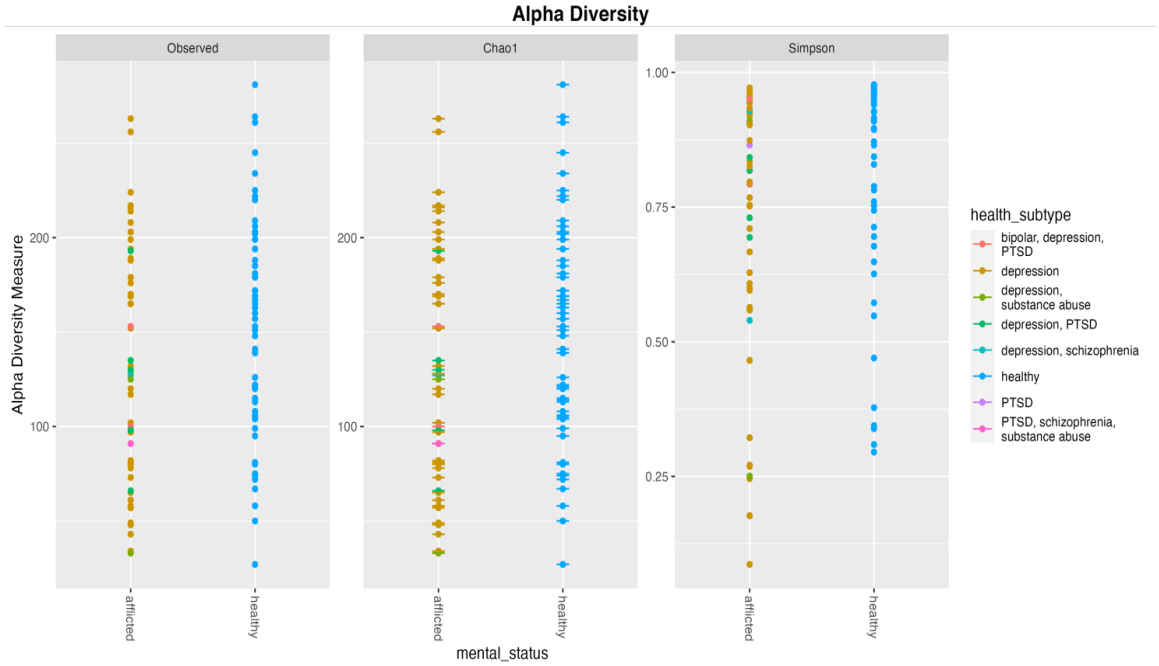

Figure 52. Alpha diversity metrics stratified by mental health status and colored by mental health sub-type.

Beta diversity analysis was performed using both principal coordinate analysis (PCoA) and NMDS using the Bray-Curtis dissimilarity index. This analysis presents points

in which the distance along the x and y axis represent the similarity of communities. Stratifying by mental health status and mental health sub-type and highlighting clustering within the samples highlighted trends between and within groups (Figure 53). An ordination plot using the Aitchison Distance was generated and overlapping values were still observed between the health statuses, with noted distribution of samples distance from the centroid (Figure 54). A permutational multivariate analysis (PERMANOVA) was performed and found to be significant by mental health status ($p = 0.001$), while the variance of homogeneity was also found to be non-significant ($p = 0.2296$). This indicates we would reject the null hypothesis of no difference in the centroid location according to these two statuses. A check of the variance of homogeneity of mental health sub-types was found to be significant (p-value 0.04) and therefore unreliable to perform this testing.

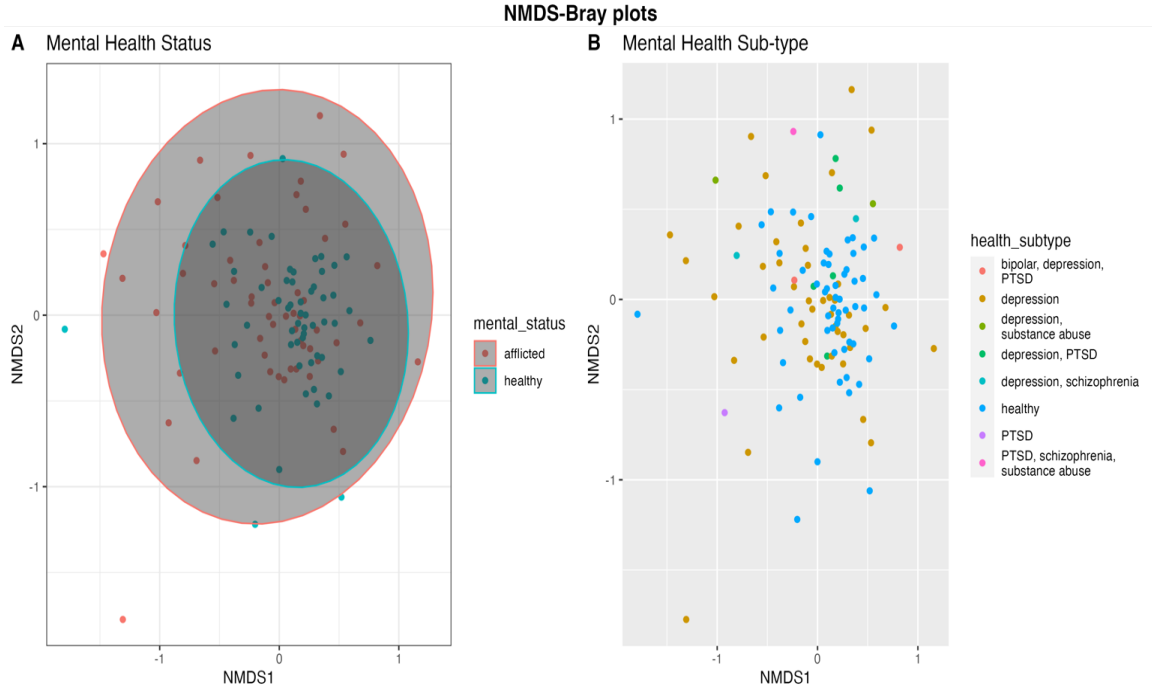

Figure 53. NMDS-Bray plots stratified by mental health status (A), mental health sub-type (B).

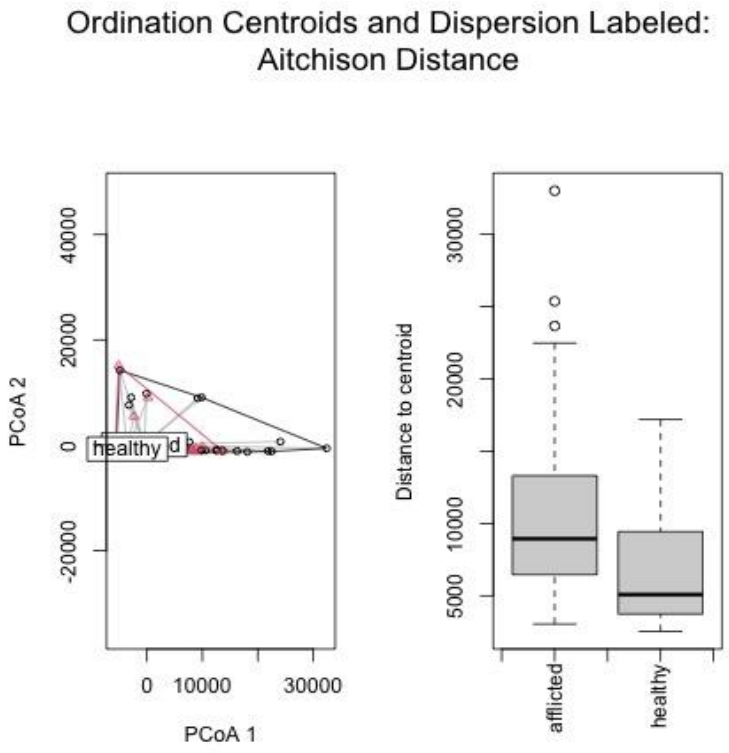

Figure 54. Ordination using Aitchison Distance (left) and stratified by diet at timepoint baseline (rice bran) and day 12 (apple slices).

Differential analysis was performed to determine significant differences in the Genera present between the two mental health statuses. Three approaches were employed, the first is the non-parametric Wilcoxon test, and the second is ANOVA-like differential expression (ALDEx2), and finally a differential algorithm based on negative binomial distribution (DESeq 2). In addition, because of the multiple comparisons being performed, the Benjamini and Hochberg (BH) correction was applied to the p-values, as appropriate. Each test has features that are particularly useful when performing differential analysis and were used to determine the continuity of results.

The Wilcoxon method indicated significantly differentiated taxa by diet, regardless of timepoint (p-value 6.616e-05), with four Phylum specifically contributing to significance even after BH FDR corrections (Table 31). When comparing the healthy donors with those afflicted with depression (only, or with another mental health disease), significant results were obtained (p-value 0.0001087), with three Phylum contributing significantly, which were identified in the comparison between healthy and afflicted mental health status (Table 32). Finally, when comparing the healthy donors with those afflicted with PTSD (only, or with another mental health disease), significant results were also obtained (p-value 0.00425), with two Phylum contributing significantly, which were identified in the comparison between healthy and afflicted mental health status (Table 33).

Table 31. Significant Phylum between mental health status, calculated with a Wilcoxon rank sum test, with continuity correction (p-value**) and BH FDR correction (BH_FDR).**

Phyla	**p-value**	**BH_FDR**
Proteobacteria	6.62E-05	6.62E-05
Verrucomicrobia	6.18E-03	6.18E-03
Firmicutes	1.78E-02	1.78E-02
Bacteroidetes	4.86E-02	4.86E-02

Table 32. Significant Phylum between healthy mental health samples and those afflicted with depression, calculated with a Wilcoxon rank sum test, with continuity correction (p-value**) and BH FDR correction (BH_FDR).**

Phyla	**p-value**	**BH_FDR**
Proteobacteria	1.09E-04	1.09E-04
Verrucomicrobia	5.67E-03	5.67E-03
Firmicutes	2.58E-02	2.58E-02

Table 33. Significant Phylum between healthy mental health samples and those afflicted with PTSD, calculated with a Wilcoxon rank sum test, with continuity correction (p-value**) and BH FDR correction (BH_FDR).**

Phyla	**p-value**	**BH_FDR**
Proteobacteria	4.25E-03	4.25E-03
Verrucomicrobia	1.22E-02	1.22E-02

The second method employed was ALDEx2 is a Co-Occurrence of Domains Analysis (CoDA) method, developed for next-generation sequencing analysis, which employs Monte-Carlo sampling from a Dirichlet distribution with a small non-zero sum. The ALDEx2 is a much more conservative approach, however, did find one significant Phylum (*Firmicutes*) significant between mental health status, falling within the first and third quartiles after the CLR transformation (Figure 55). This is consistent with the Wilcox method results described above.

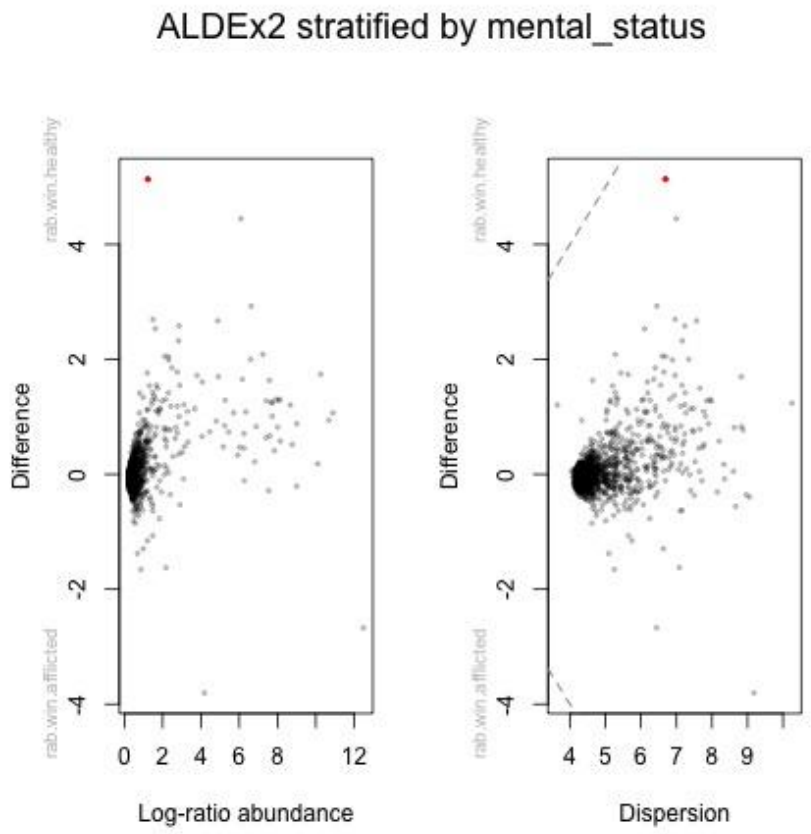

Figure 55. ALDEx2 log ratio abundance (left) and dispersion (right) plots for OTU's stratified by diet, indicating no significant results.

Genera were found to be significantly different between diets using the DESeq2 method (N=2), both associating with the afflicted mental health status (positive) (Figure 56, Table 34). Performing a crosswise comparison between healthy donors with those afflicted with depression (only, or with another mental health disease), also found significant results in the same two Genera (Figure 57). The final comparison between healthy donors and those with PTSD (only, or with another mental health disease), showed one common genera (*Faecalibacterium*) and two additional Genera (*Bacteroides* and

Collinsella), although the associations were all to the healthy status over the afflicted PTSD status (Figure 58). These results do compare overlap with some results found using the Wilcoxon and ALDEx2 methods, as the genera *Faecalibacterium* belongs to the Phyla Firmicutes.

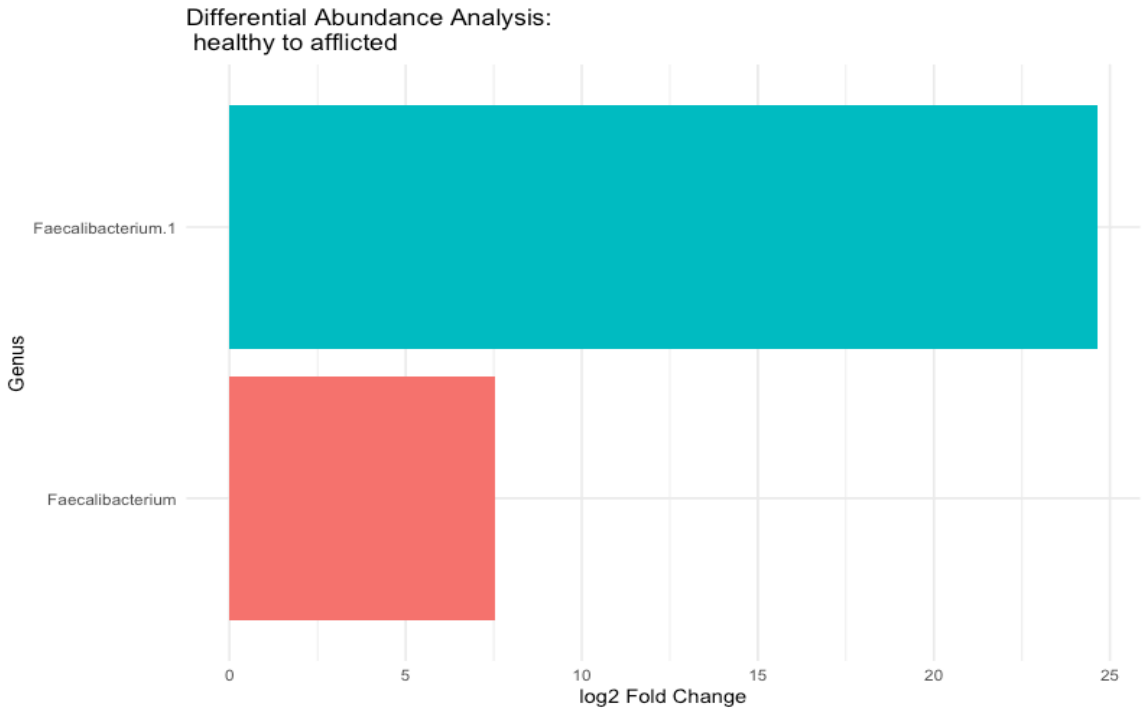

Figure 56. Differential abundance analysis, between varying mental health. P-values were adjusted using the BH correction and filtered (p-value <0.05). The fold change direction (log2) relates to the stronger association with afflicted (positive) over healthy (negative

Table 34. Top significant genera differentially expressed by variable with BH corrected p-value shown.

Phyla	Genera	Mental health status	HtoD	HtoP
Firmicutes	*Faecalibacterium*	8.58E-08	9.63E-08	5.83E-06
Firmicutes	*Faecalibacterium.1*	5.98E-38	1.15E-37	NA
Bacteroidaceae	*Bacteroides*	NA	NA	0.01429763
Actinobacteria	*Collinsella*	NA	NA	0.00204975

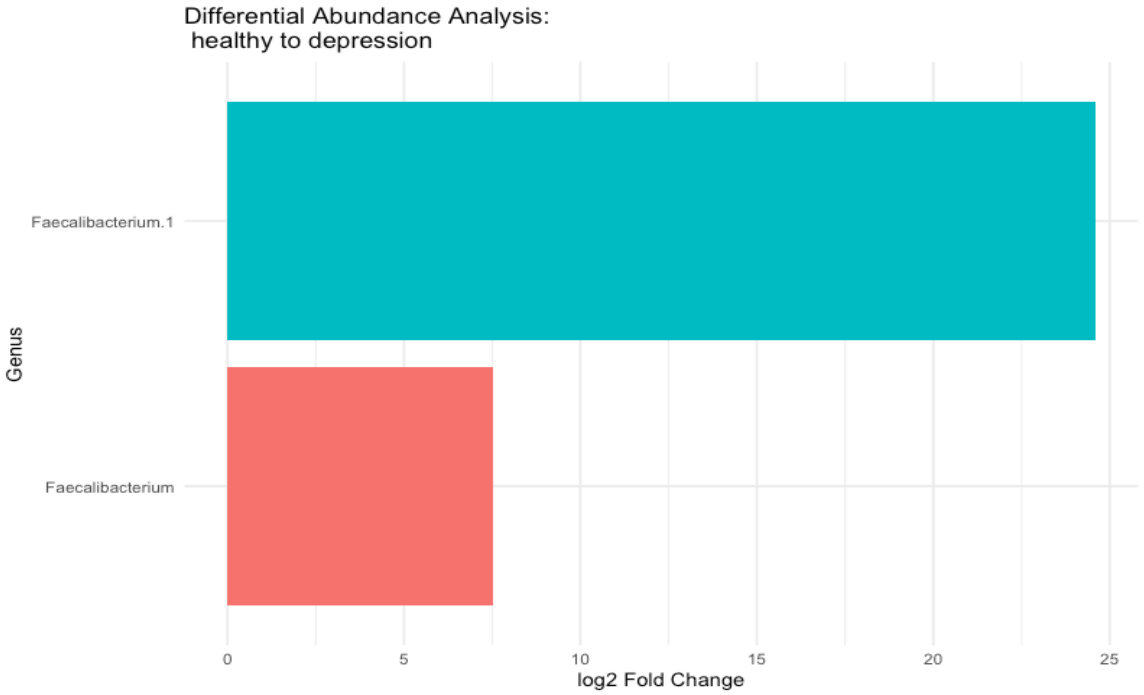

Figure 57. Differential abundance analysis, between mental health status of healthy and those with depression. P-values were adjusted using the BH correction and filtered (p-value <0.05). The fold change direction (log2) relates to the stronger association with afflicted (positive) over healthy (negative).

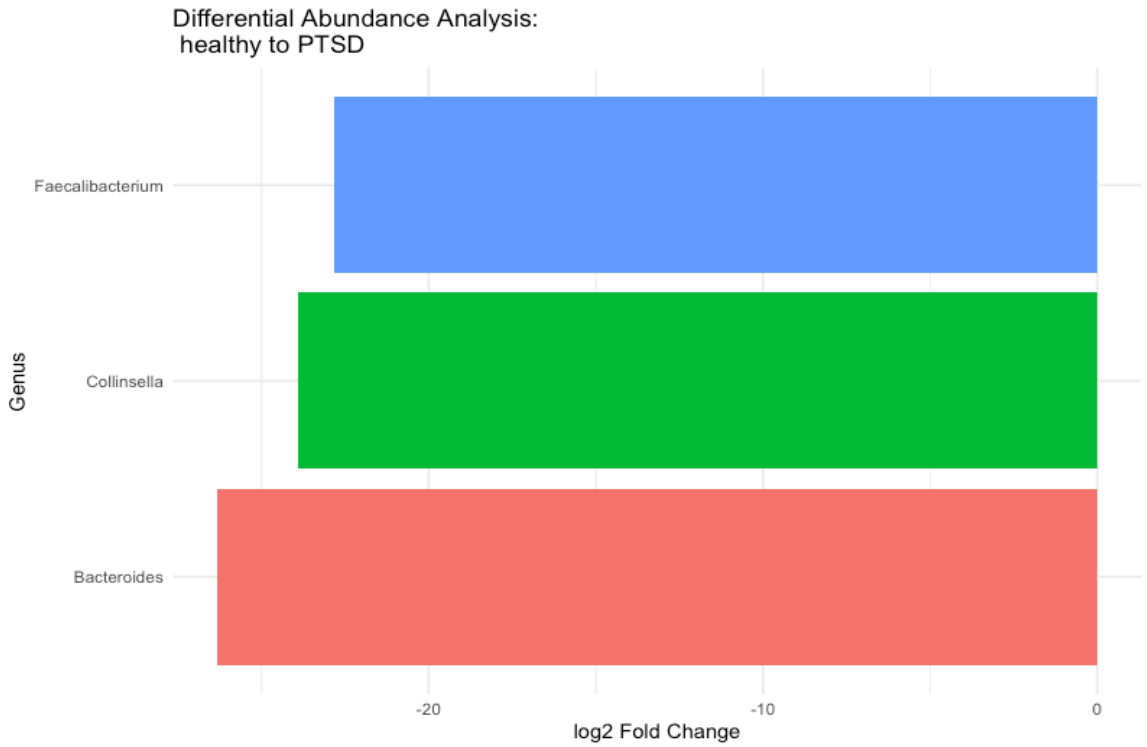

Figure 58. Differential abundance analysis, between mental health status of healthy and those with depression. P-values were adjusted using the BH correction and filtered (p-value <0.05). The fold change direction (log2) relates to the stronger association with healthy (negative) over afflicted (positive).

Prediction modeling was performed, in R using two methods – the first a CODA method using an R software package called rms, and the second using a R software package Selbal (Lüdecke, n.d.; UVic-omics, n.d.). To begin, the full model was fit, and a grid search was performed to determine the optimal value for penalty (simple penalty = 1, non-linear penalty = 200). Plotting the resulting log odds ratio showed the associations were linear, however, to correct for the degrees of freedom, cubic spline was used in the full model (Figure 59). PC1 – PC3 were reviewed to determine the strength of prediction with PC1 having the highest strength, representing 62% of the diversity. A full bootstrap resampling was then performed to determine the model performance, with decent results for the model

prediction (Figure 60). The mean absolute error was 0.041, the mean squared error 0.0022, and the 90th quantile of absolute error was 0.066. Both the prediction of depression or PTSD over healthy mental status was worse using this method, with the 90th quantile of absolute error being 0.1 and .068, respectively, however, not significantly.

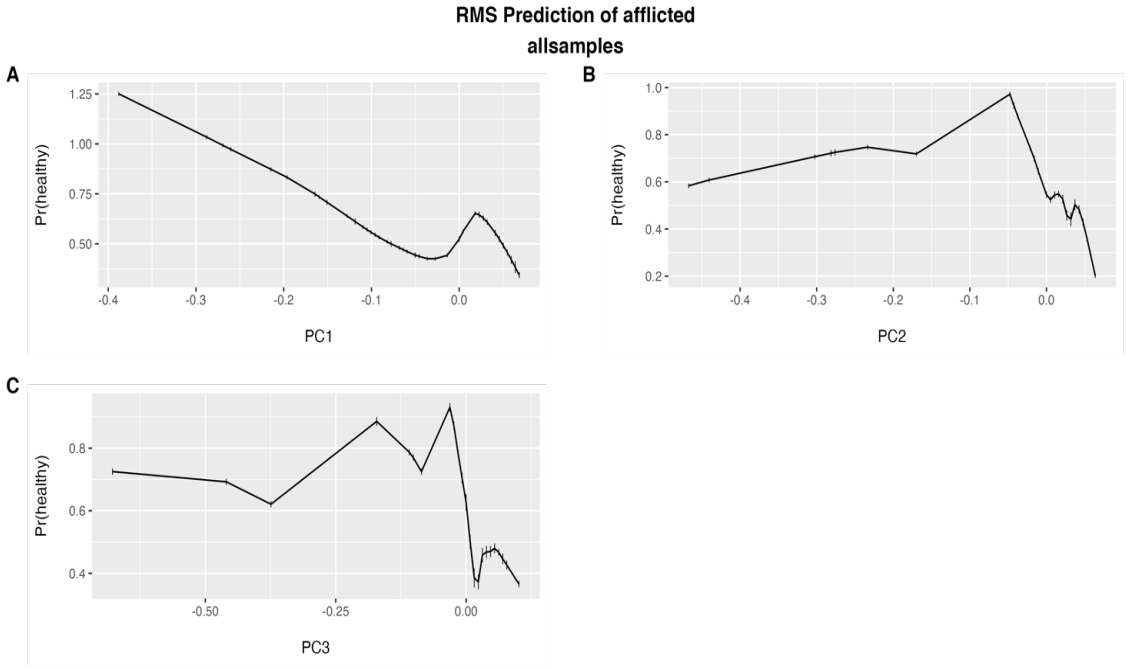

Figure 59. RMS prediction values of all samples, for mental health afflicted status, stratified by PC1, PC2, and PC3.

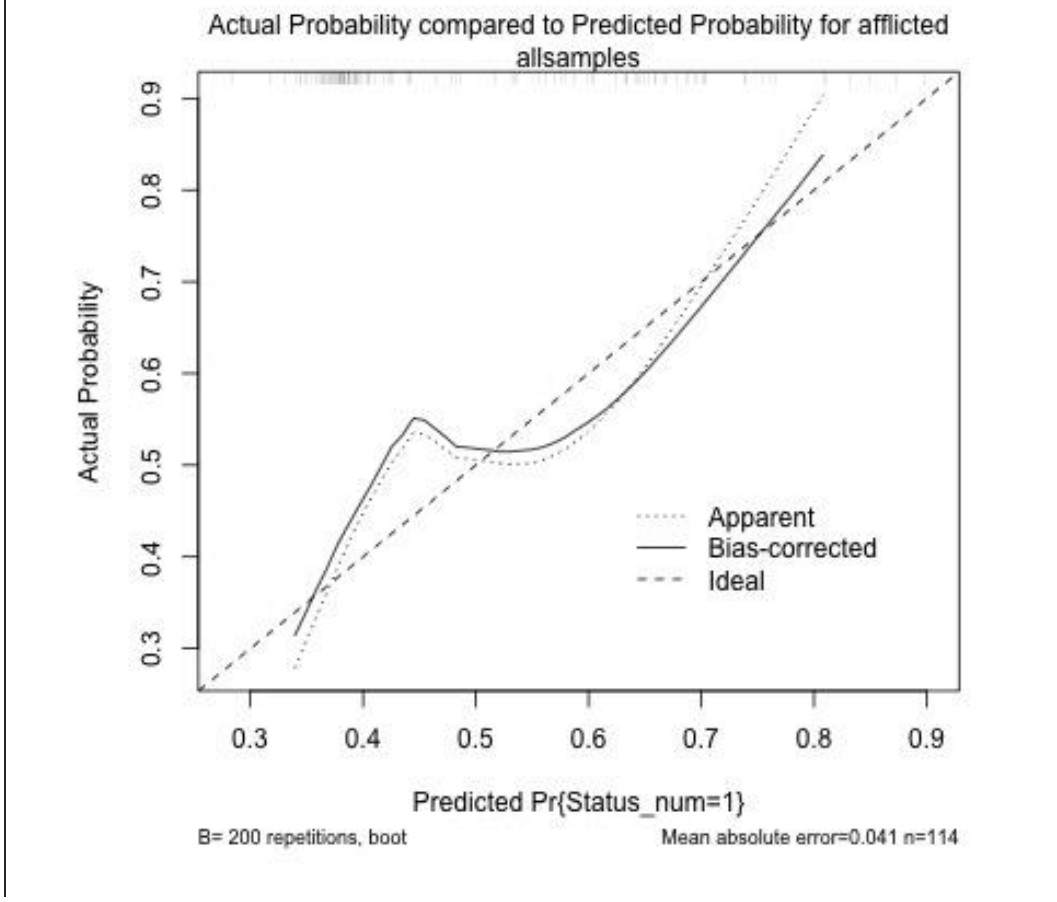

Figure 60. RMS prediction performance probability for all samples, to determine mental health afflicted status.

Selbal uses a forward-selection method for identification of taxa groups whose relative abundance is associated with a particular response variable. This microbial signature can then be used as a predictor for group identification by performing multiple regressions, adding a new taxon with each iteration. Rare taxa were removed (N<200) to balance bias. The Phyla with the strongest predictor for healthy status was *Proteobacteria*,

and three for afflicted: *Verrucomicrobia*, *Synergistetes* and *Spirochaetes* (Figure 61). The discrimination value of the area under the curve (AUC) is established when no additional variable (taxa) improves the current optimization parameter (Figure 62). In addition, a cross-validation procedure is performed to explore the robustness of the balance between taxa. The AUC-CV for this prediction is 0.719, the top Phyla for health status prediction (*Proteobacteria*) present in all CV, and the top Phyla for afflicted status prediction (*Verrucomicrobia*) present in 60% of all CV.

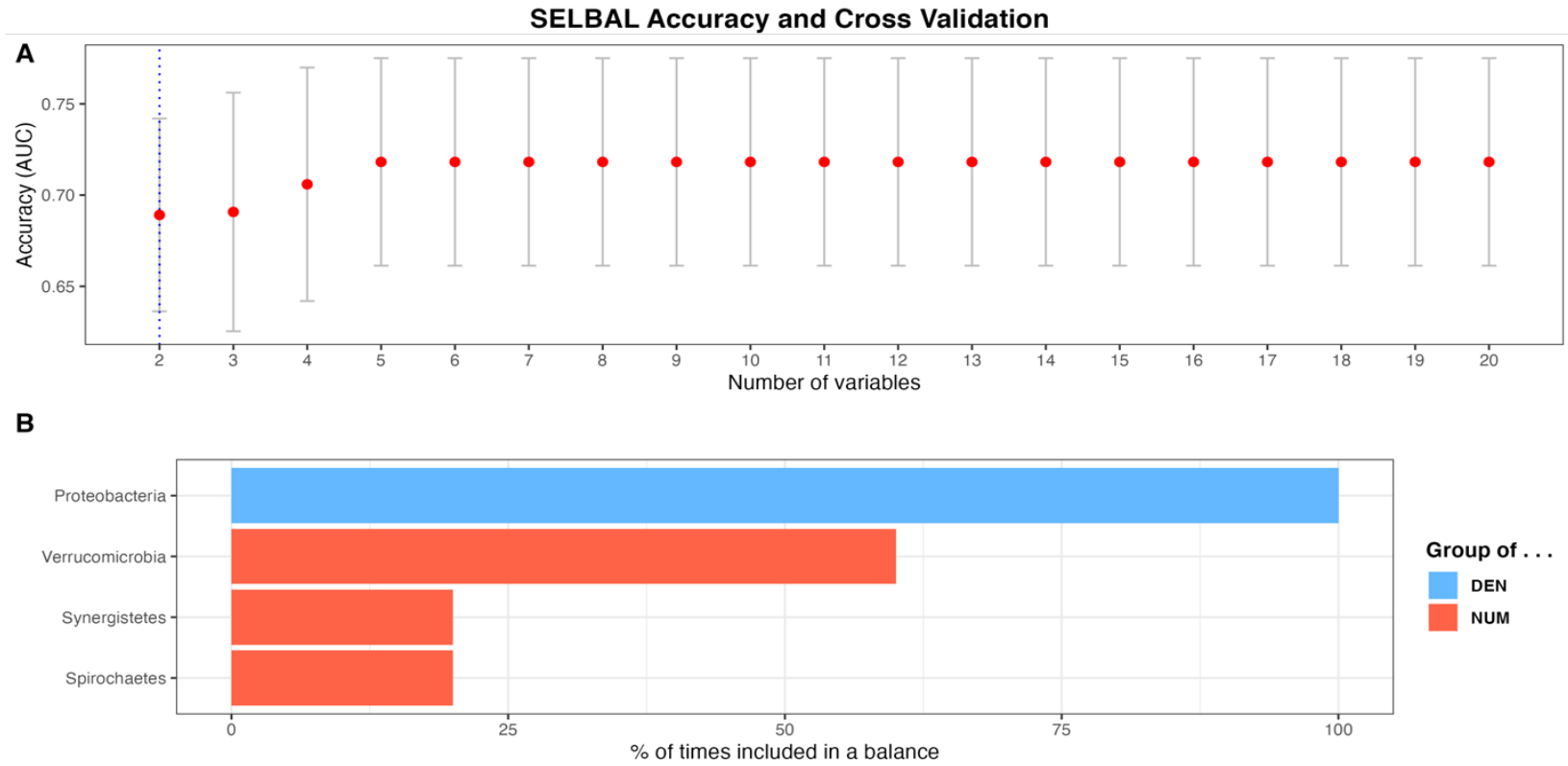

Figure 61. AUC (A) for variables and bar plot (B) representing the frequency of variables selected in CV process, defined by the numerator (rice bran) and denominator (apple slices).

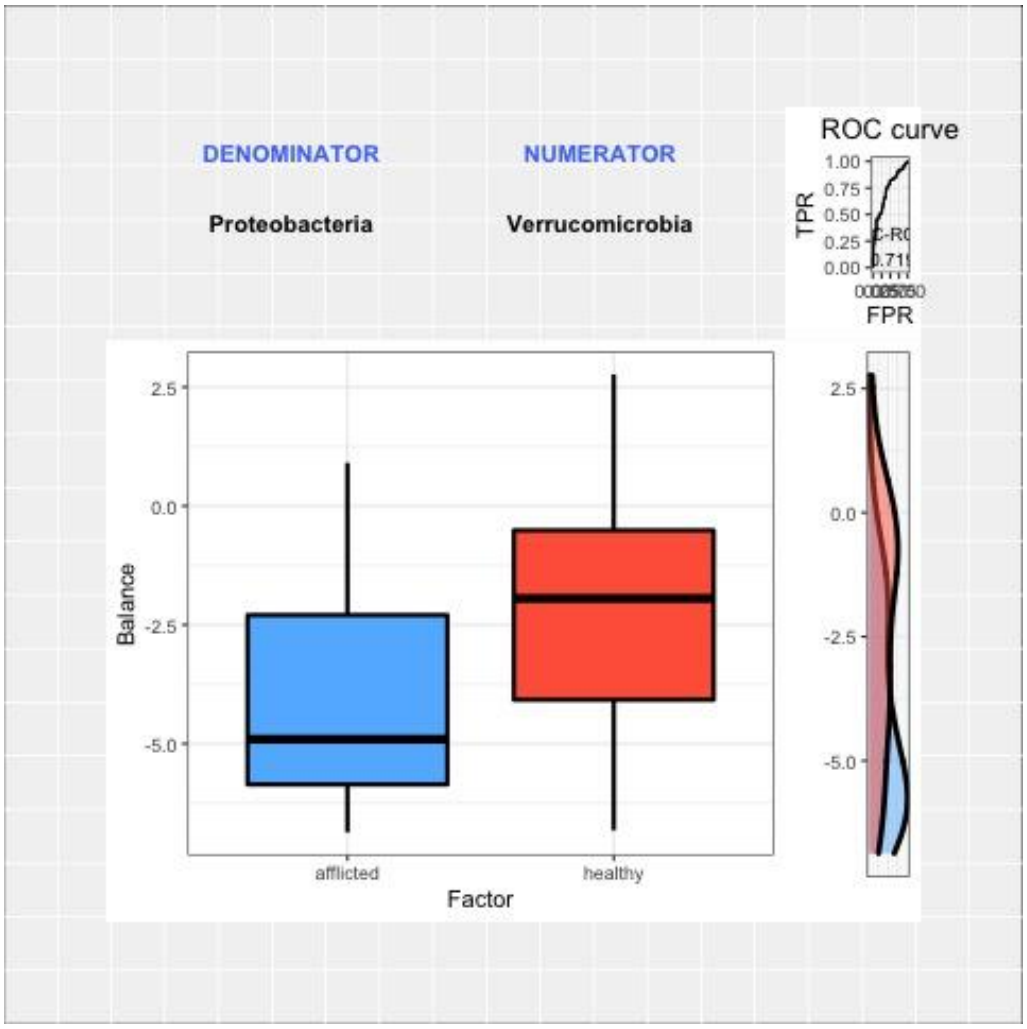

Figure 62. Selbal prediction analysis for diet, with all samples included.

Functional prediction was performed, using two methods: an R software package Tax4Fun and a QIIME2 plugin for PICRUST2. An exploration of significant OTU's (p-value <0.01) using Tax4Fun analysis revealed several predicted pathways related to alcoholism, metabolism, and longevity regulating pathway, with the top 10 KO pathways reviewed (Table 35). Utilizing a structural topic model (STM), which uses a machine learning approach to estimate relationships between text inputs, in this case KEGG

pathways, top pathways can be grouped, identified, and visualized[194]. Associations are assigned as 'topics' and plotted as an estimation towards healthy status (red) or afflicted mental health status (blue) (Figure 63). Then, these topics can be examined in the heatmap, showing the function-topic interaction. Yellow and dark blue are representative of relative abundances (high and low respectively) and were used to explore relevant pathways (Figure 63). The top pathways discovered included glycan degradation, galactose metabolism and ABC transporters. Of particular interest is the glycan degradation pathway, which has been found to be downregulated in individuals with depressed, suicidal thoughts, consistent with these findings (Serafini et al., 2011).

Table 35. Top 10 KEGG KO pathways determined by Tax4Fun.

Pathway Descriptions
alcoholism
carbon metabolism
oxidative phosphorylation
longevity regulating pathway - multiple species
nucleotide excision repair
porphyrin and chlorophyll metabolism
rna degradation
purine metabolism
starch and sucrose metabolism
purine metabolism

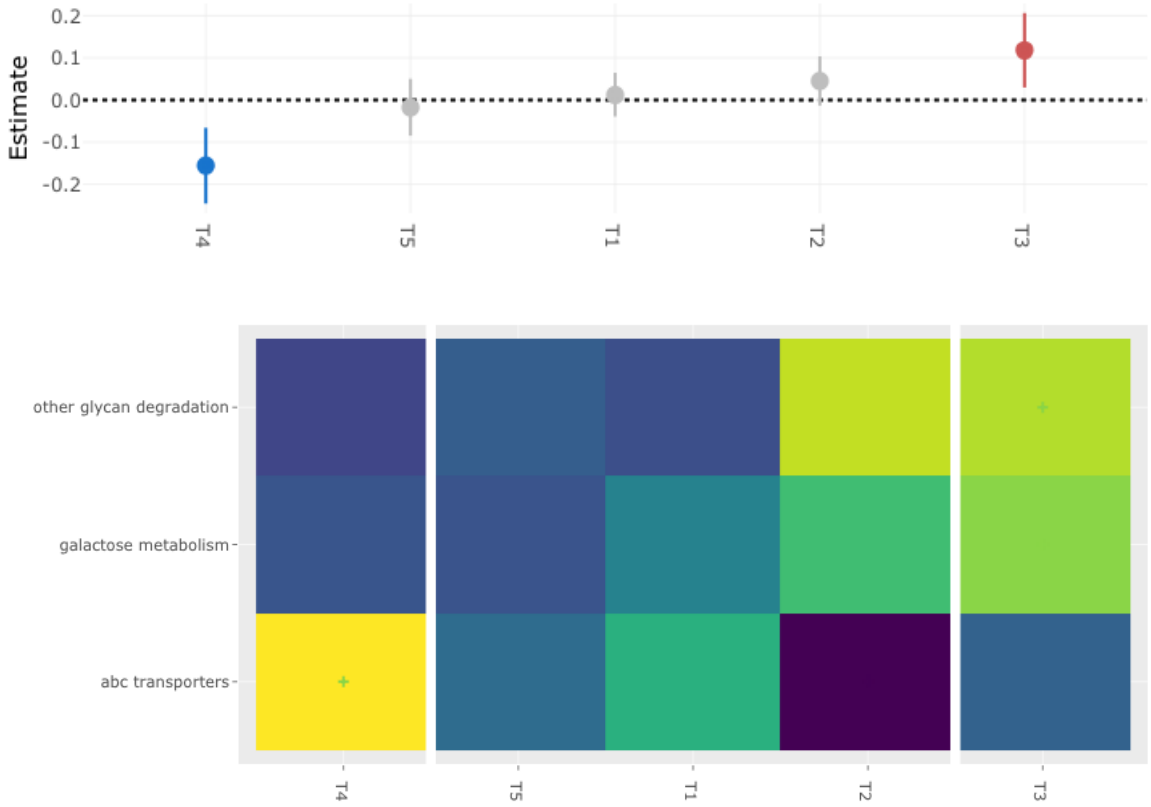

Figure 63. Functional prediction by topic with estimate cause of variance (TOP) and heat map (BOTTOM).

PICRUST2 and STAMP were employed next, to determine additional functional significance, and differentiation between the mental health status of healthy and afflicted individuals (Figure 64). Results from this prediction tool highlighted 140 significant pathways (corrected p-value <0.01), of which the top 5 significant pathways are shown (Table 36). The most significant of these being PWY-6628 (corrected p-value 3.5E-05) is super pathway of L-phenylalanine biosynthesis, recently shown to be important in the selective-decision making process of those with depression (Figure 65) (Roiser et al.,

2005). Although not in the top five, a still significant pathway that correlates to other recent research is the Kdo2-lipid A biosynthesis pathway (p-value 1.9E-03) (Figure 66) (Nguyen et al., 2021).

Table 36. Top 5 significant differentiated pathways generated from PICRUST2.

Pathway ID	p-values (corrected)	Effect size	afflicted: mean rel. freq. (%)	afflicted: std. dev. (%)	healthy: mean rel. freq. (%)	healthy: std. dev. (%)
PWY-6628	3.5E-05	0.14	0.41	0.10	0.31	0.14
PWY-6630	6.0E-05	0.13	0.40	0.10	0.31	0.14
GLYCOLYSIS-E-D	6.7E-05	0.13	0.37	0.13	0.26	0.15
PWY-7254	9.8E-05	0.13	0.32	0.18	0.19	0.18
HEMESYN2-PWY	1.6E-04	0.12	0.28	0.15	0.18	0.13

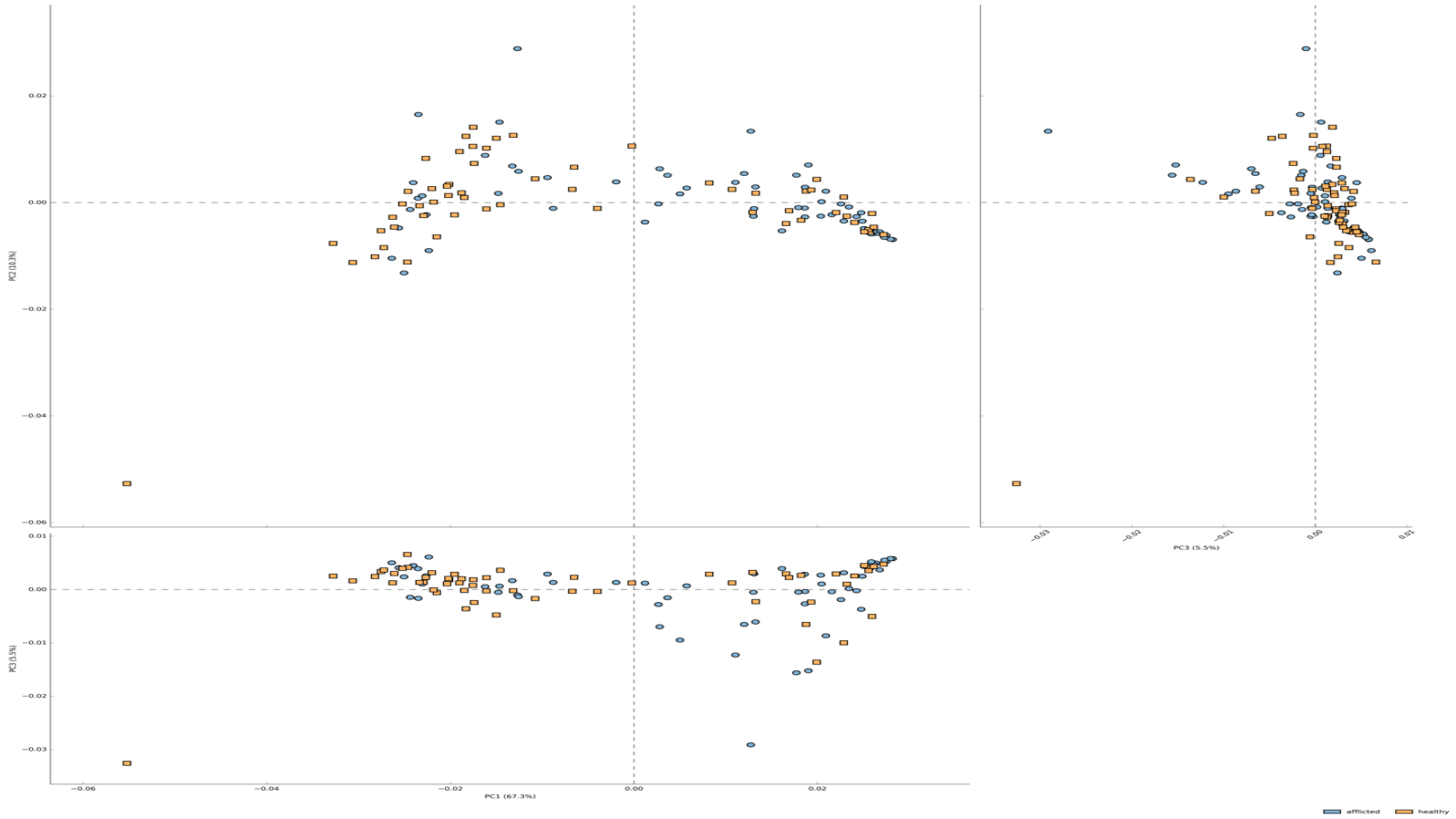

Figure 64. Crosswise comparison of PCoA 1 through PCoA3, for mental health status (color), from PICRUST2 and STAMP analysis.

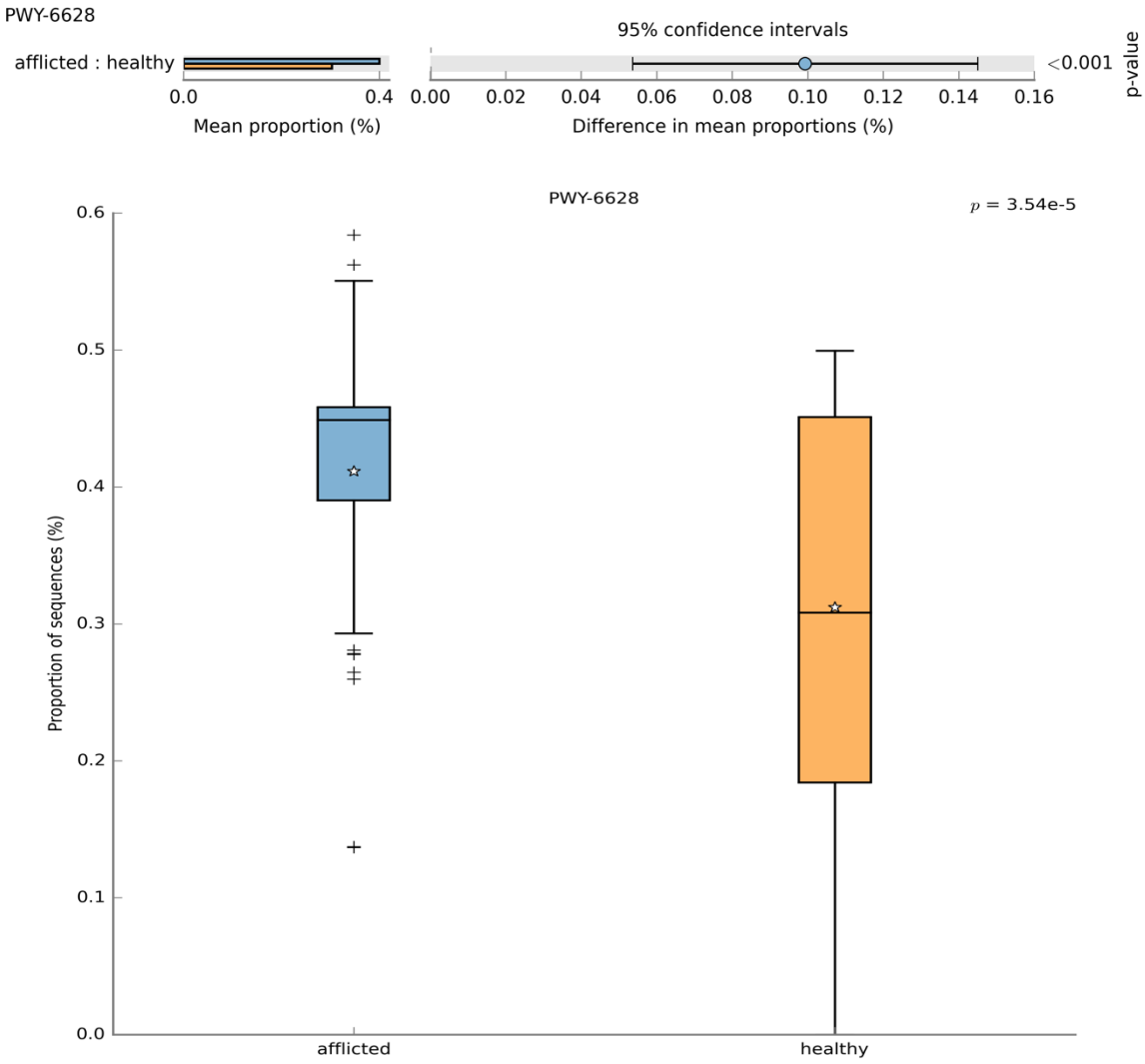

Figure 65. Most significant functional pathway, significantly differentiated between the mental health statuses (P6628-PWY), using PICRUST2 and STAMP for visualizations.

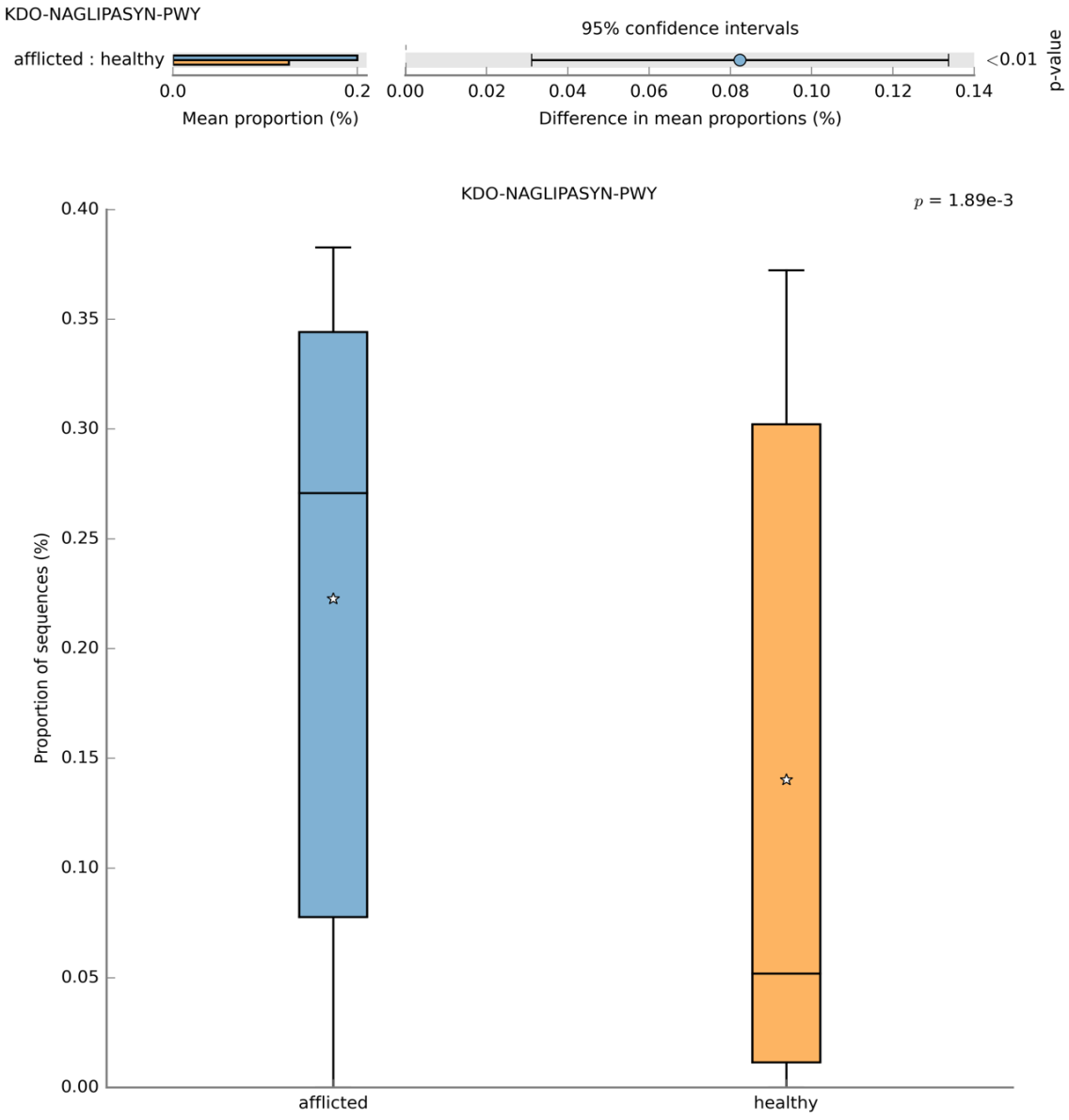

Figure 66. Recently highlighted significant functional pathway, significantly differentiated between the mental health statuses (KDO-Naglipasyn-PWY), using PICRUST2 and STAMP for visualizations.

5.4 Discussion

Exploration of the microbiome diversity between cohorts of individuals with and without mental health statuses is of critical importance. Significant relative abundance

differences between cohorts elucidate the need for microbiome research related to the onset and development of mental health (PTSD, schizophrenia, depression, bipolar disorder). Despite having differing manifestations, significant differences between phyla point to potential biological similarities between these mental health diseases. Because the sub-types were not well-balanced between gender and total value, differences could not be explored, and further studies are needed. A check on IBD status did not produce significant differences in average read length and so was not addressed, however, should be considered as a confounding factor in any future work.

The phyla *Firmicutes* had the highest number of significant OTU's, followed by *Bacteroidetes* and *Actinobacteria* in both groups. This supports previous work of two major depressive disorder studies, which also found several significant OTU's within the *Firmicutes* phyla. *Actinobacteria* has been of particular interest, due to the previous work hypothesizing that a may be related to an anti-inflammatory response, thereby increase vulnerability to PTSD (Jiang et al., 2015; Sherwin et al., 2016). When comparing the differences in relative compositions, the levels of both *Firmicutes* and *Actinobacteria* decrease, whereas Proteobacteria increase, as compared to the healthy mental status subject, highlighting potential phyla of interest. When reviewing the levels by sub-type we can see that bipolar, depression, and PTSD afflicted subjects have notably more Actinobacteria in their composition over any other sub-type, and the healthy controls. The combination of mental health diseases may be complicating finding clear correlations in microbiome studies.

A significantly lower alpha diversity within the unhealthy cohort has not been consistent between previous research on mental health disorders. In a PTSD cohort recently studied no significant differences were noted, however, in individuals with major depressive disorder and those with ADHD, significant decreases were note (Limbana et al., 2020; Prehn-Kristensen et al., 2018; Sherwin et al., 2016). These results are in line with this second finding, namely a decrease in the overall diversity of those afflicted with mental disease. We see that when averaging all mental diseases that there is a clear decrease in diversity metrics, as well as when reviewing the sub-types within those afflicted with mental disease, with the PTSD, schizophrenia and substance abuse sub-type having the lowest overall diversity with all metrics. Bray-Curtis dissimilarity matrices did not provide clear clustering differences when using NMDS1 graphs, although PERMANOVA analysis did present significant differences between phyla of the healthy and afflicted groups. Since the variance of homogeneity was found to be non-significant, this increases the confidence of these findings between these larger classifications, which was not found between each individual sub-type.

Differential analysis provided some insight into those phyla and genera that may be consequences of the illnesses presented or causing their manifestation. Four genera were found to be significant with the Wilcoxson rank sum test between healthy and afflicted individuals, including *Proteobacteria*, *Verrucomicrobia*, *Firmicutes*, and *Bacteroidetes*. Three of these phyla were also significant when comparing the healthy donors to the depression sub-type (*Proteobacteria*, *Verrucomicrobia*, *Firmicutes)* and two of these (*Proteobacteria*, *Verrucomicrobia)* were significant when comparing the healthy donors

to the PTSD sub-type. A similar result (*Firmicutes*) was found when reviewing the output of the second differential method, ALDEx2, and the third, DESeq2. DESeq2 highlight two additional phyla, however, (*Bacteroidaceae* and *Actinobacteria*) in the healthy to PTSD sub-type, that was not seen in the other methods. The fact that same phyla (*Firmicutes*) was repeatedly identified as significant increases in all three methods highlights the importance of future work attempting to better understand the possible mechanism of relation between depression and PTSD, and the dysregulation of these phyla from healthy samples. This is particularly convincing, as other research has highlighted the possible association of firmicutes in the gut with those who have depressive disorders (Huang et al., 2018). The hypothesis is that because Firmicutes can ferment carbohydrates to a variety of short-chain fatty acids (SCFA's), the decrease of SCFA's in depressed individuals will lead to a decreased intestinal barrier, and therefore stimulate an immune response, leading to inflammation and other symptoms of the disease.

The second finding from this differential analysis is the fact that the phyla *Actinobacteria*, *Firmicutes*, *Bacteroidetes*, and *Proteobacteria* were highlighted using different methods. Recent studies have highlighted the importance of the tryptophan metabolism, which is believed to produce microbial metabolites, or neuro-active metabolites, which have been suggested to alter the function of the gut-brain axis (GBA) (Kaur et al., 2019). This pathway has been associated with *Actinobacteria, Firmicutes, Proteobacteria and Bacteroidetes and Fusobacteria* – 4 of 5 phyla that were significantly different between our groups. Selbal correlated to several of the phyla already highlighted, including *Proteobacteria* and *Verrucomicrobia*, while adding two additionally significant

phyla, *Synergistetes* and *Spirochaetes*. When running the prediction analysis, the strongest predictor for healthy status was *Proteobacteria*, and for afflicted: *Verrucomicrobia.* Again, these two phyla have been highlighted in recent work

There are several reasons to explain for some of the variation between differential analysis approaches. First, may be related to the differences in uses of the CRL basis, of which the Wilcoxon method uses the geometric mean, whereas the ALDEx2 method uses the IQLR. The Bayesian resampling with a non-zero prior may also be altering the results, as employed with the ALDEx2 method. The median log2 fold difference by median log2 dispersion illustrates the effect size by variability, highlighting the differentially abundant taxon where the difference most exceeds the dispersion.

Several functional pathways were identified as statistically significant between cohorts. Functional pathways that were found to be significant also correlated with recent studies. One recent schizophrenic study highlighted the Kdo2-lipid A biosynthesis pathway (KDO-LIPOSYN-PKWY) as significantly differentiated between groups, which was also significant within this analysis (Nguyen et al., 2021). Additionally, the PWY-6628 (corrected p-value 3.5E-05) is super pathway of L-phenylalanine biosynthesis, recently shown to be important in the selective-decision making process of those with depression (Roiser et al., 2005). It has been shown that a depletion of phenylalanine and tyrosine resulted in changes to the reward, punishment cues of healthy individuals that mirrored what was seen in depressed individuals.

Limitations of the study include the homogeneity of the cohort's race. Expanding the findings to other races is important to corroborating these findings, and to potentially

find additional differences between the cohorts. Increasing the overall size of the cohorts will also allow for stratification between age and BMI groups within each study status, which may indicate additional microbiome differences. Expanding the overall number of those represented will also strengthen the power of the study, and perhaps identify other stratifying demographic-related information in the cohort. It would also be prudent to include other geographical areas with similar diets and water sources, to ensure that the study results are not limited to the population explored.

While the cohort did provide information about the type of mental illness diagnosed, the percentage of respondents was low, and so the data could not be stratified to a more specific mental illness while still maintaining a balanced cohort for race, age, and BMI. Improved studies would include more specificity into the type of mental illness, and therefore provide a more direct connection to the true biological mechanisms of the disease, and those predicted. Being able to parse differences from these various mental disorders is critical, as the onset, symptoms, and severity of each subtype does differ from one another. In expanding the number of individuals within the study it may be found that similarities exist between subtypes, or groups of sub-types. Finally, it would also be important to have clear confounding health-related information on these individuals to ensure other conditions like alcoholism or diseases like IBD, are not impacting the findings of the study. In relation to the study design, additional limitations include the number of samples, per donor. Having no controls within the project, is a severe limitation, as our previous work has shown the impact that positive and negative controls can have on the reproducibility and reliability of the study.

The final limitation relates to predictive modeling without follow-up confirmation. Future work should not only focus on expanding the study cohort, but also work to better understand some of the functional pathways in animal models, to determine their true significance. Designing studies that can utilize oral antibiotics or amino-acids can help to elucidate the functional components identified within this work. It will be important when designing such studies that there is a balance in the demographic information already described, as well as limiting studies to singular sub-types. It may also be worthwhile to expand the human cohorts to additional sequencing beyond the 16S rRNA sequencing of the V4 region, as there may be additional detail that can be ascertained.

REFERENCES

Aagaard, K., Ma, J., Antony, K. M., Ganu, R., Petrosino, J., & Versalovic, J. (2014). The placenta harbors a unique microbiome. *Science Translational Medicine*, *6* (237). https://doi.org/10.1126/scitranslmed.3008599

Acinas, S. G., Marcelino, L. A., Klepac-Ceraj, V., & Polz, M. F. (2004). Divergence and Redundancy of 16S rRNA Sequences in Genomes with Multiple rrn Operons. *Journal of Bacteriology*, *186* (9), 2629–2635. https://doi.org/10.1128/JB.186.9.2629-2635.2004

Aguiar-Pulido, V., Huang, W., Suarez-Ulloa, V., Cickovski, T., Mathee, K., & Narasimhan, G. (2016). Metagenomics, Metatranscriptomics, and Metabolomics Approaches for Microbiome Analysis. *Evolutionary Bioinformatics*, *12s1*, EBO.S36436. https://journals.sagepub.com/doi/pdf/10.4137/EBO.S36436

Ahn, J., Yang, L., Paster, B. J., Ganly, I., Morris, L., Pei, Z., & Hayes, R. B. (2011). Oral microbiome profiles: 16s rRNA pyrosequencing and microarray assay comparison. *PLoS ONE*, *6* (7), 1–6. https://doi.org/10.1371/journal.pone.0022788

Allaband, C., McDonald, D., Vázquez-Baeza, Y., Minich, J. J., Tripathi, A., Brenner, D. A., Loomba, R., Smarr, L., Sandborn, W. J., Schnabl, B., Dorrestein, P., Zarrinpar, A., & Knight, R. (2019). Microbiome 101: Studying, Analyzing, and Interpreting Gut Microbiome Data for Clinicians. In *Clinical Gastroenterology and Hepatology* (Vol. 17, Issue 2, pp. 218–230). W.B. Saunders. https://doi.org/10.1016/j.cgh.2018.09.017

Allali, I., Arnold, J. W., Roach, J., Cadenas, M. B., Butz, N., Hassan, H. M., Koci, M., Ballou, A., Mendoza, M., Ali, R., & Azcarate-Peril, M. A. (2017). A comparison of sequencing platforms and bioinformatics pipelines for compositional analysis of the gut microbiome. *BMC Microbiology*, *17* (1), 194. https://doi.org/10.1186/s12866-017-1101-8

Alves, A. V., Sanjinez-Argandoña, E. J., Linzmeier, A. M., Cardoso, C. A. L., & Macedo, M. L. R. (2016). Food Value of Mealworm Grown on Acrocomia aculeata Pulp Flour. *PLoS ONE*, *11* (3), e0151275. https://doi.org/10.1371/journal.pone.0151275

Amann, R. I., Ludwig, W., & Schleifer, K. H. (1995). Phylogenetic identification and in situ detection of individual microbial cells without cultivation. In *Microbiological Reviews* (Vol. 59, Issue 1, pp. 143–169). https://doi.org/10.1128/mmbr.59.1.143-169.1995

Andersen, S. B., Shapiro, B. J., Vandenbroucke-Grauls, C., & de Vos, M. G. J. (2019). Microbial evolutionary medicine: from theory to clinical practice. *The Lancet Infectious Diseases*. https://doi.org/10.1016/S1473-3099 (19)30045-3

Anderson, M. J. (2005). *PERMANOVA Permutational multivariate analysis of variance A computer program*. http://www.stat.auckland.ac.nz/~mja

Apprill, A., Mcnally, S., Parsons, R., & Weber, L. (2015). Minor revision to V4 region SSU rRNA 806R gene primer greatly increases detection of SAR11

bacterioplankton. *Aquatic Microbial Ecology*, *75* (2), 129–137. https://doi.org/10.3354/ame01753

Aßhauer, K. P., Wemheuer, B., Daniel, R., & Meinicke, P. (2015). Tax4Fun: Predicting functional profiles from metagenomic 16S rRNA data. *Bioinformatics*, *31* (17), 2882–2884. https://doi.org/10.1093/bioinformatics/btv287

ATCC. (n.d.). *Microbiome Research Solutions*. Retrieved August 16, 2019, from https://www.atcc.org/microbiome

Atherton, J. C. (2006). The pathogenesis of Helicobacter pylori-induced gastro-duodenal diseases. In *Annual Review of Pathology* (Vol. 1, pp. 63–96). Annual Reviews Inc. https://doi.org/10.1146/annurev.pathol.1.110304.100125

Bäckhed, F., Ley, R. E., Sonnenburg, J. L., Peterson, D. A., & Gordon, J. I. (2005). Host-bacterial mutualism in the human intestine. In *Science* (Vol. 307, Issue 5717, pp. 1915–1920). https://doi.org/10.1126/science.1104816

Bahl, M. I., Bergström, A., & Licht, T. R. (2012). Freezing fecal samples prior to DNA extraction affects the Firmicutes to Bacteroidetes ratio determined by downstream quantitative PCR analysis. *FEMS Microbiology Letters*, *329* (2), 193–197. https://doi.org/10.1111/j.1574-6968.2012.02523.x

Bajaj, J. S., Fagan, A., Gavis, E. A., Kassam, Z., Sikaroodi, M., & Gillevet, P. M. (2019). Long-term Outcomes after Fecal Microbiota Transplant in Cirrhosis. *Gastroenterology*. https://doi.org/10.1053/j.gastro.2019.01.033

Bajaj, J. S., Fagan, A., Sikaroodi, M., Kakiyama, G., Takei, H., Degefu, Y., Pandak, W. M., Hylemon, P. B., Fuchs, M., John, B., Heuman, D. M., Gavis, E., Nittono, H., Patil, R., & Gillevet, P. M. (2019). Alterations in Skin Microbiomes of Patients With Cirrhosis. *Clinical Gastroenterology and Hepatology*, *0* (0). https://doi.org/10.1016/j.cgh.2019.03.028

Bastiaanssen, T. F. S., Cowan, C. S. M., Claesson, M. J., Dinan, T. G., & Cryan, J. F. (2018). Making Sense of ⋯ the Microbiome in Psychiatry. *International Journal of Neuropsychopharmacology*, *22* (1), 37–52. https://doi.org/10.1093/ijnp/pyy067

Beckman Coulter. (n.d.). *AMPure XP, PCR Purification*. Retrieved November 23, 2021, from https://www.beckman.com/reagents/genomic/cleanup-and-size-selection/pcr

Biocyc. (n.d.). *MetaCyc superpathway of menaquinol-8 biosynthesis II*. Retrieved March 3, 2021, from https://biocyc.org/META/NEW-IMAGE?type=PATHWAY&object=PWY-6263

Bland, J. M., & Altman, D. G. (1996). Statistics Notes: Measurement Error. *BMJ*, *312* (7047), 1654. https://doi.org/10.1136/bmj.312.7047.1654

Bojic, S., Falco, M. M., Stojkovic, P., Ljujic, B., Gazdic Jankovic, M., Armstrong, L., Markovic, N., Dopazo, J., Lako, M., Bauer, R., & Stojkovic, M. (2020). Platform to study intracellular polystyrene nanoplastic pollution and clinical outcomes. *Stem Cells*. https://doi.org/10.1002/stem.3244

Bokulich, N. A., Kaehler, B. D., Rideout, J. R., Dillon, M., Bolyen, E., Knight, R., Huttley, G. A., & Gregory Caporaso, J. (2018). Optimizing taxonomic classification of marker-gene amplicon sequences with QIIME 2's q2-feature-classifier plugin. *Microbiome*, *6* (1), 90. https://doi.org/10.1186/s40168-018-0470-z

Bolyen, E., Rideout, J. R., Dillon, M. R., Bokulich, N. A., Abnet, C. C., Al-Ghalith, G. A., Alexander, H., Alm, E. J., Arumugam, M., Asnicar, F., Bai, Y., Bisanz, J. E., Bittinger, K., Brejnrod, A., Brislawn, C. J., Brown, C. T., Callahan, B. J., Caraballo-Rodríguez, A. M., Chase, J., … Caporaso, J. G. (2019). Reproducible, interactive, scalable and extensible microbiome data science using QIIME 2. *Nature Biotechnology*, *37* (8), 852–857. https://doi.org/10.1038/s41587-019-0209-9

Borrelle, S. B., Ringma, J., Lavender Law, K., Monnahan, C. C., Lebreton, L., McGivern, A., Murphy, E., Jambeck, J., Leonard, G. H., Hilleary, M. A., Eriksen, M., Possingham, H. P., de Frond, H., Gerber, L. R., Polidoro, B., Tahir, A., Bernard, M., Mallos, N., Barnes, M., & Rochman, C. M. (2020). Predicted growth in plastic waste exceeds efforts to mitigate plastic pollution. *Science*, *369* (6509), 1515–1518. https://doi.org/10.1126/SCIENCE.ABA3656

Bourne, D. G., Morrow, K. M., & Webster, N. S. (2016). Insights into the Coral Microbiome: Underpinning the Health and Resilience of Reef Ecosystems. *Annu. Rev. Microbiol*, *70*, 317–357. https://doi.org/10.1146/annurev-micro-102215-095440

Bräger, S. (2006). *Marine Nature Conservation in Europe*. https://www.researchgate.net/publication/278328811

Brandon, A. M., Gao, S. H., Tian, R., Ning, D., Yang, S. S., Zhou, J., Wu, W. M., & Criddle, C. S. (2018). Biodegradation of Polyethylene and Plastic Mixtures in Mealworms (Larvae of Tenebrio molitor) and Effects on the Gut Microbiome. *Environmental Science and Technology*, *52* (11), 6526–6533. https://doi.org/10.1021/acs.est.8b02301

Bravo, J. A., Dinan, T. G., & Cryan, J. F. (2011). Alterations in the central CRF system of two different rat models of comorbid depression and functional gastrointestinal disorders. *International Journal of Neuropsychopharmacology*, *14* (5), 666–683. https://doi.org/10.1017/S1461145710000994

Brennecke, D., Duarte, B., Paiva, F., Caçador, I., & Canning-Clode, J. (2016). Microplastics as vector for heavy metal contamination from the marine environment. *Estuarine, Coastal and Shelf Science*, *178*, 189–195. https://doi.org/10.1016/j.ecss.2015.12.003

Browne, M. A., Dissanayake, A., Galloway, T. S., Lowe, D. M., & Thompson, R. C. (2008). Ingested microscopic plastic translocates to the circulatory system of the mussel, Mytilus edulis (L.). *Environmental Science and Technology*, *42* (13), 5026–5031. https://doi.org/10.1021/es800249a

Bukin, Yu. S., Galachyants, Yu. P., Morozov, I. v., Bukin, S. v., Zakharenko, A. S., & Zemskaya, T. I. (2019). The effect of 16S rRNA region choice on bacterial community metabarcoding results. *Scientific Data*, *6* (1), 190007. https://doi.org/10.1038/sdata.2019.7

Callahan, B. J., McMurdie, P. J., & Holmes, S. P. (2017). Exact sequence variants should replace operational taxonomic units in marker-gene data analysis. *ISME Journal*, *11* (12), 2639–2643. https://doi.org/10.1038/ismej.2017.119

Callahan, B. J., McMurdie, P. J., Rosen, M. J., Han, A. W., Johnson, A. J. A., & Holmes, S. P. (2016). DADA2: High-resolution sample inference from Illumina amplicon data. *Nature Methods*, *13* (7), 581–583. https://doi.org/10.1038/nmeth.3869

Camacho, C., Coulouris, G., Avagyan, V., Ma, N., Papadopoulos, J., Bealer, K., & Madden, T. L. (2009). BLAST+: Architecture and applications. *BMC Bioinformatics*, *10* (1), 1–9. https://doi.org/10.1186/1471-2105-10-421

Canada. (n.d.). *Ocean Plastics Charter*. Retrieved January 1, 2021, from https://www.canada.ca/en/environment-climate-change/services/managing-reducing-waste/international-commitments/ocean-plastics-charter.html

Cani, P. D. (2018). Human gut microbiome: hopes, threats and promises. *BMJ Gut*, *67* (9), 1716–1725. https://doi.org/10.1136/gutjnl-2018-316723

Caporaso, J. G., Kuczynski, J., Stombaugh, J., Bittinger, K., Bushman, F. D., Costello, E. K., Fierer, N., Peña, A. G., Goodrich, J. K., Gordon, J. I., Huttley, G. A., Kelley, S. T., Knights, D., Koenig, J. E., Ley, R. E., Lozupone, C. A., McDonald, D., Muegge, B. D., Pirrung, M., … Knight, R. (2010). QIIME allows analysis of high-throughput community sequencing data. *Nature Methods*, *7* (5), 335–336. https://doi.org/10.1038/nmeth.f.303

Caporaso, J. G., Lauber, C. L., Walters, W. A., Berg-Lyons, D., Huntley, J., Fierer, N., Owens, S. M., Betley, J., Fraser, L., Bauer, M., Gormley, N., Gilbert, J. A., Smith, G., & Knight, R. (2012). Ultra-high-throughput microbial community analysis on the Illumina HiSeq and MiSeq platforms. *The ISME Journal*, *6* (8), 1621–1624. https://doi.org/10.1038/ismej.2012.8

Caussy, C., Tripathi, A., Humphrey, G., Bassirian, S., Singh, S., Faulkner, C., Bettencourt, R., Rizo, E., Richards, L., Xu, Z. Z., Downes, M. R., Evans, R. M., Brenner, D. A., Sirlin, C. B., Knight, R., & Loomba, R. (2019). A gut microbiome signature for cirrhosis due to nonalcoholic fatty liver disease. *Nature Communications*, *10* (1), 1406. https://doi.org/10.1038/s41467-019-09455-9

Chakravorty, S., Helb, D., Burday, M., Connell, N., & Alland, D. (2007). A detailed analysis of 16S ribosomal RNA gene segments for the diagnosis of pathogenic bacteria. *Journal of Microbiological Methods*, *69* (2), 330–339. https://doi.org/10.1016/j.mimet.2007.02.005

Chao, A., & Lee, S. M. (1992). Estimating the number of classes via sample coverage. *Journal of the American Statistical Association*, *87* (417), 210–217. https://doi.org/10.1080/01621459.1992.10475194

Chaudhari, D. S., Dhotre, D. P., Agarwal, D. M., Gaike, A. H., Bhalerao, D., Jadhav, P., Mongad, D., Lubree, H., Sinkar, V. P., Patil, U. K., Salvi, S., Bavdekar, A., Juvekar, S. K., & Shouche, Y. S. (2020). Gut, oral and skin microbiome of Indian patrilineal families reveal perceptible association with age. *Scientific Reports*, *10* (1), 1–13. https://doi.org/10.1038/s41598-020-62195-5

Chen, C., Song, X., Wei, W., Zhong, H., Dai, J., Lan, Z., Li, F., Yu, X., Feng, Q., Wang, Z., Xie, H., Chen, X., Zeng, C., Wen, B., Zeng, L., Du, H., Tang, H., Xu, C., Xia, Y., … Yang, H. (2017). The microbiota continuum along the female reproductive tract and its relation to uterine-related diseases. *Nature Communications*, *8*. https://doi.org/10.1038/s41467-017-00901-0

Chen, M., Wu, B.-L., Chen, T., Liu, Z., Deng, Z.-L., & Peng, L. (2016). The impact of different DNA extraction methods on the analysis of microbial diversity of oral saliva from healthy youths by polymerase chain reaction-denaturing gradient gel

electrophoresis. *Journal of Dental Sciences*, *11* (1), 54–58. https://doi.org/10.1016/j.jds.2015.08.002

Chill, S., Wu, Y., Zhou, W., & Ballew, B. (2020). *NCI-CGR/QIIME_pipeline: CGR's QIIME microbiome pipeline*. https://github.com/NCI-CGR/QIIME_pipeline

Choo, J. M., Leong, L. E. X., & Rogers, G. B. (2015). Sample storage conditions significantly influence faecal microbiome profiles. *Scientific Reports*, *5*. https://doi.org/10.1038/srep16350

Christensen, H., Andersson, A. J., Jørgensen, S. L., & Vogt, J. K. (2018). *16S rRNA Amplicon Sequencing for Metagenomics* (pp. 135–161). Springer, Cham. https://doi.org/10.1007/978-3-319-99280-8_8

Claassen, S., du Toit, E., Kaba, M., Moodley, C., Zar, H. J., & Nicol, M. P. (2013). A comparison of the efficiency of five different commercial DNA extraction kits for extraction of DNA from faecal samples. *Journal of Microbiological Methods*, *94* (2), 103–110. https://doi.org/10.1016/J.MIMET.2013.05.008

Coenye, T., & Vandamme, P. (2003). Intragenomic heterogeneity between multiple 16S ribosomal RNA operons in sequenced bacterial genomes. *FEMS Microbiology Letters*, *228* (1), 45–49. https://doi.org/10.1016/S0378-1097 (03)00717-1

Costea, P. I., Zeller, G., Sunagawa, S., Pelletier, E., Alberti, A., Levenez, F., Tramontano, M., Driessen, M., Hercog, R., Jung, F.-E., Kultima, J. R., Hayward, M. R., Coelho, L. P., Allen-Vercoe, E., Bertrand, L., Blaut, M., Brown, J. R. M., Carton, T., Cools-Portier, S., … Bork, P. (2017). Towards standards for human fecal sample processing in metagenomic studies. *Nature Biotechnology*, *July 2016*. https://doi.org/10.1038/nbt.3960

Cryan, J. F., Anderson, S. C., & Dinan, T. (2017). *The Psychobiotic Revolution: Mood, Food, and the New Science of the Gut-Brain Connection*. National Graphic Partners. https://books.google.com/books?hl=en&lr=&id=dLe-DQAAQBAJ&oi=fnd&pg=PA9&ots=C3IW55XKEL&sig=HuNUi9tObpC6PjLfoJCTVzvMx4w#v=onepage&q=teeth&f=false

Davidson, R. M., & Epperson, L. E. (2018). Microbiome sequencing methods for studying human diseases. In *Methods in Molecular Biology* (Vol. 1706, pp. 77–90). Humana Press Inc. https://doi.org/10.1007/978-1-4939-7471-9_5

de Stephanis, R., Giménez, J., Carpinelli, E., Gutierrez-Exposito, C., & Cañadas, A. (2013). As main meal for sperm whales: Plastics debris. *Marine Pollution Bulletin*, *69* (1–2), 206–214. https://doi.org/10.1016/j.marpolbul.2013.01.033

DeSantis, T. Z., Hugenholtz, P., Larsen, N., Rojas, M., Brodie, E. L., Keller, K., Huber, T., Dalevi, D., Hu, P., & Andersen, G. L. (2006). Greengenes, a chimera-checked 16S rRNA gene database and workbench compatible with ARB. *Applied and Environmental Microbiology*, *72* (7), 5069–5072. https://doi.org/10.1128/AEM.03006-05

Dill-Mcfarland, K. A., Tang, Z.-Z., Kemis, J. H., Kerby, R. L., Chen, G., Palloni, A., Sorenson, T., Rey, F. E., & Herd, P. (n.d.). *Close social relationships correlate with human gut microbiota composition OPEN*. https://doi.org/10.1038/s41598-018-37298-9

Earth Day Network. (2019). *How Much Disposable Plastic We Use*. https://www.earthday.org/2018/04/18/fact-sheet-how-much-disposable-plastic-we-use/

Earth Microbiome Project. (2011). *16S Illumina Amplicon Protocol*. http://www.earthmicrobiome.org/protocols-and-standards/16s/

Edgar, R. C. (2017). Accuracy of microbial community diversity estimated by closed- and open-reference OTUs. *PeerJ*, *5*, e3889. https://doi.org/10.7717/peerj.3889

Editorial. (2017). Overcoming Hurdles in Sharing Microbiome Data. *Nature Microbiology*, *2* (12), 1573–1573. https://doi.org/10.1038/s41564-017-0077-3

Ercolini, D., & Fogliano, V. (2018). *Food Design To Feed the Human Gut Microbiota*. https://doi.org/10.1021/acs.jafc.8b00456

Eriksen, M., Lebreton, L. C. M., Carson, H. S., Thiel, M., Moore, C. J., Borerro, J. C., Galgani, F., Ryan, P. G., & Reisser, J. (2014). Plastic Pollution in the World's Oceans: More than 5 Trillion Plastic Pieces Weighing over 250,000 Tons Afloat at Sea. *PLoS ONE*, *9* (12), e111913. https://doi.org/10.1371/journal.pone.0111913

European Nucleotide Archive (ENA). (n.d.). *European Nucleotide Archive (ENA)*. Retrieved November 24, 2021, from https://www.ebi.ac.uk/ena/browser/about/citing-ena

Evans, S. J., Bassis, C. M., Hein, R., Assari, S., Flowers, S. A., Kelly, M. B., Young, V. B., Ellingrod, V. E., & Mcinnis, M. G. (2017). The Gut Microbiome Composition Associates with Bipolar Disorder and Illness Severity HHS Public Access. *J Psychiatr Res*, *48109*, 23–29. https://doi.org/10.1016/j.jpsychires.2016.12.007

Exotic Nutrition. (n.d.). *Sugar Glider Food, Dried Mealworms, Sugar Glider Cages & Hedgehog Food*. Retrieved August 16, 2019, from https://www.exoticnutrition.com/

Ferrand, J., Patron, K., Legrand-Frossi, C., Frippiat, J. P., Merlin, C., Alauzet, C., & Lozniewski, A. (2014). Comparison of seven methods for extraction of bacterial DNA from fecal and cecal samples of mice. *Journal of Microbiological Methods*, *105*, 180–185. https://doi.org/10.1016/j.mimet.2014.07.029

Fisher Scientific. (n.d.). *MP Biomedicals FastDNA SPIN Kit for Soil*. Retrieved August 16, 2019, from https://www.fishersci.co.uk/shop/products/mp-biomedicals-fastdna-spin-kit-soil/11492400#?keyword=mp+biomedicals+fastdna+spin+kit+for+soil

Flowers, S. A., Evans, S. J., Ward, K. M., Mcinnis, M. G., & Ellingrod, V. L. (2017). Interaction Between Atypical Antipsychotics and the Gut Microbiome in a Bipolar Disease Cohort. *Pharmacotherapy*, *37* (3), 261–267. https://doi.org/10.1002/phar.1890

Fox, G. E., Stackebrandt, E., Hespell, R. B., Gibson, J., Maniloff, J., Dyer, T. A., Wolfe, R. S., Balch, W. E., Tanner, R. S., Magrum, L. J., Zahlen, L. B., Blakemore, R., Gupta, R., Bonen, L., Lewis, B. J., Stahl, D. A., Luehrsen, K. R., Chen, K. N., & Woese, C. R. (1980). The phylogeny of prokaryotes. *Science*, *209* (4455), 457–463. https://doi.org/10.1126/science.6771870

Frimodt-Møller, N. (2019). The urine microbiome – Contamination or a novel paradigm? In *EBioMedicine* (Vol. 44, pp. 20–21). Elsevier B.V. https://doi.org/10.1016/j.ebiom.2019.05.016

Gall, S. C., & Thompson, R. C. (2015). The impact of debris on marine life. *Marine Pollution Bulletin*, *92* (1–2), 170–179. https://doi.org/10.1016/j.marpolbul.2014.12.041

Gao, X., Zhang, M., Xue, J., Huang, J., Zhuang, R., Zhou, X., Zhang, H., Fu, Q., & Hao, Y. (2018). Body Mass Index Differences in the Gut Microbiota Are Gender Specific. *Frontiers in Microbiology*, *9* (JUN). /pmc/articles/PMC6023965/

Gerasimidis, K., Bertz, M., Quince, C., Brunner, K., Bruce, A., Combet, E., Calus, S., Loman, N., & Ijaz, U. Z. (2016). The effect of DNA extraction methodology on gut microbiota research applications. *BMC Research Notes*, *9* (1). https://doi.org/10.1186/s13104-016-2171-7

Gest, H. (2004). The Discovery of Microorganisms by Robert Hooke and Antoni van Leeuwenhoek, Fellows of The Royal Society. *Notes Rec. R. Soc.*, *58* (2), 187–201. https://doi.org/10.1098/rsnr.2004.0055

Geyer, R., Jambeck, J. R., & Law, K. L. (2017). Production, use, and fate of all plastics ever made. *Science Advances*, *3* (7), e1700782. https://doi.org/10.1126/sciadv.1700782

Gilbert, J. A., Blaser, M. J., Gregory Caporaso, J., Jansson, J. K., Lynch, S. v., Knight, R., Caporaso, J. G., Jansson, J. K., Lynch, S. v., & Knight, R. (2018). Current understanding of the human microbiome. *Nature Medicine*, *24* (4), 392–400. https://doi.org/10.1038/nm.4517

Gilbert, J. A., Jansson, J. K., & Knight, R. (2014). The Earth Microbiome project: Successes and aspirations. In *BMC Biology* (Vol. 12, Issue 1, p. 69). BioMed Central Ltd. https://doi.org/10.1186/s12915-014-0069-1

Gohl, D. M., Vangay, P., Garbe, J., MacLean, A., Hauge, A., Becker, A., Gould, T. J., Clayton, J. B., Johnson, T. J., Hunter, R., Knights, D., & Beckman, K. B. (2016). Systematic improvement of amplicon marker gene methods for increased accuracy in microbiome studies. *Nature Biotechnology*, *34* (9), 942–949. https://doi.org/10.1038/nbt.3601

Gomez-Gallego, C., Garcia-Mantrana, I., Salminen, S., & Collado, M. C. (2016). The human milk microbiome and factors influencing its composition and activity. *Seminars in Fetal & Neonatal Medicine*, 1–6. https://doi.org/10.1016/j.siny.2016.05.003

Gopalakrishnan, V., Spencer, C. N., Nezi, L., Reuben, A., Andrews, M. C., Karpinets, T. v, Prieto, P. A., Vicente, D., Hoffman, K., Wei, S. C., Cogdill, A. P., Zhao, L., Hudgens, C. W., Hutchinson, D. S., Manzo, T., Petaccia de Macedo, M., Cotechini, T., Kumar, T., Chen, W. S., … Wargo, J. A. (2018). Gut microbiome modulates response to anti-PD-1 immunotherapy in melanoma patients. *Science*, *359* (6371), 97–103. https://doi.org/10.1126/science.aan4236

Gotelli, N. J., & Colwell, R. K. (2001). Quantifying biodiversity: procedures and pitfalls in the measurement and comparison of species richness. *Ecology Letters*, *4* (4), 379–391. https://doi.org/10.1046/j.1461-0248.2001.00230.x

Greenblum, S., Turnbaugh, P. J., & Borenstein, E. (2012). Metagenomic systems biology of the human gut microbiome reveals topological shifts associated with obesity and inflammatory bowel disease. *Proceedings of the National Academy of Sciences of*

the United States of America, *109* (2), 594–599. https://doi.org/10.1073/pnas.1116053109

GreenGenes. (2019). *SecondGenome*. https://greengenes.secondgenome.com/

Gudra, D., Shoaie, S., Fridmanis, D., Klovins, J., Wefer, H., Silamikelis, I., Peculis, R., Kalnina, I., Elbere, I., Radovica-Spalvina, I., Hultcrantz, R., Šķenders, Ģ., Leja, M., & Engstrand, L. (2018). A widely used sampling device in colorectal cancer screening programmes allows for large-scale microbiome studies. *Gut*, gutjnl-2018-316225. https://doi.org/10.1136/gutjnl-2018-316225

H. Zahiroddini, J. Baah, & T. A. McAllister. (2006). Effects of Microbial Inoculants on the Fermentation, Nutrient Retention, and Aerobic Stability of Barley Silage . *Asian-Aust. J. Anim. Sci.*, *19* (10), 1429–1436. https://pdfs.semanticscholar.org/6330/1b0401b371691dad27e645ffc871d37a6fcb.pdf

Hammer, T. J., Sanders, J. G., & Fierer, N. (2019). Not all animals need a microbiome. In *FEMS Microbiology Letters* (Vol. 366, Issue 10, p. 117). Oxford University Press. https://doi.org/10.1093/femsle/fnz117

Heidbreder, L. M., Bablok, I., Drews, S., & Menzel, C. (2019). Tackling the plastic problem: A review on perceptions, behaviors, and interventions. In *Science of the Total Environment* (Vol. 668, pp. 1077–1093). Elsevier B.V. https://doi.org/10.1016/j.scitotenv.2019.02.437

Hemmings, S. M. J., Malan-Müller, S., van den Heuvel, L. L., Demmitt, B. A., Stanislawski, M. A., Smith, D. G., Bohr, A. D., Stamper, C. E., Hyde, E. R., Morton, J. T., Marotz, C. A., Siebler, P. H., Braspenning, M., van Criekinge, W., Hoisington, A. J., Brenner, L. A., Postolache, T. T., McQueen, M. B., Krauter, K. S., … Lowry, C. A. (2017). The Microbiome in Posttraumatic Stress Disorder and Trauma-Exposed Controls: An Exploratory Study. *Psychosomatic Medicine*, *79* (8), 936–946. https://doi.org/10.1097/PSY.0000000000000512

Heravi, F. S., Zakrzewski, M., Vickery, K., & Hu, H. (2020). Host DNA depletion efficiency of microbiome DNA enrichment methods in infected tissue samples. *Journal of Microbiological Methods*, *170*, 105856. https://doi.org/10.1016/j.mimet.2020.105856

Hsiao, E. Y., Mcbride, S. W., Hsien, S., Sharon, G., Hyde, E. R., Mccue, T., Codelli, J. A., Chow, J., Reisman, S. E., Petrosino, J. F., Patterson, P. H., & Mazmanian, S. K. (2013). Microbiota Modulate Behavioral and Physiological Abnormalities Associated with Neurodevelopmental Disorders. *Cell*, *155*, 1451–1463. https://doi.org/10.1016/j.cell.2013.11.024

Huang, Y., Shi, X., Li, Z., Shen, Y., Shi, X., Wang, L., Li, G., Yuan, Y., Wang, J., Zhang, Y., Zhao, L., Zhang, M., Kang, Y., & Liang, Y. (2018). Possible association of firmicutes in the gut microbiota of patients with major depressive disorder. *Neuropsychiatric Disease and Treatment*, *14*, 3329–3337. https://doi.org/10.2147/NDT.S188340

Hughes, D. P., Andersen, S. B., Hywel-Jones, N. L., Himaman, W., Billen, J., & Boomsma, J. J. (2011). Behavioral mechanisms and morphological symptoms of

zombie ants dying from fungal infection. *BMC Ecology*, *11* (1), 13. https://doi.org/10.1186/1472-6785-11-13
Illumina. (2011). *Quality Scores for Next-Generation Sequencing*. http://www3.appliedbiosystems.com/cms/groups/mcb_marketing/
Illumina. (2019). *MiSeq System*. https://www.illumina.com/systems/sequencing-platforms/miseq.html
J, S., W, D., E, S., K, S., & I, D. (2019). The Impact of a Diet Containing Sucrose and Systematically Repeated Starvation on the Oxidative Status of the Uterus and Ovary of Rats. *Nutrients*, *11* (7). https://doi.org/10.3390/NU11071544
Jandhyala, S. M., Talukdar, R., Subramanyam, C., Vuyyuru, H., Sasikala, M., & Reddy, N. (2015). Role of the Normal Gut Microbiota. *World Journal of Gastroenterology*, *21* (29), 8787–8803. https://doi.org/10.3748/wjg.v21.i29.8787
Jeftic, L., Sheavly, S., & Adler, E. (2009). *Marine Litter: A global Challenge*. www.unep.org/regionalseas
Jiang, H., Ling, Z., Zhang, Y., Mao, H., Ma, Z., Yin, Y., Wang, W., Tang, W., Tan, Z., Shi, J., Li, L., & Ruan, B. (2015). Altered fecal microbiota composition in patients with major depressive disorder. *Brain, Behavior, and Immunity*, *48*, 186–194. https://doi.org/10.1016/j.bbi.2015.03.016
Jones, M. B., Highlander, S. K., Anderson, E. L., Li, W., Dayrit, M., Klitgord, N., Fabani, M. M., Seguritan, V., Green, J., Pride, D. T., Yooseph, S., Biggs, W., Nelson, K. E., & Craig Venter, J. (2015). Library preparation methodology can influence genomic and functional predictions in human microbiome research. *Proceedings of the National Academy of Sciences of the United States of America*, *112* (45), 14024–14029. https://doi.org/10.1073/pnas.1519288112
Jovel, J., Patterson, J., Wang, W., Hotte, N., O'Keefe, S., Mitchel, T., Perry, T., Kao, D., Mason, A. L., Madsen, K. L., & Wong, G. K.-S. (2016). Characterization of the Gut Microbiome Using 16S or Shotgun Metagenomics. *Frontiers in Microbiology*, *7*, 459. https://doi.org/10.3389/fmicb.2016.00459
Kahlon, T. S. (2009). *Rice Bran: Production, Composition, Functionality and Food Applications, Physiological Benefits* (1st Edition). CRC Press. https://naldc.nal.usda.gov/download/33504/PDF
Kallner, A. (2018). Formulas. In *Laboratory Statistics* (pp. 1–140). Elsevier. https://doi.org/10.1016/b978-0-12-814348-3.00001-0
Kanehisa Laboratories. (n.d.). *KEGG: Kyoto Encyclopedia of Genes and Genomes*. Retrieved January 9, 2021, from https://www.genome.jp/kegg/
Kaur, H., Bose, C., & Mande, S. S. (2019). Tryptophan Metabolism by Gut Microbiome and Gut-Brain-Axis: An in silico Analysis. *Frontiers in Neuroscience*, *13*, 1365. https://doi.org/10.3389/fnins.2019.01365
Kiessling, T., Gutow, L., & Thiel, M. (2015). Marine litter as habitat and dispersal vector. In *Marine Anthropogenic Litter* (pp. 141–181). Springer International Publishing. https://doi.org/10.1007/978-3-319-16510-3_6
Kim, M., Morrison, M., & Yu, Z. (2011). Evaluation of different partial 16S rRNA gene sequence regions for phylogenetic analysis of microbiomes. *Journal of*

Microbiological Methods, *84* (1), 81–87. https://doi.org/10.1016/j.mimet.2010.10.020

Klindworth, A., Pruesse, E., Schweer, T., Peplies, J., Quast, C., Horn, M., & Glöckner, F. O. (2013). Evaluation of general 16S ribosomal RNA gene PCR primers for classical and next-generation sequencing-based diversity studies. *Nucleic Acids Research*, *41* (1), 1–11. https://doi.org/10.1093/nar/gks808

Knecht, L. D., O'Connor, G., Mittal, R., Liu, X. Z., Daftarian, P., Deo, S. K., & Daunert, S. (2016). Serotonin Activates Bacterial Quorum Sensing and Enhances the Virulence of Pseudomonas aeruginosa in the Host. *EBioMedicine*, *9*, 161–169. https://doi.org/10.1016/j.ebiom.2016.05.037

Krueger, M. C., Harms, H., & Schlosser, D. (2015). Prospects for microbiological solutions to environmental pollution with plastics. In *Applied Microbiology and Biotechnology* (Vol. 99, Issue 21, pp. 8857–8874). Springer Verlag. https://doi.org/10.1007/s00253-015-6879-4

la Rosa, P. S., Brooks, J. P., Deych, E., Boone, E. L., Edwards, D. J., Wang, Q., Sodergren, E., Weinstock, G., & Shannon, W. D. (2012). Hypothesis Testing and Power Calculations for Taxonomic-Based Human Microbiome Data. *PLoS ONE*, *7* (12), 52078. https://doi.org/10.1371/journal.pone.0052078

Lane, D. J., Pace, B., Olsen, G. J., Stahlt, D. A., Sogint, M. L., & Pace, N. R. (1985). *Rapid determination of 16S ribosomal RNA sequences for phylogenetic analyses (reverse transcriptase/dideoxynudeotide)* (Vol. 82).

Langille, M. G. I. (2018). Exploring Linkages between Taxonomic and Functional Profiles of the Human Microbiome. *MSystems*, *3* (2), e00163-17. https://doi.org/10.1128/mSystems.00163-17

Ley, R. E., Peterson, D. A., & Gordon, J. I. (2006). Ecological and Evolutionary Forces Shaping Microbial Diversity in the Human Intestine. *Cell*, *124* (4), 837–848. https://doi.org/10.1016/J.CELL.2006.02.017

Libertucci, J., & Young, V. B. (2019). The role of the microbiota in infectious diseases. In *Nature Microbiology* (Vol. 4, Issue 1, pp. 35–45). Nature Publishing Group. https://doi.org/10.1038/s41564-018-0278-4

Liebezeit, G., & Liebezeit, E. (2013). Non-pollen particulates in honey and sugar. *Food Additives and Contaminants - Part A Chemistry, Analysis, Control, Exposure and Risk Assessment*, *30* (12), 2136–2140. https://doi.org/10.1080/19440049.2013.843025

Liebezeit, G., & Liebezeit, E. (2014). Synthetic particles as contaminants in German beers. *Food Additives and Contaminants - Part A Chemistry, Analysis, Control, Exposure and Risk Assessment*, *31* (9), 1574–1578. https://doi.org/10.1080/19440049.2014.945099

Limbana, T., Khan, F., & Eskander, N. (2020). Gut Microbiome and Depression: How Microbes Affect the Way We Think. *Cureus*, *12* (8). https://doi.org/10.7759/cureus.9966

Liu, Z., Lozupone, C., Hamady, M., Bushman, F. D., & Knight, R. (2007). Short pyrosequencing reads suffice for accurate microbial community analysis. *Nucleic Acids Research*, *35*. https://doi.org/10.1093/nar/gkm541

Lüdecke, D. (n.d.). *rmse function*. Retrieved December 15, 2019, from https://www.rdocumentation.org/packages/sjstats/versions/0.15.0/topics/rmse

Lundqvist, M., Stigler, J., Elia, G., Lynch, I., Cedervall, T., & Dawson, K. A. (2008). Nanoparticle size and surface properties determine the protein corona with possible implications for biological impacts. *Proceedings of the National Academy of Sciences of the United States of America*, *105* (38), 14265–14270. https://doi.org/10.1073/pnas.0805135105

Market Research Store. (2015). *Polystyrene (PS) & Expandable Polystyrene (EPS) Market for Building & Construction, Electrical & Electronics, Packaging and Other Applications: Global Industry Perspective, Comprehensive Analysis, and Forecast*. https://www.marketresearchstore.com/report/polystyrene-expandable-polystyrene-market-for-building-z37708

Martin, R., Makino, H., Cetinyurek Yavuz, A., Ben-Amor, K., Roelofs, M., Ishikawa, E., Kubota, H., Swinkels, S., Sakai, T., Oishi, K., Kushiro, A., & Knol, J. (2016). Early-Life Events, Including Mode of Delivery and Type of Feeding, Siblings and Gender, Shape the Developing Gut Microbiota. *PLOS ONE*, *11* (6), e0158498. https://doi.org/10.1371/journal.pone.0158498

Maruvada, P., Leone, V., Kaplan, L. M., & Chang, E. B. (2017). The Human Microbiome and Obesity: Moving beyond Associations. In *Cell Host and Microbe* (Vol. 22, Issue 5, pp. 589–599). Cell Press. https://doi.org/10.1016/j.chom.2017.10.005

Mason, S. A., Welch, V. G., & Neratko, J. (2018). Synthetic Polymer Contamination in Bottled Water. *Frontiers in Chemistry*, *6*, 407. https://doi.org/10.3389/fchem.2018.00407

Mazurais, D., Ernande, B., Quazuguel, P., Severe, A., Huelvan, C., Madec, L., Mouchel, O., Soudant, P., Robbens, J., Huvet, A., & Zambonino-Infante, J. (2015). Evaluation of the impact of polyethylene microbeads ingestion in European sea bass (Dicentrarchus labrax) larvae. *Marine Environmental Research*, *112*, 78–85. https://doi.org/10.1016/j.marenvres.2015.09.009

McDonald, D., Hyde, E., Debelius, J. W., Morton, J. T., Gonzalez, A., Ackermann, G., Aksenov, A. A., Behsaz, B., Brennan, C., Chen, Y., DeRight Goldasich, L., Dorrestein, P. C., Dunn, R. R., Fahimipour, A. K., Gaffney, J., Gilbert, J. A., Gogul, G., Green, J. L., Hugenholtz, P., … Gunderson, B. (2018). American Gut: an Open Platform for Citizen Science Microbiome Research. *MSystems*, *3* (3), e00031-18. https://doi.org/10.1128/mSystems.00031-18

McMurdie, P. J., & Holmes, S. (2014). Waste Not, Want Not: Why Rarefying Microbiome Data Is Inadmissible. *PLoS Computational Biology*, *10* (4), e1003531. https://doi.org/10.1371/journal.pcbi.1003531

Methé, B. A., Nelson, K. E., Pop, M., Creasy, H. H., Giglio, M. G., Huttenhower, C., Gevers, D., Petrosino, J. F., Abubucker, S., Badger, J. H., Chinwalla, A. T., Earl, A. M., Fitzgerald, M. G., Fulton, R. S., Hallsworth-Pepin, K., Lobos, E. A., Madupu, R., Magrini, V., Martin, J. C., … White, O. (2012). A framework for human microbiome research. *Nature*, *486* (7402), 215–221. https://doi.org/10.1038/nature11209

Mohanan, N., Montazer, Z., Sharma, P. K., & Levin, D. B. (2020). Microbial and Enzymatic Degradation of Synthetic Plastics. *Frontiers in Microbiology*, *0*, 2837. https://doi.org/10.3389/FMICB.2020.580709

Molecular Devices. (n.d.). *Gemini XPS & EM Microplate Readers, Dual Monochromator Fluorometers*. Retrieved November 23, 2021, from https://www.moleculardevices.com/products/microplate-readers/fluorescent-readers/gemini-em-xps-readers#gref

Moossavi, S., Sepehri, S., Robertson, B., Bode, L., Goruk, S., Field, C. J., Lix, L. M., de Souza, R. J., Becker, A. B., Mandhane, P. J., Turvey, S. E., Subbarao, P., Moraes, T. J., Lefebvre, D. L., Sears, M. R., Khafipour, E., & Azad, M. B. (2019). Composition and Variation of the Human Milk Microbiota Are Influenced by Maternal and Early-Life Factors. *Cell Host & Microbe*, *25* (2), 324-335.e4. https://doi.org/10.1016/J.CHOM.2019.01.011

Morgan, X. C., & Huttenhower, C. (2012). Human Microbiome Analysis. *PLoS Computational Biology*, *8* (12), e1002808. https://doi.org/10.1371/journal.pcbi.1002808

Murphy, F., Ewins, C., Carbonnier, F., & Quinn, B. (2016). Wastewater Treatment Works (WwTW) as a Source of Microplastics in the Aquatic Environment. *Environmental Science and Technology*, *50* (11), 5800–5808. https://doi.org/10.1021/acs.est.5b05416

National Institutes of Health. (n.d.-a). *Depression*. Retrieved March 20, 2021, from https://www.nimh.nih.gov/health/topics/depression/index.shtml

National Institutes of Health. (n.d.-b). *Human Microbiome Project*. Retrieved September 30, 2020, from http://commonfund.nih.gov/hmp

National Institutes of Health. (n.d.-c). *Mental Illness*. Retrieved January 18, 2021, from https://www.nimh.nih.gov/health/statistics/mental-illness.shtml

National Institutes of Health. (n.d.-d). *Schizophrenia*. Retrieved March 20, 2021, from https://www.nimh.nih.gov/health/statistics/schizophrenia.shtml

National Institutes of Health. (2017a, January). *Post-Traumatic Stress Disorder (PTSD)*. https://www.nimh.nih.gov/health/statistics/post-traumatic-stress-disorder-ptsd.shtml

National Institutes of Health. (2017b, November). *Bipolar Disorder*. https://www.nimh.nih.gov/health/statistics/bipolar-disorder.shtml

Nguyen, T. T., Kosciolek, T., Daly, R. E., Vázquez-Baeza, Y., Swafford, A., Knight, R., & Jeste, D. v. (2021). Gut microbiome in Schizophrenia: Altered functional pathways related to immune modulation and atherosclerotic risk. *Brain, Behavior, and Immunity*, *91*, 245–256. https://doi.org/10.1016/j.bbi.2020.10.003

Niaounakis, M. (2017). *Management of Marine Plastic Debris*. Matthew Deans. https://books.google.com/books?hl=en&lr=&id=hWI8DgAAQBAJ&oi=fnd&pg=PP1&ots=N2H0HMJ-UH&sig=4I0-iXzWAjFwMrpA-Y22Gm0Lp6s#v=onepage&q&f=false

NIH Human Microbiome Portfolio Analysis. (2019). A review of 10 years of human microbiome research activities at the US National Institutes of Health, Fiscal Years 2007-2016. In *Microbiome* (Vol. 7, Issue 1, p. 31). NLM (Medline). https://doi.org/10.1186/s40168-019-0620-y

Novais, R. C., & Thorstenson, Y. R. (2011). The evolution of Pyrosequencing® for microbiology: From genes to genomes. *Journal of Microbiological Methods*, *86* (1), 1–7. https://doi.org/10.1016/J.MIMET.2011.04.006

Omega BioTek. (n.d.). *16S Reference*. Retrieved March 20, 2020, from http://omegabioservices.com/index.php/16s-reference/

Pace, N. R., Stahl, D. A., Lane, D. J., & Olsen, G. J. (1986). The Analysis of Natural Microbial Populations by Ribosomal RNA Sequences. In *Advances in Microbial Ecology* (9th ed., pp. 1–55). Springer, Boston, MA. https://doi.org/10.1007/978-1-4757-0611-6_1

Pallone, F. Jr. (2015). Microbead-Free Waters Act of 2015. *H.R.1321 - 114th Congress*. https://www.congress.gov/bill/114th-congress/house-bill/1321/text

Parada, A. E., Needham, D. M., & Fuhrman, J. A. (2016). Every base matters: assessing small subunit rRNA primers for marine microbiomes with mock communities, time series and global field samples. *Environmental Microbiology*, *18* (5), 1403–1414. https://doi.org/10.1111/1462-2920.13023

Parks, D. H., Tyson, G. W., Hugenholtz, P., & Beiko, R. G. (2014). STAMP: Statistical analysis of taxonomic and functional profiles. *Bioinformatics*, *30* (21), 3123–3124. https://doi.org/10.1093/bioinformatics/btu494

Pedregosa, F., Michel, V., Grisel, O., Blondel, M., Prettenhofer, P., Weiss, R., Vanderplas, J., Cournapeau, D., Pedregosa, F., Varoquaux, G., Gramfort, A., Thirion, B., Grisel, O., Dubourg, V., Passos, A., Brucher, M., Perrot andÉdouardand, M., Duchesnay, A., & Duchesnay EDOUARDDUCHESNAY, Fré. (2011). Scikit-learn: Machine Learning in Python Gaël Varoquaux Bertrand Thirion Vincent Dubourg Alexandre Passos PEDREGOSA, VAROQUAUX, GRAMFORT ET AL. Matthieu Perrot. In *Journal of Machine Learning Research* (Vol. 12). http://scikit-learn.sourceforge.net.

Prehn-Kristensen, A., Zimmermann, A., Tittmann, L., Lieb, W., Schreiber, S., Baving, L., & Fischer, A. (2018). Reduced microbiome alpha diversity in young patients with ADHD. *PLoS ONE*, *13* (7). https://doi.org/10.1371/journal.pone.0200728

Prescott, S. L. (2017). History of medicine: Origin of the term microbiome and why it matters. *Human Microbiome Journal*, *4*, 24–25. https://doi.org/10.1016/j.humic.2017.05.004

Price, M. N., Dehal, P. S., & Arkin, A. P. (2009). FastTree: Computing Large Minimum Evolution Trees with Profiles instead of a Distance Matrix. *Molecular Biology and Evolution*, *26* (7), 1641–1650. https://doi.org/10.1093/MOLBEV/MSP077

Prodan, A., Tremaroli, V., Brolin, H., Zwinderman, A. H., Nieuwdorp, M., & Levin, E. (2020). Comparing bioinformatic pipelines for microbial 16S rRNA amplicon sequencing. *PLOS ONE*, *15* (1), e0227434. https://doi.org/10.1371/JOURNAL.PONE.0227434

Qiagen. (2019a). *DNeasy PowerSoil Pro Kit*. https://www.qiagen.com/us/products/discovery-and-translational-research/dna-rna-purification/dna-purification/genomic-dna/dneasy-powersoil-pro-kit/#orderinginformation

Qiagen. (2019b). *MagAttract PowerMicrobiome DNA/RNA Kit*. https://www.qiagen.com/us/products/discovery-and-translational-research/dna-rna-purification/dna-purification/microbial-dna/magattract-powermicrobiome-dna-rna-kit/#orderinginformation
Qiagen. (2019c). *MagAttract PowerSoil DNA Kit*. https://www.qiagen.com/us/shop//sample-technologies/magattract-powersoil-dna-isolation-kit/
Qiagen. (2019d). *Pathogen Lysis Tubes*. https://www.qiagen.com/us/products/discovery-and-translational-research/lab-essentials/buffers-reagents/pathogen-lysis-tubes/#orderinginformation
Qiagen. (2019e). *QIAamp DNA Mini Kit*. https://www.qiagen.com/us/products/discovery-and-translational-research/dna-rna-purification/dna-purification/genomic-dna/qiaamp-dna-mini-kit/#orderinginformation
Qiagen. (2019f). *QIAseq 16S/ITS Region Panels*. https://www.qiagen.com/us/shop/sequencing/qiaseq-16s-its-region-panel/
Qiagen. (2019g). *QIAsymphony DSP Virus/Pathogen Kit*. https://www.qiagen.com/us/products/diagnostics-and-clinical-research/clinical-sample-processing/qiasymphony-dsp-viruspathogen-kits/#orderinginformation
Qiagen. (2019h). *QIAsymphony SP/AS instruments*. https://www.qiagen.com/us/products/discovery-and-translational-research/dna-rna-purification/instruments-equipment/qiasymphony-spas-instruments/#orderinginformation
Qiagen. (2019i). *TissueLyser II*. https://www.qiagen.com/us/products/human-id-and-forensics/automation/tissuelyser-ii/#orderinginformation
Qin, J., Li, R., Raes, J., Arumugam, M., Solvsten Burgdorf, K., Manichanh, C., Nielsen, T., Pons, N., Levenez, F., Yamada, T., Mende, D. R., Li, J., Xu, J., Li, S., Li, D., Cao, J., Wang, B., Liang, H., Zheng, H., … Wang, J. (2010). A human gut microbial gene catalogue established by metagenomic sequencing. *Nature*, *464*. https://doi.org/10.1038/nature08821
Quast, C., Pruesse, E., Yilmaz, P., Gerken, J., Schweer, T., Yarza, P., Peplies, J., & Glöckner, F. O. (2013). The SILVA ribosomal RNA gene database project: improved data processing and web-based tools. *Nucleic Acids Research*, *41* (Database issue), D590-6. https://doi.org/10.1093/nar/gks1219
R Core Team. (2014). *R: A language and environment for statistical computing. R Foundation for Statistical Computing*. Vienna, Austria.
Ranjan, R., Rani, A., Metwally, A., McGee, H. S., & Perkins, D. L. (2016). Analysis of the microbiome: Advantages of whole genome shotgun versus 16S amplicon sequencing. *Biochemical and Biophysical Research Communications*, *469* (4), 967–977. https://doi.org/10.1016/J.BBRC.2015.12.083
Roberts, M. E., Stewart, B. M., Dustin, P., & Harvard, T. (n.d.). stm: R Package for Structural Topic Models. *Journal of Statistical Software*. https://doi.org/10.18637/jss.v000.i00
Rochman, C. M., Kross, S. M., Armstrong, J. B., Bogan, M. T., Darling, E. S., Green, S. J., Smyth, A. R., & Veríssimo, D. (2015). Scientific Evidence Supports a Ban on

Microbeads. In *Environmental Science and Technology* (Vol. 49, Issue 18, pp. 10759–10761). American Chemical Society. https://doi.org/10.1021/acs.est.5b03909
Rognes, T., Flouri, T., Nichols, B., Quince, C., & Mahé, F. (2016). VSEARCH: A versatile open source tool for metagenomics. *PeerJ*, *2016* (10), e2584. https://doi.org/10.7717/peerj.2584
Roiser, J. P., McLean, A., Ogilvie, A. D., Blackwell, A. D., Bamber, D. J., Goodyer, I., Jones, P. B., & Sahakian, B. J. (2005). The Subjective and Cognitive Effects of Acute Phenylalanine and Tyrosine Depletion in Patients Recovered from Depression. *Neuropsychopharmacology*, *30* (4), 775. https://doi.org/10.1038/SJ.NPP.1300659
Rothschild, D., Weissbrod, O., Barkan, E., Kurilshikov, A., Korem, T., Zeevi, D., Costea, P. I., Godneva, A., Kalka, I. N., Bar, N., Shilo, S., Lador, D., Vila, A. V., Zmora, N., Pevsner-Fischer, M., Israeli, D., Kosower, N., Malka, G., Wolf, B. C., … Segal, E. (2018). Environment dominates over host genetics in shaping human gut microbiota. *Nature*, *555* (7695), 210–215. https://doi.org/10.1038/nature25973
Ryan, P. G., Cole, G., Spiby, K., Nel, R., Osborne, A., & Perold, V. (2016). Impacts of plastic ingestion on post-hatchling loggerhead turtles off South Africa. *Marine Pollution Bulletin*, *107* (1), 155–160. https://doi.org/10.1016/j.marpolbul.2016.04.005
Salah Ud-Din, A. I. M., & Roujeinikova, A. (2017). Methyl-accepting chemotaxis proteins: a core sensing element in prokaryotes and archaea. In *Cellular and Molecular Life Sciences* (Vol. 74, Issue 18, pp. 3293–3303). Birkhauser Verlag AG. https://doi.org/10.1007/s00018-017-2514-0
Salonen, A., Nikkilä, J., Jalanka-Tuovinen, J., Immonen, O., Rajilić-Stojanović, M., Kekkonen, R. A., Palva, A., & de Vos, W. M. (2010). Comparative analysis of fecal DNA extraction methods with phylogenetic microarray: Effective recovery of bacterial and archaeal DNA using mechanical cell lysis. *Journal of Microbiological Methods*, *81* (2), 127–134. https://doi.org/10.1016/j.mimet.2010.02.007
Sanger, F., Nicklen, S., & Coulson, A. R. (1977). DNA sequencing with chain-terminating inhibitors. *Proceedings of the National Academy of Sciences of the United States of America*, *74* (12), 5463–5467. https://doi.org/10.1073/pnas.74.12.5463
Segal, L. N., Clemente, J. C., Tsay, J. C. J., Koralov, S. B., Keller, B. C., Wu, B. G., Li, Y., Shen, N., Ghedin, E., Morris, A., Diaz, P., Huang, L., Wikoff, W. R., Ubeda, C., Artacho, A., Rom, W. N., Sterman, D. H., Collman, R. G., Blaser, M. J., & Weiden, M. D. (2016). Enrichment of the lung microbiome with oral taxa is associated with lung inflammation of a Th17 phenotype. *Nature Microbiology*, *1* (5), 1–11. https://doi.org/10.1038/nmicrobiol.2016.31
Sender, R., Fuchs, S., & Milo, R. (2016). Are We Really Vastly Outnumbered? Revisiting the Ratio of Bacterial to Host Cells in Humans. In *Cell* (Vol. 164, Issue 3, pp. 337–340). Cell Press. https://doi.org/10.1016/j.cell.2016.01.013
Serafini, G., Pompili, M., Innamorati, M., Giordano, G., Tatarelli, R., Lester, D., Girardi, P., & Dwivedi, Y. (2011). Glycosides, Depression and Suicidal Behaviour: The Role

of Glycoside-Linked Proteins. *Molecules*, *16* (3), 2688. https://doi.org/10.3390/MOLECULES16032688
Shannon, C. E., & Weaver, W. (1949). *The Mathematical Theory of Communication*.
Sharon, G., Segal, D., Ringo, J. M., Hefetz, A., Zilber-Rosenberg, I., Rosenberg, E., & Collier, R. J. (2010). Commensal bacteria play a role in mating preference of Drosophila melanogaster Author (s). *PNAS*, *107* (46), 20051–20056. https://doi.org/10.1073/pnas
Sherwin, E., Rea, K., Dinan, T. G., & Cryan, J. F. (2016). A gut (microbiome) feeling about the brain. In *Current Opinion in Gastroenterology* (Vol. 32, Issue 2, pp. 96–102). Lippincott Williams and Wilkins. https://doi.org/10.1097/MOG.0000000000000244
Simpson, E. H. (1949). Measurement of diversity. In *Nature* (Vol. 163, Issue 4148, p. 688). Nature Publishing Group. https://doi.org/10.1038/163688a0
Sina. (2003). *Yellow mealworm digest plastic*. http://news.sina.com.cn/c/2003-12-30/16251466914s.shtml
Sinha, R., Abu-Ali, G., Vogtmann, E., Fodor, A. A., Ren, B., Amir, A., Schwager, E., Crabtree, J., Ma, S., Abnet, C. C., Knight, R., White, O., Huttenhower, C., & Huttenhower, C. (2017). Assessment of variation in microbial community amplicon sequencing by the Microbiome Quality Control (MBQC) project consortium. *Nature Biotechnology*, *35* (11), 1077. https://doi.org/10.1038/nbt.3981
Smith, B., Li, N., Andersen, A. S., Slotved, H. C., & Krogfelt, K. A. (2011). Optimising bacterial DNA extraction from faecal samples: comparison of three methods. *The Open Microbiology Journal*, *5*, 14–17. https://doi.org/10.2174/1874285801105010014
Solutions, T. N. I. for E. P. (n.d.). *UNEA Resolution 3/7 Marine Litter and Microplastics*. Retrieved January 1, 2021, from https://nicholasinstitute.duke.edu/plastics-policies/unea-resolution-37-marine-litter-and-microplastics
Song, S. J., Amir, A., Metcalf, J. L., Amato, K. R., Xu, Z. Z., Humphrey, G., & Knight, R. (2016). Preservation Methods Differ in Fecal Microbiome Stability, Affecting Suitability for Field Studies. *MSystems*, *1* (3). https://doi.org/10.1128/msystems.00021-16
SPEX Sample Prep. (2010). *Geno/Grinder - Automated Tissue Homogenizer and Cell Lyser*. https://www.spexsampleprep.com/2010genogrinder
Stewart, C. J., Ajami, N. J., O'Brien, J. L., Hutchinson, D. S., Smith, D. P., Wong, M. C., Ross, M. C., Lloyd, R. E., Doddapaneni, H., Metcalf, G. A., Muzny, D., Gibbs, R. A., Vatanen, T., Huttenhower, C., Xavier, R. J., Rewers, M., Hagopian, W., Toppari, J., Ziegler, A.-G., … Petrosino, J. F. (2018). Temporal development of the gut microbiome in early childhood from the TEDDY study. *Nature*, *562* (7728), 583–588. https://doi.org/10.1038/s41586-018-0617-x
Stokholm, J., Blaser, M. J., Thorsen, J., Rasmussen, M. A., Waage, J., Vinding, R. K., Schoos, A. M. M., Kunøe, A., Fink, N. R., Chawes, B. L., Bønnelykke, K., Brejnrod, A. D., Mortensen, M. S., Al-Soud, W. A., Sørensen, S. J., & Bisgaard, H. (2018). Maturation of the gut microbiome and risk of asthma in childhood. *Nature Communications*, *9* (1), 1–10. https://doi.org/10.1038/s41467-017-02573-2

SwiftBiosciences. (n.d.). *Swift Amplicon 16S+ITS Panel*. Retrieved August 16, 2019, from https://swiftbiosci.com/swift-amplicon-16s-its-panel/

Teng, F., Darveekaran Nair, S. S., Zhu, P., Li, S., Huang, S., Li, X., Xu, J., & Yang, F. (2018). Impact of DNA extraction method and targeted 16S-rRNA hypervariable region on oral microbiota profiling. *Scientific Reports*, *8* (1), 1–12. https://doi.org/10.1038/s41598-018-34294-x

The Nicholas Institute for Environmental Policy Solutions. (n.d.). *20 Years of Government Responses to the Global Plastic Pollution Problem*. Retrieved January 1, 2021, from https://nicholasinstitute.duke.edu/publications/20-years-government-responses-global-plastic-pollution-problem

The PICRust Project. (2013). *How PICRUSt Works*. http://picrust.github.io/picrust/tutorials/algorithm_description.html#algorithm-description

The SILVA ribosomal RNA database project. (2017). *High Quality Ribosomal RNA Database*. https://www.arb-silva.de/

ThermoFisher Scientific. (n.d.-a). *GeneAmp™ PCR System 9700 and 9800 Fast Thermal Cycler, IQ User-Performed Test Procedures*. Retrieved November 23, 2021, from https://www.thermofisher.com/order/catalog/product/4339386

ThermoFisher Scientific. (n.d.-b). *KingFisher Flex System*. Retrieved August 24, 2019, from https://www.thermofisher.com/us/en/home/life-science/dna-rna-purification-analysis/automated-purification-extraction/kingfisher-flex.html

ThermoFisher Scientific. (n.d.-c). *MagMAX Microbiome Ultra Nucleic Acid Isolation Kits*. Retrieved August 3, 2019, from https://www.thermofisher.com/us/en/home/life-science/dna-rna-purification-analysis/automated-purification-extraction/automated-magmax-kits-nucleic-acid-extraction/magmax-microbiome-extraction-kits.html

Thomas, V., Clark, J., & Doré, J. (2015). Fecal microbiota analysis: an overview of sample collection methods and sequencing strategies. *Future Microbiology*, *10* (9), 1485–1504. https://doi.org/10.2217/fmb.15.87

Thompson, R. C. (2006). Plastic debris in the marine environment: consequences and solutions. *Marine Nature Conservation in Europe*, 107–271. https://www.researchgate.net/profile/Stefan_Braeger/publication/278328811_Marine_Nature_Conservation_in_Europe_2006_Proceedings_of_the_Symposium_May_2006/links/557f552008aeb61eae261777/Marine-Nature-Conservation-in-Europe-2006-Proceedings-of-the-Symposium

Tsukuda, M., Kitahara, K., & Miyazaki, K. (2017). Comparative RNA function analysis reveals high functional similarity between distantly related bacterial 16 S rRNAs. *Scientific Reports*, *7* (1), 9993. https://doi.org/10.1038/s41598-017-10214-3

Turnbaugh, P. J., Ley, R. E., Hamady, M., Fraser-Liggett, C., Knight, R., & Gordon, J. I. (2007). The human microbiome project: exploring the microbial part of ourselves in a changing world. *Nature*. https://doi.org/10.1038/nature06244

Turner, A. (2016). Heavy metals, metalloids and other hazardous elements in marine plastic litter. *Marine Pollution Bulletin*, *111* (1–2), 136–142. https://doi.org/10.1016/j.marpolbul.2016.07.020

Urbanek, A. K., Rybak, J., Wróbel, M., Leluk, K., & Mirończuk, A. M. (2020). A comprehensive assessment of microbiome diversity in Tenebrio molitor fed with polystyrene waste. *Environmental Pollution*, *262*, 114281. https://doi.org/10.1016/j.envpol.2020.114281

UVic-omics. (n.d.). *selbal: selection of balances for microbial signatures*. Retrieved January 17, 2021, from https://github.com/UVic-omics/selbal

van Rossum, G.; Drake, F. L. (2009). Python 3 Reference Manual. In *CreateSpace*. CreateSpace.

Vécsei, L., Szalárdy, L., Fülöp, F., & Toldi, J. (2013). Kynurenines in the CNS: Recent advances and new questions. In *Nature Reviews Drug Discovery* (Vol. 12, Issue 1, pp. 64–82). Nature Publishing Group. https://doi.org/10.1038/nrd3793

Ventola, C. L. (2015). The Antibiotic Resistance Crisis: Part 1: Causes and Threats. *Pharmacy and Therapeutics*, *40* (4), 277. https://www.ncbi.nlm.nih.gov/pmc/articles/PMC4378521/

Walker, W. A., & Shuba Iyengar, R. (2014). Breastmilk, Microbiota and Intestinal Immune Homeostasis. *Pediatric Research*, *77* (1–2), 220. https://doi.org/10.1038/pr.2014.160

Wampach, L., Heintz-Buschart, A., Hogan, A., Muller, E. E. L., Narayanasamy, S., Laczny, C. C., Hugerth, L. W., Bindl, L., Bottu, J., Andersson, A. F., de Beaufort, C., & Wilmes, P. (2017). Colonization and succession within the human gut microbiome by archaea, bacteria, and microeukaryotes during the first year of life. *Frontiers in Microbiology*, *8* (MAY). https://doi.org/10.3389/fmicb.2017.00738

Wang, Y., & Zhang, Y. (2015). Investigation of gut-associated bacteria in tenebrio molitor (Coleoptera: Tenebrionidae) larvae using culture-dependent and DGGE methods. *Annals of the Entomological Society of America*, *108* (5), 941–949. https://doi.org/10.1093/aesa/sav079

Wang, Z., Zolnik, C. P., Qiu, Y., Usyk, M., Wang, T., Strickler, H. D., Isasi, C. R., Kaplan, R. C., Kurland, I. J., Qi, Q., & Burk, R. D. (2018). Comparison of Fecal Collection Methods for Microbiome and Metabolomics Studies. *Frontiers in Cellular and Infection Microbiology*, *8*, 301. https://doi.org/10.3389/fcimb.2018.00301

Waring, R. H., Harris, R. M., & Mitchell, S. C. (2018). Plastic contamination of the food chain: A threat to human health? In *Maturitas* (Vol. 115, pp. 64–68). Elsevier Ireland Ltd. https://doi.org/10.1016/j.maturitas.2018.06.010

Weiss, S., Xu, Z. Z., Peddada, S., Amir, A., Bittinger, K., Gonzalez, A., Lozupone, C., Zaneveld, J. R., Vázquez-Baeza, Y., Birmingham, A., Hyde, E. R., & Knight, R. (2017). Normalization and microbial differential abundance strategies depend upon data characteristics. *Microbiome*, *5* (1), 27. https://doi.org/10.1186/s40168-017-0237-y

Werner, J. J., Zhou, D., Caporaso, J. G., Knight, R., & Angenent, L. T. (2011). Comparison of Illumina paired-end and single-direction sequencing for microbial 16S rRNA gene amplicon surveys. *The ISME Journal*, *6* (7), 1–4. https://doi.org/10.1038/ismej.2011.186

Wesolowska-Andersen, A., Bahl, M. I., Carvalho, V., Kristiansen, K., Sicheritz-Pontén, T., Gupta, R., & Licht, T. R. (2014). Choice of bacterial DNA extraction method from fecal material influences community structure as evaluated by metagenomic analysis. *Microbiome*, *2* (1), 19. https://doi.org/10.1186/2049-2618-2-19

Wessely, S. (2009). Surgery for the treatment of psychiatric illness: the need to test untested theories. *Journal of the Royal Society of Medicine*, *102* (10), 445. https://doi.org/10.1258/JRSM.2009.09K038

Willey, J. M., Sherwood, L. M., & Woolverton, C. J. (2014). *Prescott's Microbiology* (9th Editio). McGraw Hill.

Willis, A. D. (2019). Rarefaction, Alpha Diversity, and Statistics. *Frontiers in Microbiology*, *10* (OCT), 2407. https://doi.org/10.3389/fmicb.2019.02407

Woese, C. R. (1987). Bacterial Evolution. *Microbiollogical Reviews*, *51* (2), 221–271. https://www.ncbi.nlm.nih.gov/pmc/articles/PMC373105/pdf/microrev00049-0051.pdf

Xi, Y., Yuefen, P., Wei, W., Quan, Q., Jing, Z., Jiamin, X., & Shuwen, H. (2019). Analysis of prognosis, genome, microbiome, and microbial metabolome in different sites of colorectal cancer. *Journal of Translational Medicine*, *17* (1), 353. https://doi.org/10.1186/s12967-019-2102-1

Xia, Y., & Sun, J. (2017). Hypothesis testing and statistical analysis of microbiome. In *Genes and Diseases* (Vol. 4, Issue 3, pp. 138–148). Chongqing yi ke da xue, di 2 lin chuang xue yuan Bing du xing gan yan yan jiu suo. https://doi.org/10.1016/j.gendis.2017.06.001

Yang, B., Wang, Y., & Qian, P.-Y. (2016). Sensitivity and correlation of hypervariable regions in 16S rRNA genes in phylogenetic analysis. *BMC Bioinformatics*, *17* (1), 135. https://doi.org/10.1186/s12859-016-0992-y

Yang, S. S., Wu, W. M., Brandon, A. M., Fan, H. Q., Receveur, J. P., Li, Y., Wang, Z. Y., Fan, R., McClellan, R. L., Gao, S. H., Ning, D., Phillips, D. H., Peng, B. Y., Wang, H., Cai, S. Y., Li, P., Cai, W. W., Ding, L. Y., Yang, J., … Criddle, C. S. (2018). Ubiquity of polystyrene digestion and biodegradation within yellow mealworms, larvae of Tenebrio molitor Linnaeus (Coleoptera: Tenebrionidae). *Chemosphere*, *212*, 262–271. https://doi.org/10.1016/J.CHEMOSPHERE.2018.08.078

Yang, Y., Wang, J., & Xia, M. (2020). Biodegradation and mineralization of polystyrene by plastic-eating superworms Zophobas atratus. *Science of the Total Environment*, *708*, 135233. https://doi.org/10.1016/j.scitotenv.2019.135233

Yang, Y., Yang, J., Wu, W.-M. M., Zhao, J., Song, Y., Gao, L., Yang, R., & Jiang, L. (2015a). Biodegradation and Mineralization of Polystyrene by Plastic-Eating Mealworms: Part 1. Chemical and Physical Characterization and Isotopic Tests. *Environmental Science and Technology*, *49* (20), 12080–12086. https://doi.org/10.1021/acs.est.5b02661

Yang, Y., Yang, J., Wu, W.-M., Zhao, J., Song, Y., Gao, L., Yang, R., & Jiang, L. (2015b). Biodegradation and Mineralization of Polystyrene by Plastic-Eating Mealworms: Part 2. Role of Gut Microorganisms. *Environmental Science and Technology*, *49* (20), 12087–12093. https://doi.org/10.1021/ACS.EST.5B02663

Yatsunenko, T., Rey, F. E., Manary, M. J., Trehan, I., Dominguez-Bello, M. G., Contreras, M., Magris, M., Hidalgo, G., Baldassano, R. N., Anokhin, A. P., Heath, A. C., Warner, B., Reeder, J., Kuczynski, J., Caporaso, J. G., Lozupone, C. A., Lauber, C., Clemente, J. C., Knights, D., … Gordon, J. I. (2012). *Human gut microbiome viewed across age and geography*. *486* (7402), 222–227. https://doi.org/10.1038/nature11053

Yuan, S., Cohen, D. B., Ravel, J., Abdo, Z., & Forney, L. J. (2012). Evaluation of Methods for the Extraction and Purification of DNA from the Human Microbiome. *PLoS ONE*, *7* (3), e33865. https://doi.org/10.1371/journal.pone.0033865

Zambrana, L. E., McKeen, S., Ibrahim, H., Zarei, I., Borresen, E. C., Doumbia, L., Boré, A., Cissoko, A., Douyon, S., Koné, K., Perez, J., Perez, C., Hess, A., Abdo, Z., Sangaré, L., Maiga, A., Becker-Dreps, S., Yuan, L., Koita, O., … Ryan, E. P. (2019). Rice bran supplementation modulates growth, microbiota and metabolome in weaning infants: a clinical trial in Nicaragua and Mali. *Scientific Reports*, *9* (1). https://doi.org/10.1038/s41598-019-50344-4

Zierer, J., Jackson, M. A., Kastenmüller, G., Mangino, M., Long, T., Telenti, A., Mohney, R. P., Small, K. S., Bell, J. T., Steves, C. J., Valdes, A. M., Spector, T. D., & Menni, C. (2018). The fecal metabolome as a functional readout of the gut microbiome. *Nature Genetics*, *50* (6), 790–795. https://doi.org/10.1038/s41588-018-0135-7

ZymoResearch. (2019). *ZymoBIOMICS Microbial Community Standards*. https://www.zymoresearch.com/collections/zymobiomics-microbial-community-standards

BIOGRAPHY

Samantha Sevilla Chill graduated from Mother McAuley Liberal Arts High School in Chicago, Illinois, in 2006. She received her Bachelor of General Science from Seattle University, in Seattle, Washington, in 2010. She received her Master of Forensic Science in Forensic Molecular Biology from the George Washington University, in Washington, D.C., in 2012. For the past six years she has been employed at the Frederick National Laboratory for Cancer Research (FNLCR), operated by Leidos Biomedical Research. Currently, she works as a Bioinformatics Analyst I in the Biomedical Informatics and Data Science division.